National Library
of Canada

Acquisitions and
Bibliographic Services Branch

395 Wellington Street
Ottawa, Ontario
K1A 0N4

Bibliothèque nationale
du Canada

Direction des acquisitions et
des services bibliographiques

395, rue Wellington
Ottawa (Ontario)
K1A 0N4

Your file Votre référence

Our file Notre référence

NOTICE

The quality of this microform is heavily dependent upon the quality of the original thesis submitted for microfilming. Every effort has been made to ensure the highest quality of reproduction possible.

If pages are missing, contact the university which granted the degree.

Some pages may have indistinct print especially if the original pages were typed with a poor typewriter ribbon or if the university sent us an inferior photocopy.

Reproduction in full or in part of this microform is governed by the Canadian Copyright Act, R.S.C. 1970, c. C-30, and subsequent amendments.

AVIS

La qualité de cette microforme dépend grandement de la qualité de la thèse soumise au microfilmage. Nous avons tout fait pour assurer une qualité supérieure de reproduction.

S'il manque des pages, veuillez communiquer avec l'université qui a conféré le grade.

La qualité d'impression de certaines pages peut laisser à désirer, surtout si les pages originales ont été dactylographiées à l'aide d'un ruban usé ou si l'université nous a fait parvenir une photocopie de qualité inférieure.

La reproduction, même partielle, de cette microforme est soumise à la Loi canadienne sur le droit d'auteur, SRC 1970, c. C-30, et ses amendements subséquents.

Canada

University of Alberta

Capillary Gel Electrophoresis and DNA

by

Daniel Figeys ©

A thesis submitted to the Faculty of Graduate Studies and Research in partial fulfillment of the requirements for the degree of Doctor of Philosophy

Department of Chemistry

Edmonton, Alberta
Spring 1995

National Library of Canada
Acquisitions and Bibliographic Services Branch
395 Wellington Street
Ottawa, Ontario
K1A 0N4

Bibliothèque nationale du Canada
Direction des acquisitions et des services bibliographiques
395, rue Wellington
Ottawa (Ontario)
K1A 0N4

Your file Votre référence

Our file Notre référence

THE AUTHOR HAS GRANTED AN IRREVOCABLE NON-EXCLUSIVE LICENCE ALLOWING THE NATIONAL LIBRARY OF CANADA TO REPRODUCE, LOAN, DISTRIBUTE OR SELL COPIES OF HIS/HER THESIS BY ANY MEANS AND IN ANY FORM OR FORMAT, MAKING THIS THESIS AVAILABLE TO INTERESTED PERSONS.

L'AUTEUR A ACCORDE UNE LICENCE IRREVOCABLE ET NON EXCLUSIVE PERMETTANT A LA BIBLIOTHEQUE NATIONALE DU CANADA DE REPRODUIRE, PRETER, DISTRIBUER OU VENDRE DES COPIES DE SA THESE DE QUELQUE MANIERE ET SOUS QUELQUE FORME QUE CE SOIT POUR METTRE DES EXEMPLAIRES DE CETTE THESE A LA DISPOSITION DES PERSONNE INTERESSEES.

THE AUTHOR RETAINS OWNERSHIP OF THE COPYRIGHT IN HIS/HER THESIS. NEITHER THE THESIS NOR SUBSTANTIAL EXTRACTS FROM IT MAY BE PRINTED OR OTHERWISE REPRODUCED WITHOUT HIS/HER PERMISSION.

L'AUTEUR CONSERVE LA PROPRIETE DU DROIT D'AUTEUR QUI PROTEGE SA THESE. NI LA THESE NI DES EXTRAITS SUBSTANTIELS DE CELLE-CI NE DOIVENT ETRE IMPRIMES OU AUTREMENT REPRODUITS SANS SON AUTORISATION.

ISBN 0-612-01690-0

Canadä

Edmonton, April 1995

I, Norman J. Dovichi, authorize Daniel Figeys to use, for his thesis, the material published in the following papers.

Figeys, D. and Dovichi, N.J. Mobility of single stranded DNA as a function of cross-linker concentration in polyacrylamide capillary gel electrophoresis. Journal of Chromatography 645:311-317 (1993).

Figeys, D., Arriaga, E., Renborg, A., and Dovichi, N.J. Use of the fluorescent intercalating dyes POPO-3, YOYO-3 and YOYO-1 for ultrasensitive detection of double stranded DNA separated by capillary electrophoresis with hydroxypropylmethyl cellulose and non-crosslinked polyacrylamide. Journal of Chromatography A, 669:205-216 (1994).

Figeys, D., Renborg, A., and Dovichi, N.J. Labeling of double stranded DNA by ROX-dideoxycytosine triphosphate using terminal deoxynucleotidyl transferase and separation by capillary electrophoresis, Analytical Chemistry 66:4382-4383 (1994).

Figeys D., Renborg A., and Dovichi, N.J. Spatial and temporal depletion of ions from noncrosslinked denaturing polyacrylamide in capillary electrophoresis, Electrophoresis 15:1512-1517 (1994).

Figeys, D. and Dovichi, N.J. Effect of the age of noncrosslinked polyacrylamide on the separation of DNA sequencing samples, Journal of Chromatography A submitted.

Figeys, D. and Dovichi, N.J. Multiple separations of DNA sequencing fragments with a noncrosslinked polyacrylamide filled capillary: capillary electrophoresis at 300V/cm, Journal of Chromatography, submitted.

Dr. N.J. Dovichi
Department of Chemistry
University of Alberta
Edmonton, Alberta, Canada
T6G-2G2

Edmonton, April 1995

I authorize Daniel Figeys to use, for his thesis, the material published in the following papers.

Figeys, D., Arriaga, E., Renborg, A., and Dovichi, N.J. Use of the fluorescent intercalating dyes POPO-3, YOYO-3 and YOYO-1 for ultrasensitive detection of double stranded DNA separated by capillary electrophoresis with hydroxypropylmethyl cellulose and non-crosslinked polyacrylamide. Journal of Chromatography A, 669:205-216 (1994).

Figeys, D., Renborg, A., and Dovichi, N.J. Labeling of double stranded DNA by ROX-dideoxycytosine triphosphate using terminal deoxynucleotidyl transferase and separation by capillary electrophoresis, Analytical Chemistry 66:4382-4383 (1994).

Figeys D., Renborg A., and Dovichi, N.J. Spatial and temporal depletion of ions from noncrosslinked denaturing polyacrylamide in capillary electrophoresis, Electrophoresis 15:1512-1517 (1994).

Annika Renborg
Department of Chemistry
University of Alberta
Edmonton, Alberta, Canada
T6G-2G2

Edmonton, April 1995

I authorize Daniel Figeys to use, for his thesis, the material published in the following paper.

Figeys, D., Arriaga, E., Renborg, A., and Dovichi, N.J. Use of the fluorescent intercalating dyes POPO-3, YOYO-3 and YOYO-1 for ultrasensitive detection of double stranded DNA separated by capillary electrophoresis with hydroxypropylmethyl cellulose and non-crosslinked polyacrylamide. Journal of Chromatography A, 669:205-216 (1994).

Dr. Edgar Arriaga
Department of Chemistry
University of Alberta
Edmonton, Alberta, Canada
T6G-2G2

University of Alberta

Library Release Form

Name of Author: Daniel Figeys

Title of Thesis: Capillary Gel Electrophoresis and DNA

Degree: Doctor of Philosophy

Year this Degree Granted: 1995

Permission is hereby granted to the University of Alberta Library to reproduce single copies of this thesis and to lend or sell such copies for private, scholarly, or scientific research purposes only.

The author reserves all other publication and other rights in association with the copyright in the thesis, and except as hereinbefore provided, neither the thesis nor any substantial portion thereof may be printed or otherwise reproduced in any material form whatever without the author's prior written permission

9247 Interlake North, apt. 3
Seattle, Washington, USA
WA98103

April 19,1995

University of Alberta

Faculty of Graduate Studies and Research

The undersigned certify that they have read, and recommend to the Faculty of Graduate Studies and Research for acceptance, a thesis entitled **Capillary Gel Electrophoresis and DNA** submitted by **Daniel Figeys** in partial fulfillment of the requirements for the degree of **Doctor of Philosophy**.

Dr. Norman J. Dovichi

Jed Harrison

Dr. D. J. Harrison

Frederick J Cantwell

Dr. F. Cantwell

Glen Loppnow

Dr. G. Loppnow

Wm Paranchych

Dr. W. Paranchych

Gary Slater

Dr. G. Slater

April 19,1995

Abstract

Capillary gel electrophoresis (CGE) is a rapid method of separation of biological samples. Promising applications of CGE include the separation of DNA sequencing samples (ssDNA) and double-stranded DNA (dsDNA). CGE allows faster separation of DNA with equal or higher resolution versus conventional polyacrylamide gel electrophoresis (PAGE). In CGE the samples are separated in series, thus the gel-filled capillary is used for a few subsequent separations in order to reduce the experimental time. However, the reproducibility and the stability of CGE is a major problem.

The first step to do before studying the reproducibility of CGE is to find the optimum polyacrylamide concentration. The total gel concentration (%T) has been studied previously. In Chapter 2, the effect of the concentration of cross-linker (%C) in polyacrylamide on the separation of ssDNA is studied. High %C gives higher resolution with longer separation time than 0%C. The number of fragments that can be separated seems to increase as the %C decreases. This means that 0 %C polyacrylamide would be more useful than high %C polyacrylamide for DNA sequencing applications.

In chapter 3, the stability of 5%T 0%C polyacrylamide is studied by looking at the effects that aging polyacrylamide, and buffer transference numbers have on the conductivity of polyacrylamide. It is shown that by using aged polyacrylamide (6 days or more), more stable conductivity profiles are obtained.

In Chapter 4, we look at the effect that the stabilization of the conductivity of polyacrylamide has on the separation of ssDNA. First, it is demonstrated that as the polyacrylamide ages (i.e. yielding more stable conductivity) the migration times of the DNA fragments for subsequent sequencing runs are more stable. Second, stable multiple sequencing runs are reported by reversing the polarity for a short period of time between each run.

In the first part of Chapter 5, dsDNA are labeled with the novel intercalating dyes YOYO-1, YOYO-3, and POPO-3 and separated on polyacrylamide and hydroxypropylmethylcellulose. The limit of detection (3σ) is 1 molecule of a 6kb DNA fragment. In the second part, terminal deoxynucleotidyl transferase and ROX-dideoxycytosinetriphosphate are used to covalently label dsDNA.

Acknowledgments

The first and foremost person I would like to thank is my wife Rachel, who supported me during the last three and half years. She spent a lot of time helping me to comprehend the English language and cope with my long working hours.

My thanks go also to Dr. Norman Dovichi, my supervisor. I came to join his group from a classical thermodynamic laboratory, and I had little knowledge in the field of analytical chemistry. I gained tremendous experience by working in his group. He gave me the freedom of selecting my field of research. The most remarkable thing about Norm is his patience.

I also want to thank all my co-workers in Norm's group and the members of the Department of Chemistry. Through their experience, I learned a lot about chemistry. In particular, I would like to thank the people who worked on projects with me: Edgar Arriaga, David Chen, Annika Renborg, and Hussain Ahmadzadeh. I also thank all the previous members of Norm's group who taught me about capillary electrophoresis and DNA sequencing. Thanks everyone!

Finally, I would like to thank the organizations that contributed financially to this thesis: the Natural Science and Engineering Research Council of Canada, le FCAR, the Alberta Heritage Foundation for Medical Research, and the University of Alberta.

Table of Contents

1. Introduction.......1

1.1 Introduction.......2

1.2 DNA.......4

1.2.1 DNA Sample Preparation.......8

1.2.1.1 Single Stranded DNA.......8

1.2.1.1.1 Protocol 1. Two-Step Protocol.......11

1.2.1.1.2 Protocol 2. Cycle Sequencing.......13

1.2.1.2 Restriction Fragment.......13

1.3 Electrophoresis.......16

1.3.1 Theoretical Aspects.......17

1.3.2 Capillary Gel Electrophoresis.......25

1.3.2.1 Sieving Medium and Capillary Wall Treatment.......26

1.3.2.1.1 Polyacrylamide.......26

1.3.2.1.2 Cellulose Derivatives.......27

1.3.2.1.3 Preparation of Coated Capillaries.......31

1.3.2.2 Difference in Transference Numbers.......33

1.3.2.3 Detection in Capillary Electrophoresis.......38

1.3.2.3.1 General Survey.......38

1.3.2.3.2 Fluorescence Detection.......40

1.3.2.4 DNA sequencing.......47

1.4 Bibliography.......53

2. Effect of Cross-linker Concentration on the Separation of Single-stranded DNA.......61

2.1 Introduction.......62

2.2 Experimental.......63

2.3 Results and Discussion.......65

2.4 Conclusions 79

2.5 Bibliography 80

3. Stability of Linear Polyacrylamide Used for Capillary Electrophoresis. 83

3.1 Introduction 84

3.2 Experimental 85

3.3 Results 86

3.3.1 Effect of $\Delta\kappa_{depletion}$ 90

3.3.1.1 Age of Polyacrylamide 90

3.3.1.2 Depletion of Ions 95

3.3.1.3 Depletion of Ions- Temporal Evolution of Spatial Profile 100

3.3.1.4 Relaxation Due to Diffusion 102

3.3.1.5 Effect of Adding KCl 104

3.3.1.6 Effect of 5%T Linear Polyacrylamide-Filled Reservoir. . 106

3.3.2 Effect of $\Delta\kappa_{template}$ 106

3.4 Discussion 111

3.5 Conclusions 117

3.6 Bibliography 118

4. Effects of Aging of Linear Polyacrylamide on the Separation of Single-Stranded DNA. 121

4.1 Introduction 122

4.2. Experimental 124

4.3 Effects of Aging Polyacrylamide on the Separation of Sequencing Samples 126

4.3.1 Results and Discussion 126

4.3.3 Conclusions 138

4.4 Multiple Runs of DNA Sequencing Samples 138

4.4.1 Results and Discussion 138

4.4.2 Conclusions 145

4.5 Bibliography 146

5. Labeling and Separation by Capillary Electrophoresis of Double-Stranded DNA...... 148
  5.1 Introduction 149
    5.1.1 Intercalating Dyes 151
    5.1.2 ROX-Dideoxycytosine Triphosphate 155
  5.2 Intercalating Dye Experiments 156
    5.2.1 Experimental 156
    5.2.2 Results and Discussion 158
      5.2.2.1 Base Pair-to-Dye Molecule Ratio 158
      5.2.2.2 Ionic Strength 160
      5.2.2.3 Separation Matrix Composition 163
      5.2.2.4 Detection Limits 175
  5.3 ROX-Dideoxycytosine Triphosphate 177
    5.3.1 Experiment 177
    5.3.2 Results and Discussion 177
  5.4 Conclusions 179
  5.5 Bibliography 182
6. Conclusion 185
  6.1 Bibliography 191
APPENDIX A Calculation of the Friction Coefficient and the Gel Pore Size........ 193
  A.1 Slope 195
  A.2 Intercept 195
APPENDIX B More Multiple Runs of DNA Sequencing Samples 197

List of Tables

Table 1.1 Some restriction endonucleases and their recognition sequence............... 15

Table 2.1 Least squares slope and intercept from a plot of migration time, in minutes, versus the fragment length, in bases, for fragments ranging in size from 60 to 240 bases in length.. 70

Table 2.2 Least squares slope (S) and intercept (I) from a plot of mobility versus N^{-1}, where N is the fragment length in bases... 73

Table 2.3 Least squares slope and intercept from a plot of resolution versus N^{-1}, where N is the fragment length in bases... 78

Table 5.1 Characteristics of the dyes. 154

Table 5.2 Limits of detection of intercalated dyes.. 176

List of Figures

Figure 1.1 General structure of a nucleotide...5

Figure 1.2 The sugar (2'-deoxyribose) found in DNA....................................5

Figure 1.3 The four bases found in DNA...6

Figure 1.4 Phosphate groups attached to the ribose...6

Figure 1.5 The structure of a short polynucleotide...7

Figure 1.6 A) Hydrogen bonds between two polynucleotides **B)** details of hydrogen bonds between bases...9

Figure 1.7 Sequence of M13mp18 from the priming site of the universal(-21) primer. The primer sequence is underline...10

Figure 1.8 Two-step protocol for DNA sequencing.......................................12

Figure 1.9 Cycle sequencing..14

Figure 1.10 General set-up for capillary electrophoresis.................................18

Figure 1.11 Double layer at the capillary surface..20

Figure 1.12 Polymerization of acrylamide...28

Figure 1.13 Different forms of polyacrylamide..29

Figure 1.14 Constitution and conformation of a cellulose molecule.....................30

Figure 1.15 Cellulose derivatives used in capillary electrophoresis......................30

Figure 1.16 Coating of the inside wall of a capillary with acrylamide...................32

Figure 1.17 Effect of different medium on the transference number of a cation and an anion...34

Figure 1.18 Cartoon of a change in ionic concentration at the capillary.................36

Figure 1.19 Change in ionic concentration for all possible changes in transference number at the reservoir...37

Figure 1.20 Sheath flow cuvette arrangement for post column detection................42

Figure 1.21 One-color laser induced fluorescence detection system.....................43

Figure 1.22 Optical alignment and signal..45

Figure 1.23 Two-color laser induced fluorescence detection system.....................46

Figure 1.24 Simulated separation of DNA fragments by capillary gel electrophoresis..48

Figure 1.25 Predicted mobility versus the fragment length for different polymer concentrations. This is a schematic diagram...50

Figure 1.26 Predicted mobility versus fragment length for reptation with orientation. This is a schematic diagram...52

Figure 2.1A Separation of M13mp18 ddATP sample on a 6%T 0%C 35 cm long x 50 μm id x 190 μm od capillary at -300V/cm...66

Figure 2.1B Separation of M13mp18 ddATP sample on 6%T 0.5%C..................67

Figure 2.1C Separation of M13mp18 ddATP sample on 6%T 2.5%C..................68

Figure 2.1D Separation of M13mp18 ddATP sample on 6%T 5%C at -300 V/cm.....69

Figure 2.2 Average mobility versus the inverse of fragment length for different polymers..72

Figure 2.3 Average number of theoretical plates versus fragment length for different concentrations of cross-linker...75

Figure 2.4 Average resolution versus fragment length for different concentrations of cross-linker...77

Figure 3.1 Current versus time for a 14-day old 5%T linear polyacrylamide run at -300 V/cm..88

Figure 3.2 W_1 versus the age of polyacrylamide..91

Figure 3.3 W_3 versus the age of polyacrylamide..93

Figure 3.4 W_O versus the age of polyacrylamide..94

Figure 3.5 Conductivity profile at the injection end for different ages of polyacrylamide..97

Figure 3.6 Conductivity profile at the ground end for different ages of polyacrylamide 99

Figure 3.7 Change in conductivity versus the total length of capillary cut from the injection end of 1-day old capillaries (full lines) and 9-days old capillaries (dotted lines) for different run times (shown as minutes). 101

Figure 3.8 Change in conductivity versus relaxation time (no voltage applied) for polyacrylamide previously run for 6 hours at -300V/cm. 103

Figure 3.9 Effect of KCl on the conductivity of polyacrylamide 105

Figure 3.10 Effect of polyacrylamide-filled reservoirs on the conductivity in the capillary. 107

Figure 3.11 Change in conductivity versus relaxation time 109

Figure 3.12 Change in conductivity versus the number of injections of DNA template 110

Figure 3.13 Electric field versus the distance from the cathodic end of the capillary... 116

Figure 4.1 Four subsequent separations of M13mp18 ddATP terminated sequencing samples at -300V/cm on a 35 cm long capillary filled with 1-day old linear polyacrylamide 127

Figure 4.2 Four subsequent separations of M13mp18 ddATP terminated sequencing samples at -300V/cm on a 32.1 cm long capillary filled with 20-day old linear polyacrylamide 129

Figure 4.3 Three subsequent separations of M13mp18 ddATP terminated sequencing sample at -300 V/cm on a 36 cm long capillary 130

Figure 4.4 Four subsequent separations of M13mp18 ddATP terminated sequencing sample at -300 V/cm on a 36 cm long capillary 131

Figure 4.5 Mobilities for base 91 and base 252 versus the age of linear polyacrylamide for four subsequent sequencing runs 132

Figure 4.6 Resolution for base 91 versus the age of linear polyacrylamide for four subsequent sequencing runs. 134

Figure 4.7 Δt for base 91-93 versus the age of polyacrylamide for four subsequent runs. 135

Figure 4.8 Peak widths for base 91 versus the age of polyacrylamide for four subsequent runs. 136

Figure 4.9 Theoretical plates for base 91 versus the age of polyacrylamide for four subsequent sequencing runs. 137

Figure 4.10 Multiple runs of M13mp18 ddATP on a 33 cm x 32 µm id x 143 µm od capillary at -300V/cm. 139

Figure 4.11 Average current in the capillary used for 19 DNA sequencing runs. 141

Figure 4.12 Mobility for different peaks for 19 runs. 142

Figure 4.13 Mobility versus current for four subsequent runs done on a one-day old capillary. 143

Figure 4.14 Resolution versus number of runs for different peaks. 144

Figure 5.1 Structures of the intercalating dyes POPO-3, YOYO-1, and YOYO-3...... 153

Figure 5.2 Number of theoretical plates versus base pair 159

Figure 5.3 Normalized peak height versus base pair 161

Figure 5.4 Theoretical plates versus NaCl concentration. 162

Figure 5.5 Separation of ϕx174 RF/HaeIII digest intercalated with YOYO-3 on different HPMC at -200V/cm with 1XTBE, 0.1M NaCl. 164

Figure 5.6 Separation of ϕx174 RF/HaeIII digest intercalated with YOYO-3 on different linear polyacrylamide at -200V/cm with 1XTBE, 0.1M NaCl. 165

Figure 5.7 Mobility versus reciprocal fragment length for different polymers. 166

Figure 5.8 Theoretical plates versus fragment lengths for different polymers........ 167

Figure 5.9 Resolution versus fragment length for different polymers........ 169

Figure 5.10 Separation of 100-bp ladder intercalated with YOYO-3 on HPMC 0.4% at -200V/cm with 1XTBE, 0.1M NaCl........ 170

Figure 5.11A Separation of a 123-bp ladder........ 171

Figure 5.11B Expanded area of Figure 5.11A from 18 to 20 minutes........ 172

Figure 5.12 Separation of λ DNA/ Hind III.. 173

Figure 5.13 Separation of Taq I digest of M13mp18. 174

Figure 5.14 Separation of ϕx174 RF/Hae III on a 28.6 cm capillary filled with HPMC 0.4% and 1XTBE 0.1MNaCl at -100V/cm. 178

Figure 5.15 Separation of ϕx174 RF/Hae III on a 30 cm capillary filled with 5%T LPA and 1XTBE 0.1MNaCl at -300V/cm........ 180

Figure B.1 14 runs of sequencing samples on the same capillary at -300V/cm. 198

Figure B.2 15 runs of M13mp18 ddGTP sequencing samples on the same capillary at -300V/cm. 199

Figure B.3 7 runs of M13mp18 ddATP sequencing samples on the same capillary at -300V/cm. 200

List of Symbols, Nomenclature, and Abbreviations

A: adenine

A_o: baseline

A_1: peak height

A_2: equal to ($2^{0.5}$ σ)

$A_{2,i}$ and $A_{2,j}$: A_2 values for two subsequent peaks

$\overline{A_2}$: average of $A_{2,i}$ and $A_{2,j}$

bp: base pair

C: cytosine

C_i: concentration of ion i

C_p: concentration of the polymer

CE: capillary electrophoresis

CGE: capillary gel electrophoresis

CIEF: capillary isoelectric focussing

CITP: capillary isotachophoresis

cp: centiPoise

CZE: capillary zone electrophoresis

D: diffusion coefficient

$\overline{D}$: average diffusion coefficient for two subsequent peaks

$D_{b\text{-}b}$: distance between two bases

dATP: 2'-deoxyadenosine 5'-triphosphate

dCTP: 2'-deoxycytidine 5'-triphosphate

ddATP: dideoxyadenosine 5'-triphosphate

ddNTP: dideoxynucleotide 5'-triphosphate

dGTP: 2'-deoxyguanosine 5'-triphosphate

DNA: deoxyribonucleic acid

dNTP: deoxynucleotide 5'-triphosphate

dTTP: 2'-deoxythymidine 5'-triphosphate

dUTP: deoxyuridyl 5'-triphosphate

dsDNA: double-stranded DNA

E: electric field

EDTA: ethylenediamine tetraacetic acid

EthD; ethidium homodimer

F: Faraday constant

F_e: the electric force

F_f: the friction force

f: friction coefficient

G: guanine

H: plate height

HEC: hydroxyethylcellulose

HMEC: hydroxymethylethylcellulose

HPMC: hydroxypropylmethylcellulose

I: intercept

i: current

id: inner diameter

k: constant

k': proportionality constant

k_b: Boltzman constant

κ_o: steady-state conductivity in the absence of ionic transport

kb: kilobase

L: length of the capillary

LED: light emitting diode

m: mass of the DNA fragment

MECC: micellar electrokinetic capillary chromatography

MOPS: 3-[N-morpholino]propanesulfonic acid

N: length of the chain expressed by the number of nucleotides in the fragment

N^*: fragment length for the onset of biased reptation with orientation

N_{bead}: number of pores filled by the fragment

N_p: number of theoretical plates

NMR: nuclear magnetic resonance

od: outer diameter

pmt: photomultiplier tube

POPO: benzothiazolium-4-pyridinium dimer

Q: effective charge on the whole fragment

q: effective charge on the part of the fragment in one average gel pore

R: resolution

R_{10}: resolution for fragments differing by 10 base pairs

R_g: radius of gyration

R_k: resistance of the capillary at equilibrium with no stress applied (steady-state resistance)

R_p: radius of a DNA sphere

R_t: resistor

r: mean radius of the pore of polyacrylamide

r_p: thickness of the polymer

S: slope

SDS: sodium dodecylsulfate

ssDNA: single-stranded DNA

T: thymine

T: transference number

T_c and T_r: transference numbers of the cation in the buffer reservoirs and in polyacrylamide respectively

T_p: temperature

T_+ and T_-: transference numbers of a cation and an anion

TB: buffer made of TRIS and borate

TBE: buffer made of TRIS, borate and EDTA

TEMED: N,N,N',N'-tetramethylethylene-diamine

TOTO: benzothiazolium-4-quinolinium dimer

TRIS: tris(hydroxymethyl)aminomethane

t : time

t_m: migration time

$t_{m,i}$ and $t_{m,j}$: migration times for two subsequent peaks

UV: ultraviolet

V: applied voltage

W_i and W_j : baseline peak widths for two subsequent peaks

x: distance from one end of the capillary

YOYO: benzoxazolium-4-quinolinium dimer

%C: cross-linker concentration

%T: weight percent of monomer plus cross-linker

α: constant of proportionality

α_s: pore size of the gel

β: proportionality constant

Δ BP: difference in fragment length in base pairs

$\Delta\kappa$: change in conductivity induced at the capillary tip

$\Delta\kappa_{depletion}$: depletion of ions effect

$\Delta\kappa_{template}$: effect of the template in a DNA sequencing sample

$\Delta\kappa_S$: change in conductivity generated by the application of a stress

ΔL: length trimmed from the capillary

Δt_m: difference in migration time of two fragments

Δt_{sub}: difference in migration time between two subsequent peaks

$\Delta\mu_e$: difference in electrophoretic mobility between two subsequent peaks

δL: characteristic distance over which depletion is noticed

ε: dielectric constant of the medium

ε_c: friction coefficient

ε_0: permitivity of vacuum

ζ: wall zeta-potential

η: viscosity of the medium

κ: conductivity

Λ_i: ionic conductivity of ion i

μ: mobility

μ_+ and μ_-: mobilities of a cation and an anion

μ_e: electrophoretic mobility

$\overline{\mu_e}$: average electrophoretic mobility for two subsequent peaks

μ_o: electroosmotic mobility

μ_{zero}: mobility of a fragment in absence of a gel

μ_∞: mobility of the longest fragments

v: total velocity

v_e: electrophoretic velocity

v_o: electroosmotic velocity

σ^2: peak variance

σ_A^2: peak variance due to adsorption

σ_C^2: peak variance due to convection

σ_{cond}^2: peak variance due to conductivity difference

σ_D^2: peak variance due to diffusion

σ_{det}^2: peak variance due to detection effect

σ_{inj}^2: peak variance due to injection effect

σ_J^2: peak variance due to joule heating

σ_{pH}^2: peak variance due to pH difference

σ_t^2: migration time variance

CHAPTER 1

INTRODUCTION

1.1 Introduction

The analysis of biologically important molecules has become one of the leading fields of research in chemistry. DNA is an important biological molecule. It contains all the information necessary for the creation and maintenance of life. The human genome is made of 50,000 to 100,000 genes of some 3,000,000 kb(kilobase), distributed among 23 chromosomes[1,2]. Sometimes the information contained in DNA is damaged or lost. When the damage occurs in a gene or a gene-related sequence, the effect can be catastrophic. For example, cystic fibrosis is a very common genetic disease among Caucasians. Individuals with this disease produce a large quantity of mucus in their respiratory and gastrointestinal systems, causing respiratory problems and susceptibility to lung infections. The gene causing cystic fibrosis was identified and sequenced[3-5]. Although there is still no effective treatment available for this disease, the information gained by sequencing its gene has led scientists to refocus their research.

The human genome project is aimed at determining the entire genome sequence. The information gained from this project should generate new understanding, and hopefully, new treatments for genetic diseases. Current automated sequencers, based on slab gel electrophoresis using polyacrylamide, can generate 2000 bases of finished sequence per day. At this rate, 1.5 million instrument-days would be required to sequence the human genome[6]. One way of decreasing the time required for an analysis is to increase the electric field applied to the polyacrylamide. Capillary gel electrophoresis(CGE) allows high electric fields to be used[7,8] due to the efficient dissipation of the heat through the capillary wall. It also allows a lesser amount of sample to be used; however, capillary gel electrophoresis needs an improvement of the throughput, and the reproducibility of polyacrylamide. Obviously, the throughput of capillary gel electrophoresis can be increased by running capillaries in parallel[9-12]. Only a few studies of the behavior of polyacrylamide filled capillaries for DNA sequencing have been published[13]. Parts of this thesis address the effect of different parameters on the behavior of polyacrylamide for the separation of DNA sequencing samples.

The understanding of how the gel composition affects the separation of DNA sequencing samples is a key element in improving the reproducibility and performance of CGE. Polyacrylamide gels are obtained by the copolymerization of acrylamide and N,N'-methylenebisacrylamide (cross-linker). Polyacrylamide also contains a buffer and a denaturing agent. The effects of the acrylamide concentration[14], and the denaturing agent[15] on the separation of DNA sequencing samples have been previously studied. In chapter 2 of this thesis, we have completed these studies by looking at the effects of the cross-linker concentration on the separation of DNA sequencing samples.

The separation of samples by CGE is done in a serial manner. In order to improve the throughput of CGE, it is important to reduce the experimental time. One way of reducing the experimental time is to use the gel for more than one separation; however, an important increase in separation time (can double) and a decrease in resolution are often observed, when subsequent runs are performed on the same gel. Thus, it is important to find out what causes this increase in separation time and to stabilize it. There is a steady decrease of current through the gel filled capillary during electrophoresis. This decrease in current is related to the longer separation time and lower resolution, which is due to changes in transference numbers at the reservoir:capillary interfaces(see section 1.3.2.2). The changes in transference numbers and the parameters that affect them are studied in Chapter 3. In Chapter 4, the results from chapter 3 are used to stabilize the separation time of DNA sequencing samples.

Restriction fragment analysis is also an important part of the human genome project. In Chapter 5 of this thesis, we used different approaches to label double-stranded DNA. Also, the separation of double-stranded DNA on polyacrylamide and hydroxypropylmethylcellulose is reported.

1.2 DNA

DNA[1,2] is a long polymeric molecule made of four different monomers linked together in series. The basic unit of DNA is the nucleotide monomer (Figure 1.1). Nucleotides are made up of three distinct components: a sugar, a base, and a phosphate. In DNA, the sugar component is a pentose called 2'-deoxyribose (Figure 1.2) and it is presented as the Haworth structure. Ribose has a hydroxyl group in position 2', but in the case of DNA, this hydroxyl group is replaced by a hydrogen.

Four different bases are encountered in DNA. Two are single-ring molecules called pyrimidines, and two are double-ring molecules called purines (Figure 1.3). The two pyrimidine molecules are cytosine(C) and thymine(T), and the purine molecules are adenine(A) and guanine(G). They are attached to the sugar at the 1' position by a C-N bond replacing the hydroxyl group of the 2'-deoxyribose sugar. The nitrogen used in the bond is in bold in Figure 1.3. The sugar and the bases attached together are nucleosides called adenosine, guanosine, cytidine, and thymidine.

The phosphate component of the nucleotide is made of up to three individual phosphate groups (Figure 1.4) linked together linearly. The phosphate groups are attached at the 5' position of the 2'-deoxyribose. The three components linked together are nucleotides called 2'-deoxyadenosine 5'-triphosphate, 2'-deoxyguanosine 5'-triphosphate, 2'-deoxycytidine 5'-triphosphate, and 2'-deoxythymidine 5'-triphosphate.

The molecule of DNA is built by linking the different monomers to form a polynucleotide. The attachment is done by the formation of a phosphodiester bond between the 5'- phosphate group of one nucleotide and the 3'-end of the 2'-deoxyribose. Only one phosphate group is involved in the phosphodiester bond; the other phosphate groups on the nucleotide are removed during the polymerization. Two distinct ends are apparent on the DNA (Figure 1.5). The 5'- end of the polynucleotide is a triphosphate group and the 3'-end of the polynucleotide is a hydroxyl group. The different terminal

Figure 1.1 General structure of a nucleotide.

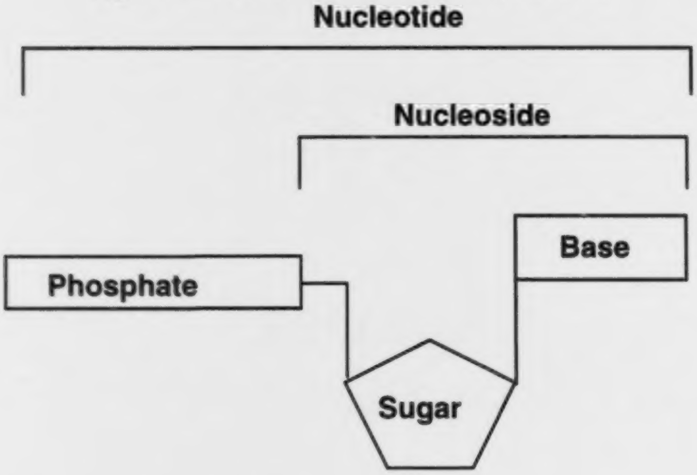
Nucleotide
Nucleoside
Base
Phosphate
Sugar

Figure 1.2 The sugar (2'-deoxyribose) found in DNA.

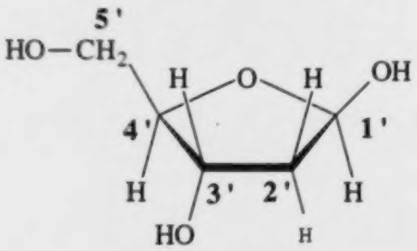
5'
HO—CH2
H
O
H
OH
4'
1'
H
3'
2'
H
HO
H

Figure 1.3 The four bases found in DNA.

Purines

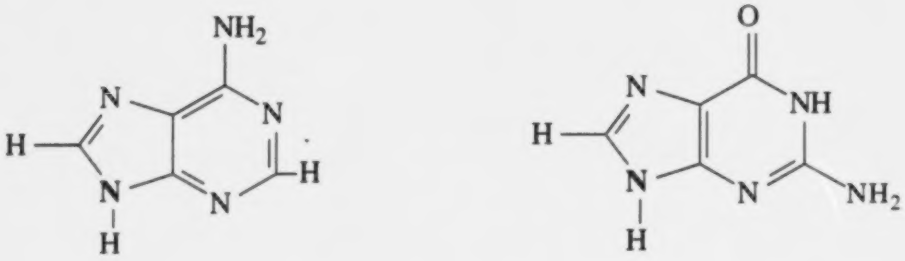
NH2
N
N
H
N
N
H
H
O
N
NH
H
N
N
NH2
H

adenine

guanine

Pyrimidines

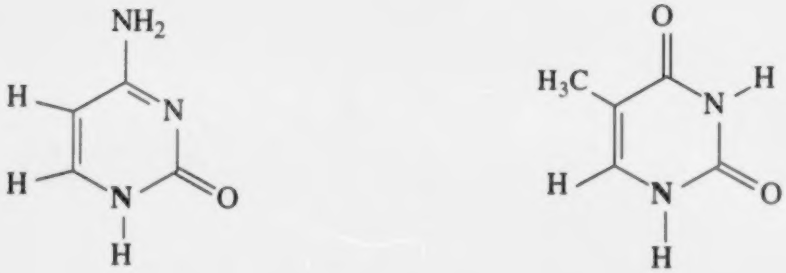
NH2
H
N
H
N
O
H
O
H3C
N
H
H
N
O
H

cytosine

thymine

Figure 1.4 Phosphate groups attached to the ribose.

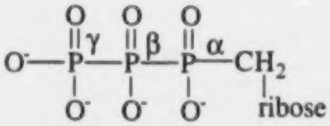

$$O^{-}-\underset{O^{-}}{\overset{O}{\overset{\|\gamma}{P}}}-\underset{O^{-}}{\overset{O}{\overset{\|\beta}{P}}}-\underset{O^{-}}{\overset{O}{\overset{\|\alpha}{P}}}-\underset{\text{ribose}}{CH_2}$$

Figure 1.5 The structure of a short polynucleotide.

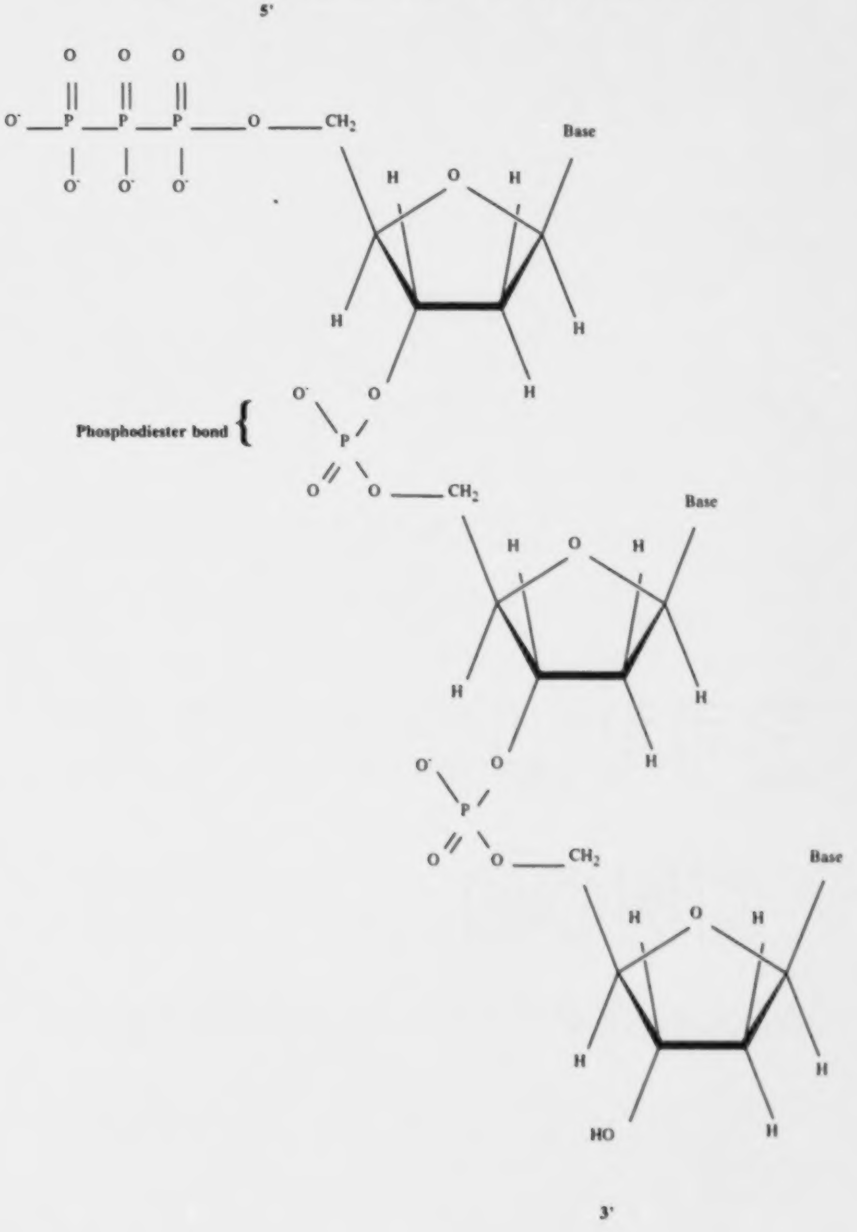
5'
O
O
O
O⁻
P
P
P
O
CH₂
O⁻
O⁻
O⁻
Base
H
O
H
H
H
O⁻
O
H
Phosphodiester bond
P
O
O
CH₂
Base
H
O
H
H
H
O⁻
O
H
P
O
O
CH₂
Base
H
O
H
H
H
HO
H
3'

groups confer a different reactivity to each end of the polynucleotide. It seems that there is no limitation to the number of nucleotides present in the polynucleotide. Thousands of nucleotides to hundreds of millions of nucleotides can be joined together to form a polynucleotide. Also, there is no limitation to the order in which the nucleotides can be joined together. Thus, the different sequence possibilities of polynucleotides are 4^n, where n is the number of bases. For a short polynucleotide of 10 nucleotides the number of different sequences is already 1, 048, 576.

In nature, DNA is usually found as a double helix, or double-stranded DNA composed of two polymer molecules bound together by hydrogen bonds between the bases. In the cases of the DNA used in this thesis, some are single stranded DNA (M13mp18) and some are double-stranded DNA (restriction fragments) . Chargaff discovered that for all the cases of double-stranded DNA, the ratio of adenine:thymine, and the ratio of guanine:cytosine were one to one. Any other base ratios were different than one to one. These results are explained by the fact that the adenines of one polymer molecule bind only with the thymines of the other polymer molecule, and the guanines of one polymer molecule only bind with the cytosines of the other polymer molecules (Figure 1.6). Adenines form two hydrogen bonds with thymines and cytosines form three hydrogen bonds with guanines. Because of structural constraints, any other base pairings are unfavorable. Thus, the sequence for one of the polynucleotides is complementary to the sequence of the other polynucleotide; however, the two polynucleotides are antiparallel, which means that one polynucleotide runs in the 5'→3' direction and the other runs in the 3'→5' direction.

1.2.1 DNA Sample Preparation

1.2.1.1 Single Stranded DNA

All the single stranded DNA samples were generated using M13mp18 template and ROX labeled universal primers (-21). Figure 1.7 gives the sequence of part of the

Figure 1.6 A) Hydrogen bonds between two polynucleotides B) details of hydrogen bonds between bases.

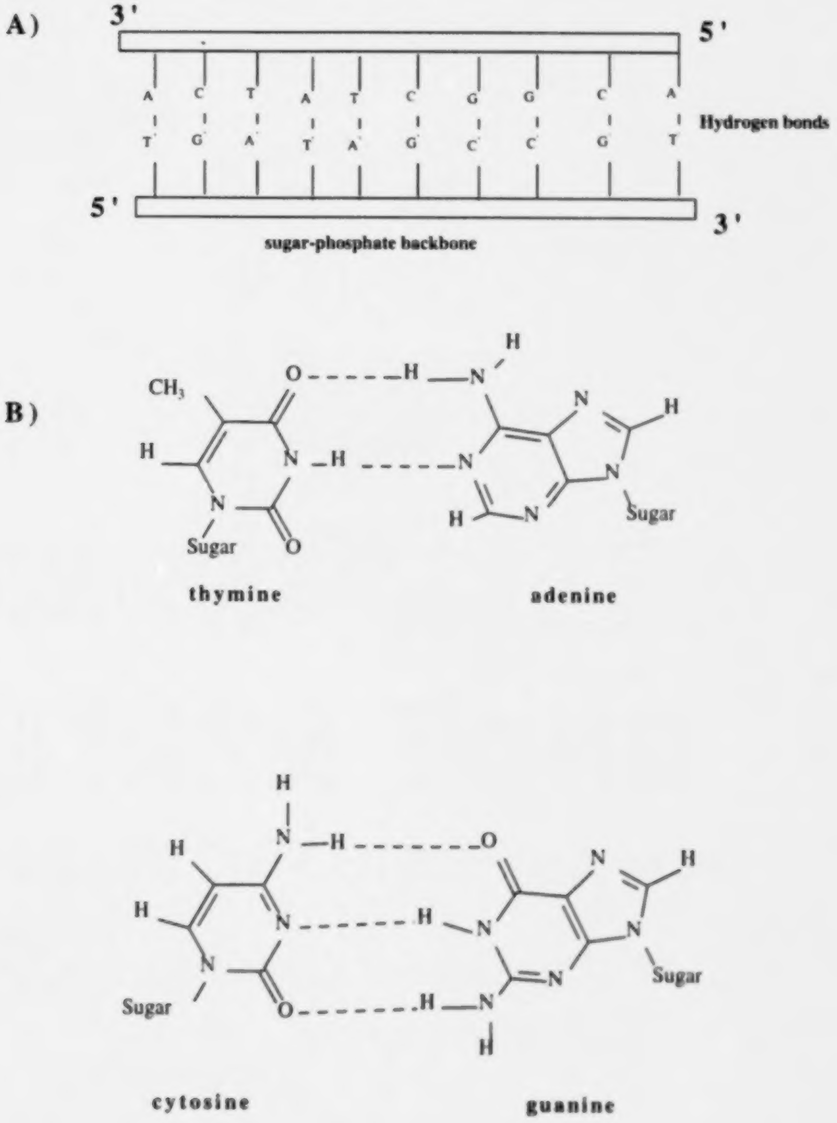
A)
3'
5'
A C T A T C G G C A
T G A T A G C C G T
Hydrogen bonds
5'
3'
sugar-phosphate backbone
B)
CH₃
Sugar
thymine
adenine
cytosine
guanine

Figure 1.7 Sequence of M13mp18 from the priming site of the universal(-21) primer. The primer sequence is underline.

```
1                                                            50
TGTAAAACGA  CGGCCAGTGC  CAAGCTTGCA  TGCCTGCAGG  TCGACTCTAG

51                                                          100
AGGATCCCCG  GGTACCGAGC  TCGAATTCGT  AATCATGGTC  ATAGCTGTTT

101                                                         150
CCTGTGTGAA  ATTGTTATCC  GCTCACAATT  CCACACAACA  TACGAGCCGG

151                                                         200
AAGCATAAAG  TGTAAAGCCT  GGGGTGCCTA  ATGAGTGAGC  TAACTCACAT

201                                                         250
TAATTGCGTT  GCGCTCACTG  CCCGCTTTCC  AGTCGGGAAA  CCTGTCGTGC

251                                                         300
CAGCTGCATT  AATGAATCGG  CCAACGCGCG  GGGAGAGGCG  GTTTGCGTAT

301                                                         350
TGGGCGCCAG  GGTGGTTTTT  CTTTTCACCA  GTGAGACGGG  CAACAGCTGA

351                                                         400
TTGCCCTTCA  CCGCCTGGCC  CTGAGAGAGT  TGCAGCAAGC  GGTCCACGCT

401                                                         450
GGTTTGCCCC  AGCAGGCGAA  AATCCTGTTT  GATGGTGGTT  CCGAAATCGG

451                                                         500
CAAAATCCCT  TATAAATCAA  AAGAATAGCC  CGAGATAGGG  TTGAGTGTTG
```

M13mp18 template and the priming site. Base number one in this sequence is the base number 6292 from the first A in the unique HpaI site (GTTAAC) found in the wild type M13. Throughout this thesis, only one termination DNA samples were used.

1.2.1.1.1 Protocol 1. Two-Step Protocol

Single stranded DNA sequencing sample can be generated using a two-step protocol (Figure 1.8) [16,17]. We used M13mp18 as a template (the piece of DNA to be sequenced) to generate a single terminated sample of known sequence. This sample is used as a standard for the study in this thesis. A primer is added to a solution of template. Primers are short pieces of DNA of known sequence that are complementary to one part of the template. In our case, we used a ROX labeled universal primer. In step one, the primers anneal to the templates. This means that the templates and the primers are now bound by hydrogen bonds between the complementary bases. In the second step, the annealed primers are extended at their 3'-end by T7 DNA polymerase (Sequenase) in the presence of the four dNTPs and terminated using one of the ddNTP. The polymerase adds bases at the 3'-end of the primers according to the complementary rule. Because the solution also contains one ddNTP sometimes the polymerase will incorporate a ddNTP. The extension will then stop because ddNTPs do not have a 3'- hydroxyl end. To obtain a DNA sequencing sample, four reactions are carried out using the four ddNTPs, and then the final solutions are mixed together before electrophoresis. In this thesis, only one ddNTP was used at a time to generate a quarter of the sequence because we are interested in using the sample only as a standard. Also, because we are interested in studying the effects of different parameters on the separation of DNA by capillary electrophoresis, it is important to be able to resolve the longest fragments.

The advantage of using the two-step protocol with Sequenase for capillary electrophoresis is that although the peak heights decrease exponentially with the fragment

Figure 1.8 Two-step protocol for DNA sequencing.

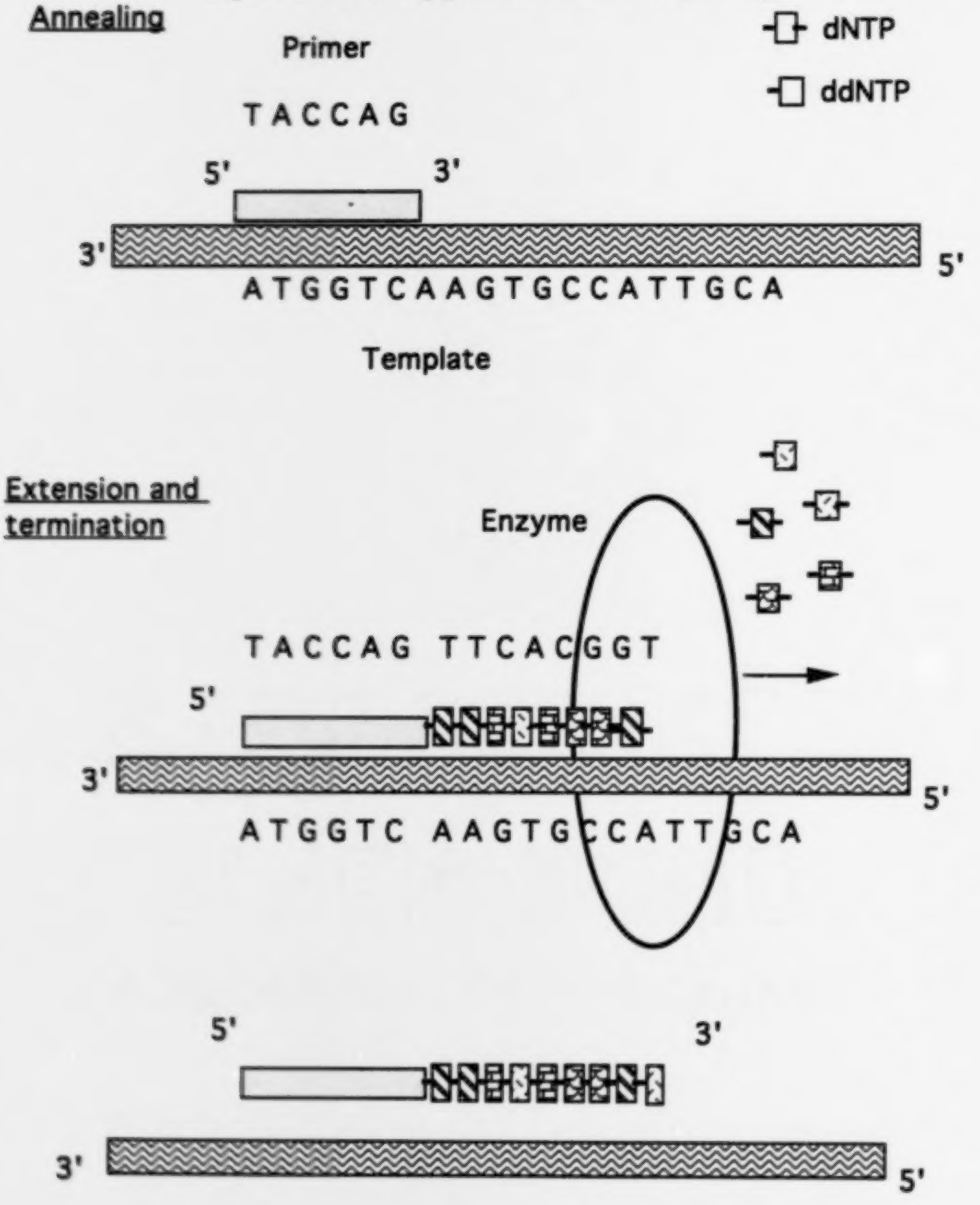
Annealing
Primer
dNTP
ddNTP
TACCAG
5'
3'
3'
5'
ATGGTCAAGTGCCATTGCA
Template
Extension and termination
Enzyme
TACCAG TTCACGGT
5'
3'
5'
ATGGTC AAGTGCCATTGCA
5'
3'
3'
5'

lengths, the peak heights are uniform for similar fragment lengths. This protocol needs a relatively large amount of template and primer. Most of the primer is not used for sequencing and generates an intense peak. This protocol has been widely used for DNA sequencing by capillary gel electrophoresis[8,18-26].

1.2.1.1.2 Protocol 2. Cycle Sequencing

In the case of protocol 1, only the primers annealed to the templates are elongated and the rest of the primers are not used. Thus, only a small amount of sample is generated. It is possible to modify protocol 1 in order to obtain more sample by repeating the protocol many times[17]. This process is done by using a thermostable enzyme to extend the primers. The first and second steps of protocol 2 (Figure 1.9) are similar to the two first steps of protocol 1 except that the enzyme is different. Then, in a third step, the temperature of the solution is raised to 95°C, which causes the DNA fragments to separate from the templates. Because the templates are now free of any other DNA, it is possible to re-anneal some primers and do the cycle again. In our experiment, the three steps were cycled 30 times.

1.2.1.2 Restriction Fragment

Double-stranded DNA can be cut by restriction endonucleases. These enzymes cut DNA at specific recognition sequences, and generate different sizes of DNA fragments. Some restriction endonucleases cut exactly in the middle of the recognition sequence, resulting in blunt end fragments. Other restriction endonucleases cut asymmetrically at the recognition sequence, resulting in overhangs at the ends (sticky ends) of the fragments. Table 1.1 gives the recognition sequence for some restriction enzymes. Cutting DNA with restriction enzymes is used in recombinant DNA technology for generating DNA fragments to be inserted in a vector. In this thesis, we used DNA standards (commercially available) already cut as well as home made restriction fragments.

Figure 1.9 Cycle sequencing.

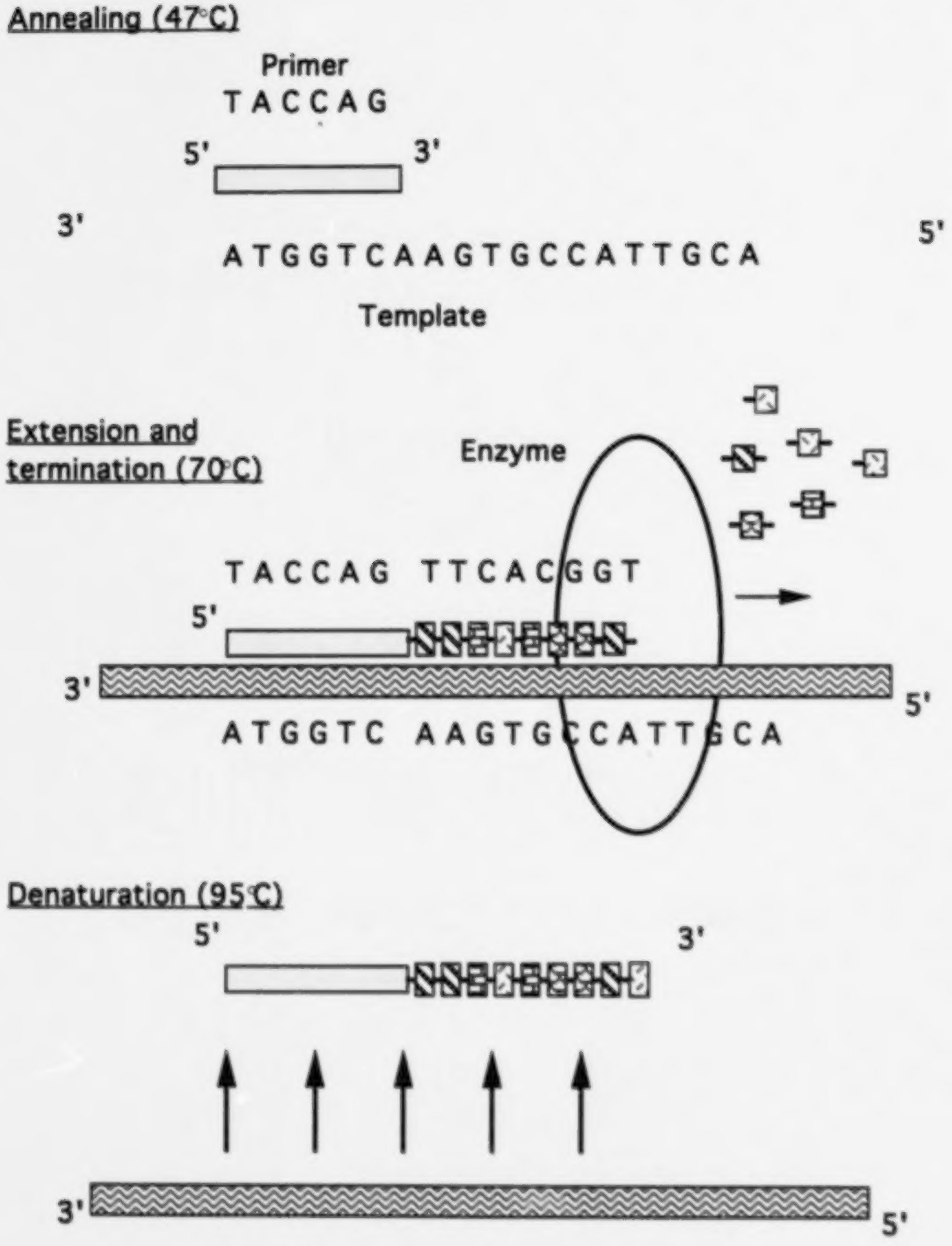
Annealing (47°C)
Primer
TACCAG
5'
3'
3'
ATGGTCAAGTGCCATTGCA
5'
Template
Extension and termination (70°C)
Enzyme
TACCAG TTCACGGT
5'
3'
5'
ATGGTC AAGTGCCATTGCA
Denaturation (95°C)
5'
3'
3'
5'

Table 1.1 Some restriction endonucleases and their recognition sequence.

Enzyme	Recognition sequence	Type of end
EcoRI	GAATTC	Sticky
HaeIII	GGCC	Blunt
HindIII	AAGCTT	Sticky
TaqI	TCGA	Sticky

1.3 Electrophoresis

The migration of electrically charged particles in solution due to an electric field is called electrophoresis. Electrophoresis is a descendant of the work of Faraday[27,28]. The introduction of his laws of electrolysis in 1791 started generations of work on electrolytic techniques. In 1807, Reuss did the initial observation of electroosmosis. Helmholtz worked on electroosmosis and electrophoresis. He concluded that electricity was divided into definite elementary portions, called "atom" of electricity (electron)[29]. The first measurement of transport numbers of ions and conductivity was done by Hittorf in 1858. His work clarified how the ions contribute to the passage of electricity in solution. Kohlrauch[30] worked on ion migration and moving boundaries. He showed that the conductivity of a solution is composed of separate contributions from each ion[29]. In 1903, Arrhenius won the Nobel prize for his dissociation theory of ions. This work was one of the major precursors of the evolution of electrophoresis. Then, in the 1930's, Tiselius[31,32] published the mobilities of proteins and built the first apparatus for moving boundary electrophoresis. In 1948, Tiselius won the Nobel Prize for his work on the moving boundary method. The 1950's and 1960's saw the introduction of electrophoresis in gels: in 1955, Smithies published his work on the electrophoresis of protein in starch; in 1959 Raymond and Weintraub reported electrophoresis of proteins in polyacrylamide gel and in 1961 Hjertén reported electrophoresis in agarose gel. Finally, in 1967 Hjertén[33] introduced the technique of capillary electrophoresis.

In classical free solution electrophoresis, two electrodes are introduced in a solution and an electric field is applied. The resolution obtained by this technique is poor due to joule heating which creates convection in the solution and causes band broadening. To eliminate this problem Hjertén[33] proposed two solutions:

"There are at least two obvious alternative approaches to the problem of eliminating convection in free solution. One alternative involves the use of a cell of very narrow cross-

section ...In the other alternative, the convective movement of a liquid element is not suppressed, but is instead directed into a periodic orbit."

In his paper, Hjertén reported the use of the second method because the ultrasensitive detectors needed to use very narrow cross-section cells were not available. Since then, ultrasensitive detection techniques have been introduced. In fact, the technique used by Hjertén has been replaced by capillary electrophoresis. The convection is reduced by efficient elimination of the heat through the glass wall and the high ratio of glass surface to the separation medium's volume.

Many capillary electrophoresis techniques have been used in the past years[34]. In this thesis, capillary zone electrophoresis(CZE) and capillary gel electrophoresis(CGE) have been used.

1.3.1 Theoretical Aspects

Capillary electrophoresis (CE) can be described as any separation of analytes done in a capillary tube and driven by the presence of charges on the analytes or other molecules. In this technique, an electric field is applied between the two ends of a capillary (Figure 1.10). One end is kept at high voltage in a PLEXIGLAS box(dashed box) and the other end is kept at ground potential. Detection is usually done near the ground end using on-column or post-column detectors.

All capillary electrophoretic methods involve electrophoresis, and some involve electroosmosis. Any charged particles will move in its surrounding electrolyte when subjected to an electric field. If the inside wall of the capillary is not charged, only electrophoresis will occur. The migration velocity of an ion is[35]

$$v_e = \frac{\mu_e V}{L} = \mu_e E \qquad (1.1)$$

Figure 1.10 General set-up for capillary electrophoresis.

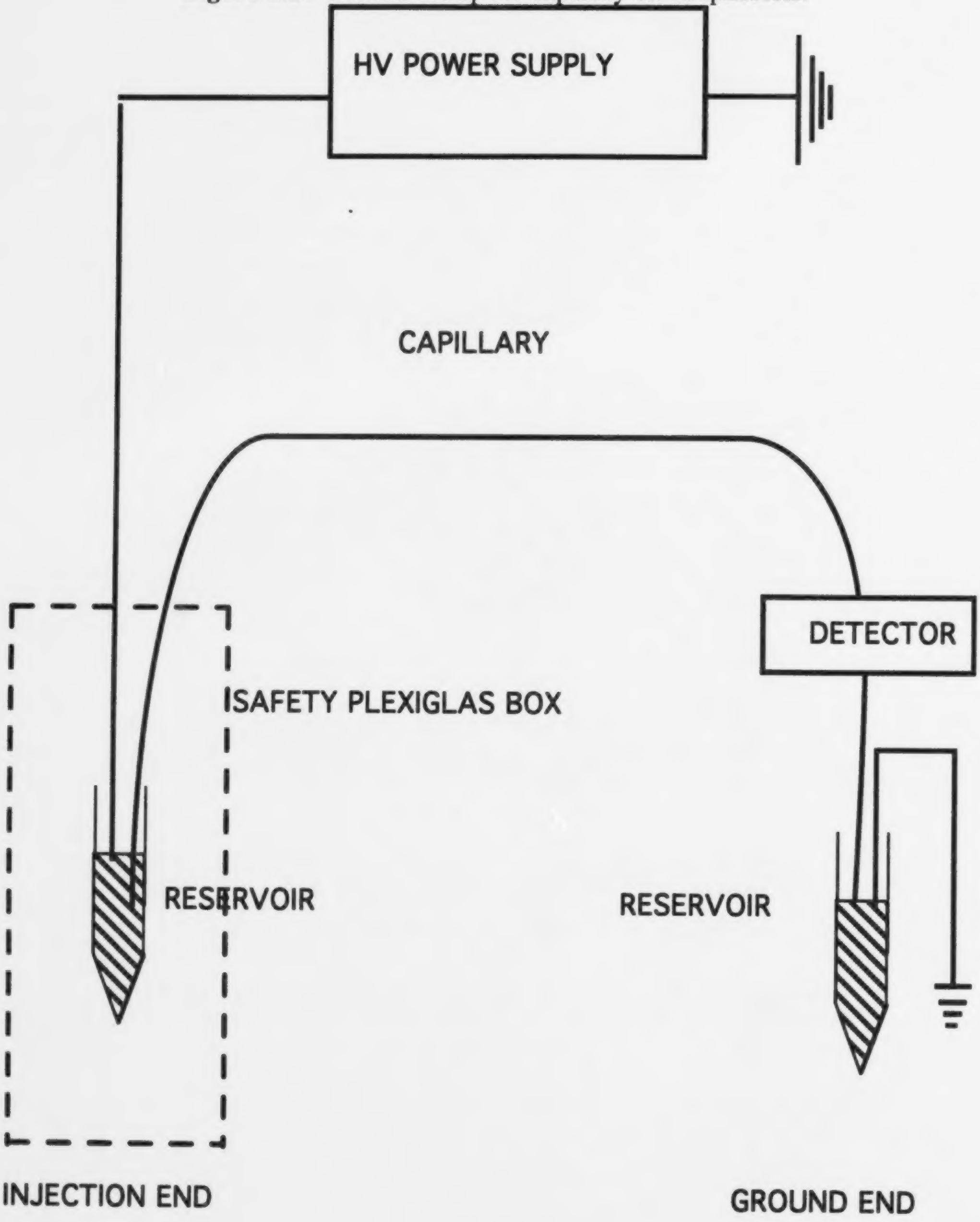
HV POWER SUPPLY
CAPILLARY
DETECTOR
SAFETY PLEXIGLAS BOX
RESERVOIR
RESERVOIR
INJECTION END
GROUND END

where v_e is the electrophoretic velocity, μ_e is the electrophoretic mobility, V is the applied voltage, L is the length of the capillary, and E is the average electric field. This equation assumes that the electric field is constant throughout the capillary. When the electric field is far from being constant this equation will fail to describe the mobility.

Electroosmosis[36] is the flow of a liquid caused by the creation of an electric field at the thin interface between the silica surface and the separation medium. In the case of a fused silica capillary, the inside wall contains some silanol groups. These silanol groups deprotonate in neutral to alkaline medium, resulting in a negatively charged stationary surface. Cations from the medium move to this surface in order to counter the negative charges and to create an ionic atmosphere (Figure 1.11) . A compromise between electrostatic attraction and diffusion creates a thin double layer. The ionic atmosphere is composed of two regions: the Stern-Helmholz layer and the Gouy-Chapman layer[37]. The Stern-Helmholz layer is close to the wall surface and is formed of adsorbed cations that are essentially fixed. This layer is not involved in the electrokinetic process. Away from the capillary wall is the Gouy-Chapman layer, which is a diffused layer of cations in constant equilibrium with the rest of the solution. The charge density of excess ions decreases exponentially in the Gouy-Chapman layer(ionic atmosphere). The thickness of this double layer is in the range of 1 to 10 nm[38]. During capillary electrophoresis, an electric field is applied tangentially to the double layer along the axis of the capillary. This electric field forces the excess cations in the ionic atmosphere to move parallel to the wall. The solvent molecules immediately in contact with the surface experience a force toward the negative electrode. An equilibrium is obtained between the electric forces and the viscous forces, which results in a solution flow. The velocity of the solution (electroosmotic velocity, v_o) is proportional to the electric field and inversely proportional to the viscosity of the medium according to equation 1.2. The velocity of the solution is zero at the wall, and increases within the ionic atmosphere to finally reach v_o at some distance (1-10nm) away from the wall.

Figure 1.11 Double layer at the capillary surface.

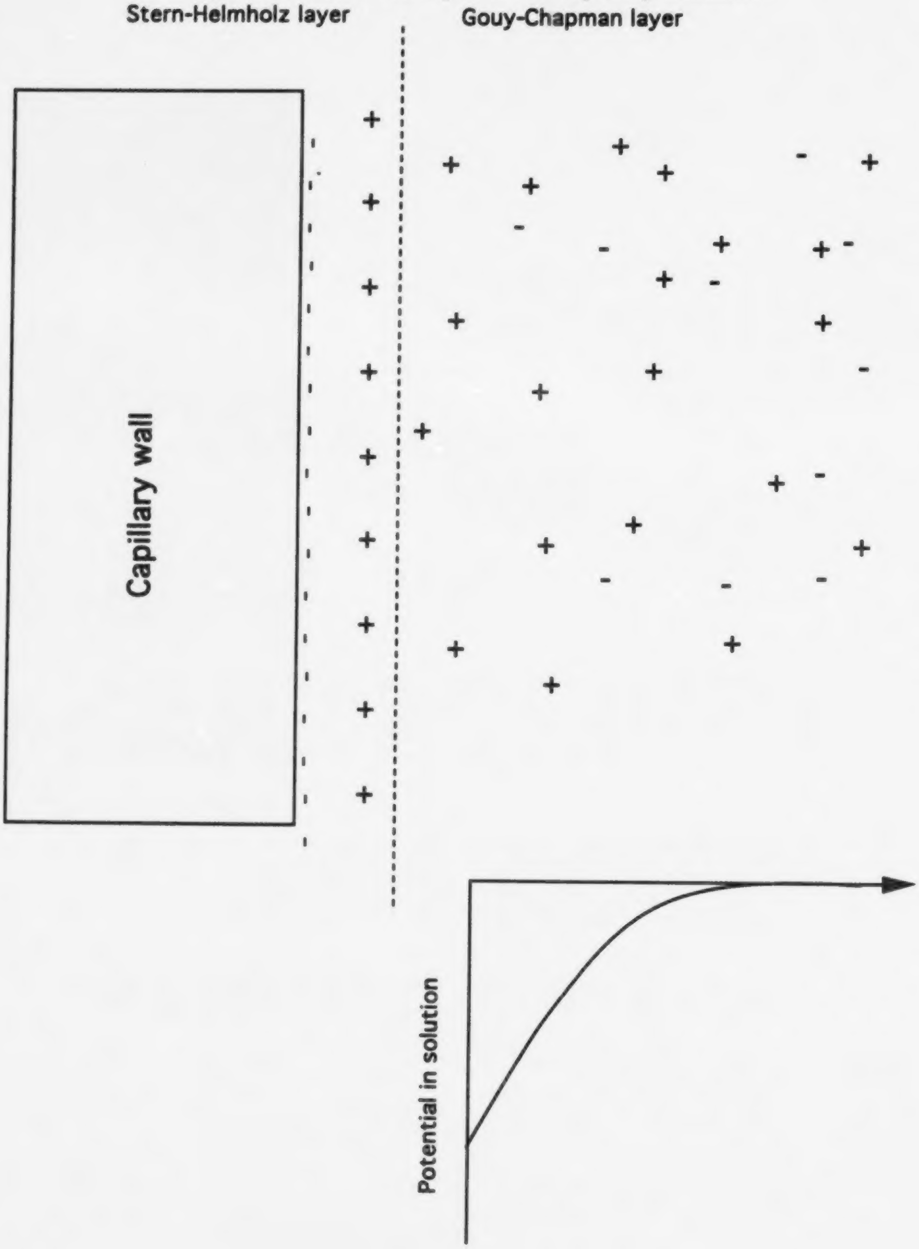
Stern-Helmholz layer
Gouy-Chapman layer
Capillary wall
Potential in solution

$$v_o = \frac{\mu_o V}{L} = \mu_o E = \frac{\varepsilon \varepsilon_0 \zeta}{\eta} E \qquad (1.2)$$

where μ_o is the electroosmotic mobility, ε is the dielectric constant of the medium, ε_0 is the permitivity of vacuum, ζ is the wall zeta-potential, and η is the viscosity of the medium. The zeta-potential is the electric potential at the plane of shear. A few papers have been published on how to control electroosmosis[39-47] by applying an electric field perpendicular to the capillary. The electroosmosis can also be modified by changing the number of silanol groups, which decreases the zeta-potential, and/or by increasing the viscosity of the medium.

The electrophoretic and the electroosmotic velocities are not orthogonal, thus they add to give the total velocity (v).

$$v = v_e + v_o = \frac{(\mu_e + \mu_o) V}{L} = (\mu_e + \mu_o) E \qquad (1.3)$$

The migration time(t_m) is the distance to reach the detector divided by the velocity. Thus, a faster separation can be achieved with good resolution if the electric field is high and the length of the capillary is short.

$$t_m = \frac{L}{v} = \frac{L^2}{V (\mu_e + \mu_o)} = \frac{L}{E (\mu_e + \mu_o)} \qquad (1.4)$$

In the rate theory of column band broadening, the plate height (H) is related to the number of theoretical plates (N_p) and is also related to the peak variance (σ^2) by equation 1.5:

$$\overline{H} = \frac{L}{N_p} = \frac{\sigma^2}{L} \qquad (1.5)$$

Thus, the number of theoretical plates is related to the variance of the peak and to the inverse of the length[48]. Peak broadening in capillary electrophoresis is affected by diffusion (σ_D^2), convection (σ_C^2), Joule heating (σ_J^2), adsorption (σ_A^2), conductivity difference (σ_{cond}^2), and pH difference (σ_{pH}^2). There is also an injection effect (σ_{inj}^2) and a detection effect (σ_{det}^2) on the peak width. Those variances contribute to the total variance according to equation 1.6.

$$\sigma^2 = \sigma_D^2 + \sigma_C^2 + \sigma_J^2 + \sigma_A^2 + \sigma_{cond}^2 + \sigma_{pH}^2 + \sigma_{inj}^2 + \sigma_{det}^2 \tag{1.6}$$

In the case of the separation of proteins, the adsorption variance can become quite important because the positively charged proteins are adsorbed onto the capillary wall. When large diameter capillaries, or high conductivity buffers are used, the convection and the Joule heating variances can be a problem[49]. When the sample is injected from a different buffer than the running buffer, the conductivity variance can become important. If, however, the experiment is done properly, σ_D^2 is the major factor affecting the total migration time variance(σ_t^2) and thus $\sigma_t^2 \approx \sigma_D^2$. The σ_D^2 is related to the migration time through the Stoke-Einstein equation:

$$\sigma_t^2 \approx \sigma_D^2 = 2\,D\,t_m \tag{1.7}$$

where D is the diffusion coefficient. An expression for the number of theoretical plates[35] can be obtained by combining equations 1.4, 1.5, and 1.7.

$$N_p = \frac{L^2}{\sigma_t^2} \approx \frac{L^2}{2\,D\,t_m} = \frac{L^2}{2\,D\left(\dfrac{L^2}{(\mu_e + \mu_o)\,V}\right)} = \frac{(\mu_e + \mu_o)\,V}{2\,D} \tag{1.8}$$

The previous equation indicates that the number of theoretical plates is related to the applied voltage and to the total mobility. Thus, the number of theoretical plates can be increased by increasing the voltage, or by increasing the total mobility. Increasing the total mobility is not easy to do. The electrophoretic mobility can be increased by decreasing the solution viscosity, or by increasing the mass to charge ratio. As stated previously, the electroosmotic mobility can be increased by reducing the viscosity of the solution, or by increasing the number of silanol groups. Another way of increasing the number of theoretical plates is to decrease the diffusion coefficient, which is easily done by using a more viscous medium for the separation; however, using a more viscous medium will change the electroosmotic mobility because it is related to the viscosity of the medium through equation 1.2. Equation 1.8 also indicates that the number of theoretical plates is not related to the length of the capillary. In practice, the length of the capillary influences the number of theoretical plates because the contributions from other band broadening factors are not always zero.

The number of theoretical plates is usually calculated from the width of the peak and the migration time. If we assume that the peak is of a Gaussian shape (i.e. only diffusion broadening), the peak width and the migration time can be obtained by fitting a Gaussian curve to the data using equation 1.9. The assumption that the peak is of a Gaussian shape is only valid when the peak width is smaller than the migration time. Equation 1.9 was used within this limit.

$$\text{signal} = A_0 + A_1 \exp\left(-\left[\frac{(t - t_m)}{A_2}\right]^2\right) \qquad (1.9)$$

where A_o is the baseline, A_1 is the peak height, A_2 is equal to $(2^{0.5}\sigma)$, and t is the time. From the results of the fitting, the number of theoretical plates can be calculated according to equation 1.10:

$$N_p = \left(\frac{t_m}{\sigma_t}\right)^2 = 2\left(\frac{t_m}{A_2}\right)^2 \qquad (1.10)$$

The number of theoretical plates does not indicate if the separation is achieved. Another parameter used to indicate the efficiency of the separation is the resolution. The resolution (R) between two peaks i and j is defined as:

$$R = 2\,\frac{(t_{m,j} - t_{m,i})}{(W_j + W_i)} \qquad (1.11)$$

where $t_{m,j}$ and $t_{m,i}$ are the migration times for the two peaks and W_j and W_i are the baseline peak widths (4σ). The two peaks can be fitted with a Gaussian function and the resolution calculated using equation 1.12:

$$R = \frac{\Delta t_{sub}}{2.83\,\overline{A_2}} \qquad (1.12)$$

where Δt_{sub} is the difference in migration time between the two subsequent peaks, and $\overline{A_2}$ is the average of $A_{2,j}$ and $A_{2,i}$. The resolution is also related to the number of theoretical plates according to equation 1.13:

$$R = 0.25\,\frac{\Delta\mu_e}{\overline{\mu_e} + \mu_o}\sqrt{N_p} = 0.18\,\frac{\Delta\mu_e}{(\overline{\mu_e} + \mu_o)^{0.5}}\sqrt{\frac{V}{\overline{D}}} \qquad (1.13)$$

where $\Delta\mu_e$ is the difference in electrophoretic mobility between two peaks, $\overline{\mu_e}$ is the average electrophoretic mobility, and $\overline{D}$ is the average diffusion coefficient. This equation indicates that in order to double the resolution, the voltage has to quadruple. This is only true if μ_e, μ_o, and $\overline{D}$ are independent of voltage, that is not always the case (e.g. see section 1.3.2.4). The increase in voltage is limited by Joule heating in the capillary.

Capillary zone electrophoresis fails to separate compounds with similar mass-to-charge ratios. We are interested in the separation of dsDNA and ssDNA, thus capillary gel electrophoresis is used instead of open tube capillary electrophoresis; however, the theoretical aspect can be extended to capillary gel electrophoresis.

1.3.2 Capillary Gel Electrophoresis

One way of separating compounds of similar mass-to-charge ratios, like DNA fragments, is to introduce a sieving medium in the capillary. Although this technique is called capillary gel electrophoresis, matrices other than gel are also included in this technique. Gels and entangled solutions are used as separation media.

The motion of a DNA molecule in an electric field can be described by Newton's law[50]:

$$m \frac{d^2x}{dt^2} = F_e - F_f \tag{1.14}$$

where m is the mass of the DNA fragment, x is the position, t is the time, F_e is the electric force, and F_f is the friction force. In steady state, the electric force is counter-balanced by the friction force ($F_e = F_f$).

$$Q\,E = f \frac{dx}{dt} \tag{1.15}$$

where Q is the charge of the analyte, E is the electric field, f is the friction coefficient, and $\frac{dx}{dt}$ is the analyte velocity. The steady state velocity (v) is given by:

$$v = \frac{dx}{dt} = \frac{Q\,E}{f} = \mu\,E \tag{1.16}$$

Q is linearly related to the DNA fragment length. Gels are structured separation media. This means that the relation between f, the DNA fragment length, and the properties of the gel is not simple. Depending on the conformation of the DNA fragment, the relation between f and the fragment length changes. Thus, it is not obvious how μ is going to change with the fragment length. Different models have been proposed to explain the changes in μ with the fragment length (see section 1.3.2.4).

DNA fragments do not separate by CZE because the mobility is only slightly dependent on the DNA fragment size. The separation gel provides a structured environment which allows separation of DNA fragments according to their size. Another advantage of using a sieving medium is that electroosmosis is negligible in high viscosity media.

Gel electrophoresis on gelatin and agar has been used for about 100 years[27,28]. Only in the mid 1950's did the interest for gel electrophoresis increase. Starch[51], agarose[52], and Polyacrylamide[53] are used for slab gel electrophoresis. Agarose and polyacrylamide have been transferred to capillary electrophoresis. In the last few years, many other polymers have been proposed for the separation of different analytes; however, agarose[54,55], polyacrylamide[55], and cellulose derivatives have been consistently used. In this work, polyacrylamide and a cellulose derivative were used for the separation of DNA.

1.3.2.1 Sieving Medium and Capillary Wall Treatment

1.3.2.1.1 Polyacrylamide

Polyacrylamide[56,57] is a general name for many different polymers based on acrylamide. Polyacrylamide is obtained by the polymerization of an acrylamide with or without a crosslinker. Acrylamide ($H_2C{=}CHCONH_2$, 2-propenamide) is a white, crystalline solid. It was first prepared in 1893 from acryloyl chloride and ammonia. Acrylamide was commercially produced in 1954 from acrylonitrile.

$$CH_2{=}CHCN + H_2SO_4{\cdot}H_2O \rightarrow CH_2{=}CHCONH_2{\cdot}H_2SO_4 \text{ (1 hour at 90-100 °C)} \quad (1.17)$$

Acrylamide exhibits high solubility in water, has good thermal stability, and a good shelf life; however, if heated above its melting point (84.5 °C) acrylamide can undergo a vigorous polymerization reaction. The amide group and the electron deficient double bond are the two reactive centers of acrylamide. Acrylamide is usually polymerized in solution using the free-radical polymerization method. Many different sources of free radicals can be used including[56,57]: peroxides, persulfates, redox couples, ultrasonic energy, UV light, and ionization energy. Righetti *et al.*[58,59] have studied different sources of radicals for the polymerization of acrylamide. In our case, a redox couple made of ammonium persulfate and TEMED (N,N,N',N'-tetramethylethylene-diamine) was used. The polymerization of acrylamide[60] with ammonium persulfate and TEMED is described in Figure 1.12.

Two types of polyacrylamide are of interest for electrophoresis (Figure 1.13). The first one is the cross-linked polyacrylamide. It is a gel obtained by the copolymerization of acrylamide and a cross-linking agent. The result is a three dimensional cross-linked gel. Righetti *et al.*[61-64] have studied the polymerization of different acrylamido monomers and cross-linking agents. The one most commonly used for electrophoresis is N,N'-methylenebisacrylamide. Capillary electrophoresis with cross-linked polyacrylamide has been used to obtain high resolution separation of short DNA sequencing fragments. In the last few years, a second type of polyacrylamide has been used for capillary electrophoresis. It is called linear polyacrylamide and is obtained by polymerization of acrylamide on its own. In both cases, the kinetic properties of the polymerization depend on the initial concentrations of the monomers, of ammonium persulfate and of TEMED, the presence of different buffer systems, the presence of denaturing agents (such as formamide or urea), the presence of terminators, the presence of oxygen, the temperature, and the pressure[58,59,63-72].

1.3.2.1.2 Cellulose Derivatives

Cellulose[73,74] is one of the most abundant polymers on earth. Its chain like structure is formed of 1,4–β-D linked polyanhydro glucopyranose (Figure 1.14). The intramolecular hydrogen bonds in cellulose cause the molecule to be stiff and rigid. The intermolecular hydrogen bonds cause the molecules to organize themselves in a parallel arrangement called fibers. Cellulose fibers are not soluble in water, thus, to be useful for

Figure 1.12 Polymerization of acrylamide.

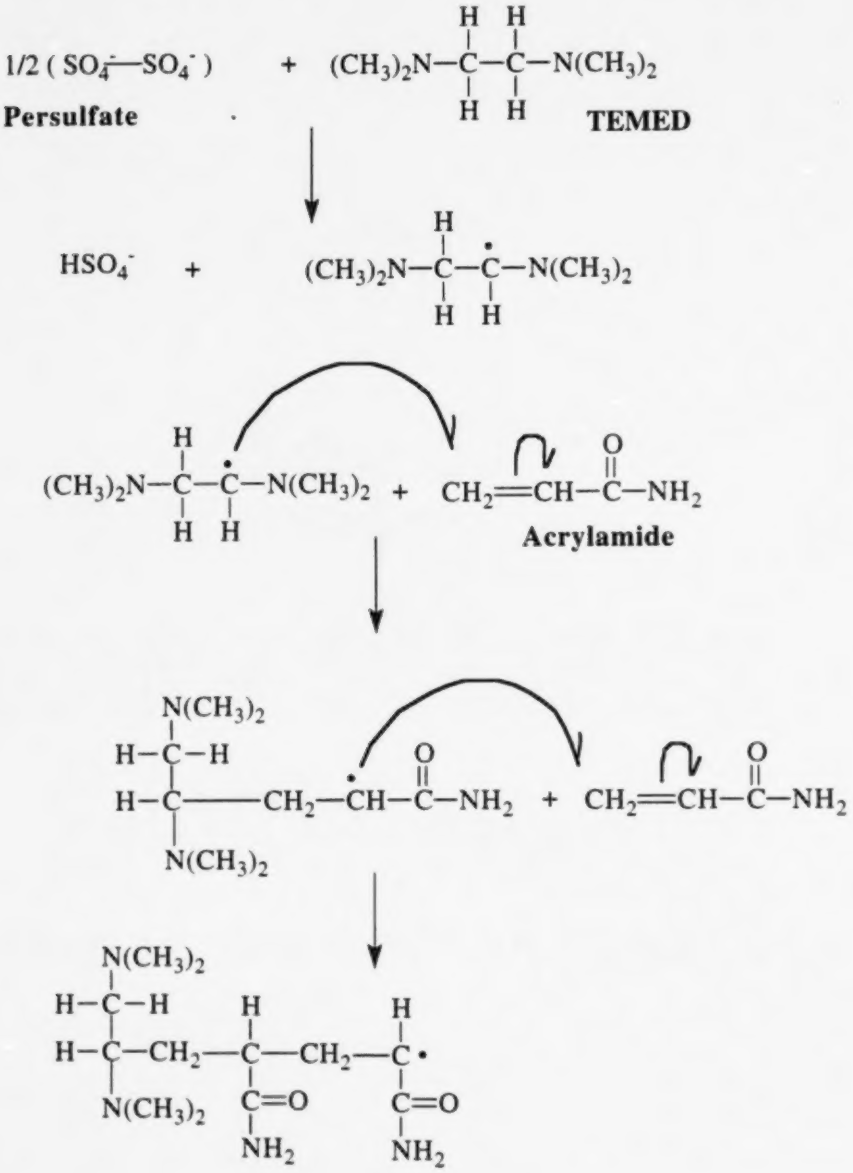
1/2 (SO4⁻—SO4⁻)
+
(CH3)2N—C—C—N(CH3)2
Persulfate
TEMED
HSO4⁻
+
(CH3)2N—C—C—N(CH3)2
(CH3)2N—C—C—N(CH3)2 + CH2═CH—C—NH2
Acrylamide
CH2—CH—C—NH2 + CH2═CH—C—NH2

Figure 1.13 Different forms of polyacrylamide.

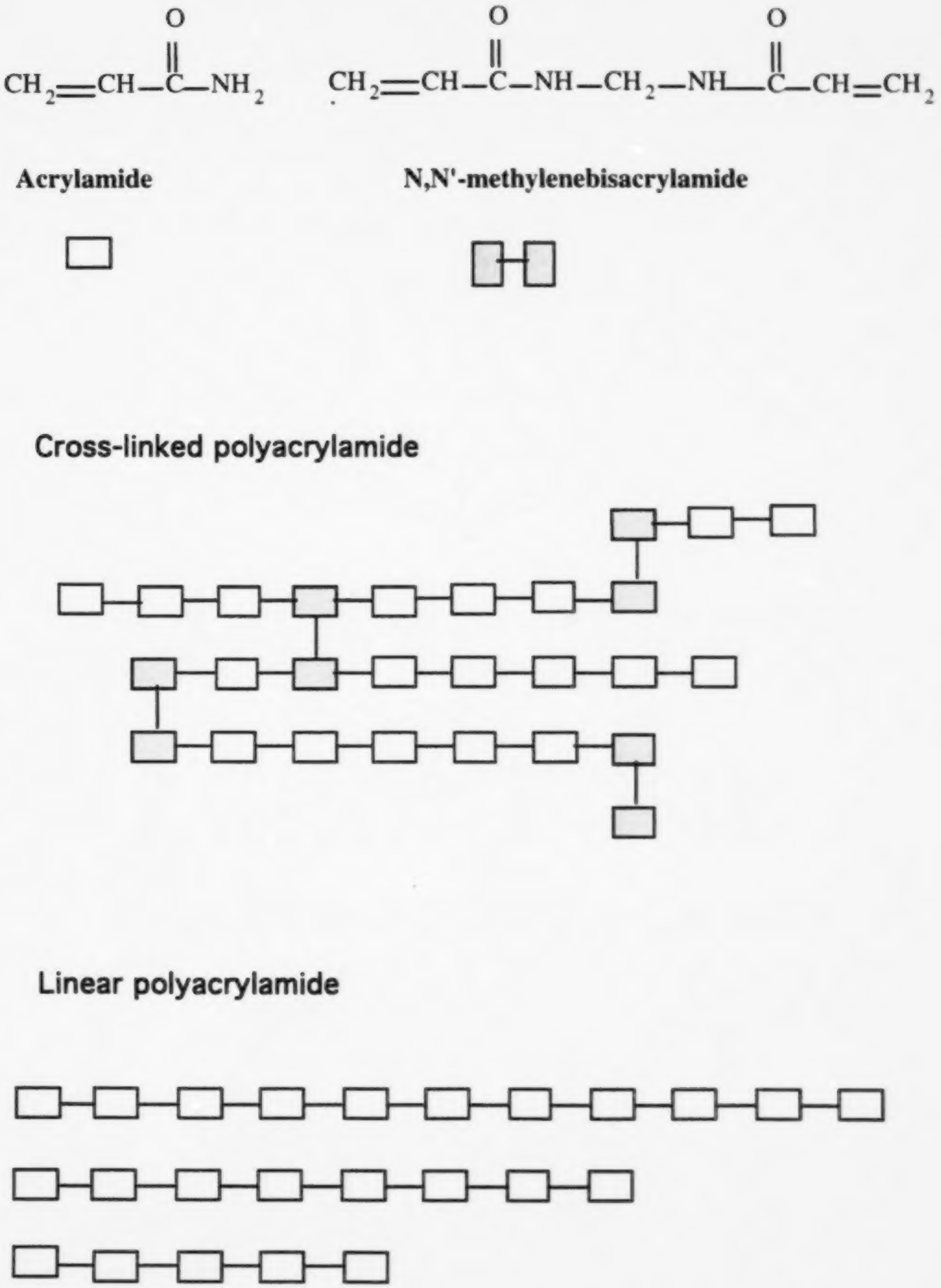

$$CH_2{=}CH{-}\overset{\overset{O}{\|}}{C}{-}NH_2$$

$$CH_2{=}CH{-}\overset{\overset{O}{\|}}{C}{-}NH{-}CH_2{-}NH{-}\overset{\overset{O}{\|}}{C}{-}CH{=}CH_2$$

Acrylamide
N,N'-methylenebisacrylamide
Cross-linked polyacrylamide
Linear polyacrylamide

Figure 1.14 Constitution and conformation of a cellulose molecule.

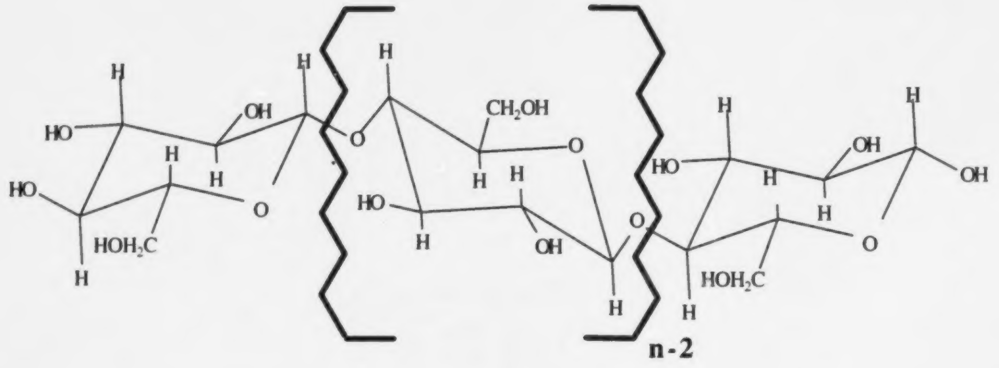

Figure 1.15 Cellulose derivatives used in capillary electrophoresis.

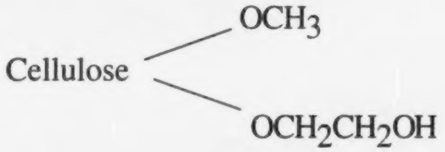

$$\text{Cellulose}\begin{cases}OCH_3\\ OCH_2CH_2OH\end{cases}$$

HMEC

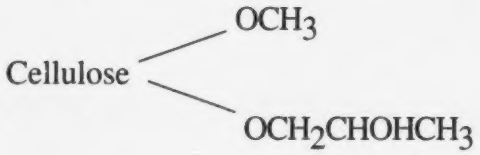

$$\text{Cellulose}\begin{cases}OCH_3\\ OCH_2CHOHCH_3\end{cases}$$

HPMC

Cellulose ——OCH_2CH_2OH

HEC

capillary electrophoresis, cellulose has to be derivatized to make it soluble. Only a few derivatives of cellulose are used in capillary electrophoresis: hydroxyethylcellulose (HEC), hydroxymethylethylcellulose (HMEC), and hydroxypropylmethylcellulose (HPMC), Figure 1.15. These three derivatives are non-ionic, and thus, not affected by electrophoresis.

HPMC was selected to perform electrophoresis in our experiment. It is commercially available as a white powder. The powder is dissolved in water to the appropriate viscosity. Different viscosities (molecular size ranges) are available. The one used in our experiment is quoted as 4000 cp (centiPoise) at 2% (W/V) of HPMC in water. Most of our experiments were done at a lower viscosity by diluting a main 2% solution of HPMC to 0.4% solution.

HPMC, as linear polyacrylamide, does not form a gel when dissolved in water. Over a certain concentration threshold of HPMC, the interactions between polymer molecules, force them to form a mesh-like structure[75]. The solution of mesh-like structure is called an entangled solution. The advantages of an entangle solution compared to the rigid cross-linked gel is that good resolution can be obtained for the separation of dsDNA using a low viscosity medium and a short experimental time.

1.3.2.1.3 Preparation of Coated Capillaries

Electroosmosis destroys the separation efficiency in capillary gel electrophoresis. The electroosmotic force can be so strong as to expel part of the polymer from the capillary when a low viscosity polymer is used. In order to reduce the electroosmotic force, the inside wall of the capillary can be coated. In our experiment, a silanizing agent was attached (γ-methacryloxypropyl trimethoxysilane) to the silanol group (Si-O$^-$) on the inside wall, which reacts with acrylamide as demonstrated in Figure 1.16. In the case of polyacrylamide filled capillaries, the coating was done at the same time as the polymerization of the acrylamide of interest inside the capillary. In the case of cellulose,

Figure 1.16 Coating of the inside wall of a capillary with acrylamide.

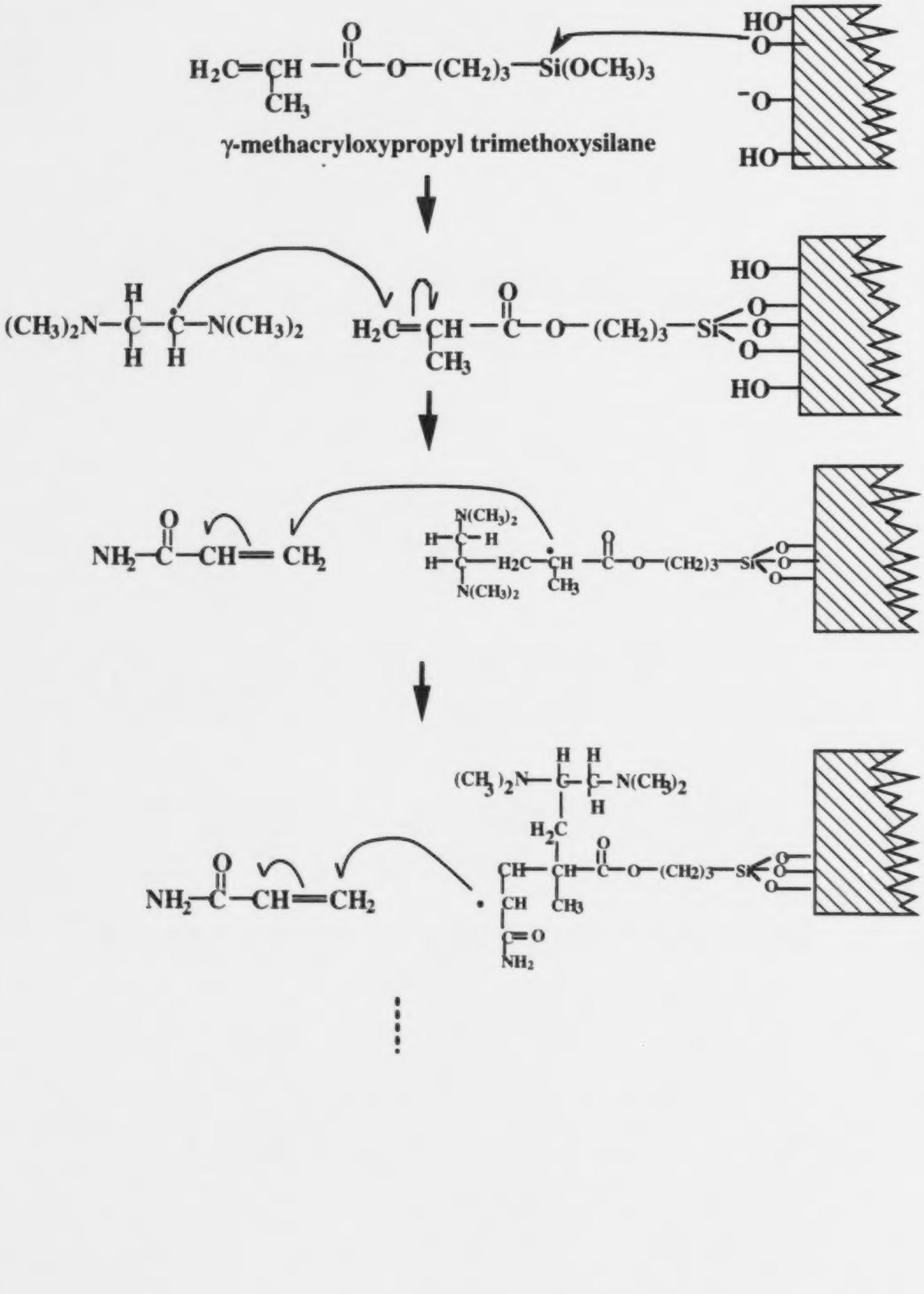
γ-methacryloxypropyl trimethoxysilane
$H_2C{=}C(CH_3)H{-}C(=O){-}O{-}(CH_2)_3{-}Si(OCH_3)_3$
HO
O
$^-$O
HO
$(CH_3)_2N{-}CH_2{-}\dot{C}H{-}N(CH_3)_2$
$NH_2{-}C(=O){-}CH{=}CH_2$

the silanizing agent ,attached to the wall, was first reacted with acrylamide to form a layer of polyacrylamide on the wall, then the cellulose was introduced in the capillary by pressure. Thus, the cellulose was not attached to the wall.

1.3.2.2 Difference in Transference Numbers

In capillary gel electrophoresis, a buffer system is used to maintain conductivity. In most of our experiments, 1xTBE (buffer made of TRIS, borate and EDTA) was used as buffer. The main charge carriers in 1xTBE are borate anions and TRIS cations. During electrophoresis, the borate migrates towards the anode, and the TRIS migrates towards the cathode. The fraction of current carried by any ion is called the transference number (T), and is given by equations 1.18 and 1.19 for a two ion system:

$$T_+ = \frac{\mu_+}{\mu_+ + \mu_-} \tag{1.18}$$

$$T_- = \frac{\mu_-}{\mu_+ + \mu_-} \tag{1.19}$$

where T_+ and T_- are the transference numbers of the cation and the anion, and μ_+ and μ_- are the mobilities of the cation and the anion.

The sum of the transference numbers for all the ions is one. Figure 1.17 shows an example of transference number using fictive mobility values. Let us say that in free solution, the cation has a mobility of 1 and the anion a mobility of 2. Thus the cation transports 1/3 of the current and the anion 2/3 of the current. Polyacrylamide is more structured than free solution and imposes different friction forces for different ion sizes. When the ions are in polyacrylamide the cation being bigger encounters more friction forces than in free solution and its mobility decreases to 0.5. The anion also encounters more friction forces than in free solution, but not as much as the cation because the anion is smaller. Thus, the anion mobility decreases to 1.5. In polyacrylamide the cation transports

Figure 1.17 Effect of different medium on the transference number of a cation and an anion.

In Solution

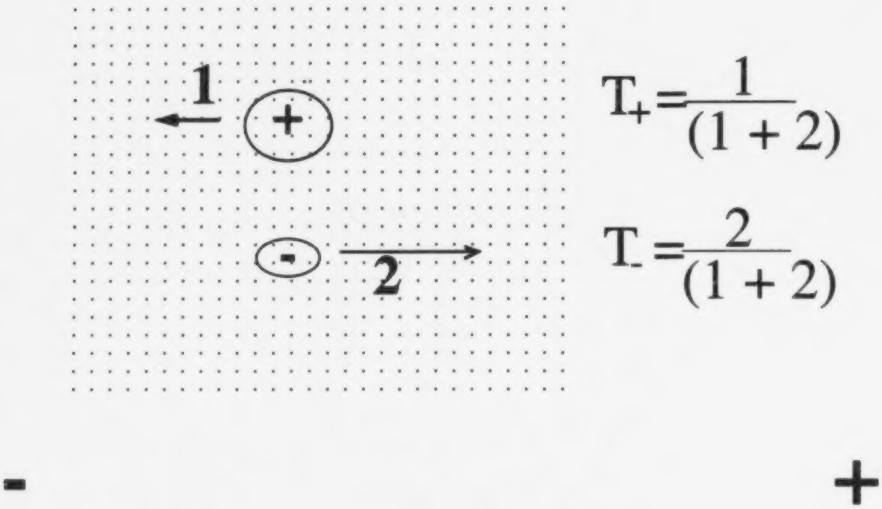

$$T_+ = \frac{1}{(1 + 2)}$$

$$T_- = \frac{2}{(1 + 2)}$$

In Polyacrylamide

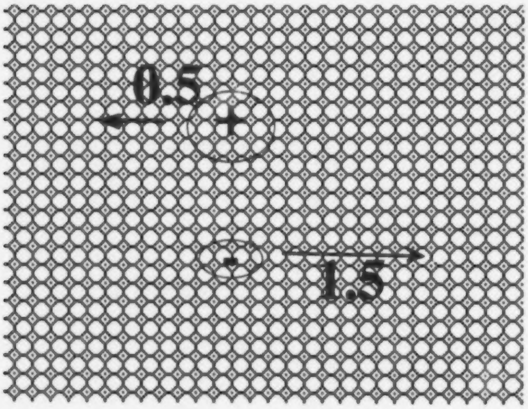

$$T_+ = \frac{0.5}{(0.5 + 1.5)}$$

$$T_- = \frac{1.5}{(0.5 + 1.5)}$$

1/4 of the current and the anion 3/4 of the current. The amount of current transported by the ions is different in solution(buffer reservoir) than in the polyacrylamide. The change in transference number at the capillary:reservoir interfaces produces a change in the concentration of ions at those interfaces[76-78]. At one end of the capillary the ionic concentration increases, and at the other end the ionic concentration decreases. The change in ionic concentration induces a change in the electric field. The electric field is lower through the high ionic concentration area and is higher through the area of low ionic concentration.

Figure 1.18 shows a cartoon of the change in ionic concentration happening at one end of the capillary. In this case, a depletion of ions is shown. At time T_0 the concentration of ions is uniform everywhere. Then, if 5 electrons flow in an outside circuit (not shown), the same amount of charge would have to cross a plane in the solution in order to keep the electroneutrality. The amount of charges carried by the ions will depend on their transference number. In this example, the transference number of the cation increases at the capillary:reservoir interface, and the inverse is true for the anion. After the five ions have crossed the boundaries (time T_1), the ionic composition is lower in the interface, but unchanged in the bulk of the capillary and the reservoir. Figure 1.19 shows the change in ionic composition for all the possible changes in transference number for a cation at the reservoir:capillary interfaces. T_r and T_C are the transference numbers of the cation in the buffer reservoirs and in polyacrylamide respectively. The curves were offset in order to be more visible. When T_r=T_C, no change in ionic composition is observed; when T_r>T_C, a decrease in the ionic concentration at the cathodic end, and an increase at the anodic end are produced; and finally, when T_r>T_C, the inverse is produced. The transference number can change with the ionic strength. The extended Kohlrausch equation relates the change in concentration in time with the transference number:

$$\left(\frac{\partial c}{\partial t}\right)_x = \frac{-i}{F}\frac{dT}{dc}\left(\frac{\partial c}{\partial x}\right)_t \qquad (1.20)$$

Figure 1.18 Cartoon of a change in ionic concentration at the capillary:reservoir interface induced by change in transference numbers. At time T_o the concentration of ions is uniform everywhere. Then, Five electrons flow in an outside circuit (not shown). At time T_1, the ionic composition is lower in the interface, but unchanged in the bulk of the capillary and the reservoir

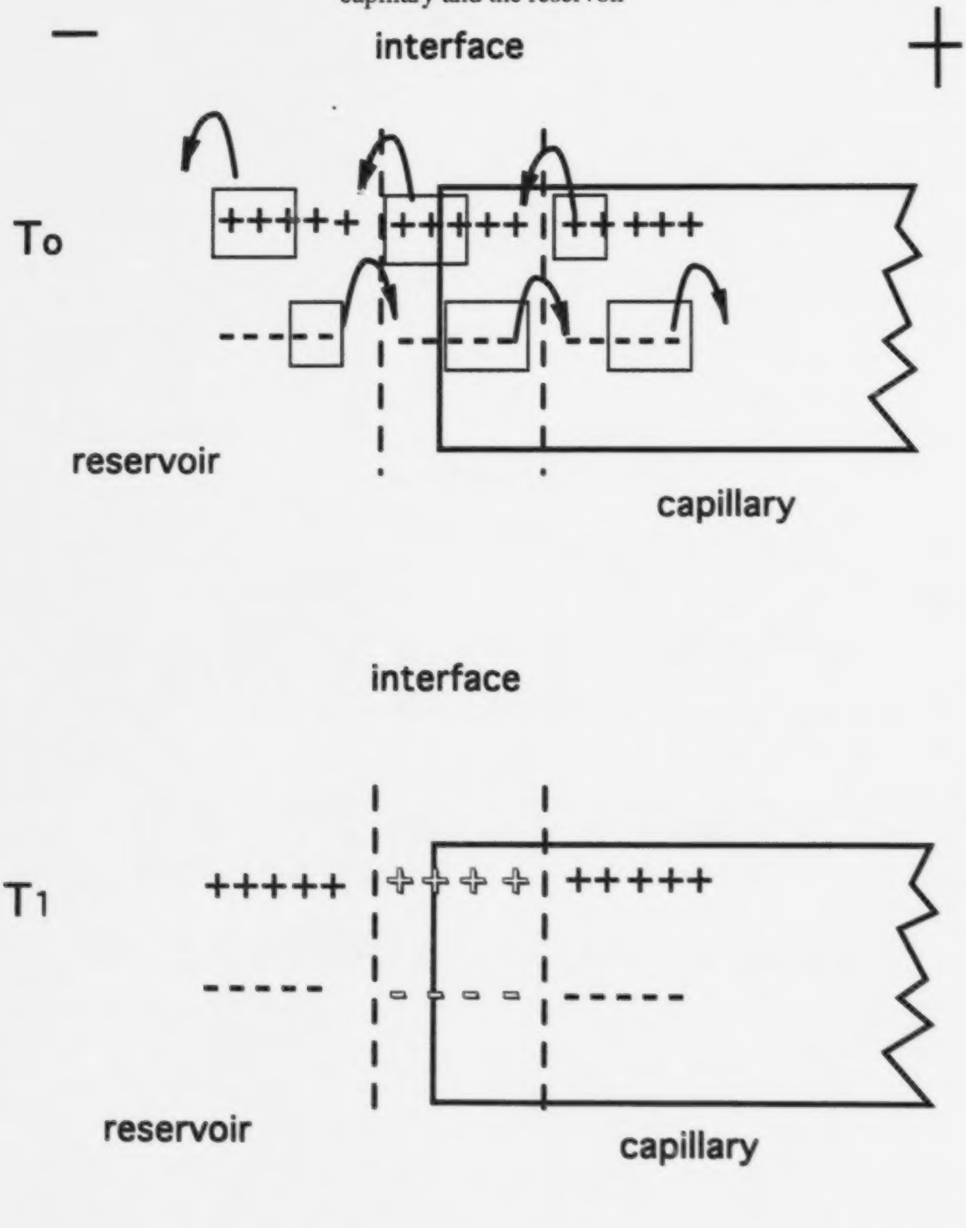
—
interface
+
To
+++++ +++++ +++++
----- ----- -----
reservoir
capillary
interface
T1
+++++ + + + + +++++
----- - - - - -----
reservoir
capillary

Figure 1.19 Change in ionic concentration for all possible changes in transference number at the reservoir:capillary interfaces.

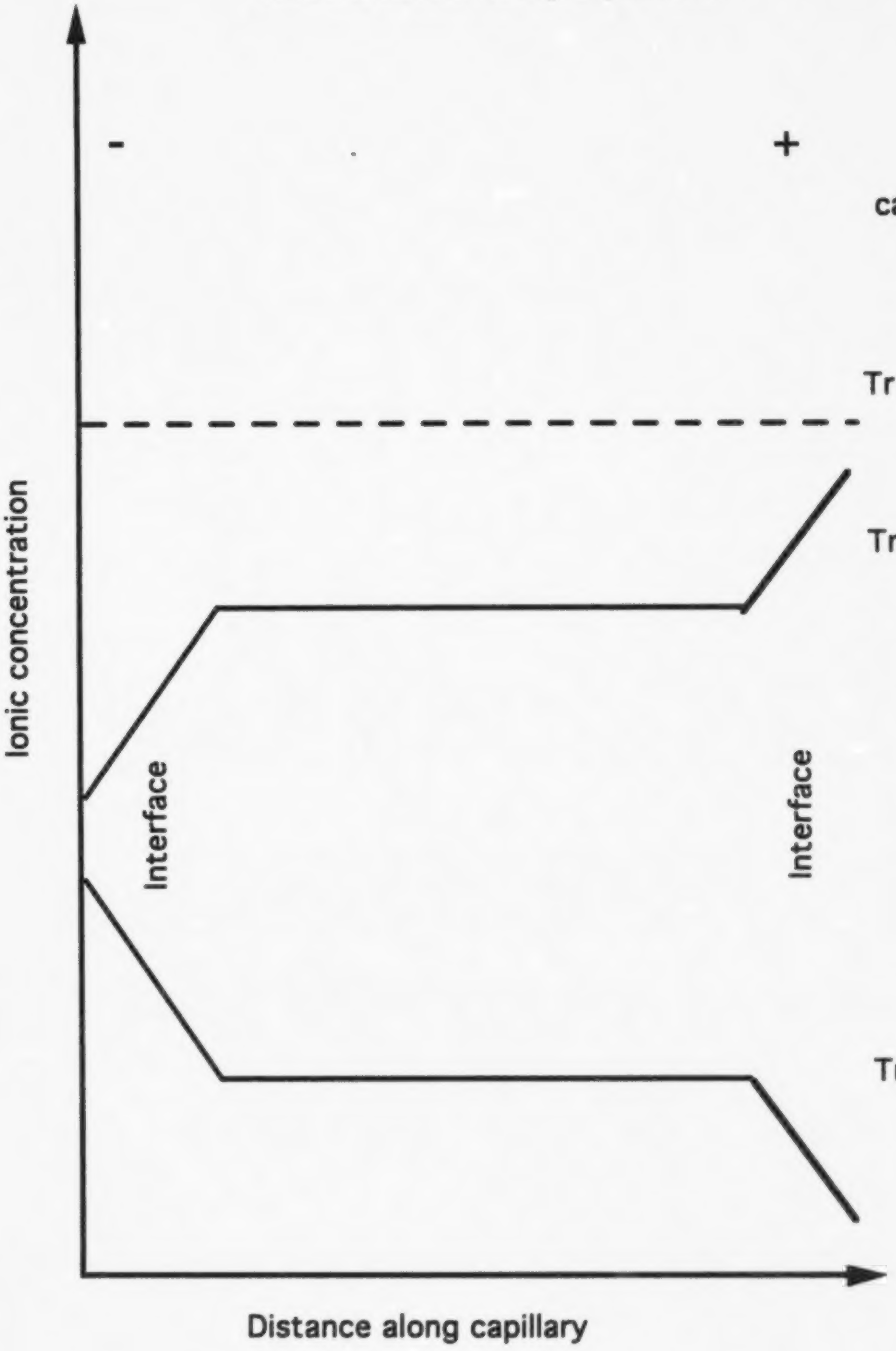
-
+
cation
Tr = Tc
Tr > Tc
Tr < Tc
Ionic concentration
Interface
Interface
Distance along capillary

where c is the concentration of an ion, t is the time, T is the transference number of an ion, x is the distance from one end of the capillary, i is the current, and F is the Faraday constant. Equations 1.20 and 1.21 can be combined to give equation 1.22.

$$\left(\frac{\partial c}{\partial t}\right)_x \left(\frac{\partial t}{\partial x}\right)_c \left(\frac{\partial x}{\partial c}\right)_t = -1 \qquad (1.21)$$

$$v = \left(\frac{\partial x}{\partial t}\right)_c = \frac{i}{F}\frac{dT}{dc} \qquad (1.22)$$

This gradient in transference number induces a movement of the two ionic areas with a velocity (v) related to the change in transference number with the ionic concentration (equation 1.22). In the case of 1xTBE, the high ionic concentration situated on the anodic side of the capillary moves out of the capillary and disappears in the buffer reservoir, and the low ionic concentration area situated on the cathodic side progresses into the capillary. Thus, an ion-depleted area forms in time at the cathodic end of the capillary (injection end). This depleted area is accompanied by a higher electric field, whereas there is a lower electric field in the rest of the capillary. With time, the electric field becomes asymmetric in the capillary. This phenomenon greatly affects the separation of DNA and is studied in this thesis.

1.3.2.3 Detection in Capillary Electrophoresis

1.3.2.3.1 General Survey

The use of low diameter tubes to do electrophoresis was limited by the detectors available for small volumes of solution. Recent developments in detection techniques have allowed for the use of small diameter capillaries for the separation and detection of samples. UV/visible absorbance, mass spectrometry, electrochemical, and fluorescence detection are now widely used in capillary electrophoresis. More exotic detection schemes like

NMR[79,80] and flame photometric detectors[81] have been reported. On-line Raman spectroscopy[82] has been coupled with capillary zone electrophoresis for the detection of methyl orange at 1×10^{-7}M. Fluorescence detection is the most sensitive method of detection for CE.

Absorbance measurement is the most popular means of detecting compounds separated by capillary electrophoresis[83]; however, its poor sensitivity limits its use for many important analytical problems. A few attempts have been made to improve absorbance detection. One way of improving the detection is by derivatizing the analyte using a strong absorbant label. For example, fluorescamine was reacted with primary amines and detected by absorbance[84]. With a 3 mm Z-shaped detector, detection limits were improved by one order of magnitude compared to the conventional system[85]. Odake *et al.*[86] used a piezoelectric transducer to detect the mechanical vibration of a capillary, induced by absorption of an intense laser light source. Waldron and Dovichi [87] used a thermooptical absorbance detector to detect phenylthiohydantoin-amino acids. The detection limit was 0.2 fmol.

Mass spectrometry is a very attractive detector, because it also gives additional information about the molecules separated by capillary electrophoresis. Electrospray ionization [88-90] is the favorite method for interfacing a capillary electrophoresis apparatus with a mass spectrometer. Fast atom bombardment is also used to couple a mass-spectrometer to a CE system. Matrix-assisted laser desorption-ionization[91] is becoming popular for coupling CE systems to mass spectrometers. Although the coupling of mass-spectrometry and CE has been developed, much more work needs to be done before this detector can compete with fluorescence and absorbance detectors in price and in detection limits.

Electrochemical detectors are also becoming more popular. Conductivity[92], potentiometry[93], and amperometry[94,95] have been used as detection schemes.

1.3.2.3.2 Fluorescence Detection

Fluorescence detection is widely used in research. It is just becoming available on the commercial systems, thus it is still less popular than UV/visible detection. Fluorescence detection has been used to detect a wide variety of compounds, separated by capillary electrophoresis. Because detection is performed at a wavelength higher than the excitation, the background noise is small. In fact, if the experiment is set up properly, the noise should be of quantum type. The signal increases linearly with the source power, and the noise increases to the square root of the excitation source power. Therefore, the signal to noise ratio increases by the square root of the source power; however, there is a limit to the increase of the signal to noise ratio due to the photobleaching of the chromophore as the power of the excitation source increases.

Lasers are usually used for the excitation of the chromophores, because they are coherent and monochromatic sources. Small light beams of high power are easily available from a laser. Other sources are not usually monochromatic and are more difficult to focus to a small diameter than a laser. Therefore, high power sources have to be used.

Only a few compounds have high enough absorptivity and quantum yield to be useful for the detection of small amounts of analyte. Thus, it is necessary to attach a highly fluorescent chromophore to most of the analytes separated by capillary electrophoresis in order to obtain reasonable detection limits. In fact, single molecule and near single molecule detection of pure dyes have been achieved[96-98]. There are a few ways used to label the analytes. The most common way is chemical derivatization. To obtain a good yield, the reaction usually has to be performed with a high concentration of analyte and chromophore. This means that although single molecule detection is achievable, the chemical labeling part is far from offering a single molecule labeling. It also means that most of the labeled analyte is never used in the analysis because of the small analyte requirement of the CE system. Amino acids and peptides [99-101], aminated monosaccharides[102], and oligosaccharides[103] were derivatized, separated and detected using a CE system with laser induced fluorescence detection.

Another way of labeling an analyte with a chromophore is to use an enzyme to catalyze the reaction. Because the enzyme decreases the activation energy, the reaction proceeds much faster than without the enzyme. Therefore, smaller concentrations of analytes can be labeled in a reasonable time. One of the reagents involved in the enzymatic reaction still needs to be chemically labeled at high concentration, but this step does not limit the enzymatic reaction. For example, different enzymes and labeled universal primers or labeled ddNTPs combinations have been used to generate DNA sequencing samples[8,18-20,104-106]. Enzymes can also be indirectly detected, using their ability to transform a weakly fluorescent chemical into a more strongly fluorescent chemical by catalyzing the breakage of bonds in the chemical[97,107,108].

In the experiments performed in this thesis, the chromophores are detected by laser induced fluorescence, using post-column excitation done in a sheath flow cuvette. The sheath flow cuvette has lower background noise than on column detection. For on column detection the laser beam is focused on the capillary, that creates a high amount of scattered light and also some impurities in the capillary's wall fluoresce. The sheath flow cuvette allows the excitation to be performed far from the surfaces, which means less background from the surfaces. A top view of a sheath flow cuvette can be seen in Figure 1.20. The square hole in the middle has 150 µm sides and the walls of the quartz chamber are 1 mm wide. The detection end of the capillary is inserted in the sheath flow cuvette. A sheath flow of buffer flows outside the capillary and brings the analytes coming out of the capillary to the excitation area. A laser beam is focused, using a microscope objective, perpendicularly to the capillary a few millimeters below the capillary tip (See the expanded portion in Figure 1.20). The fluorescence is collected at 90° using a microscope objective, focused on an iris to remove scattered light, passed through an optical bandpass filter, and detected using a photomultiplier tube(pmt) (Figure 1.21).

Figure 1.20 Sheath flow cuvette arrangement for post column detection.

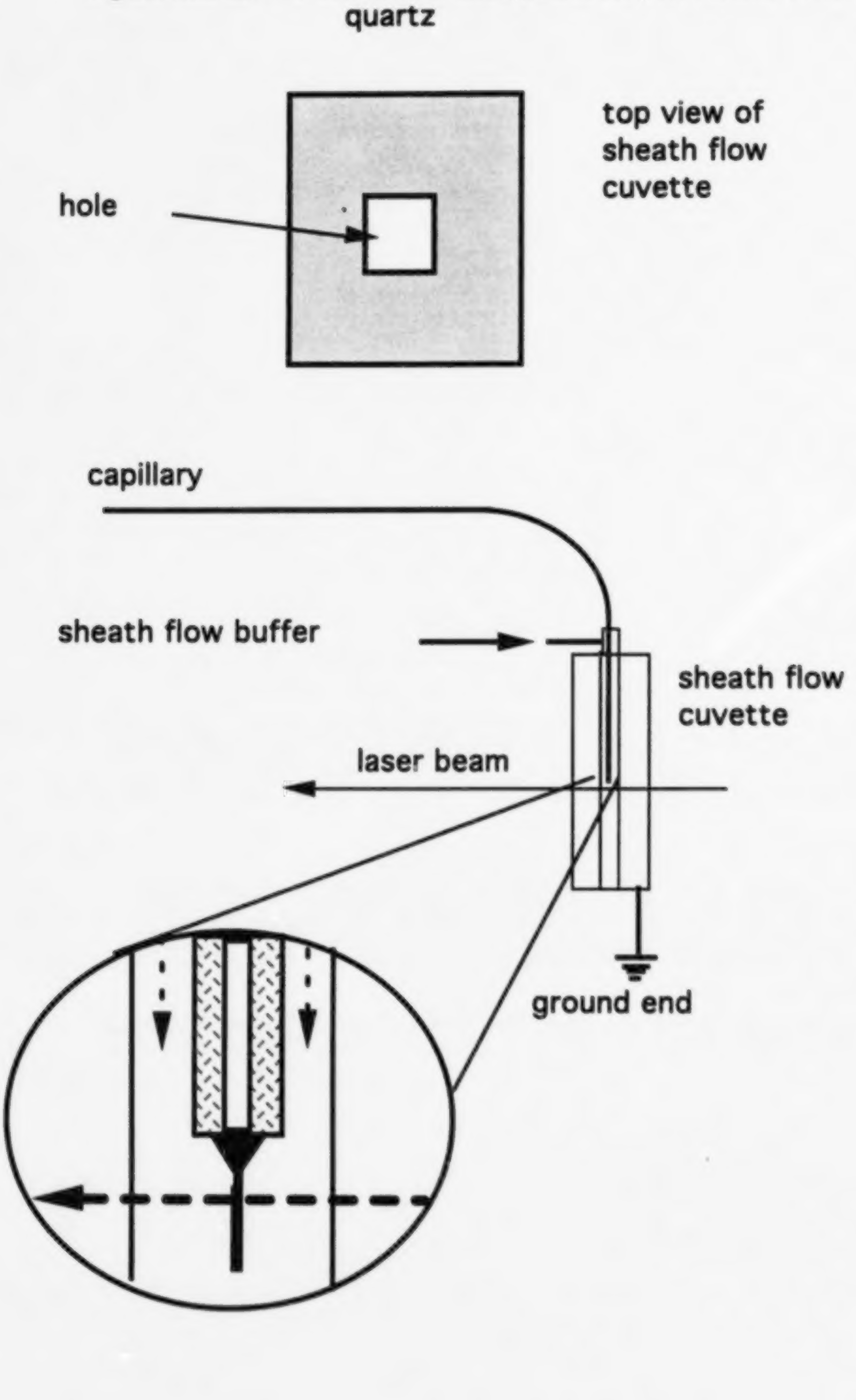
quartz
top view of sheath flow cuvette
hole
capillary
sheath flow buffer
sheath flow cuvette
laser beam
ground end

Figure 1.21 One-color laser induced fluorescence detection system.

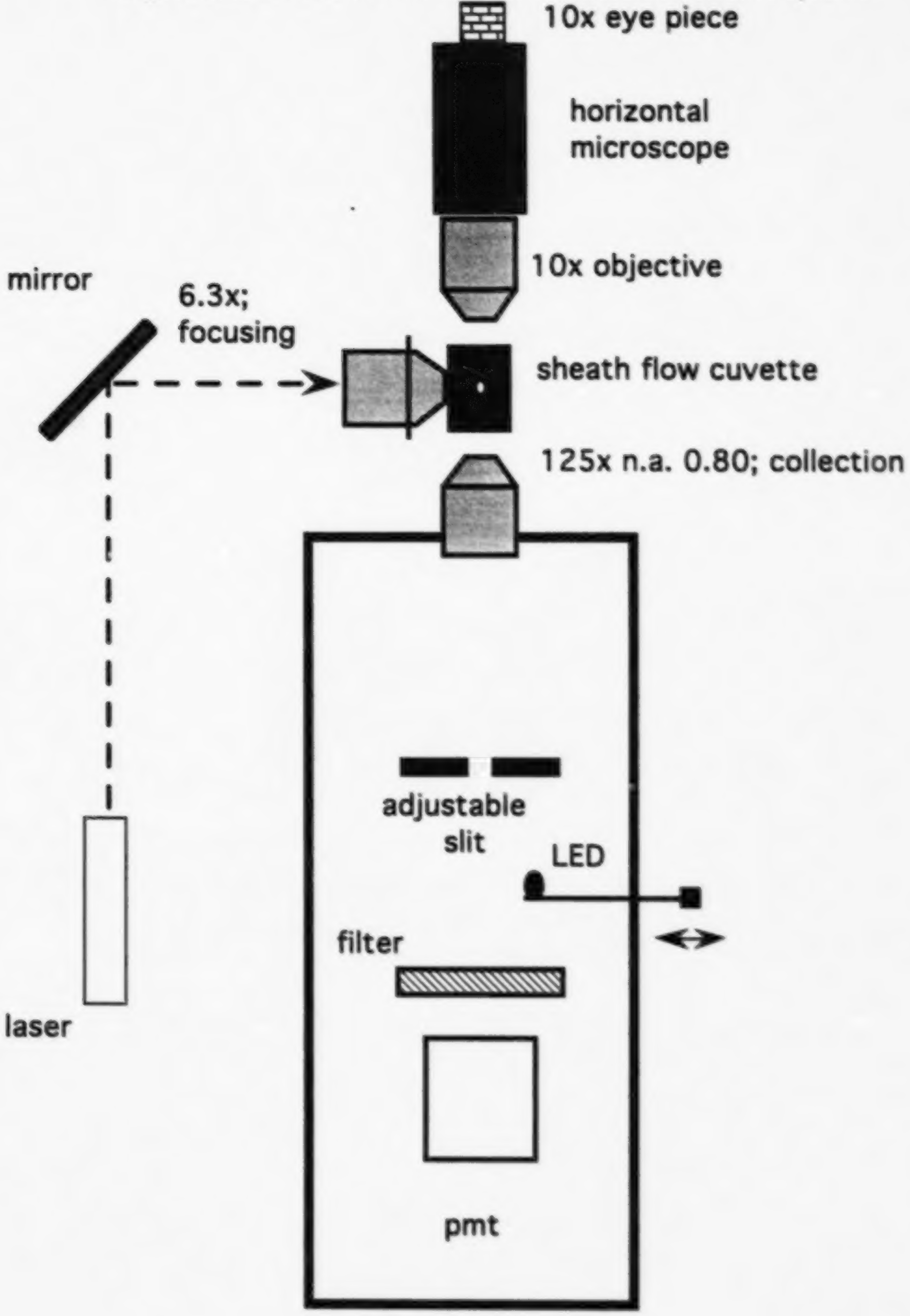
10x eye piece
horizontal microscope
10x objective
mirror
6.3x; focusing
sheath flow cuvette
125x n.a. 0.80; collection
adjustable slit
LED
filter
laser
pmt

The system is aligned using the following procedure. First, we use a horizontal microscope to view the capillary. The horizontal microscope views the side opposing the detection system and has a similar magnification as the collection objective. Then a light emitting diode (LED) is placed behind the iris in the detection system. The light from the iris passes through the collection objective and is imaged at the working distance of the collection objective.

The horizontal microscope is then moved until we see a clear image of the iris (Figure 1.22). The image of the iris is set at both the working distances of the collection objective and the horizontal microscope. Then, the sheath flow cuvette is moved until a clear image of the capillary is seen through the horizontal microscope. The capillary is at the working distance of the collection objective, and a clear image of the capillary is formed on the iris. The next step is to adjust the iris size until it matches the inside dimension of the capillary. After that, the laser beam is moved until it intersects the capillary and is well focused. The capillary is then withdrawn a few hundred micrometers above the laser beam position. This part of the alignment is only a rough alignment, and in order to obtain good signal to noise ratio a second alignment is performed. This alignment is performed by continuously electrophoresing a diluted solution of a fluorescent dye. Once the dye is flowing out of the capillary, the velocity of the sheath flow is adjusted in order to superimpose the image of the iris with the image of the fluorescence spot. In this system, the sheath flow buffer flows by gravity, which produces a very smooth flow profile. Then, the LED is turned off and removed from behind the iris, allowing the light from the fluorescent spot to reach the pmt. The signal to noise ratio is then optimized by moving the sheath flow cuvette in 3 dimensions. The laser beam is accordingly moved. The whole alignment procedure takes around 45 minutes.

For the experiment involving intercalating dyes, a two-color system was used (Figure 1.23). The difference with the one-color system is that a beam splitter (dichroic mirror) is introduced after the iris in order to separate the light in two parts. Each light fraction is

Figure 1.22 Optical alignment and signal:noise optimization

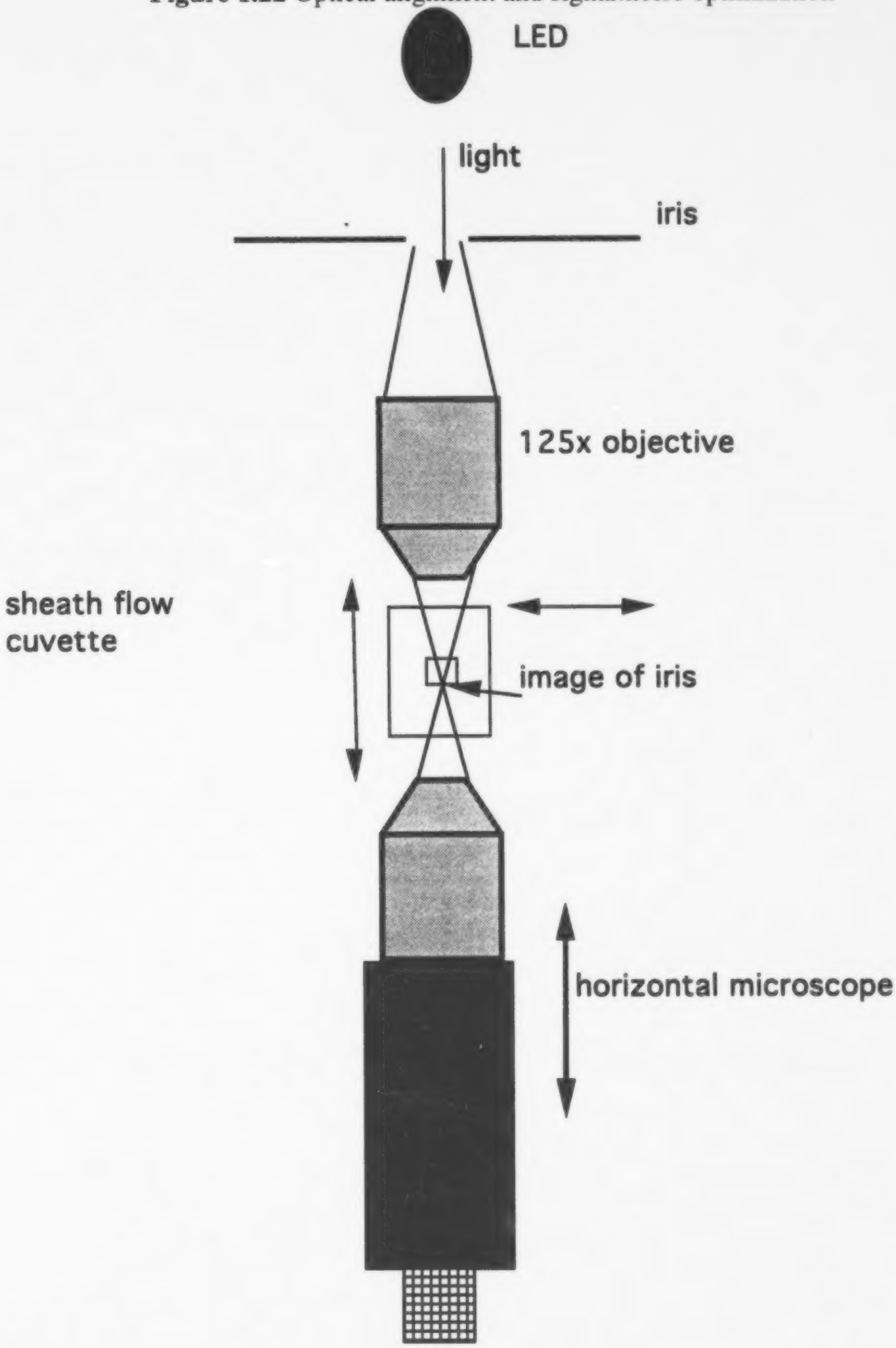
LED
light
iris
125x objective
sheath flow
cuvette
image of iris
horizontal microscope

Figure 1.23 Two-color laser induced fluorescence detection system.

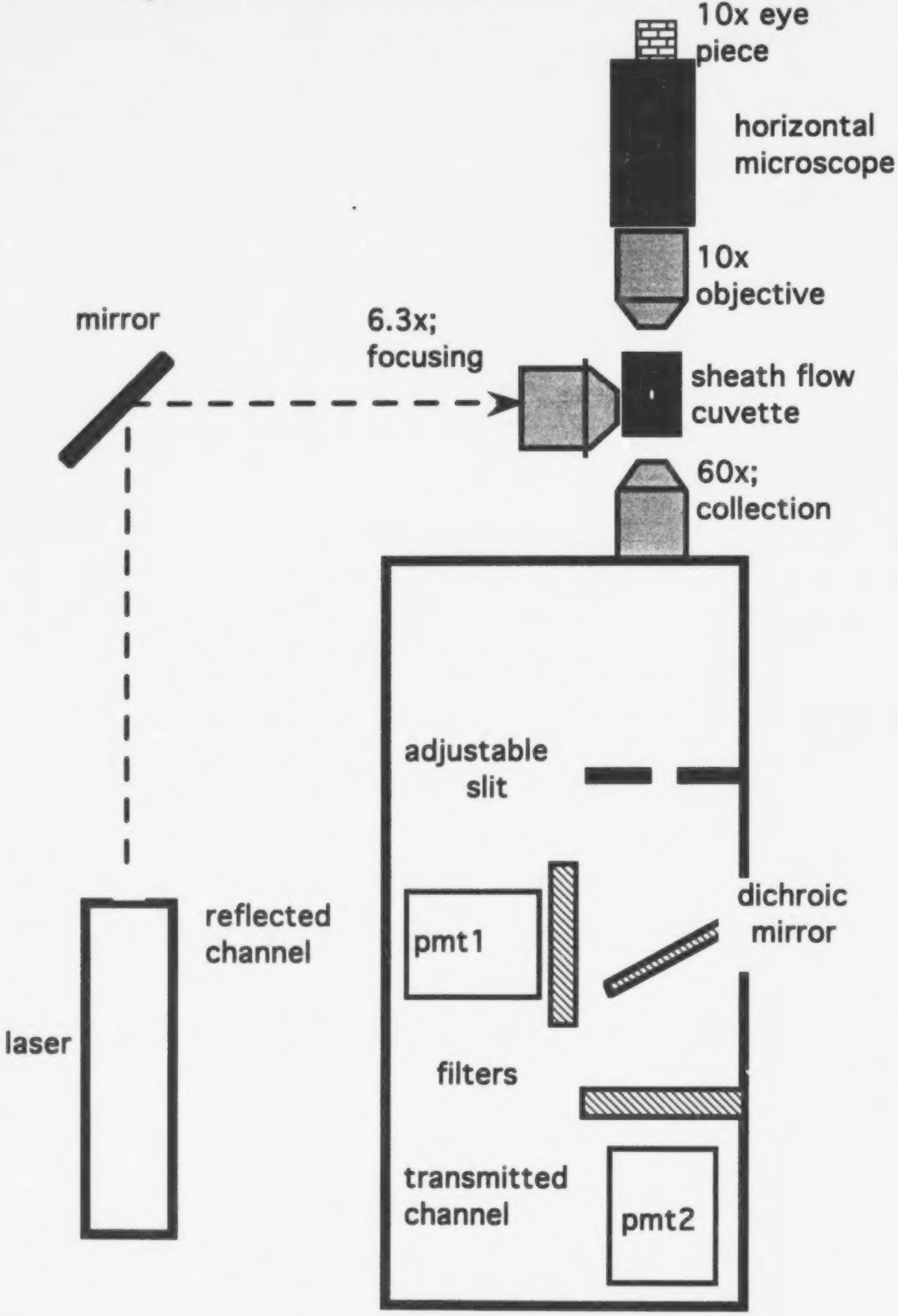
10x eye piece
horizontal microscope
10x objective
mirror
6.3x; focusing
sheath flow cuvette
60x; collection
adjustable slit
dichroic mirror
reflected channel
pmt1
laser
filters
transmitted channel
pmt2

passed through a specific filter and detected using a pmt. The alignment procedure for the two-color system is the same as the one-color system.

In this thesis, the dyes used in the experiments were selected according to the laser wavelengths available. The optical filter wavelength ranges were close to the maximum fluorescence emission of the dyes, and as far as possible from the Raman bands of water.

1.3.2.4 DNA sequencing

Gel electrophoresis is used to separate DNA sequencing fragments. In gel, DNA fragments separate according to their length. The short fragments move quickly through the gel and the long fragments move slowly through the gel; however, the movements of small fragments and big fragments through the gel are different (Figure 1.24). Short fragments move through the polymer in a spherical shape and are usually very well resolved on polyacrylamide. After a certain fragment size, the fragments have to orient to pass through the polymer. This change in conformation generates broader peaks and decreasing resolution with fragment lengths up to a point where all the fragments comigrate.

The model describing the movement of small fragments in a spherical shape is called the Ogston model[109-111]. This model assumes that the mobility of a DNA fragment is proportional to the fraction of volume available to it in the gel, as well as that DNA is a sphere. The mobility is thus related to the gel concentration according to equation 1.23:

$$\mu = \mu_o \exp\left[-\alpha C_p (r_p + R_p)^2\right] \tag{1.23}$$

where μ is the mobility, μ_o is the mobility of a fragment in absence of a gel, α is a constant of proportionality, C_p is the concentration of the polymer, r_p is the thickness of the polymer strands, and R_p is the radius of the DNA sphere. The radius of gyration of a molecule with a spherical shape is given by:

Figure 1.24 Simulated separation of DNA fragments by capillary gel electrophoresis.

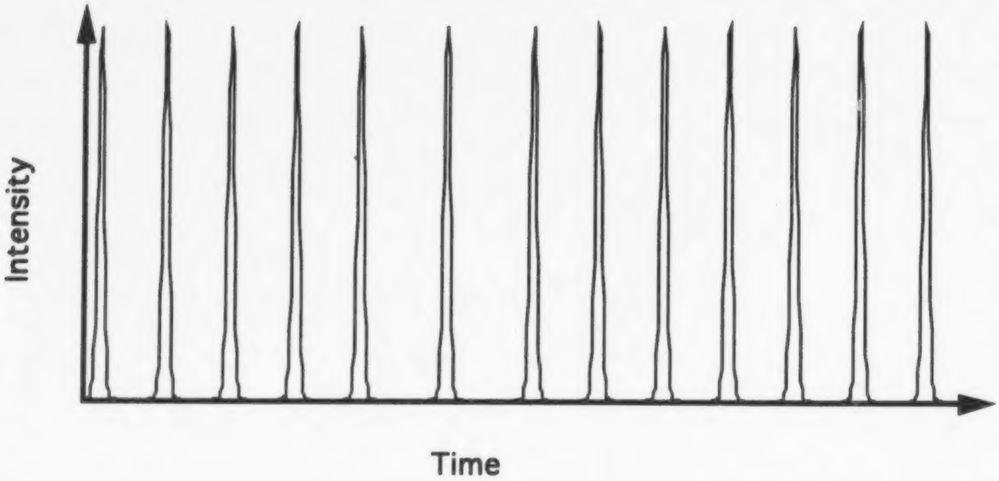
Separation of small DNA sequencing fragments

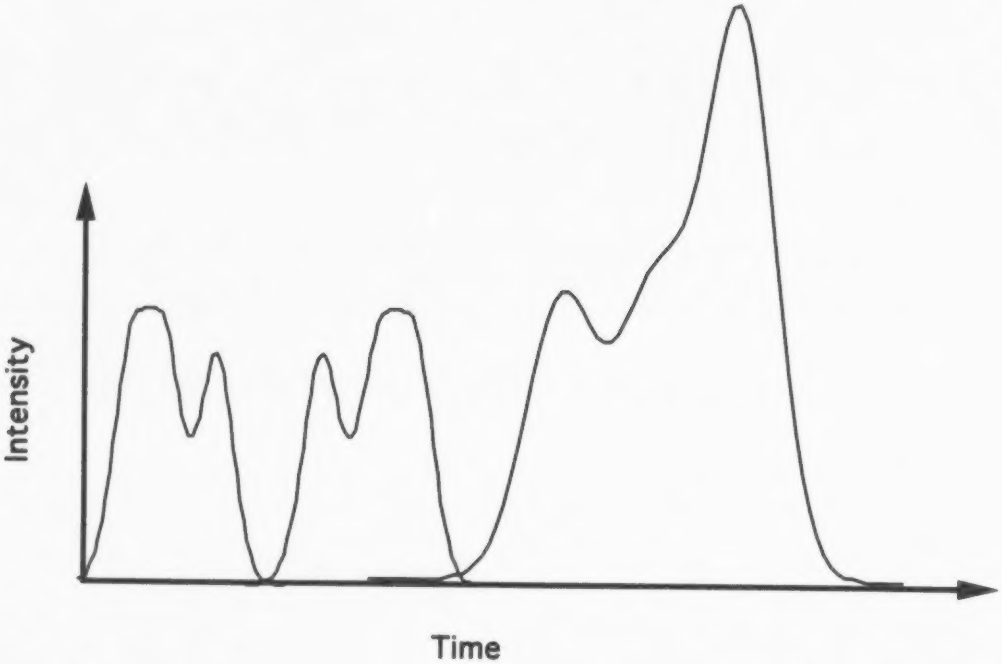
Separation of large DNA sequencing fragments

$$R_g^2 = k\,N \tag{1.24}$$

where R_g is the radius of gyration, k is a constant, and N is the length of the chain expressed by the number of nucleotides in the fragment. Equation 1.24 is valid only if the excluded volume effects are neglected or shielded; Otherwise $R_g = k\,N^{\frac{3}{5}}$. Combining equations 1.23 and 1.24 results in a relation between μ and N according to equation 1.25.

$$\mu = \mu_o \exp[-\alpha\,C_p\,k\,N] \tag{1.25}$$

This model describes well the movement of small DNA fragments in low electric fields[112]. This model predicts that for large DNA fragments, the mobilities are zero (i.e. they do not move in the polymer), which is not the case. Figure 1.25 shows the predicted mobility versus the fragment length for different polymer concentrations. An increase in polymer concentration causes the migration times to increase, and shifts the high resolution window to lower fragment sizes. The Ogston model is generally only applied in low electric fields and/or for small fragment sizes.

In the case of large fragment lengths, a second model called "reptation without orientation" applies[110-124]. In this model, the DNA fragments are considered to be too large to move from pore to pore without deformation. This model predicts that the mobility is related to the fragment length according to equation 1.26:

$$\mu = \mu_o \frac{k'}{N} \tag{1.26}$$

where k' is a proportionality constant. In high electric fields and/or for larger DNA fragments, the DNA orients and moves through the gel in a snake like motion in the direction of the migration. Equation 1.22 has to be modified to take into account the reptation with orientation (equation 1.27):

Figure 1.25 Predicted mobility versus the fragment length for different polymer concentrations. This is a schematic diagram.

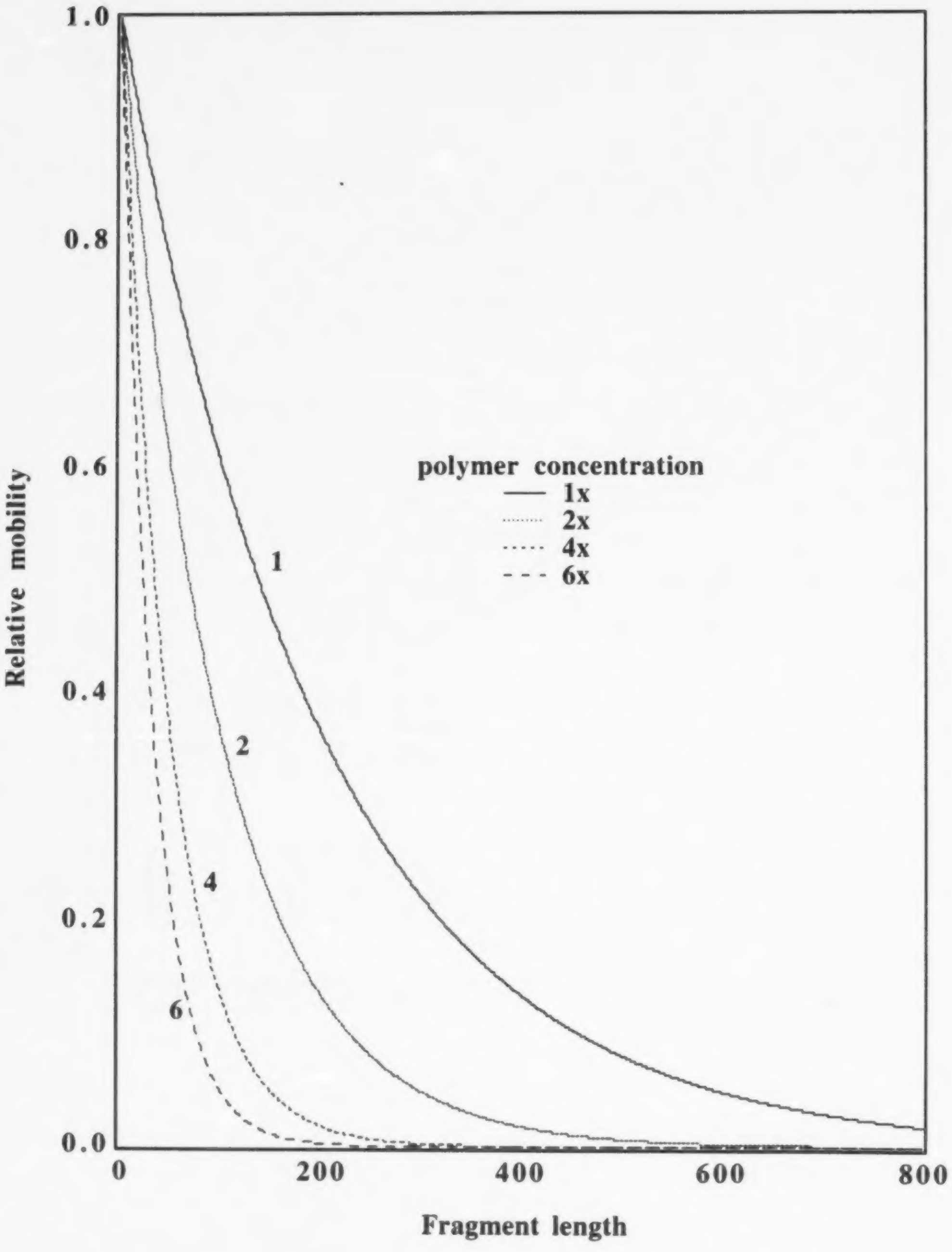

$$\mu = \frac{Q}{3\,\varepsilon_c}\left[\frac{1}{N} + \left(\frac{q\,E\,\alpha_s}{3\,k_b\,T_p}\right)^2\right] \tag{1.27}$$

where ε_c is the friction coefficient, Q is the effective charge on the whole fragment, q is the effective charge on the part of the fragment in one pore, α_s is the pore size of the gel, k_b is the Boltzman constant, and T_p is the temperature. Figure 1.26 shows a plot of the predicted mobility versus the fragment length. Only the terms in brackets were considered for the plot, the term outside the square brackets was set to one. The mobility is divided by the second term of the square brackets of equation 1.27, which is the mobility limit for a fragment of infinite size. Thus, the values on the plot represent the number of times the mobility of a fragment is higher than a fragment of infinite size. As the electric field increases, the mobility decreases faster towards the mobility limit and less fragments are separated.

In this thesis, the Ogston model was used to explain the results obtained for the smaller fragments of DNA sequencing samples, and the reptation with orientation (also called biased reptation) model was used to explain the results obtained for larger fragments; however, it seems that the biased reptation does not totally explain the results of DNA sequencing by capillary electrophoresis[50].

Figure 1.26 Predicted mobility versus fragment length for reptation with orientation. This is a schematic diagram.

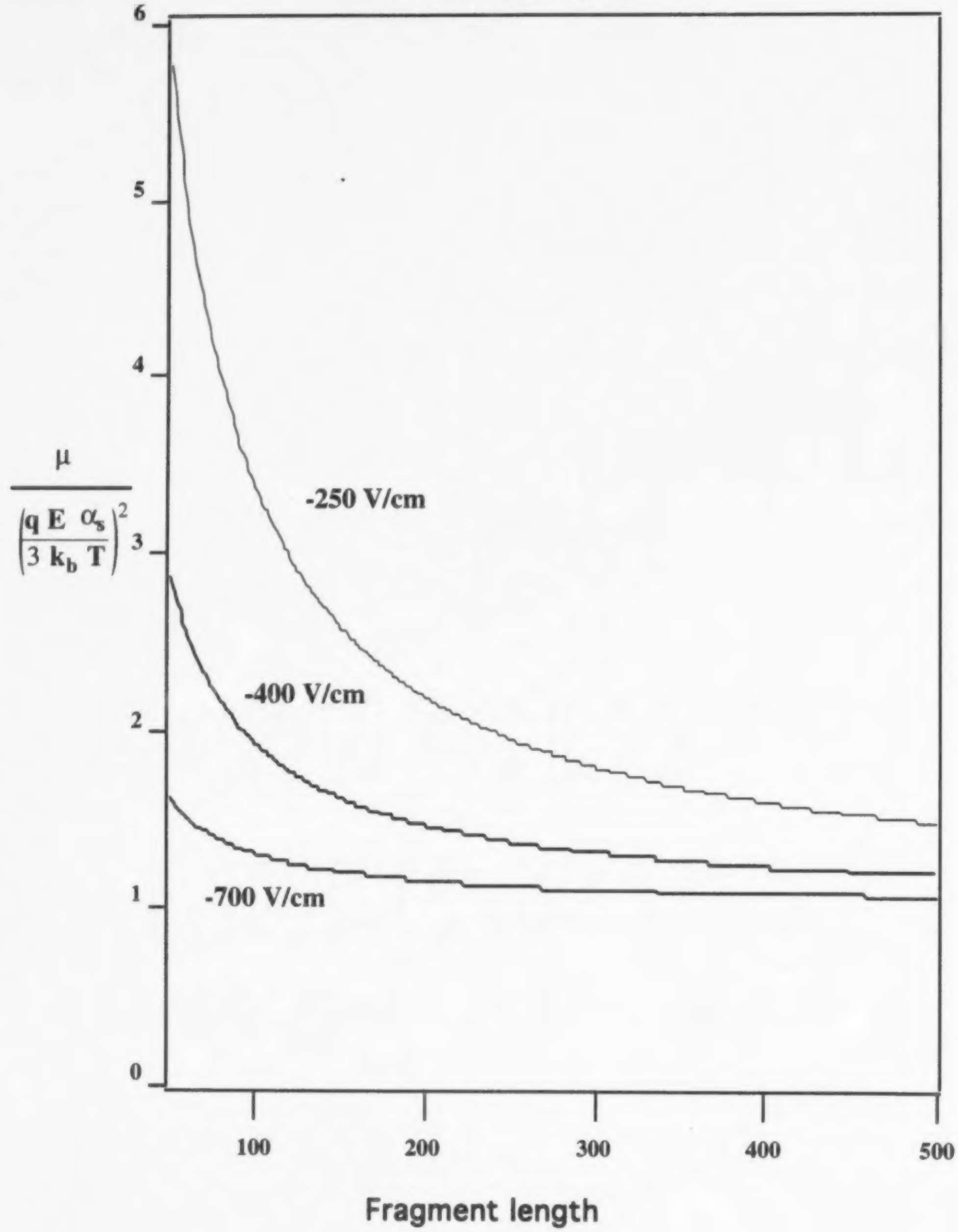

1.4 Bibliography

(1) Brown, T. A. *Genetics a Molecular Approach*; Chapman & Hall: London, 1993; Vol. 2, pp 467.

(2) Brown, T. A. *Gene Clonning, an Introduction;* 2 ed.; Chapman & Hall: London, 1990, pp 286.

(3) Riordan, J. R. *Science* **1989**, *245*, 1066-1073.

(4) Kerem, B.; Rommens, J. M.; Buchanan, J. A.; Markiewicz, D.; Cox, T. K.; Chakravarti, A.; Buchwald, M.; Tsui, L. C. *Science* **1989**, *245*, 1073-1080.

(5) Tsui, L. C. *Human Mutation* **1992**, *1*, 197-203.

(6) Barinaga, M. *C&E News* **1991**, 1589.

(7) Best, N.; Arriaga, E.; Chen, D. Y.; Dovichi, N. J. *Analytical Chemistry* **1994**, *66*, 4063-4067.

(8) Rocheleau, M. J.; Dovichi, N. J. *Journal of Microcolumn Separations* **1992**, *4*, 449-453.

(9) Takahashi, S.; Murakami, K.; Anazawa, T.; Kambara, H. *Analytical Chemistry* **1994**, *66*, 1021-1026.

(10) Huang, X. C.; Quesada, M. A.; Mathies, R. A. *Analytical Chemistry* **1992**, *64*, 2149-2154.

(11) Kambara, H.; Takahashi, S. *Nature* **1993**, *361*, 565-566.

(12) Huang, X. C.; Quesada, M. A.; Mathies, R. A. *Analytical Chemistry* **1992**, *64*, 967-972.

(13) Swerdlow, H.; Dew-Jager, K.; Gesteland, R. F. *BioTechniques* **1994**, *16*, 684-693.

(14) Harke, H. R.; Bay, S.; Zhang, J. Z.; Rocheleau, M. J.; Dovichi, N. J. *Journal of Chromatography* **1992**, *608*, 143-150.

(15) Rocheleau, M. J.; Grey, R. J.; Chen, D. Y.; Harke, H. R.; Dovichi, N. J. *Electrophoresis* **1992**, *13*, 484-486.

(16) Sanger, F.; Nicklen, S.; Coulson, A. R. *Proceedings of the National Academy of Sciences USA* **1977**, *74*, 5463-5467.

(17) Rao, V. B. *Analytical Biochemistry* **1994**, *216*, 1-14.

(18) Chen, D.; Harke, H. R.; Dovichi, N. J. *Nucleic Acids Research* **1992**, *20*, 4873-4880.

(19) Pentoney, S. L.; Konrad, K. D.; Kaye, W. *Electrophoresis* **1992**, *13*, 467-474.

(20) Swerdlow, H.; Zhang, J. Z.; Chen, D. Y.; Harke, H. R.; Grey, R.; Wu, S.; Dovichi, N. J.; Fuller, C. *Analytical Chemistry* **1991**, *63*, 2835-2841.

(21) Cohen, A. S.; Najarian, D. R.; Karger, B. L. *Journal of Chromatography* **1990**, *516*, 49-60.

(22) Ruiz-Martinez, M. C.; Berka, J.; Belenkii, A.; Foret, F.; Miller, A. W.; Karger, B. L. *Analytical Chemistry* **1993**, *65*, 2851-2858.

(23) Carson, S.; Cohen, A. S.; Belenkii, A.; Ruiz-Martinez, M. C.; Berka, J.; Karger, B. L. *Analytical Chemistry* **1993**, *65*, 3219-3226.

(24) Drossman, H.; Luckey, J. A.; Kostichka, A. J.; D'Cunha, J.; Smith, L. M. *Analytical Chemistry* **1990**, *62*, 900-903.

(25) Luckey, J. A.; Drossman, H.; Kostichka, A. J.; Mead, D. A.; D'Cunha, J.; Norris, T. B.; Smith, L. M. *Nucleic Acids Research* **1990**, *18*, 4417-4421.

(26) Smith, L. M. *Nature* **1991**, *349*, 812-813.

(27) Vesterberg, O. *Journal of Chromatography* **1989**, *480*, 1-19.

(28) Vesterberg, O. *Electrophoresis* **1993**, *14*, 1423-1429.

(29) Castellan, G. W. *Physical Chemistry;* third ed.; Addison-Wesley: London, 1983, pp 943.

(30) Kohlrauch, F. *Wiedemans Ann.(Ann. Phys. Leipzig)* **1897**, *62*, 209.

(31) Tiselius, A. *Nova Acta Regiae Societatis Scientiarum Upsaliensis* **1930**, *Ser. IV, Vol. 7*,

(32) Tiselius, A. *Transaction of the Faraday Society* **1937**, *33*, 524-531.

(33) Hjertén, S. *Chromatography Review* **1967**, *9*, 122-219.

(34) Thormann, W.; Molteni, S.; Caslavska, J.; Schmutz, A. *Electrophoresis* **1994**, *15*, 3-12.

(35) Carchon, H.; Eggermont, E. *American Laboratory* **January 1992**, 67-72.

(36) Pretorius, V.; Hopkins, B. J.; Schieke, J. D. *Journal of Chromatography* **1974**, *99*, 23-30.

(37) Knox, J. H. *Journal of Chromatography* **1994**, *680*, 3-13.

(38) Bello, M. S.; deBesi, P.; Rezzonico, R.; Righetti, P. G.; Casiraghi, E. *Electrophoresis* **1994**, *15*, 623-626.

(39) Demana, T.; Guhathakurka, U.; Morris, M. D. *Analytical Chemistry* **1992**, *64*, 390-394.

(40) Hjertén, S. *Journal of Chromatography* **1985**, *347*, 191-198.

(41) Ghowsi, K.; Gale, R. J. *Journal of Chromatography* **1991**, *559*, 95-101.

(42) Lee, C. S.; Blanchard, W. C.; Wu, C. T. *Analytical Chemistry* **1990**, *62*, 1550-1552.

(43) Lambert, W.; Middleton, D. L. *Analytical Chemistry* **1990**, *62*, 1585-1587.

(44) Vindevogel, J.; Sandra, P. *Analytical Chemistry* **1991**, *63*, 1530-1536.

(45) Janini, G. M.; Chan, K. C.; Barnes, J. A.; Muschik, G. M.; Issaq, H. J. *Journal of Chromatography* **1993**, *653*, 321-327.

(46) Chang, H. T.; Yeung, E. S. *Journal of Chromatography* **1992**, *608*, 65-72.

(47) Yao, X. W.; Wu, D.; Regnier, F. E. *Journal of Chromatography* **1993**, *636*, 21-29.

(48) Hjertén, S. *Electrophoresis* **1990**, *11*, 665-690.

(49) Davis, K. L.; Liu, K. L.; Lanan, M.; Morris, M. D. *Analytical Chemistry* **1993**, *65*, 293-298.

(50) Lu, H.; Arriaga, E.; Chen, D. Y.; Figeys, D.; Dovichi, N. J. *Journal of Chromatography* **1994**, *680*, 503-510.

(51) Smithies, O. *Biochemistry Journal* **1955**, *61*, 629-641.

(52) Hjertén, S. *Biochemistry and Biophysic Acta* **1961**, *53*, 514-517.

(53) Raymond, S.; Weintraub, L. *Science* **1959**, *130*, 711.

(54) Serwer, P. *Electrophoresis* **1983**, *4*, 375-382.

(55) Stellwagen, N. C. *Advances in Electrophoresis* **1987**, *1*, 177-228.

(56) Thomas, W. M.; Wang, D. W. In *Encyclopedia of Polymer Science and Engineering*; 2 ed.John Wiley and Sons: Toronto, 1985; Vol. 1; pp 169-211.

(57) Bikales, N. B. In *High Polymers*; E. C. Leonard, Ed.; Willey-Interscience: Toronto, 1970; Vol. 24; pp 81-103.

(58) Caglio, S.; Righetti, P. G. *Electrophoresis* **1993**, *14*, 997-1003.

(59) Righetti, P. G.; Caglio, S. *Electrophoresis* **1993**, *14*, 573-582.

(60) Tanaka, T. *Scientific American* **1981**, *244*, 124-139.

(61) Gelfi, C.; deBesi, P.; Alloni, A.; Righetti, P. G. *Journal of Chromatography* **1992**, *608*, 333-341.

(62) Righetti, P. G.; Chiari, M.; Nesi, M.; Caglio, S. *Journal of Chromatography* **1993**, *638*, 165-178.

(63) Gelfi, C.; Righetti, P. G. *Electrophoresis* **1981**, *2*, 213-219.

(64) Righetti, P. G.; Snyder, R. S. *Applied and Theoretical Electrophoresis* **1988**, *1*, 53-58.

(65) Righetti, P. G.; Gelfi, C.; Bosisio, A. B. *Electrophoresis* **1981**, *2*, 291-295.

(66) Righetti, P. G.; Gelfi, C. *Electrophoresis* **1981**, *2*, 220-228.

(67) Righetti, P. G.; Gelfi, C.; Bosisio, A. B. *Electrophoresis '82* **1983**, 147-156.

(68) Holmes, D. L.; Stellwagen, N. C. *Electrophoresis* **1991**, *12*, 612-619.

(69) Rapp, T. L.; Kowalchyk, W. K.; Davis, K. L.; Todd, E. A.; Liu, K.-L.; Morris, M. D. *Analytical Chemistry* **1992**, *64*, 2434-2437.

(70) Hjelmeland, L. M.; Allenmark, S.; AnderLan, B.; Jackiw, B. A.; Nguyen, N. Y.; Chrambach, A. *Electrophoresis* **1981**, *2*, 82-90.

(71) Righetti, P. G.; Caglio, S.; Saracchi, M.; Quaroni, S. *Electrophoresis* **1992**, *13*, 587-595.

(72) Righetti, P. G.; Bossi, A.; Giglio, M.; Vailati, A.; Lyubimova, T.; Briskman, V. A. *Electrophoresis* **1994**, *15*, 1005-1013.

(73) Felcht, U.-H. In *Cellulose and its Derivatives; Chemistry, Biochemistry and Applications*; J. F. Kennedy; G. O. Phillips; D. J. Wedlock and P. A. Williams, Ed.; John Wiley & Sons: Toronto, 1985; pp 273-284.

(74) Krassig, D. H. In *Cellulose and its Derivatives; Chemistry, Biochemistry and Applications*; J. F. Kennedy; G. O. Phillips; D. J. Wedlock and P. A. Williams, Ed.; John Wiley & Sons: Toronto, 1985; pp 3-26.

(75) Grossman, P. D.; Soane, D. S. *Journal of Chromatography* **1991**, *559*, 257-266.

(76) Spencer, M. *Electrophoresis* **1983**, *4*, 36-41.

(77) Spencer, M. *Electrophoresis* **1983**, *4*, 41-45.

(78) Spencer, M. *Electrophoresis* **1983**, *4*, 46-52.

(79) Sweedler, J. W.; al., e. *Journal of the American Chemical Society* **1994**, *116*, 7929-7930.

(80) Wu, N.; Peck, T. L.; Webb, A. G.; Magin, R. L.; Sweedler, J. V. *Analytical Chemistry* **1994**, *66*, 3849-3857.

(81) Sänger-vandeGriend, C. E.; Kientz, C. E.; Brinkman, U. A. T. *Journal of Chromatography A* **1994**, *673*, 299-302.

(82) Chen, C. Y.; Morris, M. D. *Journal of Chromatography* **1991**, *540*, 355-363.

(83) Schlabach, T.; Powers, T. *American Laboratory* **1991**, *23*, 24-25.

(84) Guzman, N. A.; Moschera, J.; Baley, C. A.; Iqbal, K.; Malick, A. W. *Journal of Chromatography* **1992**, *598*, 123-131.

(85) Moring, S. E.; Reel, R. T.; vanSoest, R. E. J. *Analytical Chemistry* **1993**, *65*, 3454-3459.

(86) Odake, T.; Kitamori, T.; Sawada, T. *Analytical Chemistry* **1992**, *64*, 2870-2871.

(87) Waldron, K. C.; Dovichi, N. J. *Analytical Chemistry* **1992**, *64*, 1396-1399.

(88) Suter, M. J. F.; DaGue, B. B.; Moore, W. T.; Lin, S. N.; Caprioli, R. M. *Journal of Chromatography* **1991**, *553*, 101-116.

(89) Huang, E. C.; Wachs, T.; Conboy, J. J.; Henion, J. D. *Analytical Chemistry* **1990**, *62*, 713A-725A.

(90) Smith, R. D.; Wahl, J. D.; Goodlett, D. R.; Hofstadler, S. A. *Analytical Chemistry* **1993**, *65*, 574A-584A.

(91) vanVeelen, P. A.; Tjaden, U. R.; vanderGreef, J.; Ingendoh, A.; Hillenkamp, F. *Journal of Chromatography* **1993**, *647*, 367-374.

(92) Avdalovic, N.; Pohl, C. A.; Rocklin, R. D.; Stillian, J. R. *Analytical Chemistry* **1993**, *65*, 1470-1475.

(93) Nann, A.; Simon, W. *Journal of Chromatography* **1993**, *633*, 207-211.

(94) Lu, W.; Cassidy, R. M. *Analytical Chemistry* **1994**, *66*, 200-204.

(95) Lu, W.; Cassidy, R. M. *Analytical Chemistry* **1993**, *65*, 1649-1653.

(96) Chen, D. Y.; Adelhelm, K.; Cheng, X. L.; Dovichi, N. J. *Analyst* **1994**, *119*, 349-352.

(97) Zhao, J. Y.; Dovichi, N. J.; Hindsgaul, O.; Gosselin, S.; Palcic, M. M. *Glycobiology* **1994**, *4*, 239-242.

(98) Chen, D. Y.; Dovichi, N. J. *Journal of Chromatography B* **1994**, *657*, 265-269.

(99) Zhao, J. Y.; Waldron, K. C.; Miller, J.; Zhang, J. Z.; Harke, H.; Dovichi, N. J. *Journal of Chromatography* **1992**, *608*, 239-242.

(100) Zhang, J. Z.; Chen, D. Y.; Wu, S.; Harke, H. R.; Dovichi, N. J. *Clinical Chemistry* **1991**, *37*, 14921496.

(101) Zhao, J.-Y.; Chen, D.-Y.; Dovichi, N. J. *Journal of Chromatography* **1992**, *608*, 117-120.

(102) Zhao, J. Y.; Diedrich, P.; Zhang, Y.; Hindsgaul, O.; Dovichi, N. J. *Journal of Chromatography B* **1994**, *657*, 307-313.

(103) Liu, J.; Shirota, O.; Novotny, M. *Journal of Chromatography* **1991**, *559*, 223-235.

(104) Igloi, G. L.; Schiefermayr, E. *BioTechniques* **1993**, *15*, 486-495.

(105) Johnson, A. F.; Struthers, M. D.; Pierson, K. B.; Mangel, W. F.; Smith, L. M. *Analytical Chemistry* **1993**, *65*, 2352-2359.

(106) Lee, L. G.; Connell, C. R.; woo, S. L.; Cheng, R. D.; McArdle, B. F.; Fuller, C. W.; Halloran, N. D.; Wilson, R. K. *Nucleic Acids Research* **1992**, *20*, 2471-2483.

(107) Hogan, B. L.; Yeung, E. S. *Analytical Chemistry* **1992**, *64*, 2841-2845.

(108) Wu, D.; Regnier, F. E. *Analytical Chemistry* **1993**, *65*, 2029-2035.

(109) Ogston, A. G. *Transaction of the Faraday Society* **1958**, *54*, 1754-1757.

(110) Luckey, J. A.; Smith, L. M. *Electrophoresis* **1993**, *14*, 492-501.

(111) Viovy, J.-L.; Duke, T. *Electrophoresis* **1993**, *14*, 322-329.

(112) Slater, G. W.; Rousseau, J.; Noolandi, J.; Turmel, C.; Lalande, M. *Biopolymers* **1988**, *27*, 509-524.

(113) Defontaines, A.-D.; Viovy, J.-L. *Electrophoresis* **1994**, *15*, 111-119.

(114) Deutsch, J. M. *Science* **1988**, *240*, 922-924.

(115) deGennes, P. G. *The Journal of Chemical Physics* **1971**, *55*, 572-579.

(116) Noolandi, J.; Slater, G. W.; Lim, H. A.; Viovy, J. L. *Science* **1989**, *243*, 1456-1458.

(117) Noolandi, J. *Advances in Electrophoresis* **1992**, *5*, 1-57.

(118) Rodbard, D.; Chrambach, A. *Proceedings of the National Academy of Sciences USA* **1970**, *65*, 970-977.

(119) Russell, T. P.; Deline, V. R.; Dozier, W. D.; Felcher, G. P.; Agrawal, G.; Wool, R. P.; Mays, J. W. *Nature* **1993**, *365*, 235-237.

(120) Slater, G. W.; Noolandi, J. *Biopolymers* **1986**, *25*, 431-454.

(121) Slater, G. W.; Rousseau, J.; Noolandi, J. *Biopolymers* **1987**, *26*, 863-872.

(122) Viovy, J. L.; Duke, T.; Caron, F. *Contemporary Physics* **1992**, *33*, 25-40.

(123) Wheeler, D.; Chrambach, A. *Electrophoresis* **1993**, *14*, 993-996.

(124) Widom, B.; Viovy, J. L.; Defontaines, A. D. *Journal De Physique I* **1991**, *1*, 1759-1784.

CHAPTER 2 [1]

EFFECT OF CROSS-LINKER CONCENTRATION ON THE SEPARATION OF SINGLE-STRANDED DNA.

---

[1] A version of this chapter has been published.
Figeys, D. and Dovichi, N.J. 1993 Journal of Chromatography 645:311-317.

2.1 Introduction

Since 1989, there have been a number of reports of DNA sequencing by capillary gel electrophoresis [1-14]. The high surface-to-volume ratio of the capillary facilitates the use of high electric fields for fast separations. Bisacrylamide is the most common cross-linking agent used in polyacrylamide gels. The cross-linker concentration (%C) is usually expressed as a weight percentage of the total monomer concentration in the gel. The weight percent of monomer plus cross-linker is denoted as %T, the total acrylamide concentration. Most workers employ 5%C polyacrylamide gels, although there have been reports on the use of much lower %C gels.

Recently, attention has focused on the use of linear polyacrylamide (0%C) in electrophoresis. These entangled polymer solutions have relatively low viscosity and they may be pumped from the capillary after use. There is hope that by refilling the capillary after every separation, it will not be necessary to realign the optical systems in automated DNA sequencers. Bode[15,16] performed the first work with linear polyacrylamide in the mid-1970s; he combined linear polyacrylamide with agarose for the separation of proteins and nucleic acids. The mobility was a function of the polymer length. Crambach *et al.* pioneered the use of linear polyacrylamide [17-19]. They compared the performance of 0%C and 5%C gels at various total acrylamide concentrations. More recently, Karger *et al.*[20] compared 0, 0.5, and 5%C gels for separation of double-stranded DNA; they also studied the effect of electric fields on the resolution of fragments 4363 and 7253 bases in length. Bocek *et al.*[21] reported that linear polyacrylamide could be pumped from a capillary through the use of a special high pressure syringe; the effect of the total acrylamide concentration was considered. Pentoney *et al.*[10] reported DNA sequencing in 10%T linear polyacrylamide at an electric field of -300 V/cm; the sequence could not be determined for fragments longer than 300 bases. Similar results have been reported by Mathies' group[12] with 9%T linear polyacrylamide. Righetti *et al.* [22] argued that the high viscosity of 10%T linear polyacrylamide eliminates any hope of refilling capillaries with that material; only low %T polyacrylamide has a sufficiently low viscosity for replacement. Righetti also pointed out that the polymerization reaction does not go to completion; at least 20% of monomer remains after polymerization. Guttman *et al.*[23] reported the use of low total percent linear polyacrylamide for the separation of double-stranded DNA; they claimed that the capillary could be reused 100 times without replacement of the separation medium.

There have been few systematic studies of the effect of gel composition on the separation parameters [24-27]. The effects of %T[24] and the denaturing agent[26] on the separation of DNA sequencing fragments have been reported. In this chapter, we complete the study of the effect of the gel composition by looking at the effect of cross-linker concentration on the mobility, the plate count, and the resolution in the separation of DNA sequencing fragments by polyacrylamide gel electrophoresis.

2.2 Experimental

Fluorescently labeled DNA sequencing samples were prepared using protocol one from Chapter 1. The reaction buffer was freshly prepared by mixing 1 µL of 10x MOPS buffer (400 mM 3-[N-morpholino]propanesulfonic acid (MOPS) pH 7.5, 500 mM NaCl, and 100 mM $MgCl_2$) and 1 µL of 10x Mn^{2+} solution (50 mM $MnCl_2$ and 150 mM isocitrate sodium salt). To the reaction buffer 1 µL of M13mp18 single stranded DNA 0.25 µg/µL (United States Biochemical, Cleveland, USA), 1 µL of ROX primer 0.4 pmol/µL (Applied Biosystems, Los Angeles, USA), 1 µL of MOPS buffer, 1 µL of Mn, 1 µL of water, and 1 µL of Sequenase13U/µL diluted 1:5 using Sequenase enzyme dilution buffer (United States Biochemical) were added. Only ddATP (3 µL of a mixture of 1mM each, dATP, dCTP,dTTP,7-deaza-dGTP, and 3.3 µM ddATP) was used as a terminating nucleotide. The annealing was done at 65°C and the elongation at 37°C. The samples were ethanol precipitated, washed, and then resuspended in 4 μL of a 49:1 mixture of formamide:0.5M EDTA at pH 8.0.

Stock solutions of 40% acrylamide - X% N,N'-methylene bisacrylamide (Bio-Rad, Toronto) were prepared monthly. Gels (6%T) were prepared daily in 5 mL aliquots by diluting the stock solution of acrylamide-bisacrylamide. The aliquots also contained 1xTBE buffer (0.54 g TRIS, 0.275 g boric acid, and 0.100 millimole disodium EDTA, diluted to 50 mL with deionized water), and 7M urea. Before polymerization, the solution was carefully degassed. Polymerization was initiated by the addition of 2 μL of N,N,N',N'-tetramethylethylene-diamine (TEMED) and 20 μL of 10% ammonium persulfate. The solutions were injected into a capillary using a modified syringe. The gels were covalently bound to the capillary wall with the use of γ–methacryloxypropyl trimethoxysilane solution. γ–methacryloxypropyl trimethoxysilane solution was introduced in the capillary 30 minutes prior to the polymerization of polyacrylamide. The solution of γ–methacryloxypropyl trimethoxysilane was prepared by mixing: 0.5 mL of water, 0.5 mL of glacial acetic acid, and 5 μL of γ–methacryloxypropyl trimethoxysilane. Linear polyacryalmide was covalently bound to the full length of the capillary; other gels were bound to the last 5-cm of the capillary. The polyimide coated fused silica capillaries were typically 35 cm long × 50 μm id × 190 μm od.

The one-spectral channel capillary electrophoresis system for DNA sequencing[5,7] has been described before in Chapter 1 (Figure 1.21). The collection objective was 60X instead of 125X. Fluorescence was induced with a green (543 nm and 0.7mW) line of a He-Ne laser. The samples were injected at 200V/cm for 60 seconds and eluted at -300 V/cm with a fresh 1× TBE buffer.

2.3 Results and Discussion

Three to six electropherograms were obtained for each value of %C studied; in all the cases, 6%T polyacrylamide was used. The order in which the gels were prepared was randomized, and fresh gels were used for each experiment. The results reported are average values. Figure 2.1 shows examples of the electropherograms obtained in each of the %C polymer. It can be seen that as the %C increases, the migration time increases. As in earlier work[24], there is a linear relationship between the fragment length and the migration time for relatively short sequencing fragments ranging from 60 to 240 bases. The slope and the intercept are summarized in Table 2.1.

The plots have a common intercept, which corresponds to a migration time of 11.7 minutes and to a mobility of 1.43×10^{-4} cm^{2}V^{-1}s^{-1} for a vanishingly small fragment. This value is slightly less than observed in the %T study[24], and presumably, results from the differences in the fluorescent labeling scheme used in the two experiments. The higher slopes for high %C polyacrylamide indicate that the sequencing is slower than in low %C polyacrylamide. This is due to higher electrophoretic friction for the higher %C.

The mobility (μ) of the DNA sequencing fragments is calculated from the migration time, t_m, using equation 2.1. Within experimental error, the mobility is identical for 2.5 and 5% C gels. The mobility increases with lower %C, and is maximum for 0%C.

$$\mu = \frac{L}{E\,t_m} = \frac{L^2}{V\,t_m} \qquad (2.1)$$

The electrophoretic behavior of long DNA fragments is described by the biased reptation model [28,29]. Fragments smaller than a given threshold are in a random coil configuration; their mobility decreases inversely with the fragment length. Fragments longer than that threshold are oriented into a linear configuration; their mobility is

Figure 2.1A Separation of M13mp18 ddATP sample on a 6%T 0%C 35 cm long x 50 µm id x 190 µm od capillary at -300V/cm.

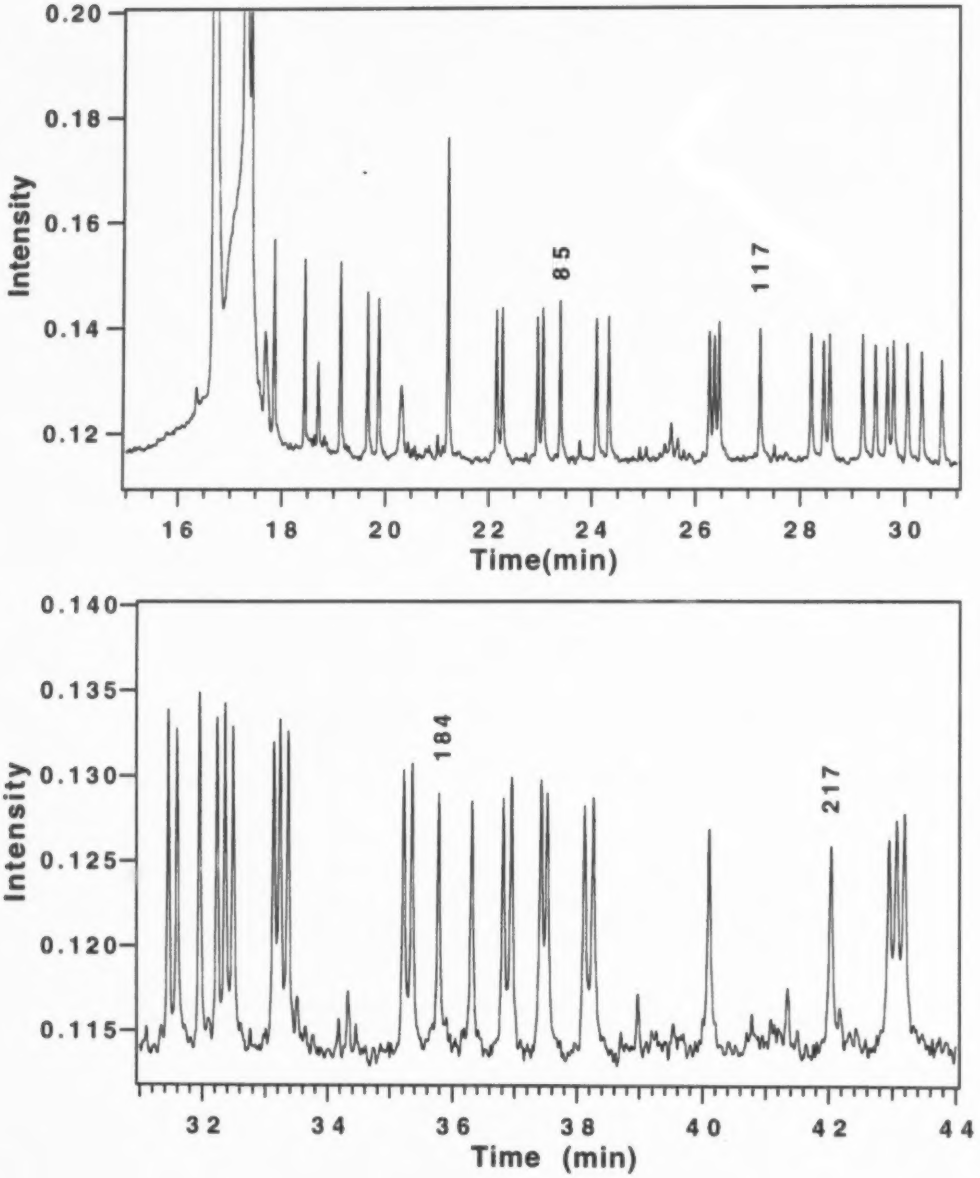

Figure 2.1B Separation of M13mp18 ddATP sample on 6%T 0.5%C.
Other conditions as in fig. 2.1.A.

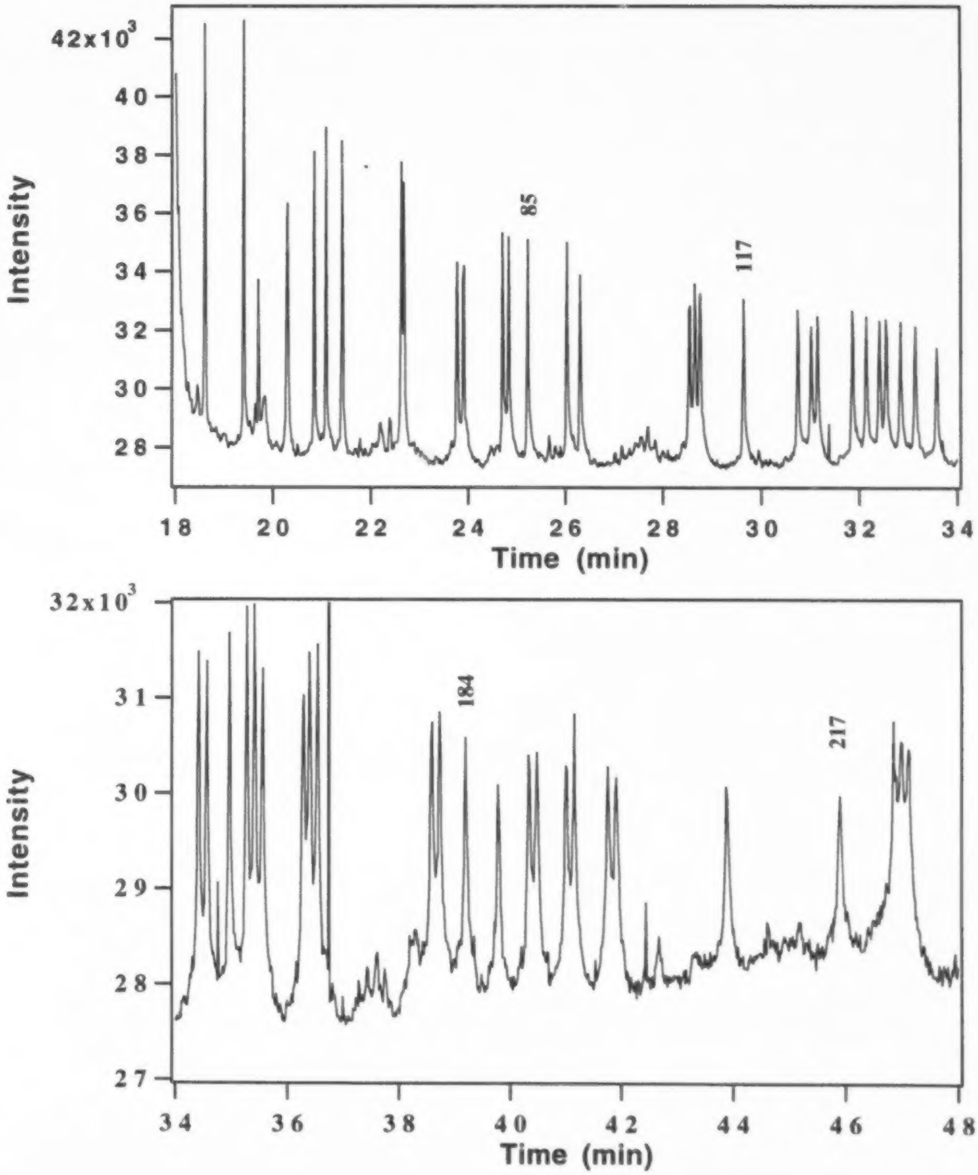

Figure 2.1C Separation of M13mp18 ddATP sample on 6%T 2.5%C. Other conditions as in fig.2.1.A.

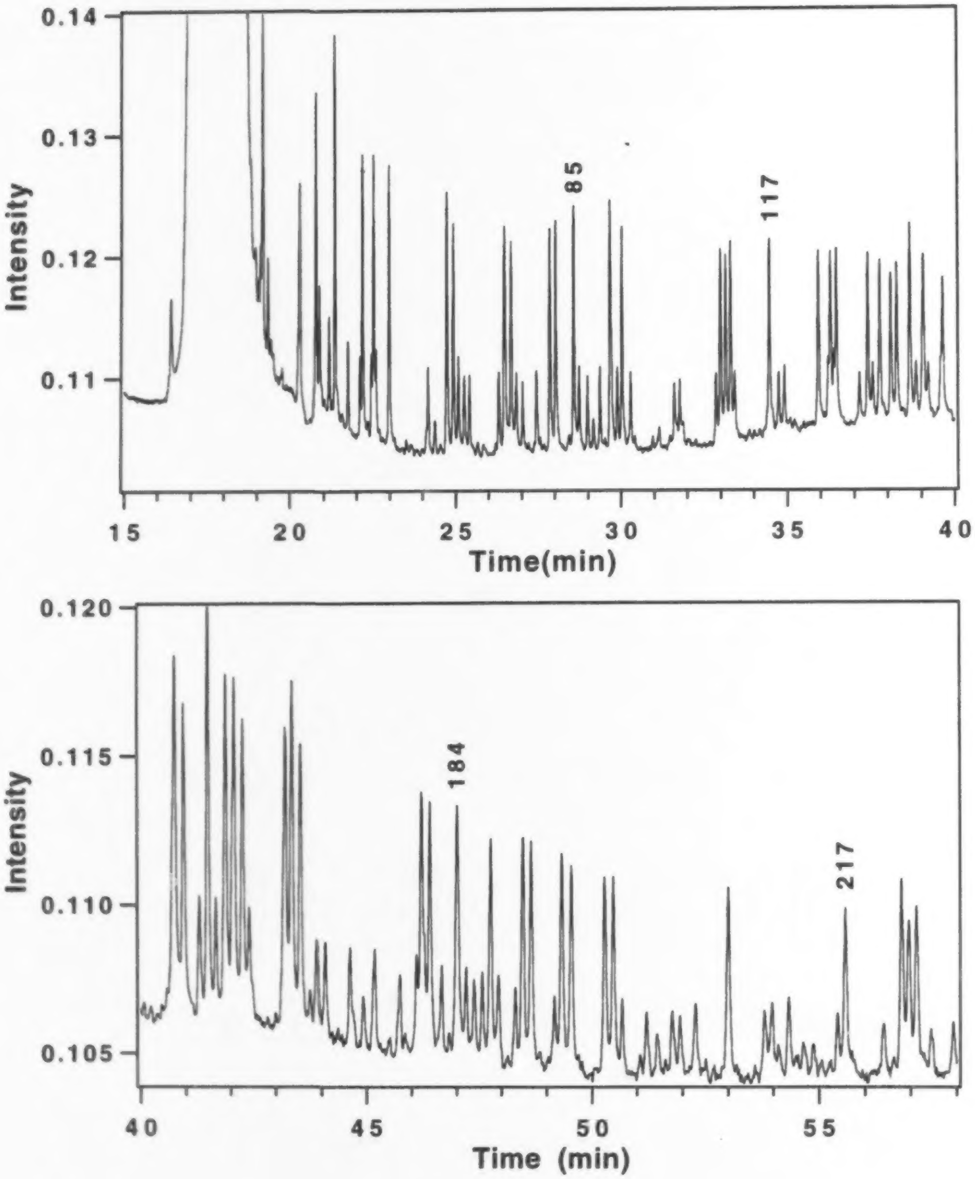

Figure 2.1D Separation of M13mp18 ddATP sample on 6%T 5%C. Other conditions as in fig. 2.1.A.

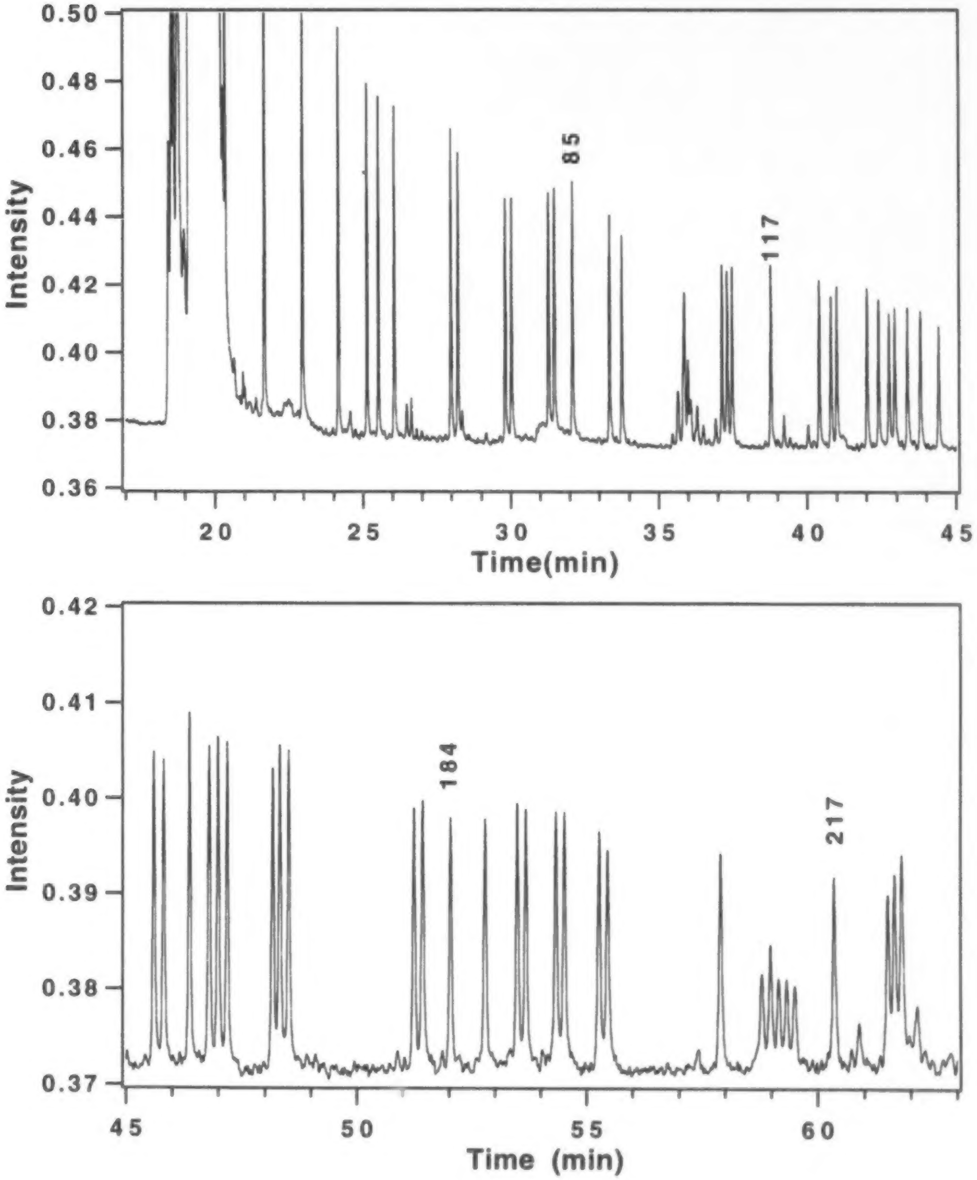

Table 2.1 Least squares slope and intercept from a plot of migration time, in minutes, versus the fragment length, in bases, for fragments ranging in size from 60 to 240 bases in length.

%C	slope (minute/base)	intercept (minute)	r
0	$1.02 \pm 0.04 \times 10^{-1}$	$1.1 \pm 0.1 \times 10^{1}$	0.9995
0.5	$1.17 \pm 0.08 \times 10^{-1}$	$1.2 \pm 0.1 \times 10^{1}$	0.9988
2.5	$1.75 \pm 0.03 \times 10^{-1}$	$1.1 \pm 0.5 \times 10^{1}$	0.9999
5.0	$1.61 \pm 0.09 \times 10^{-1}$	$1.2 \pm 0.2 \times 10^{1}$	0.9992

independent of the fragment length. The biased reptation model predicts that mobility is given by equation 1.23. This equation can be writen in a simpler form:

$$\mu = a\left(\frac{1}{N} + \frac{1}{N^*}\right) = \frac{a}{N} + \mu_\infty \qquad (2.2)$$

where a is the slope of the line, N^* is the fragment length for the onset of biased reptation with orientation, and μ_∞ is the mobility of the longest fragments. A plot of μ versus N^{-1} is shown in Figure 2.2.

The biased reptation model seems to apply to all the fragments larger than 125 bases for 0.5, 2.5, and 5%C and 200 bases in the case of 0%C. Equation 2.2 was fitted to the linear portion of the plot of mobility versus the inverse fragment length. The coefficients obtained are reported in Table 2.2.

The intercept, μ_∞, is the mobility of the longest fragments; lower %C gels generate higher mobilities for the longest fragments. The slope decreases with %C. The ratio a/μ_∞ is N^*. Fragments with N^* bases have half the mobility compared to the abscence of biased reptation with orientation. The linear polyacrylamide produces the highest values of N^*, which suggests that the non-cross-linked polymer suffers least from the effects of biased reptation with orientation.

According to the biased reptation model, the slope of equation 2.2 is inversly proportional to the frictional coefficient for migration of an elongated fragment through the gel. The decrease in slope with the increase of %C implies that the frictional force experienced by the fragment decreases with the decrease of %C (see Appendix A). This decrease in the friction coefficient with the decrease in %C is expected (the decrease between 5%C and 0%C is related to the fact that one is a cross-linked polymer, and the

Figure 2.2 Average mobility versus the inverse of fragment length for different polymers.

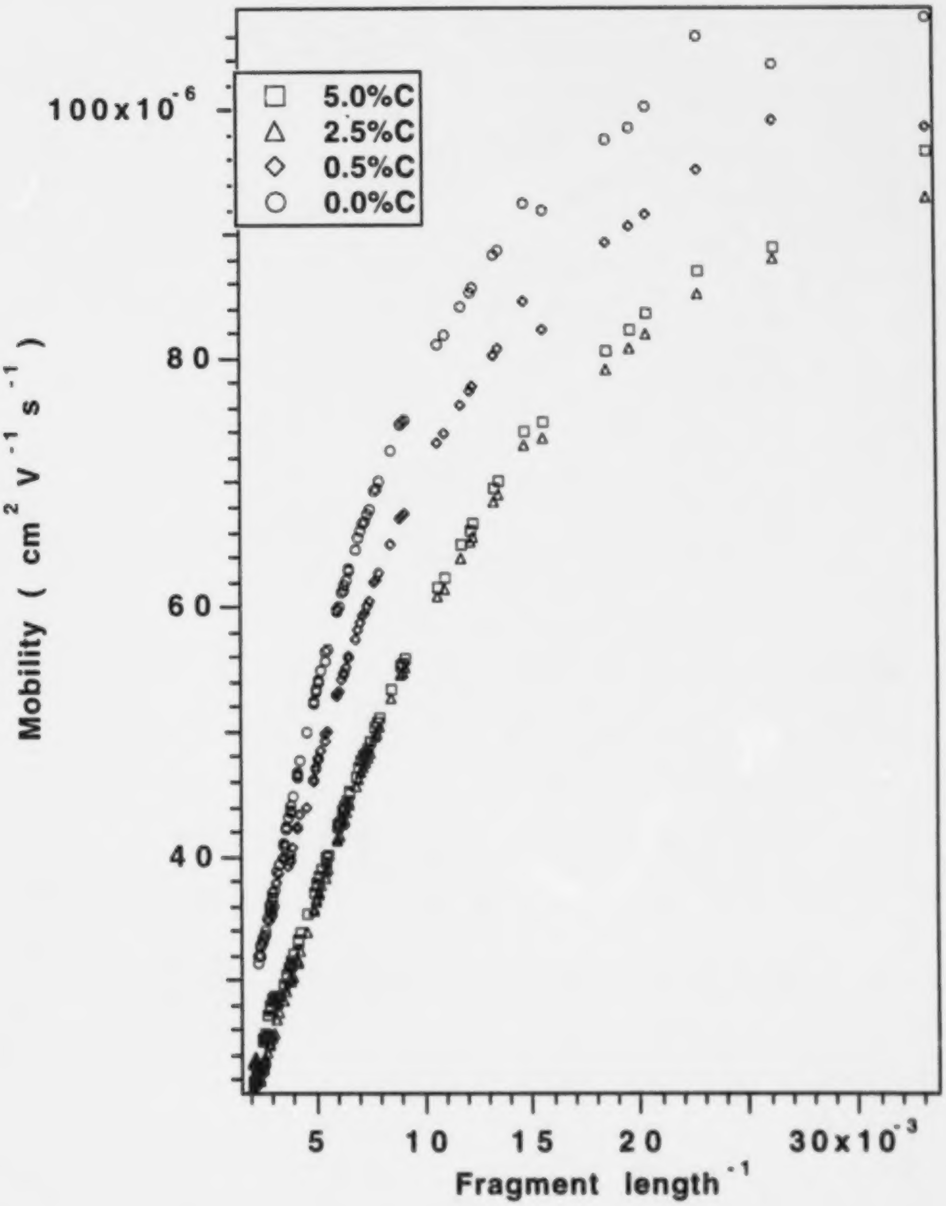

Table 2.2 Least squares slope (S) and intercept (I) from a plot of mobility versus N^{-1}, where N is the fragment length in bases. The least-squared fit was performed for fragments longer than 200 bases. N^* is found by dividing the slope by the intercept, and gives a measure of the fragment size for which biased reptation with orientation becomes significant.

%C	$S \times 10^3$	$I \times 10^5$	S^{-1}	α_S (nm)	N^*	r
0	8.11 ± 0.03	1.25 ± 0.01	123	16.5	650	0.9998
0.5	5.77 ± 0.04	1.78 ± 0.02	173	20.7	320	0.9994
2.5	5.25 ± 0.02	0.97 ± 0.01	190	17.5	540	0.9997
5.0	4.97 ± 0.02	1.23 ± 0.01	201	19.2	400	0.9997

other is a linear polymer). The intercepts from Table 2.2 are related to the radius of the pore of polyacrylamide (Appendix A). The calculated value of the pore's size (α_S) for 6%T 5%C is in agreement with a previously published result of 26 nm[30], but the published values of 110 nm for 2.5%C, and 103 nm for 0.5%C do not agree with our calculation. These huge differences are probably due to gel preparation. Holmes[30] prepared her gels at a higher concentration of TEMED and ammonium persulfate without adding urea. The pore's size differences could also be due to the fact that Holmes used Ferguson plots to calculate the pore's size and we used the reptation models.

A Gaussian function was fitted to the peaks obtained for bases 85, 117, 184, 217, 258, 309, 350 and 396 according to equation 1.9. The number of theoretical plates, N_p, was estimated using equation 1.10. The plate count, Figure 2.3, varied slightly with the fragment length; the shortest fragments produced roughly a factor of two higher plate counts compared to the longest fragments. Plate counts were lower for lower %C polyacryalmides; however, the correlation between plate counts and cross-linker concentrations is poor, r=0.62.

In zone electrophoresis, the number of theoretical plates is given by equation 2.3. Both diffusion coefficient and mobility depend on the product of fragment size and viscosity; the ratio should be independent of those two parameters [31]. Variation in plate counts with the fragment length probably is associated with the change in shape of the fragments, as they undergo transition from a random coil conformation for the small fragments, to a linear configuration for the longer fragments.

$$N_p = \frac{E\,\mu}{2\,D} \qquad (2.3)$$

Figure 2.3 Average number of theoretical plates versus fragment length for different concentrations of cross-linker.

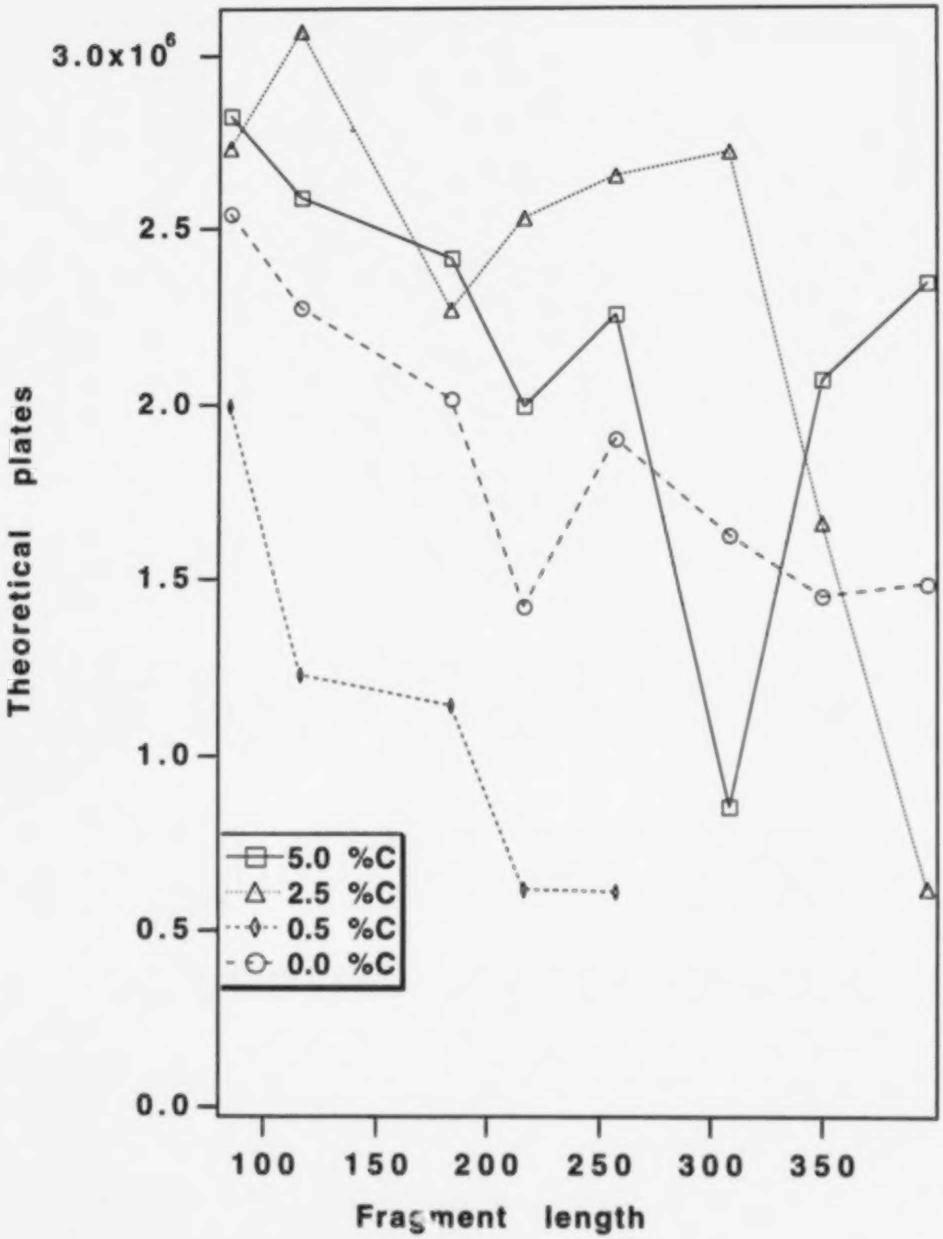

While plate counts vary slowly with fragment lengths, the spacing between adjacent peaks decreases for longer fragments. This phenomenon is a result of biased reptation with orientation, and leads to a degradation in the resolution with the fragment length. Figure 2.4 presents the resolution of adjacent fragments. We found the resolution of the adjacent peaks to be inversely proportional to the fragment length, Table 2.3. In this case, the resolution asymptotically approaches zero for long fragments as peak spacing goes to zero for long fragments. Resolution may be written as:

$$R = \frac{\beta}{N} \tag{2.4}$$

where β is a proportionality constant. The proportionality constant increases with cross-linker concentrations; there is a more rapid decrease in resolution with the fragment length for high %C gels compared with low %C gels. This result reflects the earlier onset of biased reptation for higher %C gels.

Resolution drops below 1 for fragments longer than ~250 bases for low %C gels. As a result, it would be difficult to obtain sequence information for longer fragments. This observation is consistent with the data of both Mathies and Pentoney, who were unable to obtain sequence information for fragments longer than ~300 bases in 0%C gels [10,12].

We were unable to reproduce the long column life reported by Guttman for linear polyacrylamide. After two or three injections, our capillaries inevitably failed, producing very low resolution separations. This observation is not surprising. Early reports on capillary gel electrophoresis separations of oligonucleotide standards stated that at least a hundred separations could be performed without replacing the gel. However, no group has been able to reuse gel filled capillaries for many separations when dealing with DNA sequencing samples. The high molecular weight template present in the sequencing sample

Figure 2.4 Average resolution versus fragment length for different concentrations of cross-linker.

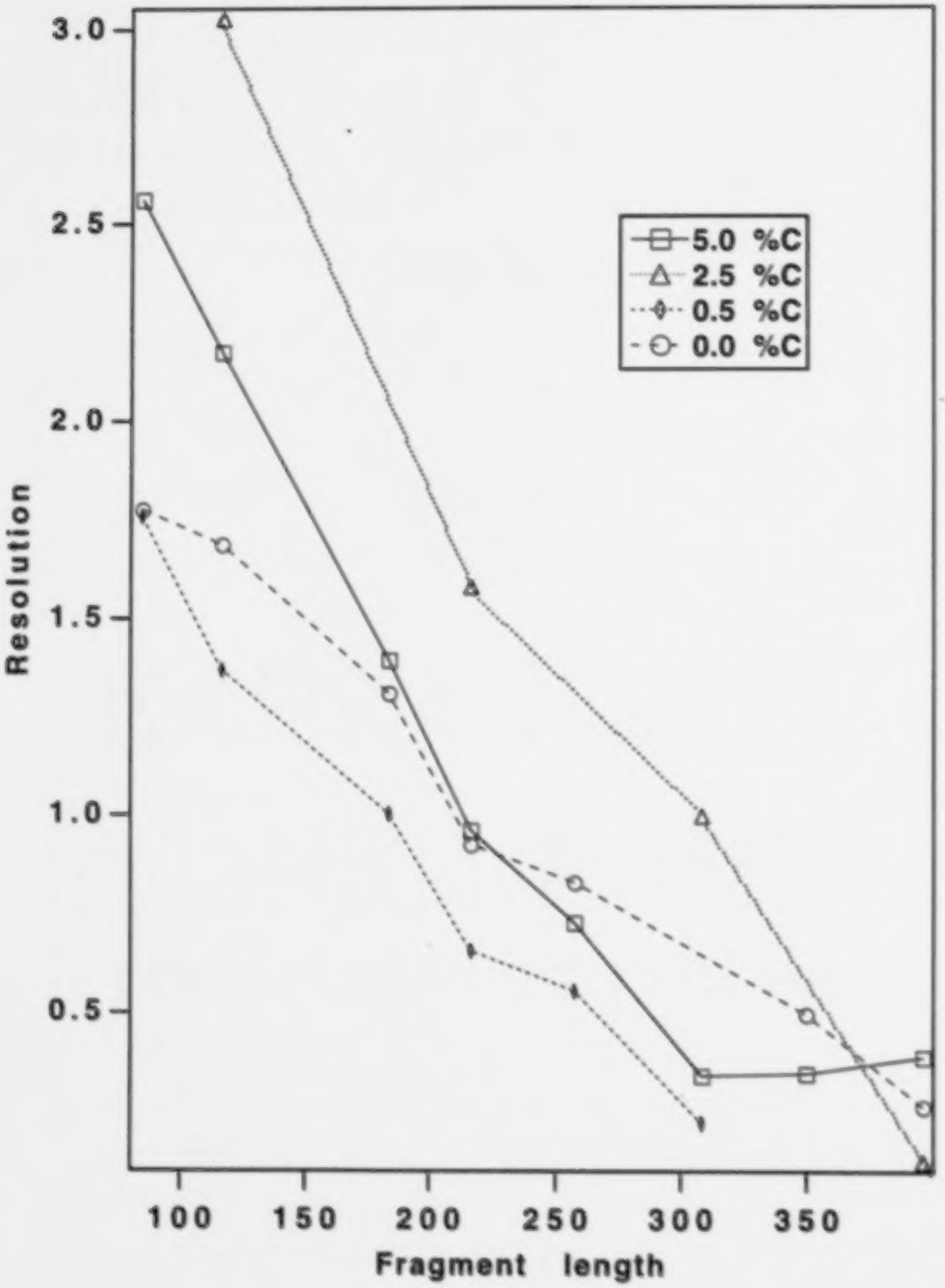

Table 2.3 Least squares slope and intercept from a plot of resolution versus N^{-1}, where N is the fragment length in bases. Slope is given to two significant figures.

%C	Slope	Intercept	r
0	160 ± 30	0.1 ± 0.2	0.93
0.5	170 ± 20	-0.1 ± 0.2	0.97
2.5	350 ± 40	-0.2 ± 0.2	0.97
5	260 ± 20	-0.3 ± 01	0.98

leads to rapid degradation of the gel performance[32]. Linear polyacrylamide is not immune to this phenomenon.

2.4 Conclusions

Mobility decreases with increasing cross-linker concentrations. The addition of cross-linker increases the electrophoretic friction of the polymer, retarding the analyte. The transition from normal mobility to the limiting mobility of reptation with orientation occurs for longer fragments as the %C is decreased. Both observations are explained by a increase in electrophoretic friction produced by a higher concentration of cross-linker.

The later onset of the effects of biased reptation with orientation for low %C polyacrylamide implies that the material would be more useful than high %C polyacrylamide for DNA sequencing applications; longer sequencing runs should be possible. The resolution is better in 2.5%-5%C than in 0%C for fragment smaller than 200 bases; however, the resolution in 2.5%-5%C decreases faster than in 0%C that mean that 0%C should be more useful for the separation of longer fragment than 2.5%-5%C.

2.5 Bibliography

(1) Swerdlow, H.; Gesteland, R. *Nucleic Acids Research* **1990**, *18*, 1415-1419.

(2) Drossman, H.; Luckey, J. A.; Kostichka, A. J.; D'Cunha, J.; Smith, L. M. *Analytical Chemistry* **1990**, *62*, 900-903.

(3) Cohen, A. S.; Najarian, D. R.; Karger, B. L. *Journal of Chromatography* **1990**, *516*, 49-60.

(4) Swerdlow, H.; Wu, S.; Harke, H.; Dovichi, N. J. *Journal of Chromatography* **1990**, *516*, 61.

(5) Swerdlow, H.; Zhang, J. Z.; Chen, D. Y.; Harke, H. R.; Grey, R.; Wu, S.; Dovichi, N. J.; Fuller, C. *Analytical Chemistry* **1991**, *63*, 2835-2841.

(6) Chen, D.; Harke, H. R.; Dovichi, N. J. *Nucleic Acids Research* **1992**, *20*, 4873-4880.

(7) Chen, D. Y.; Swerdlow, H. P.; Harke, H. R.; Zhang, J. Z.; Dovichi, N. J. *Journal of Chromatography* **1991**, 237.

(8) Karger, A. E.; Harris, J. M.; Gesteland, R. F. *Nucleic Acids Research* **1991**, *19*, 4955-4962.

(9) Luckey, J. A.; Drossman, H.; Kostichka, A. J.; Mead, D. A.; D'Cunha, J.; Norris, T. B.; Smith, L. M. *Nucleic Acids Research* **1990**, *18*, 4417-4421.

(10) Pentoney, S. L.; Konrad, K. D.; Kaye, W. *Electrophoresis* **1992**, *13*, 467-474.

(11) Rocheleau, M. J.; Dovichi, N. J. *Journal of Microcolumn Separations* **1992**, *4*, 449-453.

(12) Huang, X. C.; Quesada, M. A.; Mathies, R. A. *Analytical Chemistry* **1992**, *64*, 2149-2154.

(13) Takahashi, S.; Murakami, K.; Anazawa, T.; Kambara, H. *Analytical Chemistry* **1994**, *66*, 1021-1026.

(14) Smith, L. M. *Nature* **1991**, *349*, 812-813.

(15) Bode, H.-J. *Analytical Biochemistry* **1977**, *83*, 204-210.

(16) Bode, H.-J. *Analytical Biochemistry* **1977**, *83*, 364-371.

(17) Tietz, D.; Aldroubi, A.; Pulyaeva, H.; Guszczynski, T.; Garner, M. M.; Chrambach, A. *Electrophoresis* **1992**, *13*, 614-616.

(18) Pulyaeva, H.; Wheeler, D.; Garner, M. M.; Chrambach, A. *Electrophoresis* **1992**, 608-614.

(19) Tietz, D.; Gottlieb, M. H.; Fawcett, J. S.; Chrambach, A. *Electrophoresis* **1986**, *7*, 217-220.

(20) Heiger, D. N.; Cohen, A. S.; Karger, B. L. *Journal of Chromatography* **1990**, *516*, 33-48.

(21) Sudor, J.; Foret, F.; Bocek, P. *Electrophoresis* **1991**, *12*, 1056-1058.

(22) Chiari, M.; Nesi, M.; Fazio, M.; Righetti, P. G. *Electrophoresis* **1992**, *13*, 690-697.

(23) Guttman, A.; Wanders, B.; Cooke, N. *Analytical Chemistry* **1992**, *64*, 2348-2351.

(24) Harke, H. R.; Bay, S.; Zhang, J. Z.; Rocheleau, M. J.; Dovichi, N. J. *Journal of Chromatography* **1992**, *608*, 143-150.

(25) Righetti, P. G.; Caglio, S.; Saracchi, M.; Quaroni, S. *Electrophoresis* **1992**, *13*, 587-595.

(26) Rocheleau, M. J.; Grey, R. J.; Chen, D. Y.; Harke, H. R.; Dovichi, N. J. *Electrophoresis* **1992**, *13*, 484-486.

(27) Figeys, D.; Dovichi, N. J. *Journal of Chromatography* **1993**, *645*, 311-317.

(28) Slater, G. W.; Noolandi, J. *Biopolymers* **1985**, *24*, 2181.

(29) Lumpkin, O. J.; Déjardin, P.; Zimm, B. H. *Biopolymers* **1985**, *24*, 1573.

(30) Holmes, D. L.; Stellwagen, N. C. *Electrophoresis* **1991**, *12*, 612-619.

(31) Cheng, Y. F.; Wu, S.; Chen, D. Y.; Dovichi, N. J. *Analytical Chemistry* **1990**, *62*, 496.

(32) Swerdlow, H.; Dew-Jager, K. E.; Brady, K.; Grey, R.; Dovichi, N. J.; Gesteland, R. *Electrophoresis* **1992**, *13*, 475-483.

CHAPTER 3 [1]

STABILITY OF LINEAR POLYACRYLAMIDE USED FOR CAPILLARY ELECTROPHORESIS.

---

[1] A version of this chapter has been published.
Figeys, D., Renborg, A. and Dovichi, N.J. 1994 Electrophoresis 15:1512-1517.

3.1 Introduction

DNA sequencing samples are usually run on polyacrylamide gel[1-11] when using capillary electrophoresis. It is the only studied polymer that can be used to separate single-stranded DNA with high resolution. Other polymers such as agarose[12,13], or substituted cellulose[14,15], do not generate a high enough resolution in the range of fragment length found in sequencing samples.

Polyacrylamide is used in two forms. One is the cross-linked form[1,2,4,5,11,16] (usually with bisacrylamide), and the other one is the linear form[6-9] (without a cross-linker). Cross-linked polyacrylamide is usually a high viscosity gel. High resolutions can easily be obtained on it. Its main disadvantage is that cross-linked chains are limited in their movements. Thus, any *in situ* formation of bubbles destroys the gel. The resolution in linear polyacrylamide is lower than in identical %T cross-linked polyacrylamide [11]. The main advantage of linear polyacrylamide is its higher degree of freedom for the polymer chains. This freedom allows most of the *in situ* formation of bubbles to be accommodated. It is also less viscous than cross linked polyacrylamide; therefore, the sequencing is more rapid. Recently, linear polyacrylamide has been used for the separation of sequencing fragments over 550 bases in length[17].

The irreproducibility and variability of a gel in a high electric field is a major problem. Usually, only 2 to 4 runs can be performed on the same gel, and the migration time increases quite significantly. At the same time, the current through the capillary decreases. There have been a few studies on the effect of different parameters like %C, %T, temperature, and electric field[11,18-20] on the separation of DNA sequencing samples. These studies mainly focus on the optimization of the separation time versus the resolution.

Only a few studies of the stability, and the phenomena that occur in the gel have been published. Swerdlow *et al.*[21] studied the stability of cross- linked polyacrylamide for the separation of single-stranded DNA. They indicated that the drop in current through the gel during the electrophoresis and the amount of DNA template present in a sample could explain the increases in migration time observed in these gels. Spencer [22-24] studied the effect of charge carriers on the conductivity of polyacrylamide gel. He indicated that the formation of zones of different ionic concentrations could explain the drop in current observed in time (see section 1.3.2.2).

We wish to study the behavior of the current flow in linear polyacrylamide during electrophoresis conditions. In particular, there is often a steady decrease in current during an electrophoresis run[25]. This current drop can be quite significant. According to Ohm's law, a decrease in current is caused by an increase in resistance under the condition of a constant electric field. This decrease in current is accompanied by an increase in analyte migration times. There are two explanations for the decrease in current during an electrophoresis run. The first one is a uniform increase of the resistance throughout the capillary. Under this condition the electric field would be constant throughout the capillary and the analyte velocity would also be constant. The second explanation is that the resistance increase in a part of the capillary. Under this condition the electric field would be higher in the high resistance part and lower in the rest of the capillary. The second explanation is in agreement with the results observed because it predicts an increase in analyte migration times.

In this chapter, we present a phenomenological study of the effects of different variables on the conductivity of linear polyacrylamide in capillary electrophoresis. The effect of the age of the polymer, changes in the concentration of the charge carriers and the template are reported. The importance of each parameter and the ways of reducing their effects on the polymer are also discussed.

3.2 Experimental

Linear polyacrylamides (5%T) were prepared by taking 625 μL of a 40% acrylamide (BioRad, CA) stock solution, adding 1 mL of 5xTBE buffer [2.7 grams TRIS (ICN Biomedicals Inc., Cleveland, Ohio), 1.37 grams of boric acid (BDH Inc., Toronto, Ontario) and 1.0 mL 0.5M EDTA diluted to 50 mL in deionized filtered water), and 2.1 grams of urea (Gibco BRL, Gaithersburg, MD)] and making the solution up to 5.0 mL in deionized, filtered water. This solution was degassed for 20 minutes by bubbling argon gas through it. The polymerization reaction was initiated and catalyzed by adding 20 µL of 10% ammonium persulfate (Boehringer Mannheim Corp., Indianapolis, IN) and 2 µL N,N,N',N'-tetramethylethylenediamine (TEMED) (Gibco BRL, Gaithersburg, MD). Immediately following the addition of the initiator, the solution was injected into a fused silica capillary, (Polymicro, Phoenix, AR) with typical dimensions of 30 cm x 32 µm id x 143 µm od, which had been pretreated with γ-methacryloxypropyl trimethoxysilane (Sigma Chemical, St.Louis, MD) for one hour. All chemicals are of electrophoretic grade. The day of preparation is day zero; capillaries older than that were left to age on the bench and trimmed before use.

Current measurements were made by measuring the potential drop across a 1.1 MΩ resistor, added in series between the anodic end and the ground, and converting the voltage to current.

3.3 Results

A capillary electrophoretic system can be described as an Ohmic system. A potential E is applied through a resistor, R_t (capillary), generating a current I. Rather than dealing with resistance, it is convenient to consider the conductivity, κ, of the solution,

$$\kappa = \pi^{-1}\, r^{-2}\, R_t^{-1}\, L = \pi^{-1}\, r^{-2}\, I\, V^{-1}\quad L^{-1} = \pi^{-1} r^{-2}\, I E^{-1} \tag{3.1}$$

The conductivity of a solution is, in turn, related to the concentration of ions in the solution

$$\kappa = \sum_{1}^{n} \Lambda_i\, C_i \tag{3.2}$$

The capacitance, κ, can be divided to take into account the effect of the stress applied on the system:

$$\kappa = \kappa_k + \Delta\kappa_s \tag{3.3}$$

where κ_k is the conductivity of the capillary at equilibrium with no stress applied (steady-state conductivity). κ_k is a constant for a particular polymer concentration and a particular buffer. $\Delta\kappa_s$ is the change in conductivity generated by the application of a stress. Many stress generators were proposed to explain the decrease in current when running sequencing samples: depletion of ions at the injection end[22-24] of the capillary, created by different transference numbers in the solution and the polymer, plugging of the pore by large DNA fragments (template)[25], depletion zone created by the difference of mobilities between DNA and the main current carriers and degradation of the polymer.

The value of $\Delta\kappa_s$ can be further subdivided into two parts. The first part represents what we call the depletion of ions effect. The depletion of ions effect is represented as $\Delta\kappa_{depletion}$. The second part of $\Delta\kappa_s$ represents the effect of the template in a DNA sequencing sample ($\Delta\kappa_{template}$). Equation 3.1 can be rewritten as:

$$\kappa = \kappa_k + \Delta\kappa_{depletion} + \Delta\kappa_{template} \tag{3.4}$$

Figure 3.1 shows a typical plot of current versus time for a 14-day old 5%T linear polyacrylamide run at -300 V/cm. The data were fitted by a two-component exponential

$$I(\mu A) = 1.24\ \mu A + 0.927\ \mu A \exp\left(\frac{-t}{5.7\ \text{min}}\right) + 0.151\ \mu A \exp\left(\frac{-t}{235\ \text{min}}\right) \tag{3.5}$$

The fast component (part A) in the current decay is mainly due to the way the polymer was prepared. The polymer contains ammonium persulfate (1.75 mM) and TEMED (2.65 mM)

Figure 3.1 Current versus time for a 14-day old 5%T linear polyacrylamide run at -300 V/cm. The bottom panel represents the residual of the subtraction of the double exponential fitting from the top curve

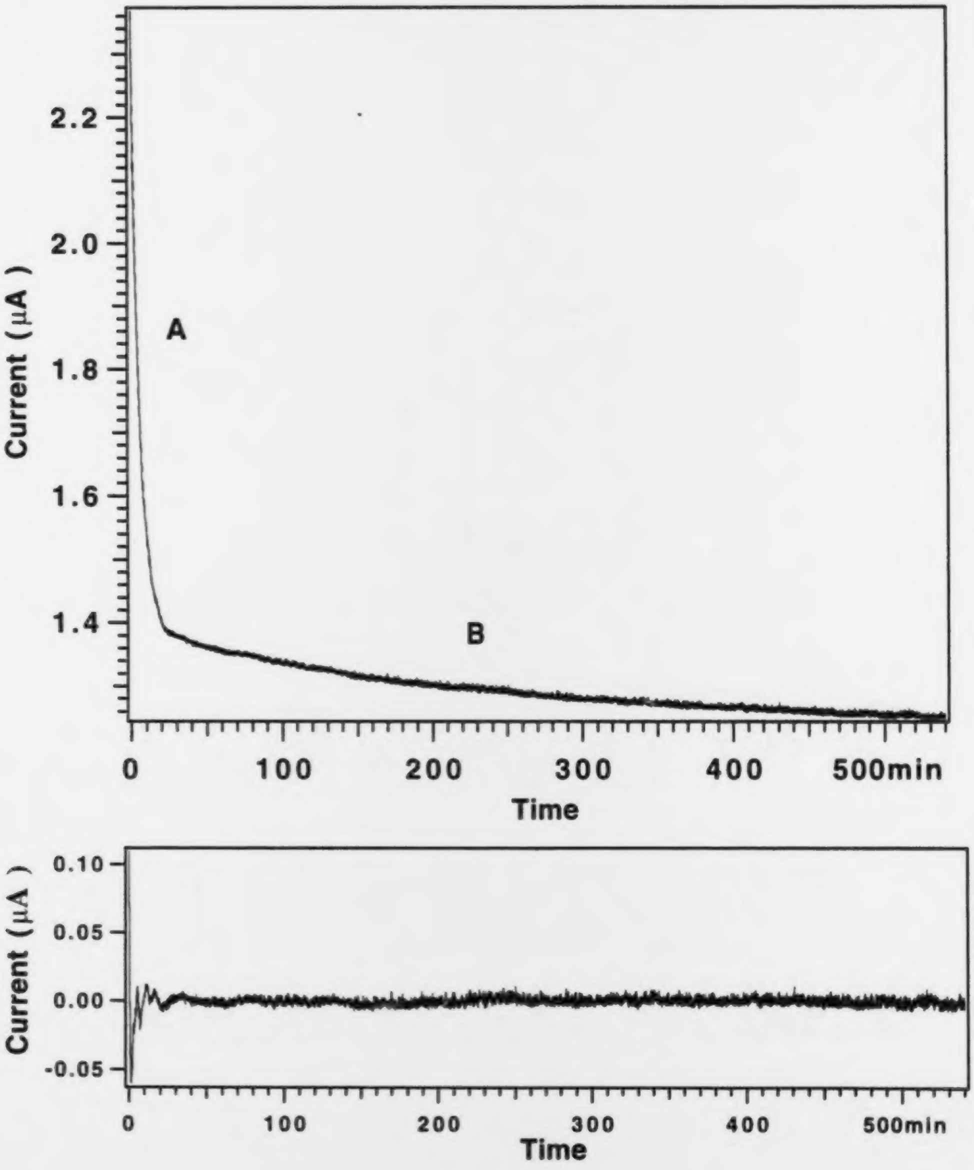

which is charged at pH=8.4. Ammonium persulfate and TEMED are not present in the 1xTBE reservoir. Thus, in part A of the curve, ammonium persulfate and TEMED are expelled from the polymer. Also, the polymer's buffer concentration is calculated to be 1xTBE by diluting 1 mL of 5xTBE in 5 mL of total volume before polymerization; however, the total volume available to the buffer is not 5 mL because of the huge concentration of urea and the formation of a polymer network. The total concentration is thus higher than 1xTBE; therefore, in the part A of the curve, the concentration of TBE inside the capillary "equilibrates" with the 1xTBE running buffer. The 5.7 minute time constant for the part A is the typical migration time for small ions. This equilibration accounts for the common practice of applying an electric field to the capillary for half an hour, or longer, before performing any separation.

In part B of the curve, the concentration difference has been corrected, and the main effects affecting the current are the ones related to equation 3.2. The second component in the current drop (part B) occurs over a much longer time period, with an exponential time constant of 235 minutes. The current dropped by about 12% due to this slow component during a 500 minute electrophoresis run. In this report, we are interested in studying the steady decrease of the current with time in part B of the curve.

In equation 3.4, κ_k is considered constant, but both $\Delta\kappa_{depletion}$ and $\Delta\kappa_{template}$ can change. It would be very difficult to separate $\Delta\kappa_{depletion}$ from $\Delta\kappa_{template}$ if both of them changed significantly at the same time. We found a way of obtaining polymers where $\Delta\kappa_{depletion}$ is significantly reduced during an appreciable period of time (see section 3.3.1.1).

The phenomenon of depletion of ions depends on the components of the buffer and the polymer used. In the case of 1xTBE buffer, TRIS is the main cation charge carrier and borate is the main anion charge carrier. The mobilities of these ions are different. Thus, a change in concentration of the charge carrier will happen at the reservoir:capillary interfaces. For 1xTBE, TRIS seems to have a higher transference number in the buffer reservoir than in the capillary. Thus, a depletion of ions happens at the injection end with time. Similarly, an increase in ions should happen at the ground end of the capillary. Spencer *et al.*[22] have shown that, in the case of normal buffers, the depletion area should always move inside the capillary, and the increase area should move out of the capillary.

3.3.1 Effect of $\Delta k_{depletion}$

3.3.1.1 Age of Polyacrylamide

We prepared many different 5%T linear polyacrylamide filled capillaries from completely different starting solutions. Because no injection of template was done in this part, $\Delta\kappa_{template}$ is zero. Each capillary was run at -300 V/cm for at least 6 hours with 1xTBE as the running buffer. Each capillary was only used once. The conductivity versus time was fitted using a double exponential decay for fresh polyacrylamides (equation 3.6). In the case of older polyacrylamide, the exponential terms from equation 3.6 were fitted separately (one exponential for each part of the conductivity profile(see Figure 3.1)). In the case of older polyacrylamides. Fitting with a double exponential instead of two separated exponential decays seems fine for fresh polyacrylamides because the terms for the depletion of ion and for the expulsion of small ions are both large. In the case of older polyacrylamides the term for the depletion of ions is much smaller than the term for the expulsion of small ions. Also, the depletion of ions happens on a longer time than the expulsion of small ions. Which means that the depletion of ions has a lot more data points to described it than the expulsion of ions. The coefficients were slightly correlated for older polyacrylamides using a double exponential.

$$\kappa(h\Omega^{-1}\ m^{-1}) = w_0 + w_1 \exp\left(\frac{-t}{w_2}\right) + w_3 \exp\left(\frac{-t}{w_4}\right) \qquad (3.6)$$

The first exponential term is related to the expulsion of small ions from the capillary during the equilibration period of the capillary with the running buffer. Our results suggest that

Figure 3.2 W_1 versus the age of polyacrylamide.

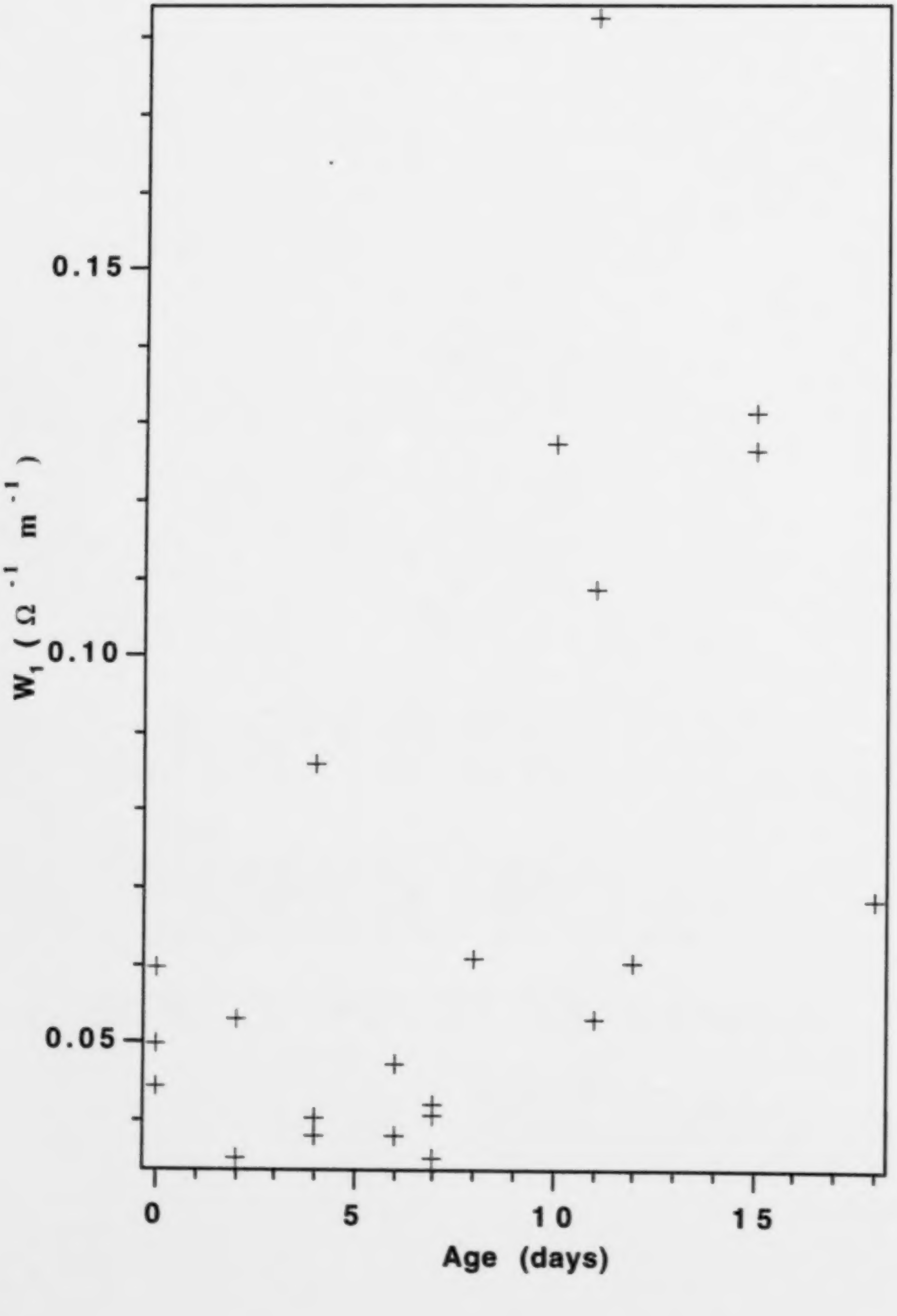

the coefficient, W_1, increases slightly with the age of the polymer (Figure 3.2). However, the time constant, W_2, for the expulsion of small ions is independent of the age of the polymer and as a median value of 8±4 minutes. These results suggest that the difference in ionic concentration between the polymer and the running buffer increases with the aging of the polyacrylamide; however, the gel structure does not seem to change sufficiently with age to affect the mobility of small ions, because the time constant is independent of the age of the polymer.

The second exponential term in the equation is related to the phenomenon of depletion of ions. The amplitude of the second exponential fit (W_3 found in equation 3.6) decreases (Figure 3.3) with the age of polyacrylamide as described by equation 3.7.

$$w_3(h\Omega^{-1}\ m^{-1}) = 1.2 \pm 0.4\ h\Omega^{-1}\ m^{-1} + 3.2 \pm 0.4\ h\Omega^{-1}\ m^{-1} \exp\left(\frac{-day}{3.5 \pm 1.2\ day}\right) \qquad (3.7)$$

This result is in agreement with the fact that the depletion of ions is smaller for older polymers than for younger polymers. It also indicates that there still is a small depletion of ions ($1.2 \pm 0.4\ h\Omega^{-1}\ m^{-1}$) in older polyacrylamides. W_4 is constant at 108 ± 50 minute.

The constant W_o is the limiting conductivity of the polymer (Figure 3.4), and increases exponentially with the age of the polymers.

$$w_0(h\Omega^{-1}\ m^{-1}) = 6.4 \pm 0.4\ h\Omega^{-1}\ m^{-1} - 4.8 \pm 0.4\ h\Omega^{-1}\ m^{-1} \exp\left(\frac{-day}{5 \pm 1\ day}\right) \qquad (3.8)$$

The maximum depletion of ions ($4.8 \pm 0.4\ h\Omega^{-1}\ m^{-1}$ for a 0-day old polyacrylamides) is 71 % of the steady-state conductivity ($6.8 \pm 0.8\ h\Omega^{-1}\ m^{-1}$). The time constant (5 ± 1 day) is the age when the depletion of ions is only 37% of the maximum depletion value ($4.8 \pm 0.4\ h\Omega^{-1}\ m^{-1}$). After 15 days, the depletion of ions is only 10% of the maximum value. These results clearly indicate that the older polyacrylamides generate

Figure 3.3 W3 versus the age of polyacrylamide.

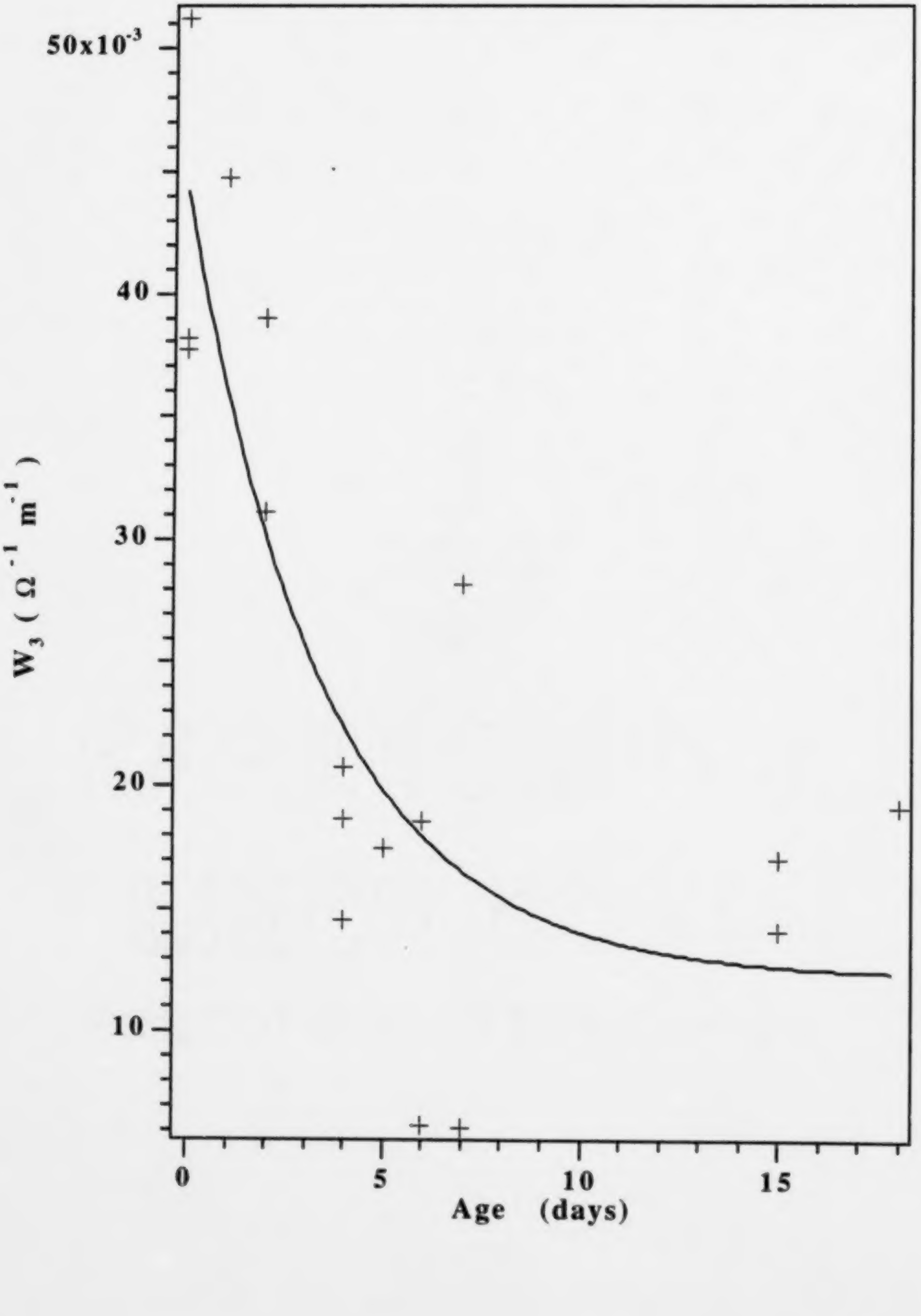

Figure 3.4 W_O versus the age of polyacrylamide.

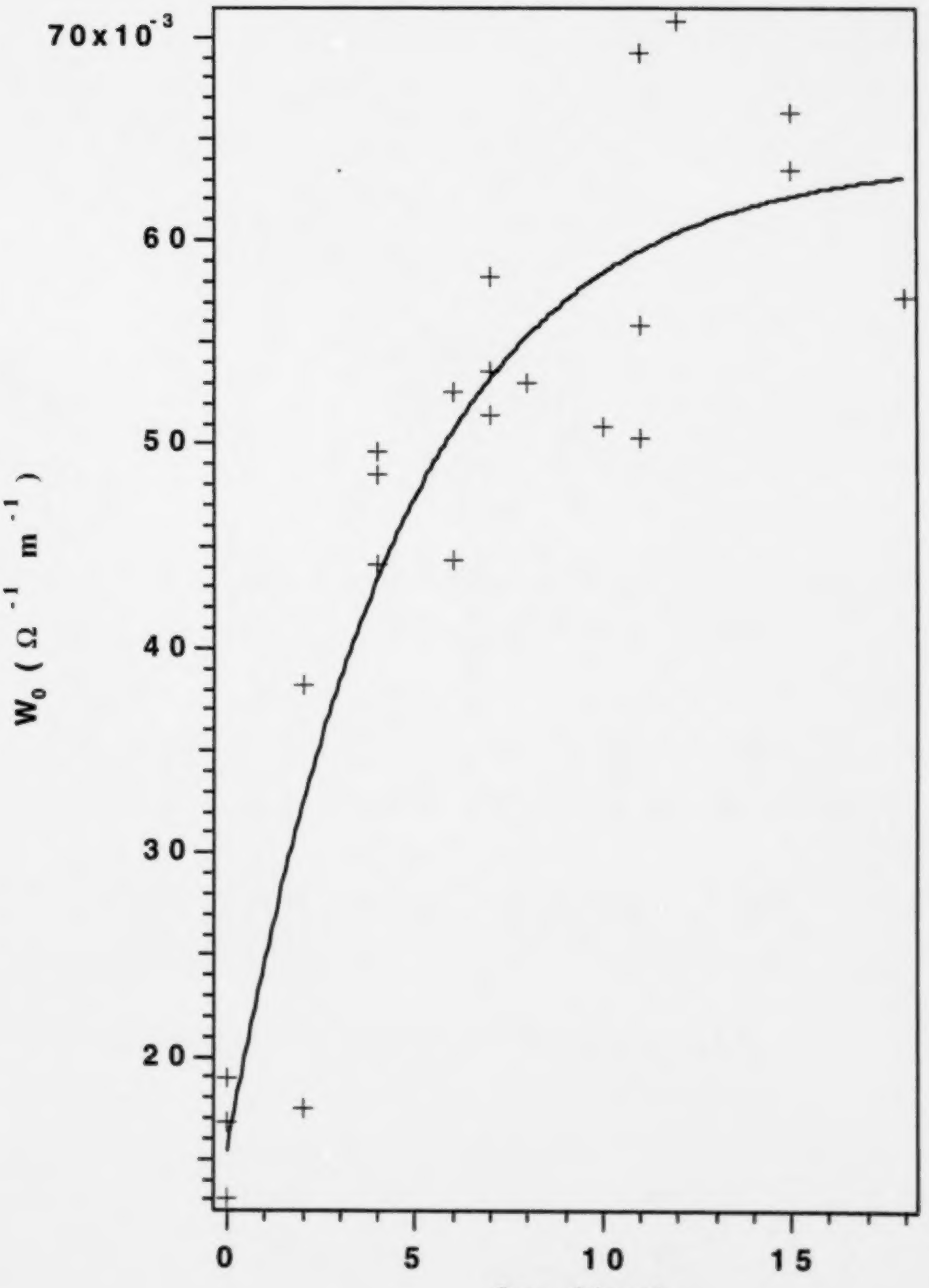

higher conductivities than the younger polyacrylamides. The steady-state conductivity of the polymer is obtained by adding up the values of W_0 and W_3 and is $6.8 \pm 0.8\ h\Omega^{-1}\ m^{-1}$. This value is the conductivity that the polymer should have after equilibration and without the depletion of ions. In the case of older polyacrylamides, the $\Delta k_{depletion}$ part is very stable, which is not the case for younger polyacrylamides.

3.3.1.2 Depletion of Ions

During electrophoresis, where a tube of polymer is immersed with each end in a buffer reservoir, a zone of decreased concentration will move into one end of the polymer, and a zone of high concentration will move out of the other end of the polymer into the buffer reservoir; the high concentration zone is dissipated in the receiving buffer reservoir.

To localize spatially the resistance change, we ran capillaries with 1xTBE for 3 hours at -300 V/cm. Then, we carefully cut parts of the capillary at the injection end. The potential was readjusted to keep the field at -300 V/cm, and the current was measured for 20 seconds. The time involved in cutting the capillary was less than a minute per cut, that means that the diffusion during the cutting was negligible. The conductivity was calculated from the value of the current according to:

$$\kappa(\Delta L) = \pi^{-1}\, r^{-2}\, I(\Delta L = 0)\ E^{-1} - \pi^{-1}\, r^{-2}\, I(\Delta L)\, E^{-1} \tag{3.9}$$

where I ($\Delta L = 0$) is the current drop across the entire capillary, and I(ΔL) is the current drop across the remainder of the capillary after length ΔL has been trimmed. We expected that applying the field for only 20 seconds would not significantly disturb the system. A conductivity profile was generated for each capillary used.

The capillary can be divided into many parts, with each part having a specific concentration of ions. The conductivity of the capillary is related to the concentration of ions in the divisions. A uniform concentration of buffer ions throughout the capillary will produce a constant conductivity versus the length of the capillary cut. Similarly, if the concentration of the buffer ions is lower in the parts cut than in the rest of the capillary, the conductivity will increase with the length cut. Inversely, if the concentration of buffer ions is higher in the parts cut than in the rest of the capillary, then the conductivity will decrease with the length cut. Figure 3.5 (full lines; left and bottom axis) shows the change in conductivity observed versus the total length of capillary cut at the injection end for different ages of polyacrylamide. In the absence of diffusion, ionic depletion leads to a sharp conductivity boundary that moves through the gel. In the presence of diffusion, this boundary is smeared. A non-linear regression algorithm was used to get the best fitting equation (equation 3.10, and dotted curve on figure) of the data (Full curve) given in Figure 3.5.

$$\kappa = \kappa_0 - \Delta\kappa \exp\left(\frac{-\Delta L}{\delta L}\right)^2 \tag{3.10}$$

Where κ_0 is the steady-state conductivity in the absence of ionic transport, $\Delta\kappa$ is the change in conductivity induced at the capillary tip, ΔL is the length trimmed from the capillary, and δL is the characteristic distance over which depletion is noticed. For the 1-day old polyacrylamide, the data are fitted by the function

$$\kappa = 7.12\ \mathrm{h}\Omega^{-1}\ \mathrm{m}^{-1} - 3.04\ \mathrm{h}\Omega^{-1}\ \mathrm{m}^{-1} \exp\left(\frac{-\Delta L}{1.6}\right)^2 \tag{3.11}$$

The data for the 4-day old polyacrylamide are fitted with

$$\kappa = 6.48\ \mathrm{h}\Omega^{-1}\ \mathrm{m}^{-1} - 1.28\ \mathrm{h}\Omega^{-1}\ \mathrm{m}^{-1} \exp\left(\frac{-\Delta L}{1.2}\right)^2 \tag{3.12}$$

while the data for the 9-day old polyacrylamide are fitted with the function

$$\kappa = 7.12\ \mathrm{h}\Omega^{-1}\ \mathrm{m}^{-1} - 0.80\ \mathrm{h}\Omega^{-1}\ \mathrm{m}^{-1} \exp\left(\frac{-\Delta L}{4.4}\right)^2 \tag{3.13}$$

Figure 3.5 Conductivity profile at the injection end for different ages of polyacrylamide.

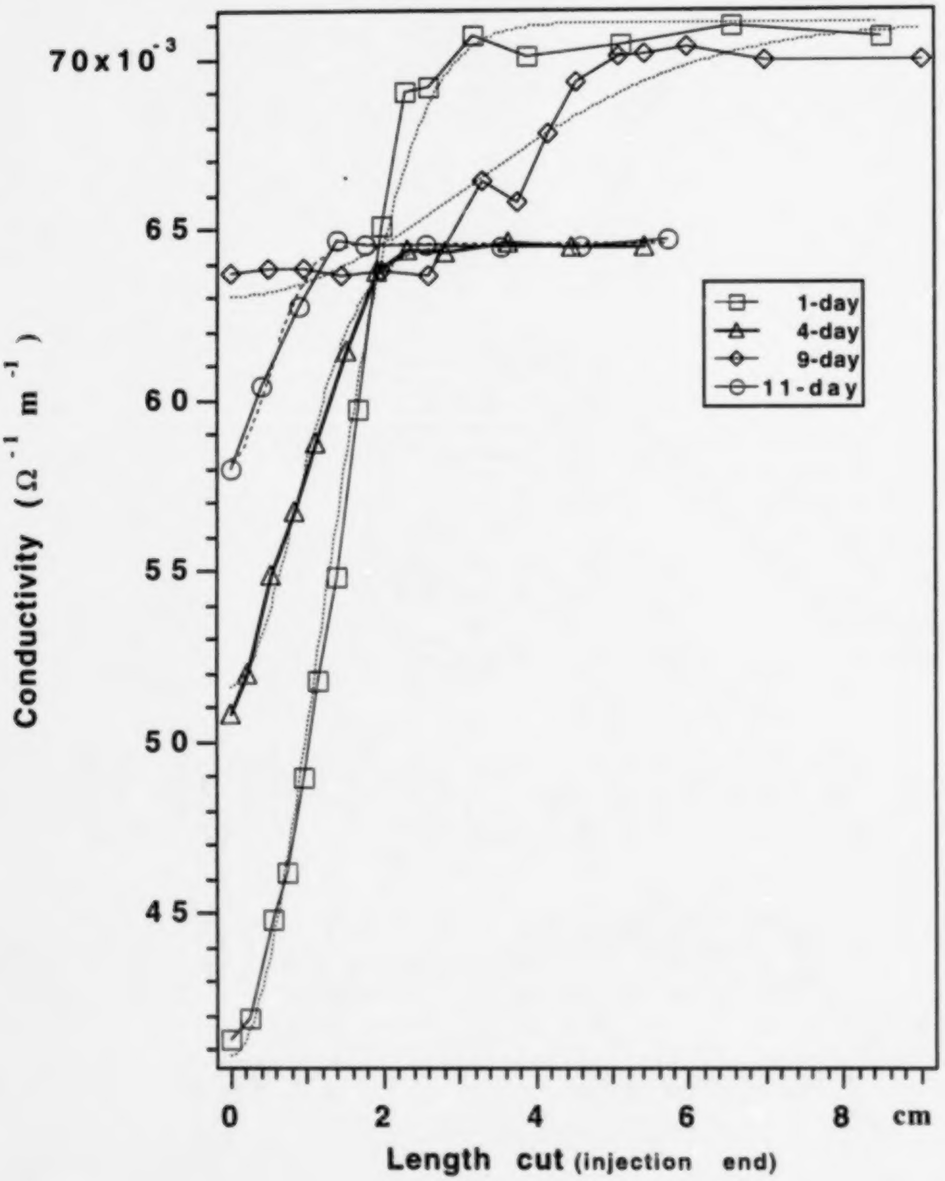

and the data for the 11-day old polyacrylamide are fitted with

$$\kappa = 6.44\ \mathrm{h}\Omega^{-1}\ \mathrm{m}^{-1} - 0.64\ \mathrm{h}\Omega^{-1}\ \mathrm{m}^{-1}\ \exp\left(\frac{-\Delta L}{0.73}\right)^{2} \qquad (3.14)$$

Notice that the steady-state conductivity of the capillaries was identical within experimental error, and has an average value of $6.8 \pm 0.4\ \mathrm{h}\Omega^{-1}\ \mathrm{m}^{-1}$. The variation of the steady-state conductivity of the capillaries is due to the 1 μm variation of the radius of the capillaries, which corresponds to a conductivity variation of $0.8\ \mathrm{h}\Omega^{-1}\ \mathrm{m}^{-1}$. The steady-state conductivity is also in agreement, within experimental error, with the result, $6.8 \pm 0.8\ \mathrm{h}\Omega^{-1}\ \mathrm{m}^{-1}$, from section 3.3.1.1. That is, aging did not affect the steady-state mobility of ions within the polymer. Also, the 1-day old polymer showed a 40% decrease in conductivity at the injection end, reaching a limit conductivity of $4.08\ \mathrm{h}\Omega^{-1}\mathrm{m}^{-1}$ at the injection tip. The region of enhanced resistance extended about 1.6 cm into the gel. This large change in conductivity at the injection end of the capillary must be associated with a significant depletion of ions from this region; roughly 40% of the ions have been expelled from the neighborhood of the injection tip of the 1-day old capillary. On the other hand, the 11-day old polyacrylamide showed a 10% decrease in conductivity at the injection end. The values of $\Delta\kappa$ decrease with the age of the polyacrylamide, which is also in agreement with the results of section 3.1.1.

The distance over which the ionic depletion occurs is large for the 9-day old polyacrylamide. A front, or region, of rapidly changing conductivity occurs between 3 to 5 cm from the injection tip. For all the other capillaries studied the area where a large depletion of ions happens is 2 cm or less.

We also cut pieces from the positive end of the capillaries (Figure 3.6). No significant changes in conductivity were observed up to 5.5 cm away from the positive end for polyacrylamides of any ages.

Figure 3.6 Conductivity profile at the ground end for different ages of polyacrylamide.

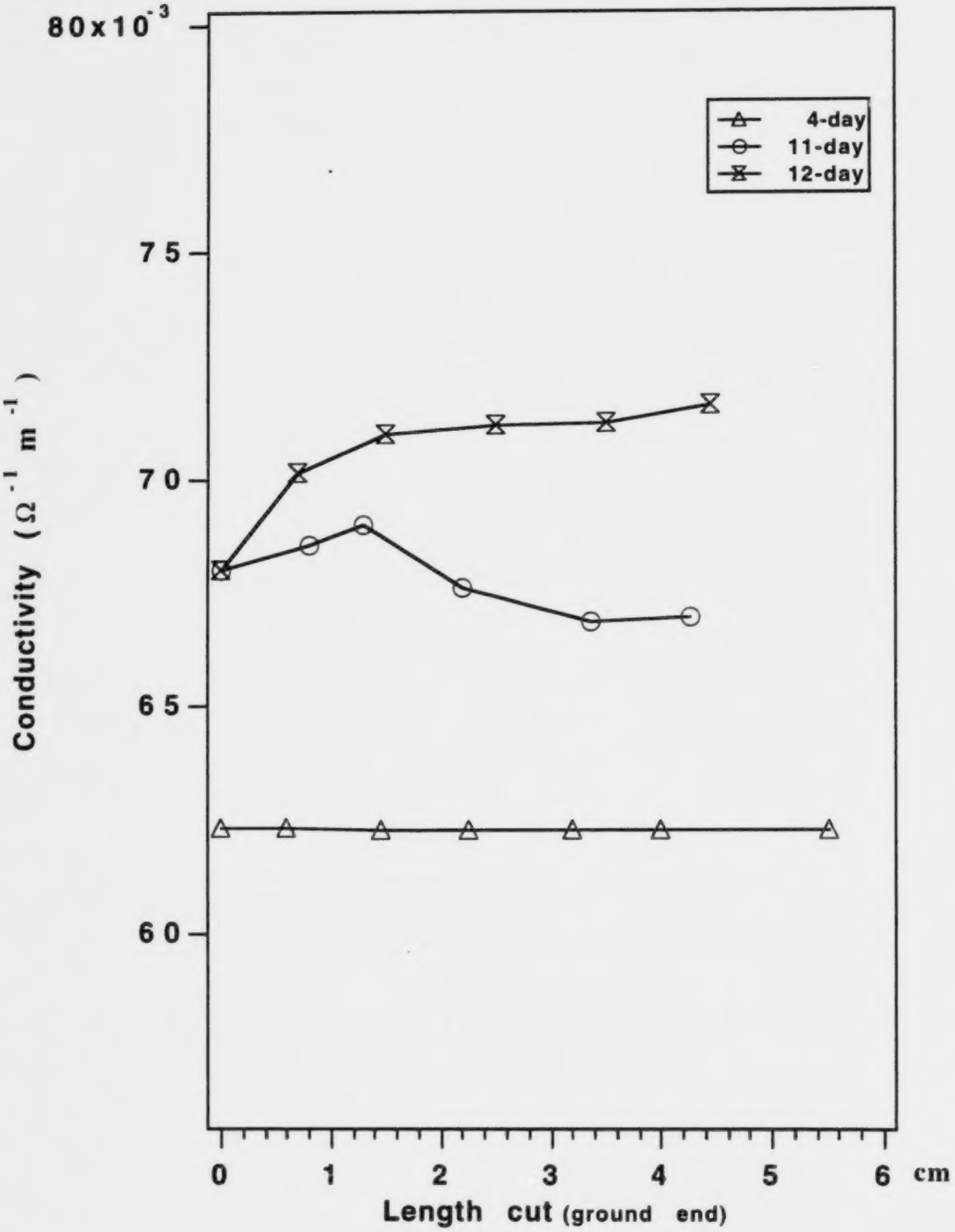

3.3.1.3 Depletion of Ions- Temporal Evolution of Spatial Profile

To study the evolution of the region of high resistance, a set of 1-day old linear polyacrylamide filled capillaries, and a set of 9-day old linear polyacrylamide filled capillaries were operated at -300 V/cm for different periods of time. Figure 3.7 shows the conductivity observed versus the total length of capillary cut for different run times for the 1-day capillaries (full lines) and the 9-day old capillaries (dotted lines).

In the case of the 1-day old polyacrylamides we can see that the depletion of ions increases significantly in time and moves in the direction of the ground end. The spreading of the depletion reaches up to 3.7 cm in 282 minutes and can not be caused by diffusion. The steady-state conductivity is 7.2 ± 0.12 $h\Omega^{-1}$ m^{-1}. There is a 22% drop in conductivity on 1.4 cm in 66 minutes and a 70% drop in conductivity on 3.7 cm in 282 minutes. The distance, over which the change of conductivity extends, is estimated by the δL term of equation 3.9. The characteristic distance for the resistance change increases linearly ($r > 0.9975$) with time:

$$\delta L = -0.27 \pm 0.18 \text{ cm} + 0.014 \pm 0.001 \text{cm min}^{-1} \; t \qquad (3.15)$$

where δL is in millimeters, and t is time in minutes. The amplitude of the conductivity change was also linearly related ($r > 0.998$) to the electrophoresis time:

$$\Delta\kappa = -0.40 \pm 0.28 \text{ h}\Omega^{-1} \text{ m}^{-1} - 0.016 \pm 0.01 \text{h}\Omega^{-1} \text{ m}^{-1} \text{ min}^{-1} \; t \qquad (3.16)$$

The linear dependence of the change of conductivity on the electrophoresis time is only approximate; the data of Figure 3.7 show an exponential decrease in conductivity with time. The conductivity is constant in the bulk of the capillary because its ionic concentration is uniform.

Figure 3.7 Change in conductivity versus the total length of capillary cut from the injection end of 1-day old capillaries (full lines) and 9-days old capillaries (dotted lines) for different run times (shown as minutes).

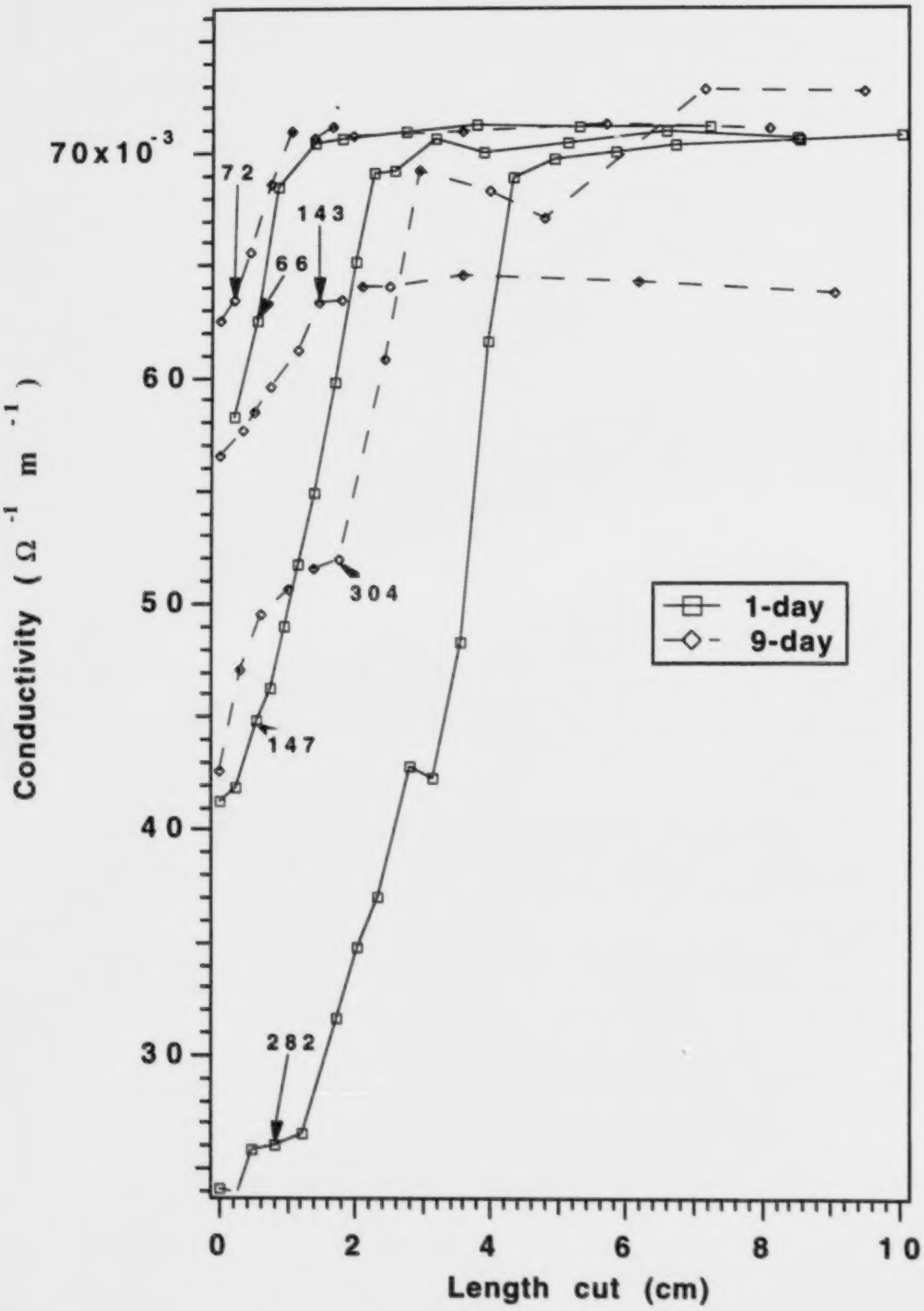

In the case of the 9-day old polyacrylamides, the depletion zone is less important. The steady-state conductivity is $6.8 \pm 0.4\ h\Omega^{-1}\ m^{-1}$. The δL term also increases linearly with time ($r > 0.997$):

$$\delta L = 0.0 \pm 0.12\ \text{cm} + 0.0083 \pm 0.0006\text{cm min}^{-1}\ t \qquad (3.17)$$

and the amplitude of the conductivity change is linearly related to the time ($r > 0.938$):

$$\Delta\kappa = 0.0 \pm 0.6\ h\Omega^{-1}\ m^{-1}\ - 0.0084 \pm 0.03 h\Omega^{-1}\ m^{-1}\ \text{min}^{-1}\ t \qquad (3.18)$$

The slopes for δL and $\Delta\kappa$ of the 9-day old polyacrylamide are around half the values of the 1-day old polyacrylamide. Thus, the depletion in a 9-day old polyacrylamide does not increase in space and value as fast as in the case of a fresh polyacrylamide.

3.3.1.4 Relaxation Due to Diffusion

A capillary was run for 6 hours at -300V/cm, then the voltage was turned off, and the capillary was let to relax in the buffer. To monitor the relaxation of the ionic depletion, the current was measured periodically after the termination of the electrophoresis run. The buffer reservoirs were replaced a few times to make sure that the change in current was not due to evaporation from the reservoirs. Figure 3.8 shows the conductivity versus the time after the voltage was turned off. The data points are denoted by the symbol "x", along with the least-squares fit (dashed curve) of an exponential to the data,

$$\kappa\ (h\Omega^{-1}\ m^{-1}) = 6.24 h\Omega^{-1}\ m^{-1} - 2.96 h\Omega^{-1}\ m^{-1} \exp\left(\frac{-t}{18.9\ \text{hours}}\right) \qquad (3.19)$$

where t is the time measured in hours. This result definitely indicates that the effect of $\Delta\kappa_{\text{depletion}}$ is reversible.

Figure 3.8 Change in conductivity versus relaxation time (no voltage applied) for polyacrylamide previously run for 6 hours at -300V/cm.

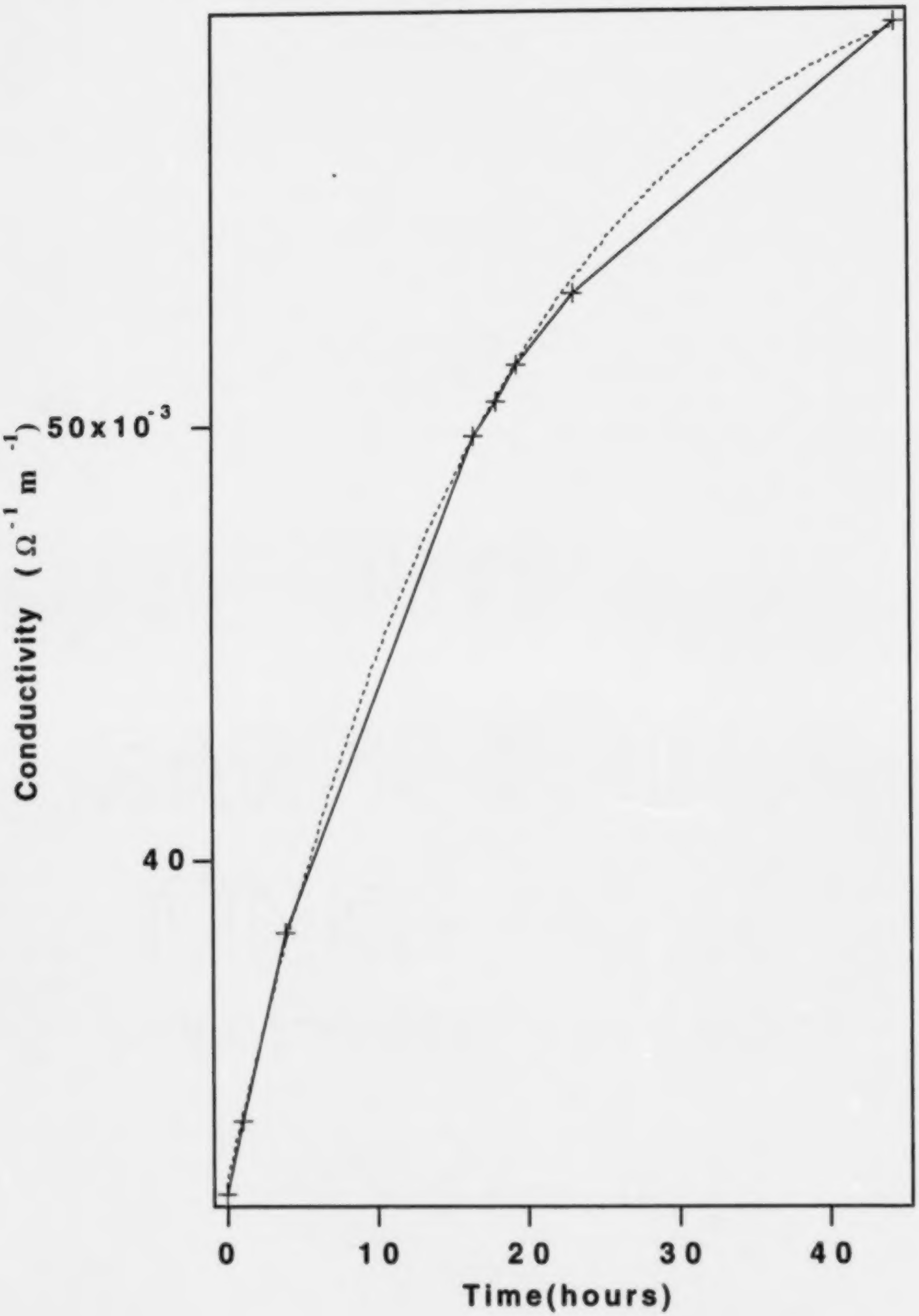

3.3.1.5 Effect of Adding KCl

The buffer reservoirs for the capillary were filled with 30mM KCl + 1xTB. Three different capillaries (7-day, 19-day, and 30-day old) were run for different times. The electric field was -300V/cm as in all the previous experiments. The profile of the conductivity for the 7-day and 19-day old polyacrylamides were established by, first, cutting at the injection end, and then, cutting at the ground end. The opposite procedure was done for the 30-day old polyacrylamide. We expected that adding KCl should help to reduce the depletion of ions, because in free solution the mobility of K^+ and Cl^- are similar. Only a small amount, compared to the buffer concentration, had to be added to make KCl the main charge carrier. The steady-state conductivity for this new buffer system is 27 ± 1 $h\Omega^{-1}\ m^{-1}$, which is four times higher than in the case of 1xTBE alone. Figure 3.9 shows the profile of the conductivity versus the length cut. In all cases the conductivity decreased when pieces of the capillaries were cut from the ground end (dotted line).

This result indicates that an increase in ionic concentration occurred at the ground end. No significant change in conductivity was noticed at the injection end, except for the 7-day old polyacrylamide, which increased by 0.6 $h\Omega^{-1}\ m^{-1}$. Thus, in the case of 30mM KCl + 1xTB, the depleted area at the injection end was expelled into the buffer reservoir, and the area of increased concentration at the ground end moved in the capillary. These results demonstrate the opposite effect than the ones observed with 1xTBE. Spencer [22-24] also described this phenomenon. The depleted area and the area of increased concentration move in or out of the capillary, depending on the change in the transference number with the change in concentration of the ions [22-24] . This change in the transference number with the concentration of ions depends on the type of ions involved in conduction. For some buffers, like 1xTBE, the depleted area moves into the capillary, and the area of increased ionic concentration moves out of the capillary; those buffers are called normal buffers. For some other buffers, like 30mM KCl + 1xTB, the depleted area moves out of the capillary,

Figure 3.9 Effect of KCl on the conductivity of polyacrylamide. Ground end is the dotted lines and injection end is the full lines.

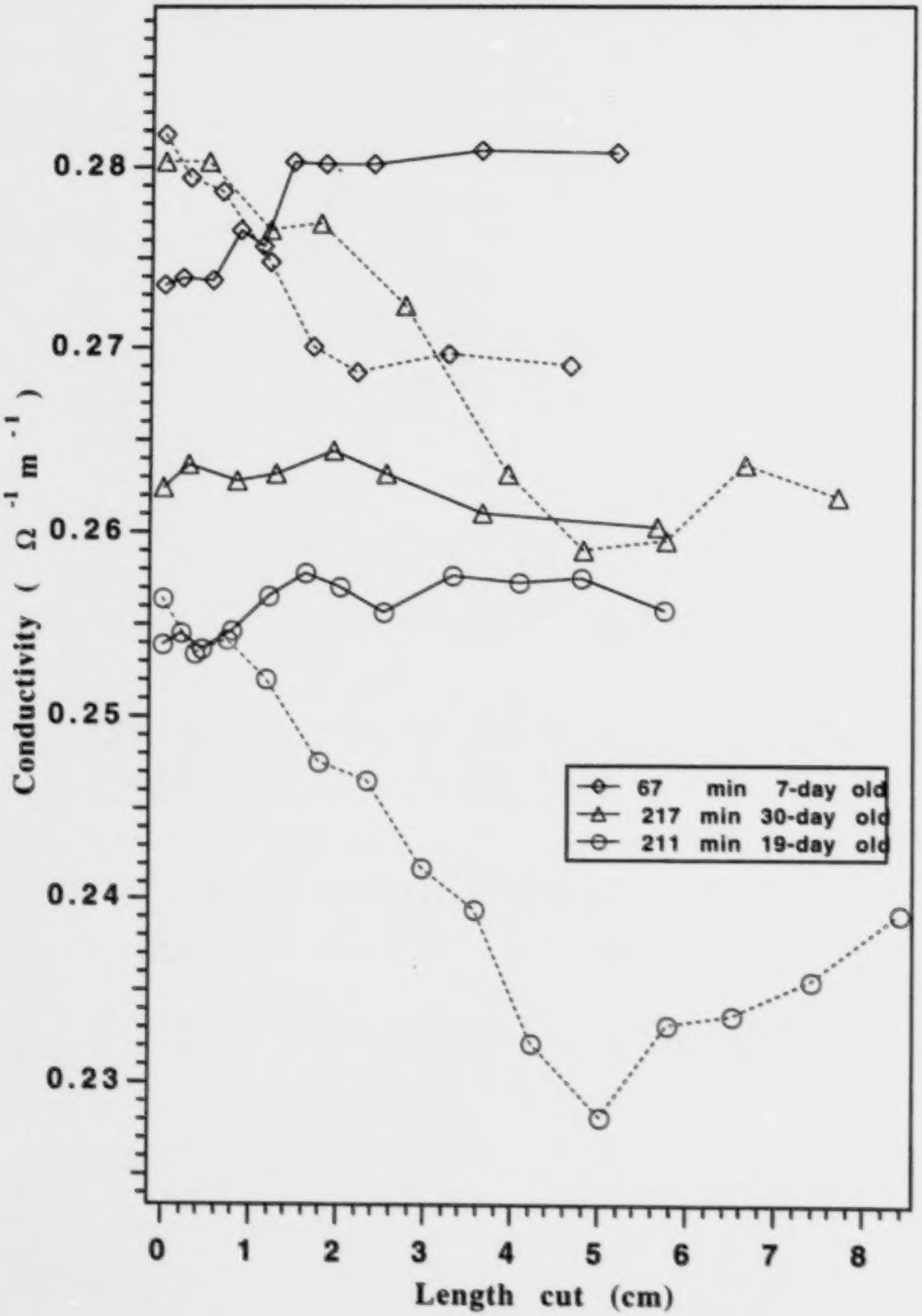

and the area of increased ionic concentration moves in the capillary; those buffers are called abnormal buffers.

3.3.1.6 Effect of 5%T Linear Polyacrylamide-Filled Reservoir

Swerdlow *et al.*[25] have noticed that by filling the buffer reservoir with the polymer and buffer of interest, the depletion of ions is reduced. In this section, we filled both reservoirs with 5%T linear polyacrylamide containing 1xTBE. The steady-state conductivity, $12.0 \pm 0.8\ \mathrm{h}\Omega^{-1}\ \mathrm{m}^{-1}$ is higher than the one obtained with the 1xTBE buffer reservoirs. This result is due to the fact that ammonium persulfate and TEMED are also present in the linear polyacrylamide-filled reservoirs. Figure 3.10 shows the conductivity profile of 13-day old capillaries run for different times. The conductivity at the ground end(dotted line) in both cases is constant. The conductivity at the injection end changes slightly; however, considering the scale of the graph, this change is small and could be due to slight differences between the polymer in the capillary and the one in the reservoir. This difference between the two polymers could be due to different kinetics of polymerization. The polymerization in the capillary is done close to room temperature because of the efficient removal of the heat in a capillary. The polymerization in a test tube is not at constant temperature, in fact, the temperature increases to over 40^0C. These results demonstrate that in the case of older polyacrylamides the depletion of ions can be eliminated if the buffer reservoirs are filled with the polymer and buffer of interest.

3.3.2 Effect of $\Delta k_{template}$

We studied the effects that injections of DNA template have on the conductivity of polyacrylamide filled capillaries. The polymers used for the experiment were older polymers and were pre-run until the current was stable. Template was injected until a drop in conductivity was noticed. Then, the capillaries were run at -300V/cm for 1 hour to simulate a sequencing run. Some capillaries were run without injecting template. The

Figure 3.10 Effect of polyacrylamide-filled reservoirs on the conductivity in the capillary. Ground end is the dotted lines and injection end is the full lines.

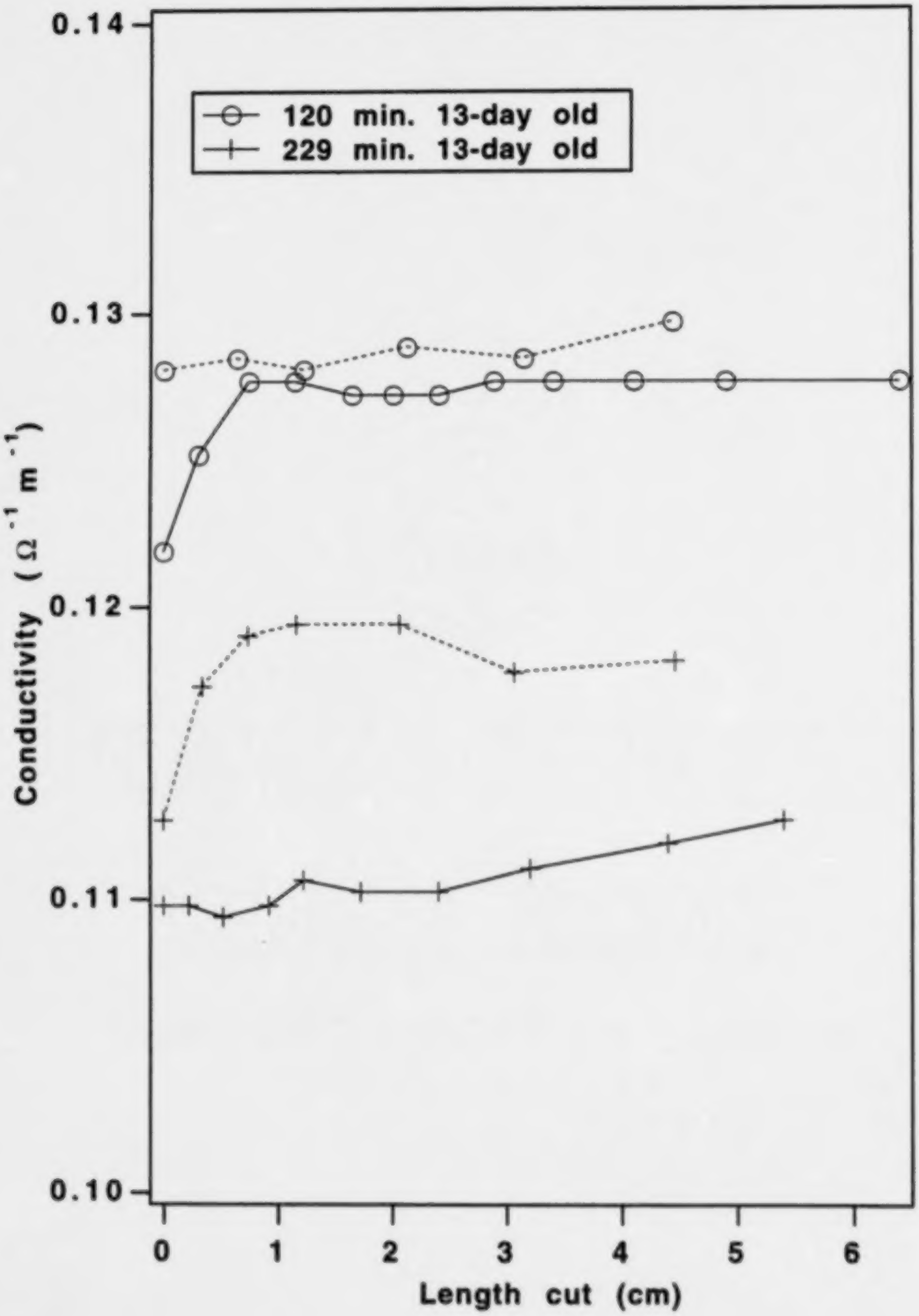

decrease in conductivity for the capillaries run with template was greater compared to the ones run without template. This result indicated that the injections of DNA template affected the separation by decreasing the conductivity. After running for one hour, the high voltage was turned off, and the capillaries were left to relax in the buffer. The current was measured (by turning the high voltage on for 60 seconds) after a period of time. Figure 3.11 shows the change in conductivity after the high voltage was turned off versus the time. It can be seen that the conductivity increases slightly for the capillaries run without DNA template after 23 hours (dotted lines). The steady-state conductivity extrapolated from an exponential fit is 7.2 ± 0.4 $h\Omega^{-1}$ m^{-1}. In the case of the capillaries with DNA template (full lines), the increase was much greater. This result clearly indicates that the decrease in conductivity observed by injecting DNA template is partly reversible if the capillary is left to relax. This result does not indicate the amount of DNA template necessary to decrease the conductivity, since a large amount of template was injected to force the conductivity to decrease.

We did four subsequent injections of template on the same capillary. Between each injection, the capillary was run for 1 hour at -300V/cm. The polymers used were older, and were only used after current was stabilized. Two different concentrations of template were used: 1 μL of M13mp18 (0.2 μg/μL) in 3 μL of formamide:EDTA, and 1 μL of M13mp18 (0.2 μg/μL) in 10 μL of formamide:EDTA. For each solution, the experiment was repeated on at least four different capillaries. The conductivity was normalized to zero by subtracting the first conductivity value from all the conductivity values for each capillary. Figure 3.12 shows the change in conductivity versus the number of injections. Injection zero means that the capillary was run without a template injection under the same conditions. The data of Figure 3.12 show that the conductivity decreases by 0.25 $h\Omega^{-1}$ m^{-1} for the most diluted template solution. In the case of the most concentrated solution, the conductivity decreases by more than 2.0 $h\Omega^{-1}$ m^{-1} within 4 runs. These results clearly indicate that a lower concentration of template has less effect on the conductivity than a

Figure 3.11 Change in conductivity versus relaxation time. The polyacrylamides were equilibrated before being used. Enough DNA template (full lines) was injected to significantly decrease the conductivity. Some runs were done without injecting DNA template (dotted lines). All the polyacrylamides are run for 1 hour at -300V/cm then allowed to relax.

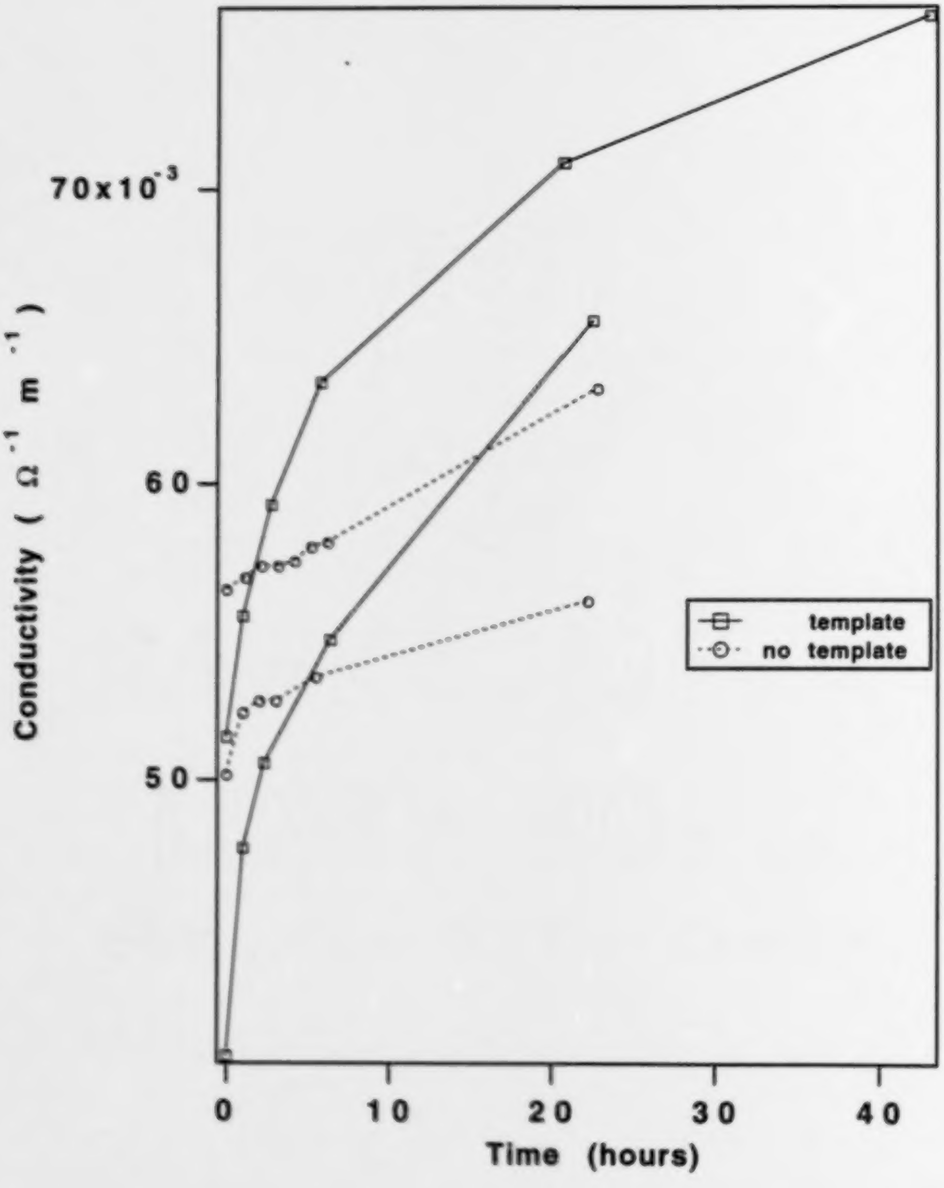

Figure 3.12 Change in conductivity versus the number of injections of DNA template. The polyacrylamides were equilibrated before being used. The injection time was 20 seconds at -300V/cm.

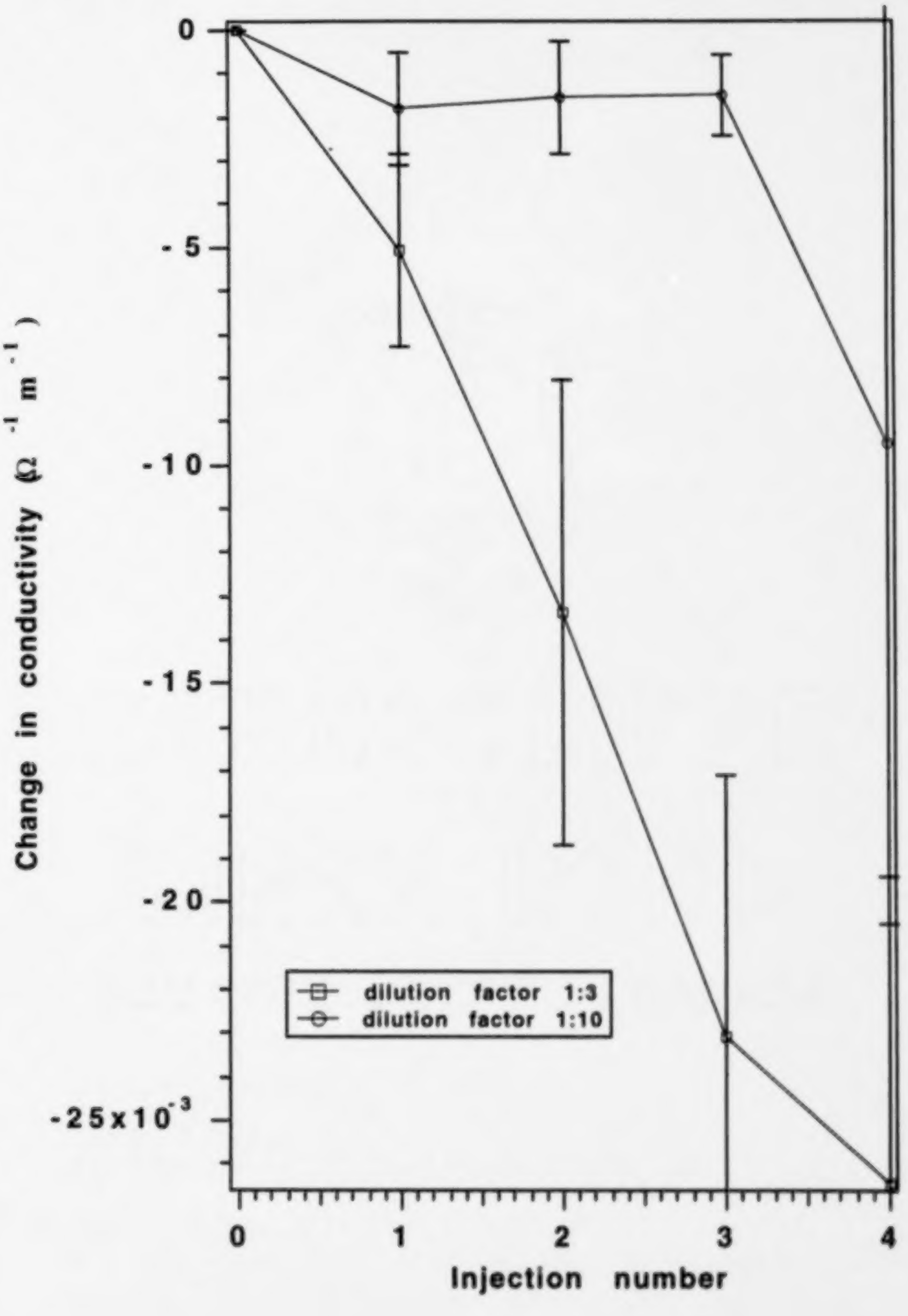

higher concentration of template. Lower concentrations of template in a sequencing sample can be obtained by cycle sequencing. These results also indicate that the difference in the buffer between the sample and the capillary does not significantly affect the conductivity.

3.4 Discussion

We have observed a change in the current of linear polyacrylamide-filled capillaries during electrophoresis. This current change is associated with a change in conductivity that is localized to the injection tip of the capillary. The current in older polyacrylamides is more stable and higher than in younger polyacrylamides. This difference in behavior of polyacrylamides is associated with the behavior at the injection (negative) tip of the capillary; the steady-state conductivity, which is the conductivity of the bulk of the capillary, showed no difference for all the capillaries.

The conductivity versus time for the different ages of polyacrylamide was fitted with a double exponential decay. The values obtained suggest that the depletion of ions decreases as the age of the polyacrylamide increases. A steady-state conductivity of 6.8 ± 0.8 $h\Omega^{-1}$ m^{-1} was calculated; the maximum value of the depletion of ions is 4.8 ± 0.4 $h\Omega^{-1}$ m^{-1}, and the time constant is 5 ± 1 days.

Clearly, the various behaviors of different ages of polyacrylamide is related to a change in the properties of polyacrylamide. Change in the properties of cross-linked polyacrylamide as it ages were previously noticed by Tanaka[26]. He noticed a change in the swelling properties between 3-day old gels and 30-day old gels. Slater *et al.* [27,28] also noticed a change in the properties of polyacrylamide with time. They found that the velocity of DNA changes if the gel is not aged before use. Caglio *et al.*[29] studied the polymerization kinetics of polyacrylamide and reported that the polymerization is finished within 1 day. Thus, the change in current with the age of the capillary that is observed can not be due to an incomplete polymerization. It could be argued that the shrinkage of the polymer could take place in time, but this would increase the polymer viscosity and decrease the steady-state conductivity of the polymer, which was not observed in this experiment. In our preparation of polyacrylamide, TBE as the buffer and 7M urea as the denaturing agent were added. In this medium, polyacrylamide could hydrolyze slowly and become partially negatively charged. Geribaldi *et al.*[30] studied lane distortions in gel electrophoresis. In their discussion they proposed that acidic groups in gels could increase with time. This hypothesis is based on studies of the hydrolysis effect on gel properties by Tanaka[31,32]. The hydrolysis of the amino group to form a carboxylic group on the polymer was also noticed in gel chromatography[33]. The presence of negative charges in the gel would disturb the mechanism of the depletion of ions and would also ensure a minimum amount of ions in the capillary. On the other hand, the presence of a charge on the polymer would change the ionic makeup of the solution, leading to a change in the steady-state conductivity of the polymer.

Depletion of ions near the injection end was proposed to explain the decrease in current versus time[22-24]. This depletion of ions could spread in the capillary with time. An increase in ionic concentration could occur at the opposite end of the capillary, but would move out of it. Our results indicate (Figures 3.5 , and 3.6) that with 1xTBE the depletion of ions at the injection end moves into the capillary with time. No depletion is observed at the ground end (Figure 3.7), probably because it moves out of the capillary. Spencer[22] predicted that in the case of a TRIS-HCl buffer the depletion of ions should occur at the cathode (injection end) with no change in concentration at the anode. Similarly, in the case of TBE, the increased concentration area at the ground end dissipates in the buffer reservoir and is not noticed at the ground end of the capillary.

The depletion of ions is larger when there is a major difference in the mobilities of the charge carriers, which is the case in a buffer such as TBE. Any such effect would change the distribution of the potential drop. Higher drops in potential are observed in the first few centimeters of the capillaries and lower drops in the rest of the capillaries. The electric field decreasing in most of the capillary would increase the migration time of DNA.

This result is in agreement with our observation of a decrease in current versus time for all the capillaries studied. Our results suggest that the depletion could reach up to 9 cm for a young polyacrylamide within 350 minutes. This behavior was also reported in the literature for different gels and different buffers. Seida *et al.* [34] studied the change in concentration of sodium sulfate in a 6.6%T 3.2%C polyacrylamide gel at 10 V. They reported an increase in the cation concentration at the cathode side and a decrease at the anode. The change in concentration was noticed quite rapidly (5 minutes) and extended quickly into the gel. Slater et al.[27,28] reported that the velocity of DNA in the first few centimeters of a gel is higher, and the velocity of DNA is lower in the last few centimeters. These results were obtained using a slab gel. Spencer [22] noticed a decrease in current of 40% for a gel (15%T) that was run for 3 hours at 100V with a buffer containing 2 mM of spermine tetrahydrochloride. A depletion area extending 40 mm was noticed on a 15%T, 80 mm long gel, run for 3 hours at 6 mA with 1 mM spermine tetrahydrochloride. Changes in pH were also noticed along the capillary. Lundahl and Hjertén[35] reported an increase in the concentration of the buffer near the cathode of a sucrose gradient U tube and the reverse effect near the anode for a 0.02 M sodium phosphate buffer. The opposite situation was obtained for the 0.04 M TRIS-HCl buffer. Kozulic[36] studied the bending of DNA bands in slab gel electrophoresis. His results suggest the presence of a voltage drop between gels and running buffers.

Our results also indicate that in the case of older polyacrylamides, the depletion of ions is less important. This result might possibly be explained by the presence of charges on the polymer. The polymer might become charged by the hydrolysis of some amino groups of polyacrylamide to carboxylate groups. The presence of charges on the stationary polymer would insure a minimum conductivity and would disturb the effect of the change in transference number. We do not have yet any direct prove or disprove of charges on the polymer. We can postulate that this amount of charge on the polymer would have to be small in order not to see any electroosmosis.

The recovery in conductivity is consistent with the diffusion of ions into the depleted zone. After 6 hours of electrophoresis, the depleted zone extends about 3 cm into the capillary. Assuming a diffusion coefficient of 2×10^{-5} cm^2 s^{-1}, the diffusion will extend about 1.2 cm from each end of the depletion zone after 19 hours. The recovery in current is consistent with the diffusion of ions into the depletion zone.

The addition of KCl transformed the buffer system from a normal buffer system to an abnormal buffer system. In this abnormal buffer system, an area of increased concentration of ions moves in the capillary at the ground end, and a depleted area at the injection end moves out of the capillary and disappears in the buffer reservoir. This abnormal behavior was also described by Spencer[22-24]. This phenomena occurred when the transference number of the ions decreases with the increase in the concentration of ions. This means that the KCl causes the reverse effect than the one observed with 1xTBE. The amount of KCl in the 1xTBE buffer could be adjusted in order that the effects on the conductivity of KCl and 1xTBE cancel out.

The 1xTBE buffer reservoirs were replaced by 5%T 1xTBE linear polyacrylamide. The depletion of ions at the injection end was not observed. These results are expected because the transference number is the same in the polyacrylamide reservoirs and the capillary. Thus, no change in ionic concentration can occur at either end of the capillary. One would expect a change in the ionic concentration near the electrodes; however, due to the size of the reservoirs compared to the capillary, the change in ionic concentration at the electrodes has a negligible effect on the conductivity.

The effect of the $\Delta\kappa_{template}$ was demonstrated in Figure 3.12. The results suggest that decreasing the amount of template in a sample will decrease the effect on the conductivity. Swerdlow *et al.*[25] also noticed an effect of the template on the conductivity when using a cross-linked polyacrylamide. In their experiment, the conductivity decreases significantly immediately after the injection, and the capillary had to be trimmed at the injection end for the conductivity to recover. The diffusion coefficient of the template is probably too small to explain the recovery of the current observed during the relaxation of the gel (Figure 3.11). Our results suggest that at high concentrations, the template induces an increase in the depletion of ions when it is passing through the depleted area.

The average electric field in this experiment is - 300V/cm, computed by dividing the voltage by the capillary length. In the case of significant ionic depletion, there will be a disproportionate voltage drop across the region of low conductivity, with a concomitant higher than the average field in the region of low conductivity, and a lower than average electric field in the remainder of the capillary.

Figure 3.13 presents a plot of the expected electric field in the capillary that has operated for 282 min. The electric field at the injection end, -800 V/cm, is much larger than the average electric field of -300V/cm. The electric field in the bulk of the capillary, -175V/cm, is less than the average field. The high electric field at the injection end of the capillary will have several important effects. First, Joule heating will be the most severe at the injection end. Second, the polymer will be subjected to the greatest stress at the injection end; the high electric field can be expected to induce damage to the polymer at the injection end. Third, electroosmotic forces will be greatest at the injection end; unless the capillary wall is carefully treated, osmosis may drive the gel from the injection end (see ref. 17); large DNA sequencing fragments are not separated in the initial portion of the capillary.

DNA sequencing papers report that the injection end of the capillary must be trimmed before use. By trimming a few millimeters from the injection end, the region of low conductivity is removed from the capillary, allowing the initial operation of the capillary at a uniform electric field. This conductivity decrease at the injection end will automatically form an electric field gradient during the separation; the electric field experienced by the DNA fragment decreases during the separation.

Figure 3.13 Electric field versus the distance from the cathodic end of the capillary.

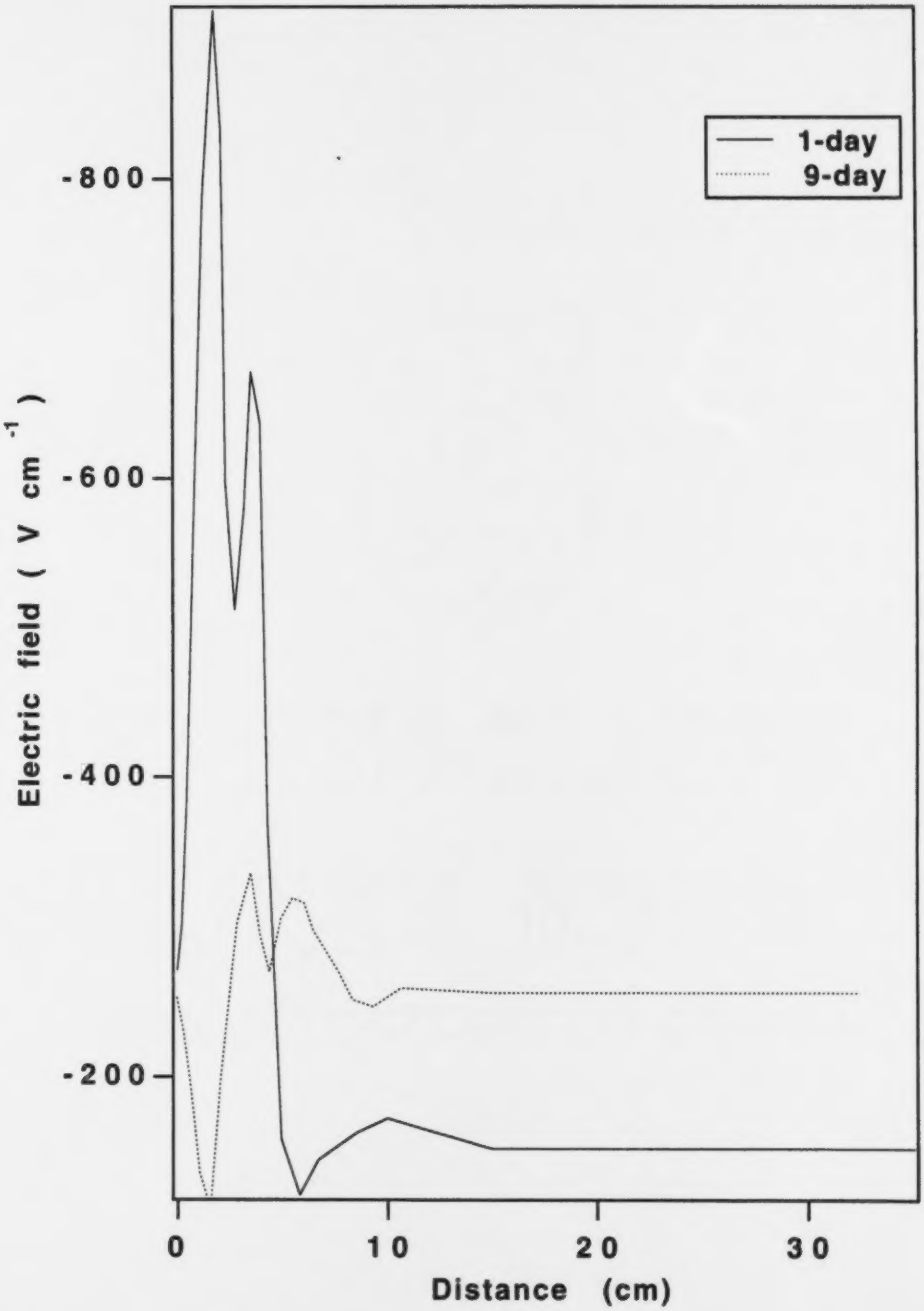

3.5 Conclusion

This report shows that older polyacrylamides generate higher and more stable currents than younger polyacrylamides. It also shows that the polyacrylamides can relax to higher currents if no field is applied. We also demonstrated that higher currents are obtained when lower concentrations of template are used.

The results on the depletion of ions obtained in this chapter, not only apply to DNA sequencing, but also to any separation done on linear polyacrylamide; the phenomena of the depletion of ions is characteristic of the polymer and the buffer used. The sample separated on linear polyacrylamide could affect the depletion of ions if its concentration was similar to the buffer.

3.6 Bibliography

(1) Baba, Y.; Matsuura, T.; Wakamoto, K.; Tsuhako, M. *Chemistry Letters* **1991**, 371-374.

(2) Chen, D.; Harke, H. R.; Dovichi, N. J. *Nucleic Acids Research* **1992**, *20*, 4873-4880.

(3) Cohen, A. S.; Najarian, D. R.; Karger, B. L. *Journal of Chromatography* **1990**, *516*, 49-60.

(4) Chen, D. Y.; Swerdlow, H. P.; Harke, H. R.; Zhang, J. Z.; Dovichi, N. J. *Journal of Chromatography* **1991**, 237.

(5) Drossman, H.; Luckey, J. A.; Kostichka, A. J.; D'Cunha, J.; Smith, L. M. *Analytical Chemistry* **1990**, *62*, 900-903.

(6) Carson, S.; Cohen, A. S.; Belenkii, A.; Ruiz-Martinez, M. C.; Berka, J.; Karger, B. L. *Analytical Chemistry* **1993**, *65*, 3219-3226.

(7) Huang, X. C.; Quesada, M. A.; Mathies, R. A. *Analytical Chemistry* **1992**, *64*, 2149-2154.

(8) Pentoney, S. L.; Konrad, K. D.; Kaye, W. *Electrophoresis* **1992**, *13*, 467-474.

(9) Ruiz-Martinez, M. C.; Berka, J.; Belenkii, A.; Foret, F.; Miller, A. W.; Karger, B. L. *Analytical Chemistry* **1993**, *65*, 2851-2858.

(10) Swerdlow, H.; Wu, S.; Harke, H.; Dovichi, N. J. *Journal of Chromatography* **1990**, *516*, 61.

(11) Figeys, D.; Dovichi, N. J. *Journal of Chromatography* **1993**, *645*, 311-317.

(12) Bocek, P.; Chrambach, A. *Electrophoresis* **1991**, *12*, 1059-1061.

(13) Bocek, P.; Chrambach, A. *Electrophoresis* **1992**, *13*, 31-34.

(14) Figeys, D.; Arriaga, E.; Renborg, A.; Dovichi, N. J. *Journal of Chromatography* **1994**, *669*, 205-216.

(15) Baba, Y.; Sumita, C.; Hide, K.; Ishimaru, N.; Samata, K.; Tanaka, A.; Tsuhako, M. *Journal of Liquid Chromatography* **1993**, *16*, 955-965.

(16) Swerdlow, H.; Gesteland, R. *Nucleic Acids Research* **1990**, *18*, 1415-1419.

(17) Best, N.; Arriaga, E.; Chen, D. Y.; Dovichi, N. J. *Analytical Chemistry* **1994**, *66*, 4063-4067.

(18) Lu, H.; Arriaga, E.; Chen, D. Y.; Figeys, D.; Dovichi, N. J. *Journal of Chromatography* **1994**, *680*, 503-510.

(19) Harke, H. R.; Bay, S.; Zhang, J. Z.; Rocheleau, M. J.; Dovichi, N. J. *Journal of Chromatography* **1992**, *608*, 143-150.

(20) Luckey, J. A.; Smith, L. M. *Analytical Chemistry* **1993**, *65*, 2841-2850.

(21) Swerdlow, H.; Dew-Jager, K.; Gesteland, R. F. *BioTechniques* **1994**, *16*, 684-693.

(22) Spencer, M. *Electrophoresis* **1983**, *4*, 46-52.

(23) Spencer, M. *Electrophoresis* **1983**, *4*, 36-41.

(24) Spencer, M. *Electrophoresis* **1983**, *4*, 41-45.

(25) Swerdlow, H.; Dew-Jager, K. E.; Brady, K.; Grey, R.; Dovichi, N. J.; Gesteland, R. *Electrophoresis* **1992**, *13*, 475-483.

(26) Tanaka, T. *Physical Review Letters* **1978**, *40*, 820-823.

(27) Slater, G. W.; Mayer, P.; Drouin, G. *Analusis Magazine* **1993**, *21*, M25-M28.

(28) Slater, G. W.; Mayer, P.; Drouin, G. *Electrophoresis* **1993**, *14*, 962-966.

(29) Caglio, S.; Righetti, P. G. *Electrophoresis* **1993**, *14*, 997-1003.

(30) Starita-Geribaldi, M.; Houri, A.; Sudaka, P. *Electrophoresis* **1993**, *14*, 773-781.

(31) Tanaka, T.; Nishio, I.; Sun, S.-T.; Ueno-Nishio, S. *Science* **1982**, *218*, 467-469.

(32) Tanaka, T.; Fillmore, D.; Sun, S.-T.; Nishio, I.; Swislow, G.; Shah, A. *Physical Review Letters* **1980**, *45*, 1636-1639.

(33) Bywater, R. P.; Marsden, N. V. B. *Journal of Chromatography Library* **1983**, *22A*, A262.

(34) Seida, Y.; Nakano, Y. *Journal of Chemical Engineering of Japan* **1991**, *24*, 755-760.

(35) Lundahl, P.; Hjertén, S. *Annal of the New York Academy of Sciences* **1973**, *216*, 253-261.

(36) Kozulic, B. *Analytical Biochemistry* **1994**, *216*, 253-261.

CHAPTER 4 [1,2]

EFFECTS OF AGING OF LINEAR POLYACRYLAMIDE ON THE SEPARATION OF SINGLE-STRANDED DNA.

---

[1] A part of this chapter has been submitted for publication.
Figeys, D., and Dovichi, N.J. 1995. Journal of Chromatography.

[2] A part of this chapter has been submitted for publication.
Figeys, D., and Dovichi, N.J. 1995. Journal of Chromatography.

4.1 Introduction

Capillary electrophoresis has become a major analytical tool in the field of biological sample analysis. In particular, DNA sequencing samples have received a lot of attention in the last few years .[1-11]

Usually, DNA sequencing samples are prepared using the Sanger *et al.* technique[12] and run on denaturing polyacrylamide gel. UV and fluorescence on column detection[2,4,6,9] were reported. Post-column fluorescence detection has also been used to achieve low limits of detection[1,3,5,7].

The preparation of samples and the detection techniques available are now very well established; however, major problems are still encountered in the preparation of suitable capillaries. The ideal capillary will allow multiple runs to be performed on it. Also, with the throughput needed for DNA sequencing , capillaries should be easy to use in an automated system. Finally, the ideal capillary needs to be stable enough to obtain the trust of the users as slab gel has achieved.

Cross-linked polyacrylamide is used to obtain high-resolutions separation of sequencing samples. Only a few reports are available on the effect of different parameters (%T, %C, temperature) on the separation of DNA[13-16]. Usually, only 2 to 3 separations can be performed on the same gel without a major change in the migration time or the occurrence of bubbles that damage the gel[17].

We studied the stability of linear polyacrylamide (Chapter 3 and see ref. [18]). We noticed that more stable current profiles are obtained with aged linear polyacrylamides than with fresh linear polyacrylamides. Less depletion of ions at the injection end was observed in aged linear polyacrylamides than in fresh linear polyacrylamides.

Typically, because physical changes induce bubbles in the gel, cross-linked polyacrylamide-filled capillaries are used within a couple of days after the polymerization. Linear polyacrylamide can be used for a much longer time after polymerization than cross-linked polyacrylamide. As it ages, the polymer's properties change. Physical changes like shrinking, swelling, or phases separation can happen due to the equilibration of pressures. Physical changes in polyacrylamide usually happen on a longer time scale than the one day necessary for the completion of the polymerization. Chemical changes can also happen, such as hydrolysis.

In the first part of this chapter we describe DNA sequencing done with linear polyacrylamide (5%T 7M urea) filled capillaries used up to 115 days after polymerization. The effects of aging polyacrylamide on the separation of a DNA sequencing standard are analyzed.

A few authors[8] proposed the use of linear polyacrylamide for the separation of DNA sequencing samples. The main advantage of low concentrations of linear polyacrylamide is that it can be refilled in a capillary by applying a suitable pressure[19]. Refilling the capillary removes the step of realigning the system usually done when changing a capillary. It allows multiple runs to be performed on the same capillary. Also, linear polyacrylamide seems to be less affected by the capillary generating bubbles, in contrast to cross-linked polyacrylamide; however, the resolution obtained with linear polyacrylamide is lower than for cross-linked polyacrylamide[15]. Also, only low concentrations of linear polyacrylamide can easily be pumped in and out of the capillary[20]. For the same reason, narrow bore capillaries would be difficult, if not impossible, to use with this technique. In wide bore capillaries, Joule heating limits the field that can be applied. Finally, after each refill, the capillary needs to be pre-run for a while to obtain a stable current. This pre-run time will depend on the viscosity of the polymer, and is typically from 20 to 30 minutes for a 5%T at -300V/cm.

Fifty runs or more were obtained on the same capillary using oligonucleotides or mixtures of oligonucleotides[21-23]. There are only a few reports on multiple runs of sequencing samples on the same capillary. Pentoney *et al.* [2] used a 10%T 7M urea linear polyacrylamide to perform 5 to 10 runs. Two millimeters of the column were cut a few minutes after each injection. This approach has also been used with cross-linked polyacrylamide to reduce the effect of bubbles at the injection end and to perform multiple runs[4,10,21]; however, this approach is not suitable for automation.

Ruiz-Martinez *et al.*[8] refilled a capillary with 6%T linear polyacrylamide and did multiple runs on it. As we previously mentioned, this approach will only be successful with low concentrations of polyacrylamide and wide bore capillaries.

Another way of increasing the throughput of a CE system is to run multiple capillaries in parallel. Huang *et al.*[6,24] used on column confocal fluorescence detection to scan many capillaries. Kambara *et al.*[7] used multiple sheathflow systems and proper optical to scan capillaries. These approaches are a good way of increasing the throughput of a system; however, arrays of capillaries will only be convenient to use if we find a way of getting multiple runs per capillary.

In the second part of this chapter, we will demonstrate the use of linear polyacrylamide for multiple sequencing on the same capillary without refilling it. Cycle sequencing was used to prepare fluorescently labeled samples, and laser induced post-column fluorescence was used as a detection scheme. This technique allows complete and simple automation of DNA sequencing on capillaries.

4.2. Experimental

The Sequitherm Cycle Sequencing kit (Cedarlane Laboratories, Hornby) and the Δtaq Cycle Sequencing kit (USB, Cleveland, Ohio) were used to prepare sequencing samples of fluorescently labeled DNA. The protocols of the kits for cycle sequencing were used with the following changes: ROX-labeled M13 universal (-21) primer (ABI, Foster City, California) was used with M13mp18 single-stranded DNA (USB, Cleveland, Ohio). Samples were ddATP terminated. The samples were covered with mineral oil and heated for five minutes at 95 ^{O}C. Cycle sequencing was performed using 30 cycles; each cycle consisting of 45 seconds at 95 ^{O}C, 45 seconds at 47 ^{O}C, and 90 seconds at 70 ^{O}C.

Samples were ethanol precipitated, washed, and resuspended in 15 to 25 μL of formamide:EDTA (49:1). Each sample was divided into 5 to 10 aliquots.

Linear polyacrylamides (5%T) were prepared by taking 1.25 mL of a 20% acrylamide (BioRad, CA) stock solution, adding 1.0 mL of 5xTBE buffer [2.7 grams TRIS (ICN Biomedicals Inc., Cleveland, Ohio), 1.37grams boric acid (BDH Inc., Toronto, Ontario), and 1.0 mL 0.5 M EDTA diluted to 50 mL in deionized filtered water)], and 2.1 grams of urea (Gibco BRL, Gaithersburg, MD), and making the solution up to 5.0 mL in deionized, filtered water. This solution was degassed for at least 20 minutes by bubbling argon gas through it. The polymerization reaction was initiated and catalyzed by adding 2 μL N,N,N',N'-tetramethylethylenediamine (TEMED) (Gibco BRL, Gaithersburg, MD), and 20 μL of 10% ammonium persulfate (Boehringer Mannheim Corp., Indianapolis, IN). Immediately following the addition of initiators, the solution was injected into fused silica capillaries, (Polymicro, Phoenix, AZ) with typical dimensions of 33 cm x 32 μm id x 143 μm od. Capillaries were pretreated for one hour with a silanizing solution. This solution was freshly prepared by mixing together 0.5 mL of water, 0.5 mL of glacial acetic acid, and 20 μL of γ-methacryloxypropyl trimethoxysilane (Sigma Chemical, St.Louis, MD). All chemicals are of electrophoretic grade. The day of preparation is day zero. Linear polyacrylamide-filled capillaries that are older than day zero were left to age on the bench and trimmed before use.

The capillary electrophoresis system and fluorescence detection system used for these experiments are an in-house design described in Chapter 1 (Figures 1.19 and 1.20). The high voltage power supply used in this experiment is a Spellman CZE1000R (Plainview, NY). Excitation of the sequencing samples is achieved by using a yellow (8 mW at 594 nm) He-Ne laser (PMS, Electro-Optics, Boulder, Colorado). Fluorescence is collected at right angles to the laser beam with a 125X microscope objective (Leitz Weizlar, Germany). The light collected is imaged onto an iris, passed through a

630DF30 band pass filter (Omega Optical., Brattleboro, VT) and detected with an R1477 photomultiplier tube (Hamamatsu, Middlesex, NJ).

4.3 Effects of Aging Polyacrylamide on the Separation of Sequencing Samples

4.3.1 Results and Discussion

Separation of sequencing samples was performed on linear polyacrylamide-filled capillaries ranging from 1- to 115-day old. Figure 4.1 shows four subsequent sequencing runs done on a 1-day old linear polyacrylamide-filled capillary at -300 V/cm, from the primer up to base 166. The migration times increase from run to run; the peak for base 91 moves from 23.7 up to 39.4 minutes (66% of increase), and the peak for base 252 moves from 43.3 up to 70.8 minutes (63% of increase) from run one to run four. Also, the peak heights decrease by a factor of ten within four sequencing runs, despite the use of a fresh sample for each sequencing run. At the same time, the current in the capillary decreases from 1.21 μA for sequencing run one to 0.70 μA for sequencing run four.

The decrease in current is due to a depletion of ions at the injection end[18]. This depletion of ions causes a localized increase in the electric field near the injection end, and a decrease of the electric field in the rest of the capillary. As well, this depletion of ions expands in the capillary with time, thus increasing the asymmetry of the electric field in the capillary. This phenomenon of depletion of ions causes the migration times to increase from sequencing run to sequencing run and results in a lower amount of sample to be injected. Depletion of ions was well described by Spencer [25-27] and was also reported in slab gel experiments[27-30]. Spencer[27] noticed a depletion of ions extending 40 mm for a 80 mm 15%T gel run at 6 mA for 3 hours with 1mM spermine tetrahydrochloride. Seida *et al.*[30] reported changes in concentration of the buffer near the two electrodes directly inserted in a gel. In this experiment, 10 V was applied on a 6.6%T 3.2%C using sodium sulfate as a buffer. Slater *et al.*[28] noticed an increase in

Figure 4.1 Four subsequent separations of M13mp18 ddATP terminated sequencing samples at -300V/cm on a 35 cm long capillary filled with 1-day old linear polyacrylamide.

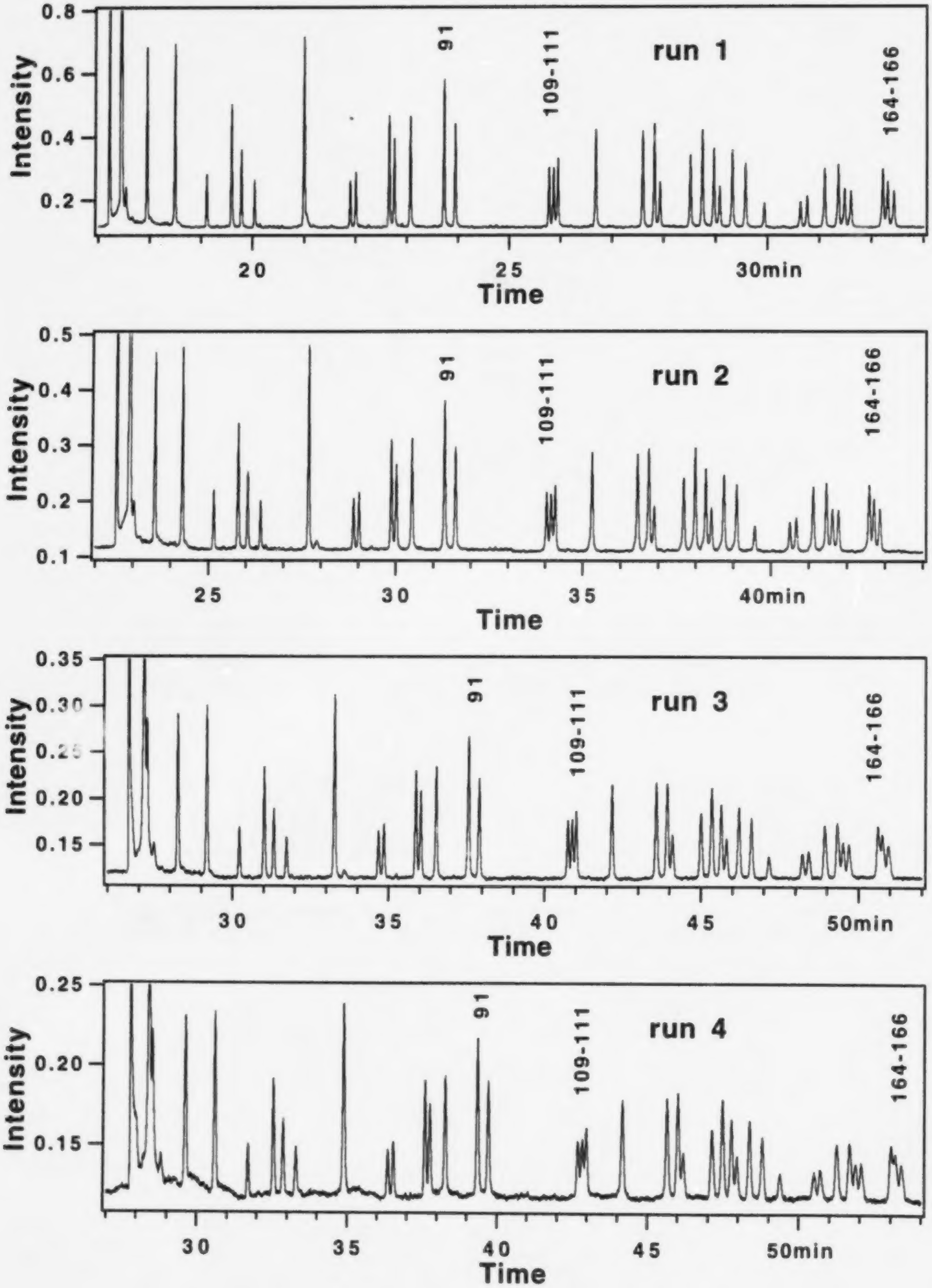

velocity of DNA in the first few centimeters of a slab gel and a decrease in the last few centimeters.

Figure 4.2 shows similar separations done on a 20-day old linear polyacrylamide-filled capillary. It can be seen that the migration time for base 91 changes only from 22.2 to 22.3 minutes (0.04% increase), and for base 252 from 38.9 to 39.1 minutes (0.6% increase). The current stays at 1.55 μA from the run one to run four. The peak heights only change by around 10%.

In a previous report[18], we have indicated that the aging of polyacrylamide allows a more stable current in time (i.e. less depletion of ions at the electric field), and thus, a more symmetric distribution of the electric field throughout the capillary. The increase in stability of polyacrylamide with age was also noticed in a different set of experiments, where a capillary was refilled with a 1-day old linear polyacrylamide and three subsequent sequencing runs were performed (Figure 4.3). The migration times change similarly to Figure 4.1. When the capillary was refilled with a 20-day old linear polyacrylamide and four subsequent sequencing runs were performed (Figure 4.4), the migration was stable within 5% RSD. These results indicate that the change in the migration times with age is not due to a capillary problem, such as bad coating of the inside wall. It is due to changes in the properties of aging polyacrylamide.

Using the migration times measured and equation 2.1 the mobilities of base 91 and base 252 were calculated. Figure 4.5 shows the calculated mobilities for base 91 and base 252 versus the age of linear polyacrylamide for four subsequent sequencing runs. The mobilities, in linear polyacrylamide less than a couple of days old, decrease by 40% for base 91, and 39% for base 252 from the sequencing run one to four. In the case of linear polyacrylamide 7- to 34-day old, mobilities decrease by an average of 6.2% for base 91 and 4.5% for base 252 within four sequencing runs. In the case of the 115-day old linear polyacrylamide-filled capillary, mobilities increase by 29% for base 91 and 35% for base 252 within four sequencing runs.

Figure 4.2 Four subsequent separations of M13mp18 ddATP terminated sequencing samples at -300V/cm on a 32.1 cm long capillary filled with 20-day old linear polyacrylamide.

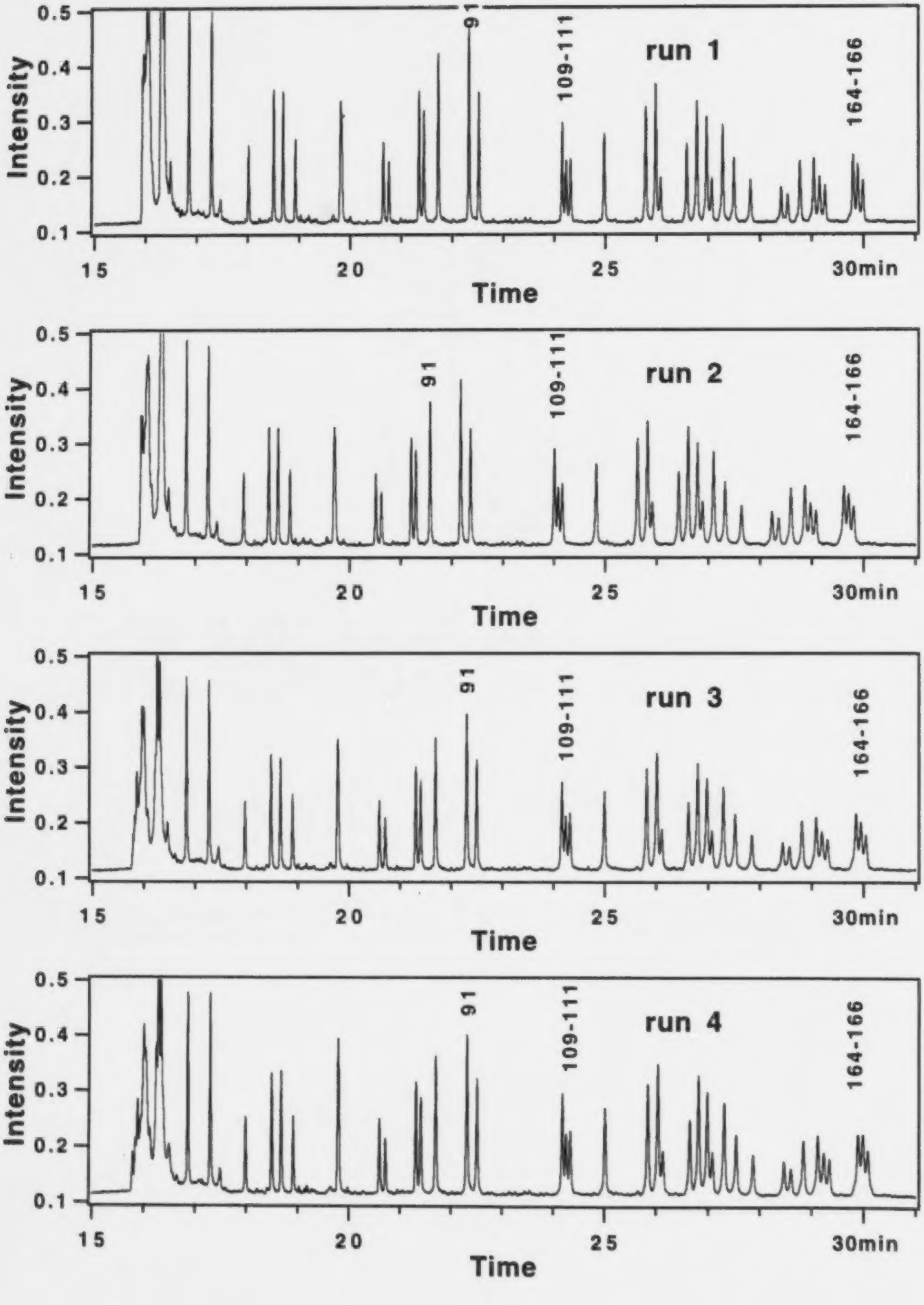

Figure 4.3 Three subsequent separations of M13mp18 ddATP terminated sequencing sample at -300 V/cm on a 36 cm long capillary. The capillary was refilled with 1-day old linear polyacrylamide before the first run, using a gas tight syringe.

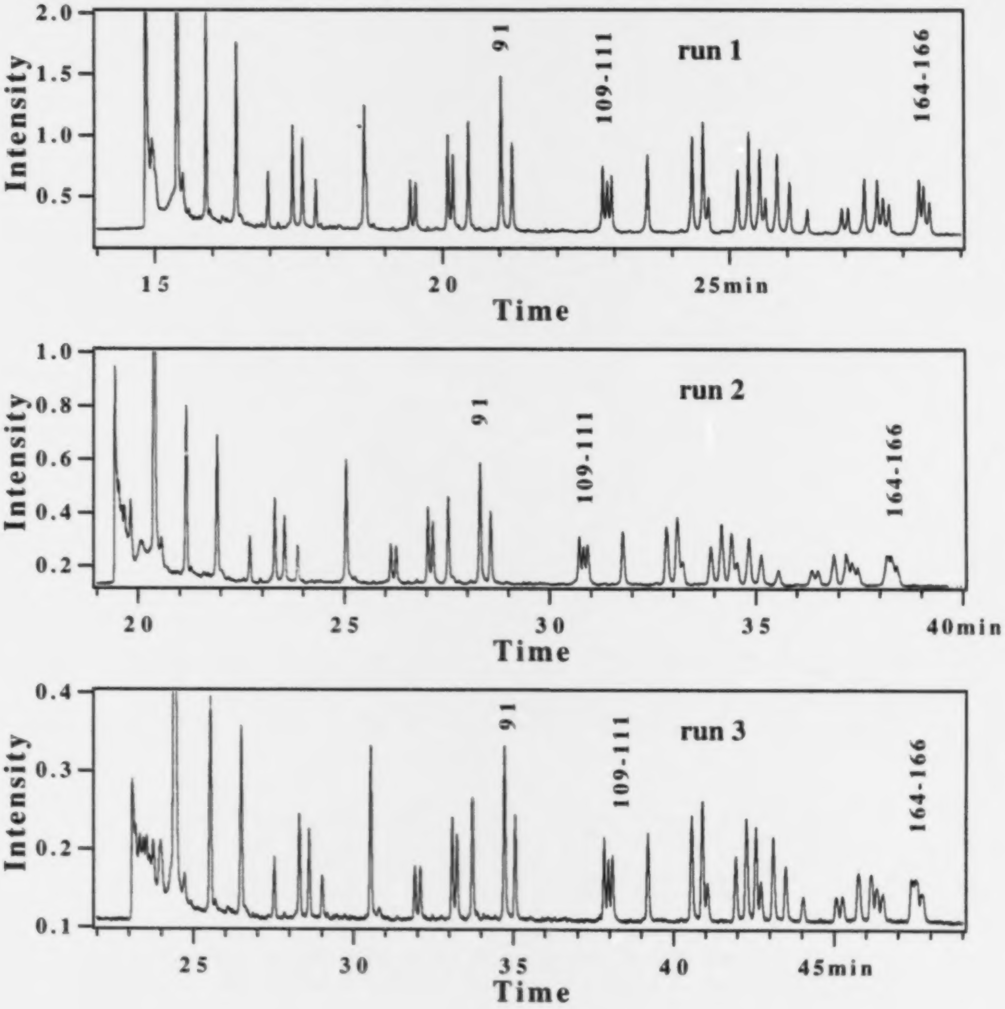

Figure 4.4 Four subsequent separations of M13mp18 ddATP terminated sequencing sample at -300 V/cm on a 36 cm long capillary. The capillary was refilled with 20-day old linear polyacrylamide before the first run, using a gas tight syringe.

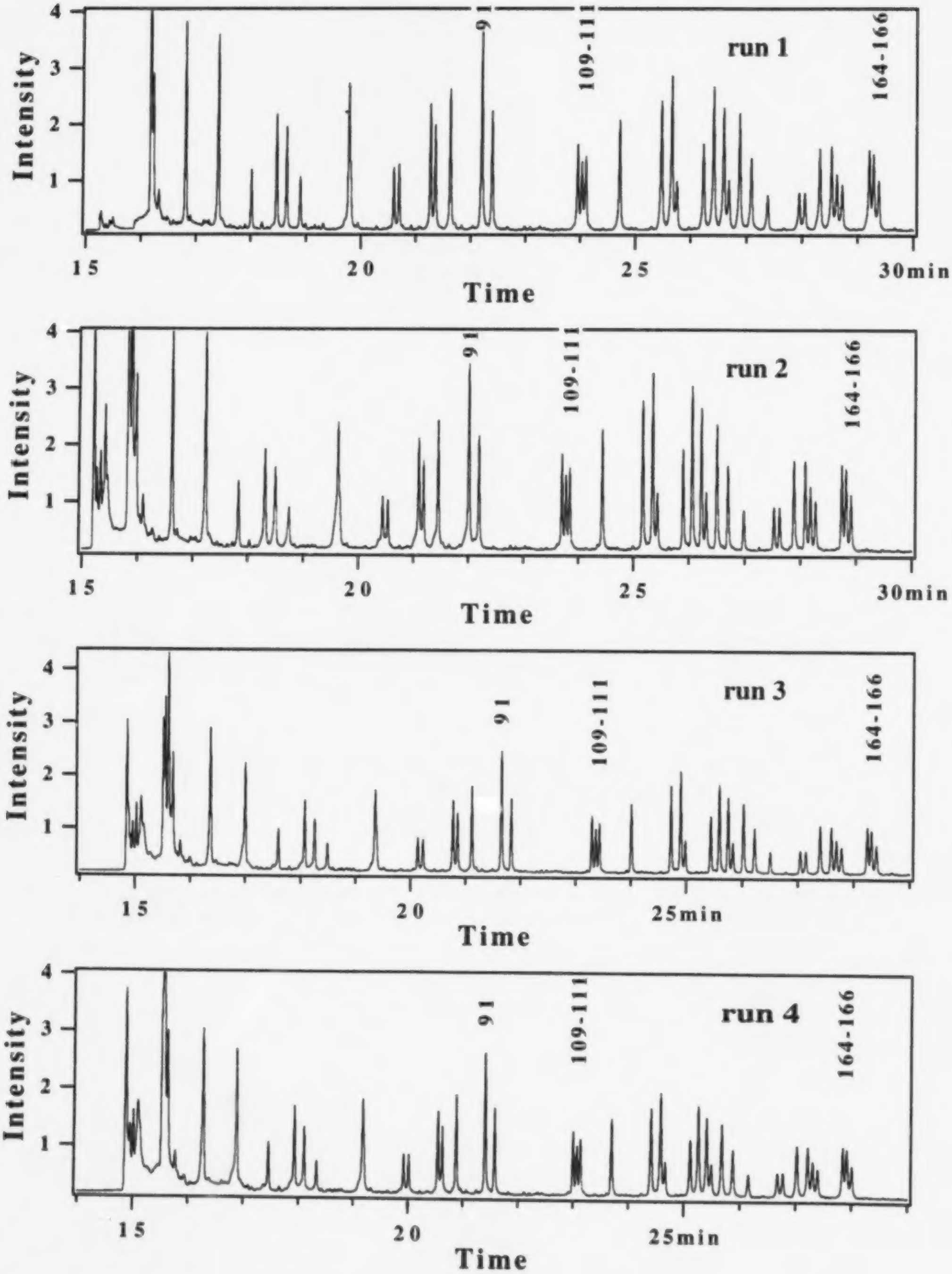

Figure 4.5 Mobilities for base 91 and base 252 versus the age of linear polyacrylamide for four subsequent sequencing runs. The run number is indicated beside each line.

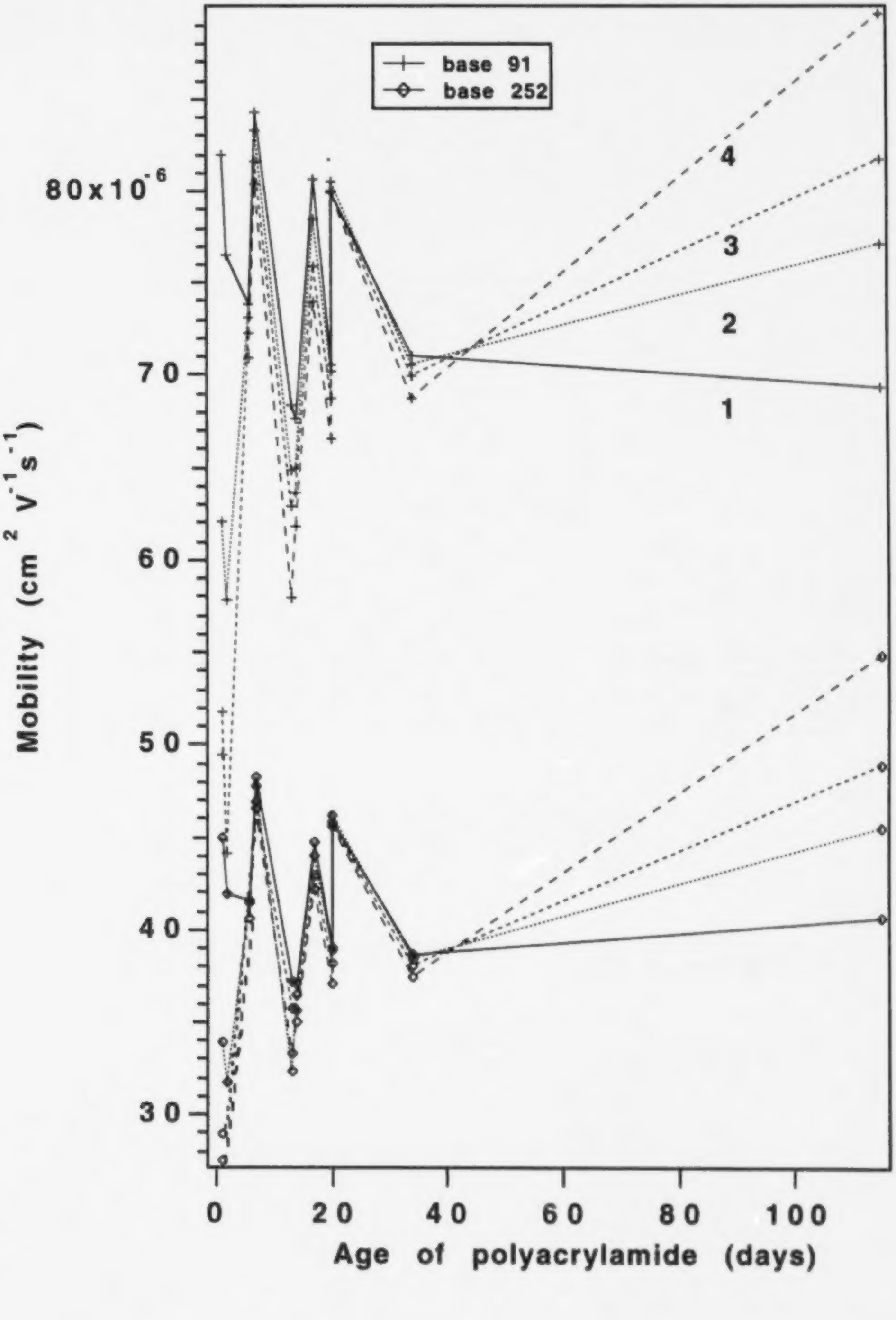

A non-linear least-squares routine was used to fit a four-parameter Gaussian function to peak 91-92 and 252-258 according to equation 1.9. From the values of migration time and A_2, the resolution (R) is calculated using equation 1.12. The resolution for base 91 (Figure 4.6) is similar for all ages of linear polyacrylamide; however, the resolution decreases with the number of sequencing runs. This decrease could be caused by a decrease in Δt and/or an increase in peak width (A_2) from run to run. Δt (Figure 4.7) is stable within the four runs for most of the different ages of linear polyacrylamide; however, in the case of the 115-day old linear polyacrylamide, there is a decrease in Δt from the sequencing run one to four, and in the case of capillaries less than 2-day old, there is an increase in Δt from the sequencing run one to four.

The peak width increases from run to run (Figure 4.8). It easily doubles for the linear polyacrylamide less than 2-day old and increases by an average of 70% for the linear polyacrylamides between 6- and 34-day old. In the case of the 115-day old linear polyacrylamide, the peak width decreases by 1%. In all the cases, except for the 115-day old linear polyacrylamide, decreases in resolutions are due to increases in peak width. For the 115 day old linear polyacrylamide, the decrease is due to a decrease in Δt. The injection contribution to the band broadening should be constant because the injection conditions were identical for all the experiments. In the case of fresh linear polyacrylamide, longitudinal diffusion increases from sequencing run to sequencing run because of the increase in migration time. For older linear polyacrylamide, migration times were fairly constant, thus the longitudinal diffusion effect would not explain the increase in the peak widths. The increase in the peak widths could be due to a structural change in the linear polyacrylamide under high electric fields.

The number of theoretical plates (N_p) is related to the migration times and the peak widths according to Equation 1.10. Figure 4.9 shows the number of theoretical plates for base 91 versus the age of linear polyacrylamide. In all the cases, except the

Figure 4.6 Resolution for base 91 versus the age of linear polyacrylamide for four subsequent sequencing runs. Base 252 was not included for clarity.

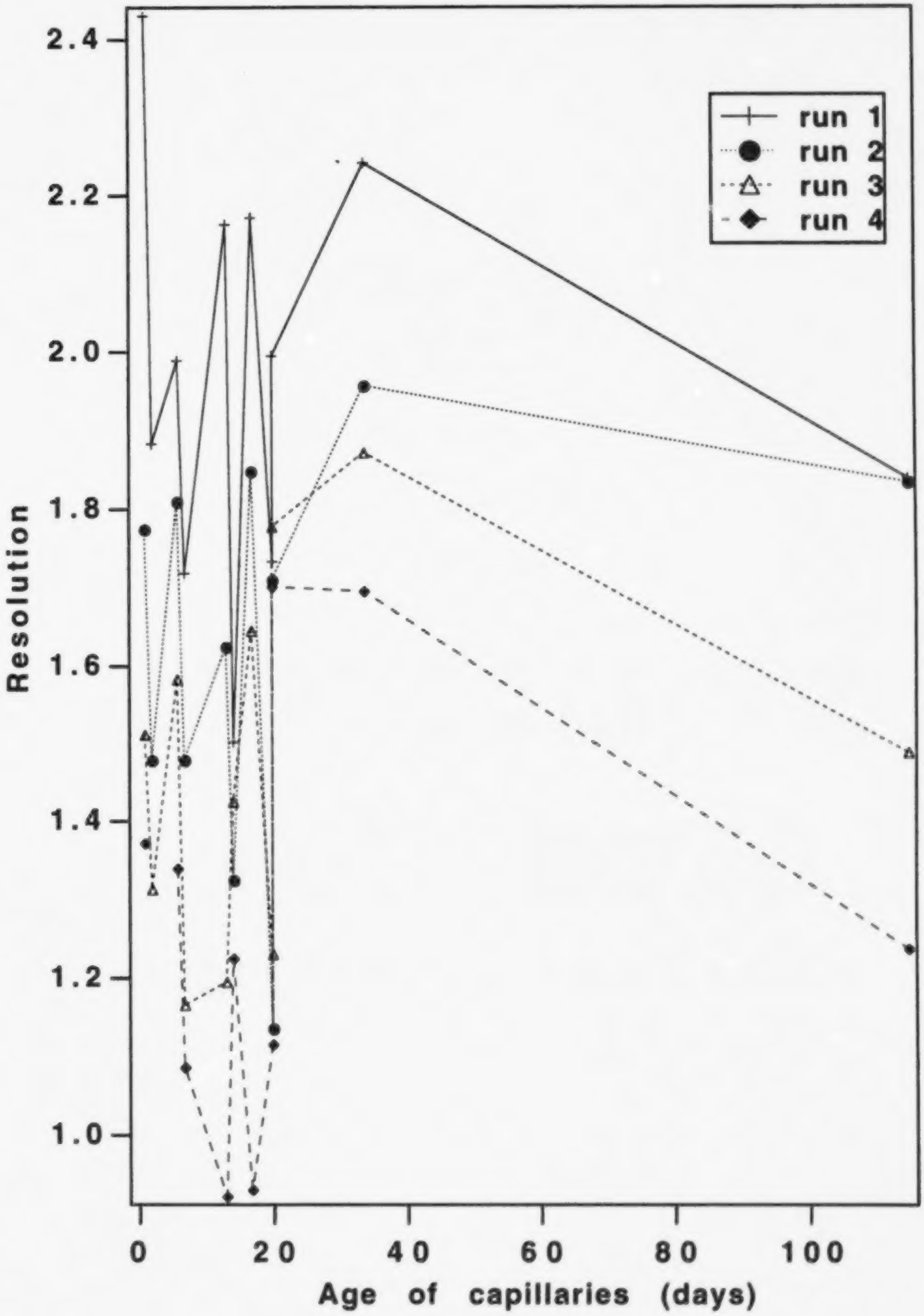

Figure 4.7 Δt for base 91-93 versus the age of polyacrylamide for four subsequent runs.

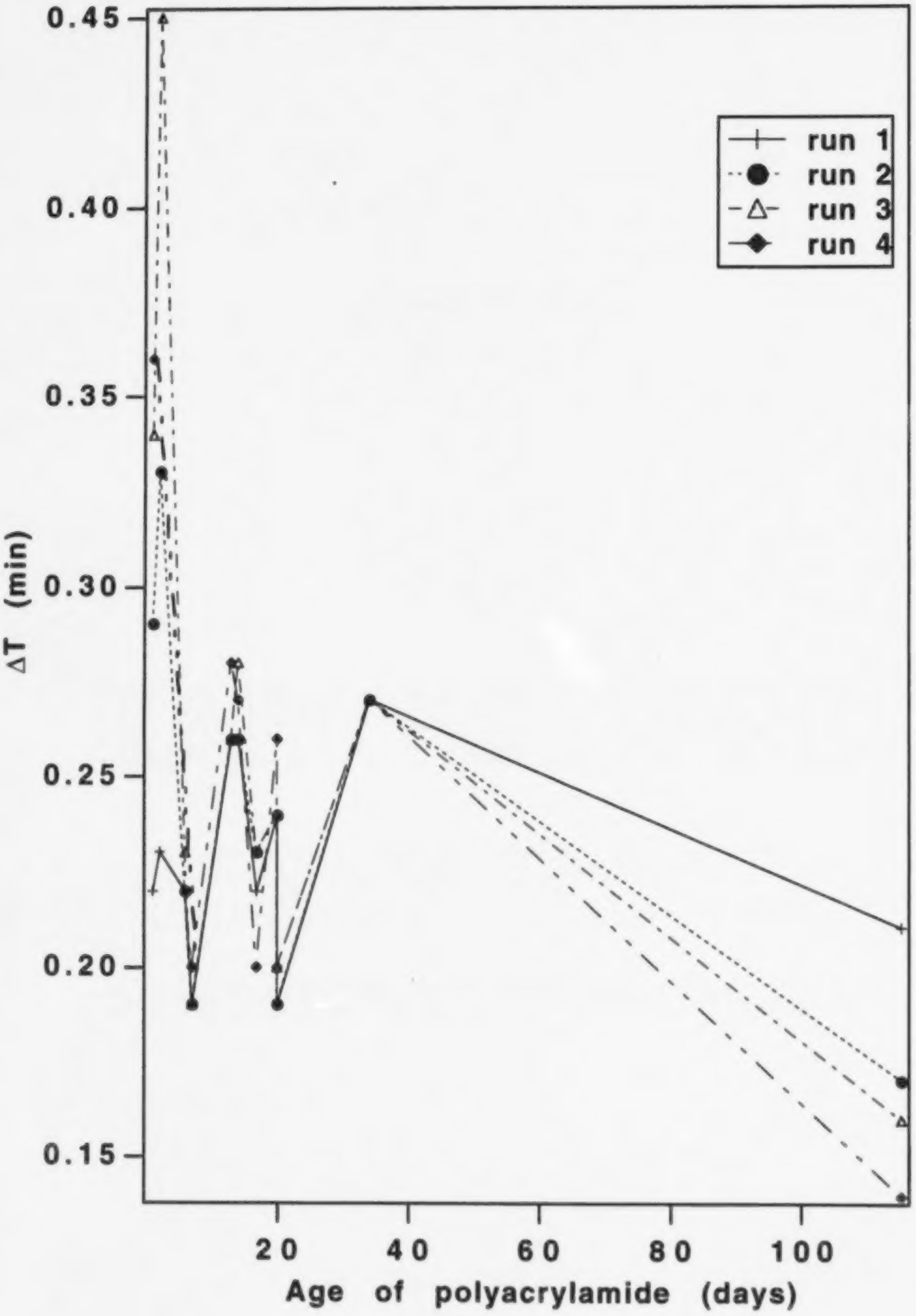

Figure 4.8 Peak widths for base 91 versus the age of polyacrylamide for four subsequent runs.

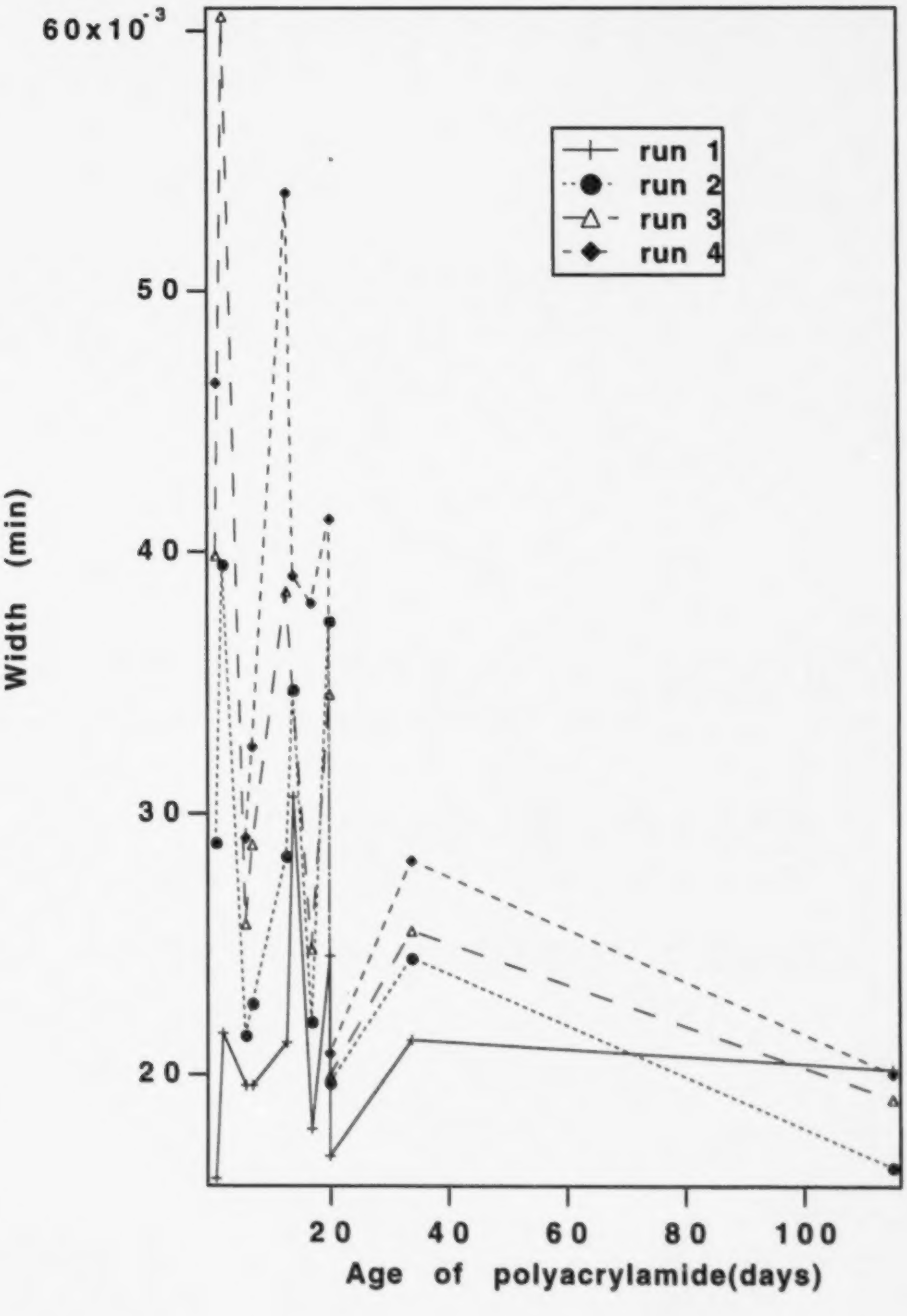

Figure 4.9 Theoretical plates for base 91 versus the age of polyacrylamide for four subsequent sequencing runs. Base 252 was not included for clarity. The run number is indicated beside each line.

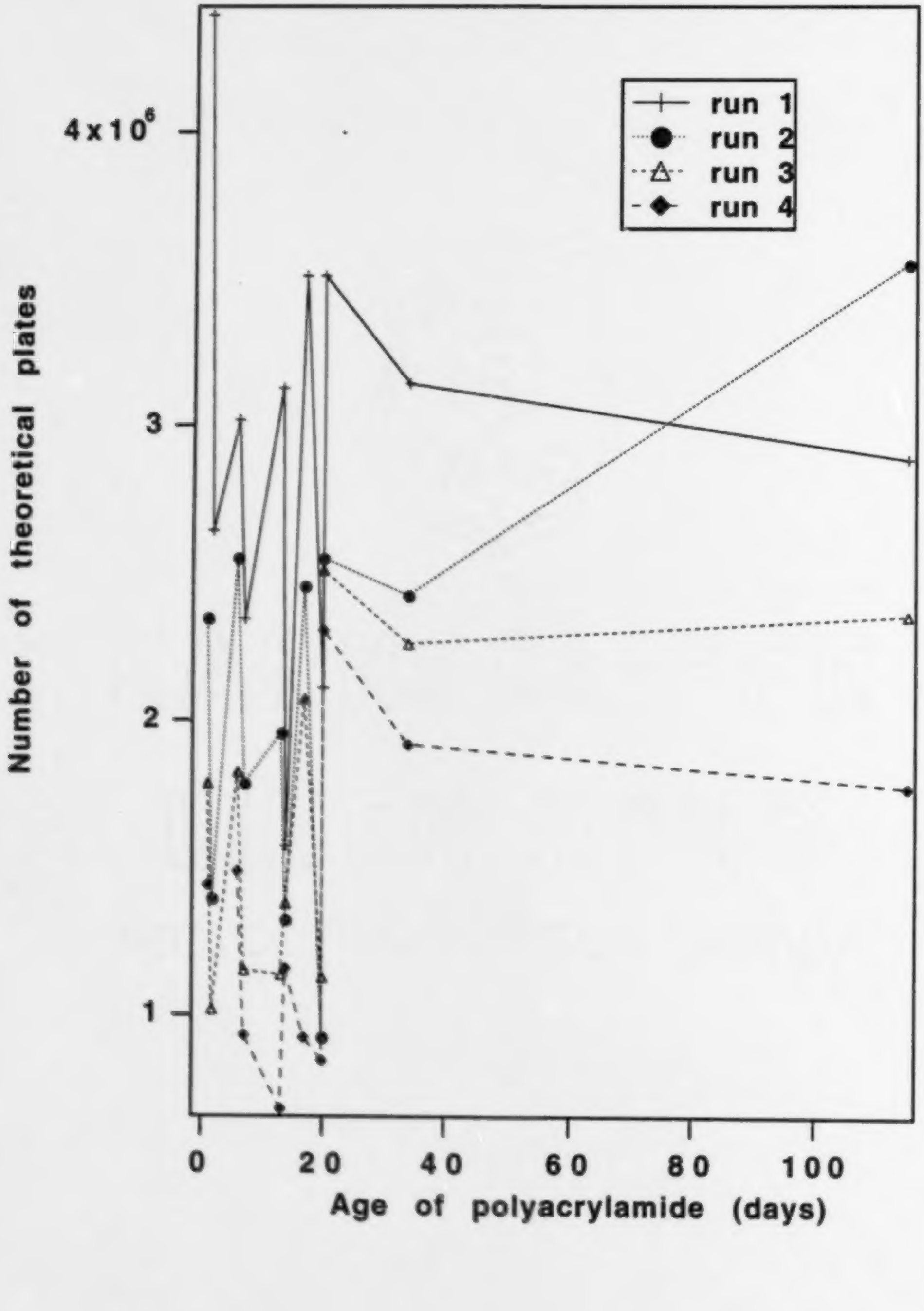

115-day old polyacrylamide, N_p decreases from run to run. In the case of fresh linear polyacrylamides (less than a couple of day old), the migration times increase by 66%, and the peak widths increase by 200%, resulting in a decrease by a factor of three in the number of theoretical plates. Linear polyacrylamide between 6- and 34-day old have migration times that increase by an average of 8%, and peak widths that increase by 70%. This results in a decrease by a factor of 2.5 in the number of theoretical plates. Finally, in the case of the 115 day old linear polyacrylamide, the migration times decrease by an average of 25%, and the peak widths increase by 1% resulting in a decrease by a factor of 1.8 in the number of theoretical plates.

4.3.3 Conclusion

Linear polyacrylamide can be used to perform subsequent sequencing runs on the same capillary if the linear polyacrylamide is aged properly before use. The migration times for aged linear polyacrylamide change by less than 8% for base 91 and 5.5% for base 252 within four sequencing runs. Sufficient resolution was obtained for DNA sequence determination.

4.4 Multiple Runs of DNA Sequencing Samples

4.4.1 Results and Discussion

The results in Chapter 3 and the results from the first part of Chapter 4 suggest that multiple runs can be performed on a capillary if a stable polymer (i.e. older polymer) is used, and if the amount of template in the sample is reduced. Older polymer-filled capillaries stabilized the migration time of DNA for four subsequent runs (Chapter 4.3); however, there is still some depletion of ions occurring in an old polyacrylamide during electrophoresis. In order to decrease the effect of the depletion of ions, the electric field was reversed between each sequencing. This voltage reversal allowed the depletion of ions at the injection end to be refilled, and thus, to decrease the effect of the depletion of

Figure 4.10 Multiple runs of M13mp18 ddATP on a 33 cm x 32 µm id x 143 µm od capillary at -300V/cm. The polarity was reversed after each run at +400V/cm for 20 minutes.

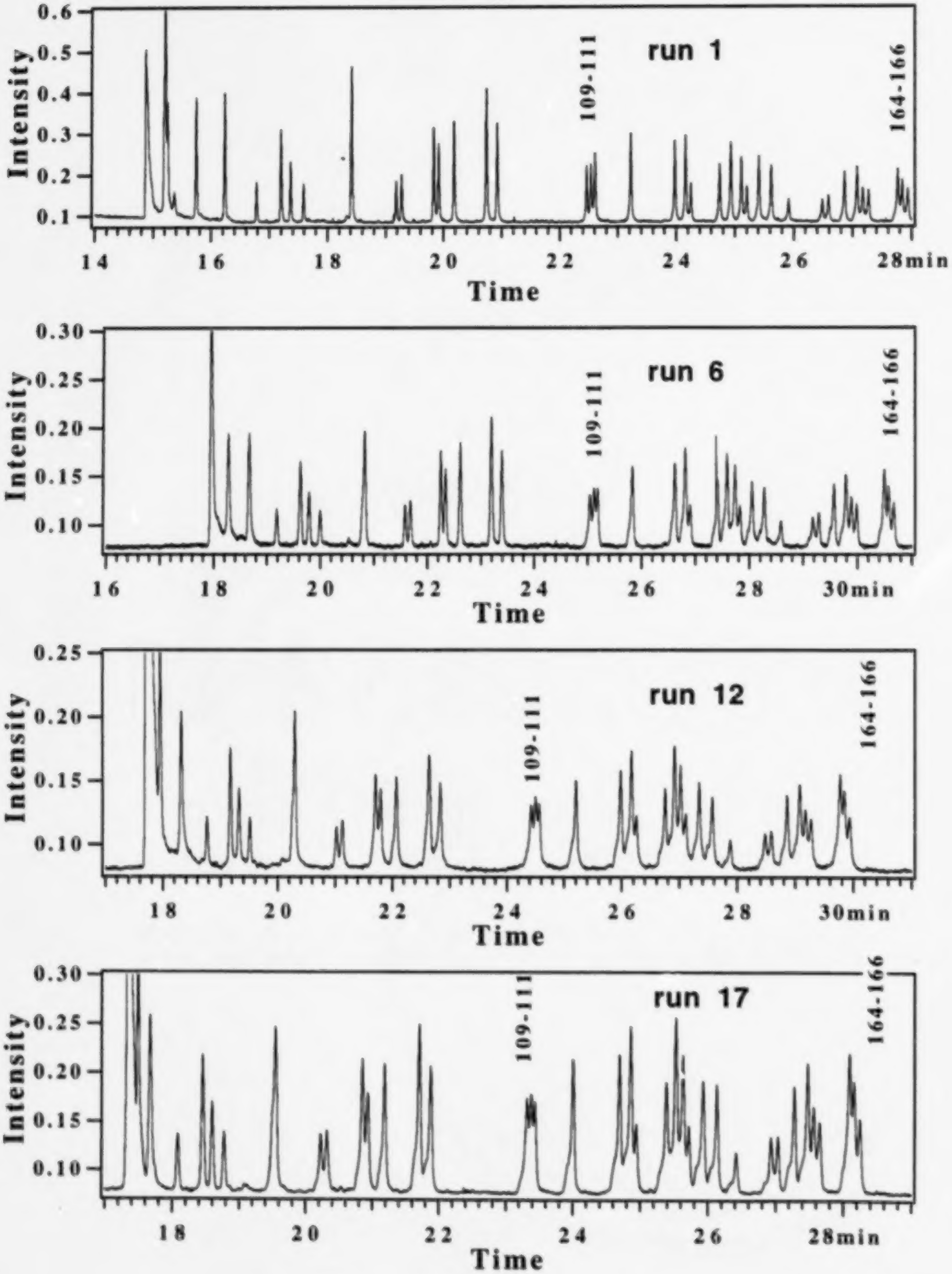

ions. To generate samples with low amounts of template, cycle sequencing was used. Figure 4.10 shows the sequence from the primer up to base 166 for four of the runs. By reversing the polarity between runs, up to 19 subsequent runs were obtained on the same capillary without refilling the capillary. The polarity was reversed for 10 to 20 minutes at +400V/cm between each run. Up to 0.4μA was recuperated by this technique. Reversing the polarity was previously proposed by Swerdlow *et al.* to eliminate the plugging of the pore by big DNA fragments[17]. The separation was reproduced a few times on different capillaries using completely different solutions (Appendix B).

Figure 4.11 shows the change in current versus the run number. There is still a slight decrease in current (1.49 to 1.29 μA) which is not compensated by reversing the polarity. It could be due to an incomplete deplugging of the pore. The increase in current from run 7 to 8 and run 13 to 14 occurred because of the overnight delay between these runs.

Figure 4.12 shows the change in mobility versus the run number. The relative standard deviation of the mobility is 3% to 6% for base 91 to base 350. Thus, the migration time is stable within 19 runs. The variation of the migration time seems to be related to the variation in the current from run to run. It can be seen more clearly on Figure 4.13 that the mobility is related to the current for four subsequent injections on a capillary without reversing the polarity. Thus, any change in current during electrophoresis affects the migration time of the analytes. This means that by stabilizing the change in current with time, the migration time will be stabilized.

The peaks for base 91, 142, 252, 350, and the next fragment after each of these bases were fitted using a Gaussian model (Equation 1.9) and the resolution was calculated using Equation 1.12. Figure 4.14 shows the resolution versus number of runs. The main decrease in the resolution occurs in the first four runs. The resolution is still very satisfactory for fragments smaller than 200 bases for all the other runs. We injected a

Figure 4.11 Average current in the capillary used for 19 DNA sequencing runs. Other conditions as in fig. 4.10.

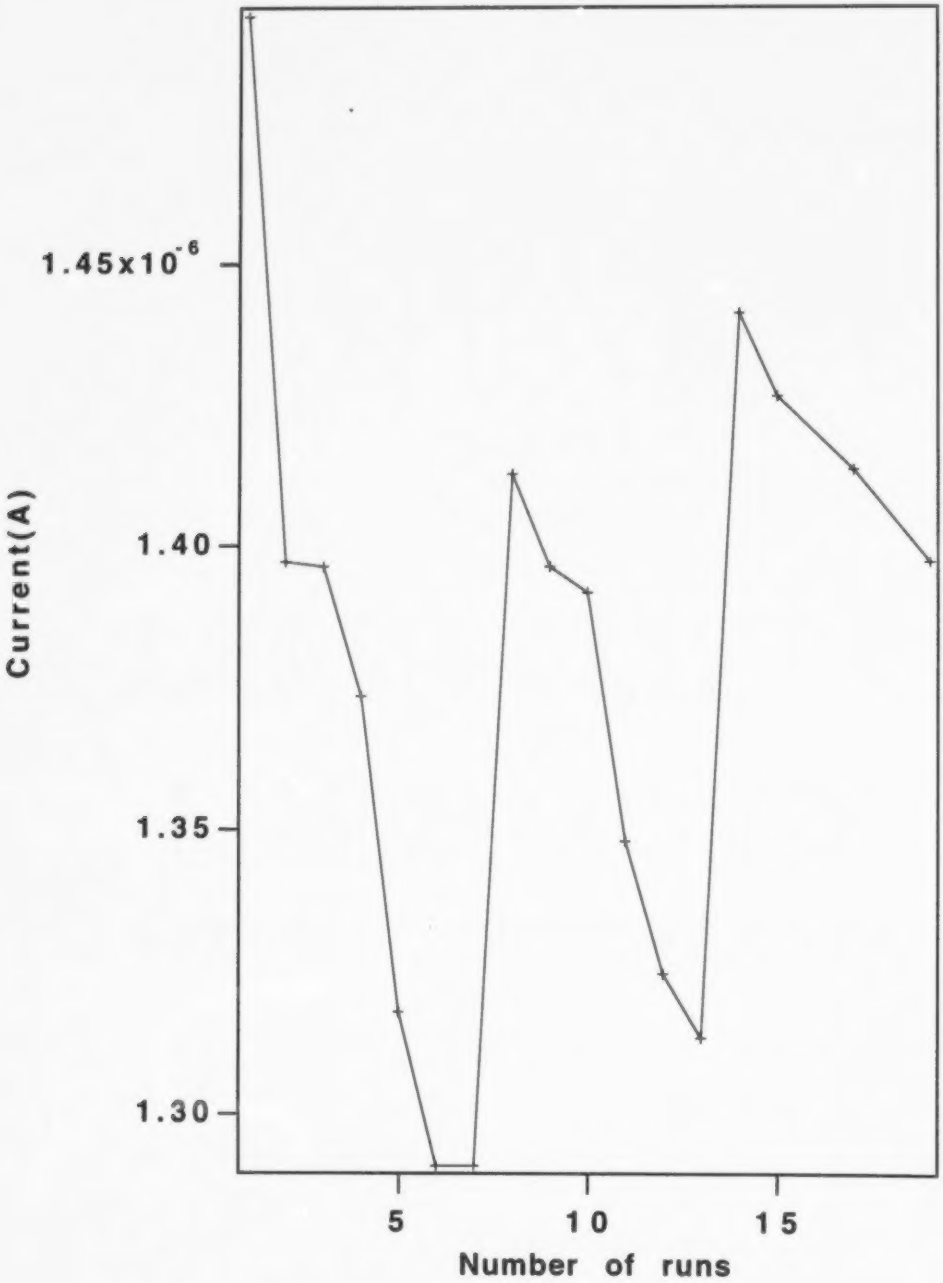

Figure 4.12 Mobility for different peaks for 19 runs. Other conditions as in fig. 4.10.

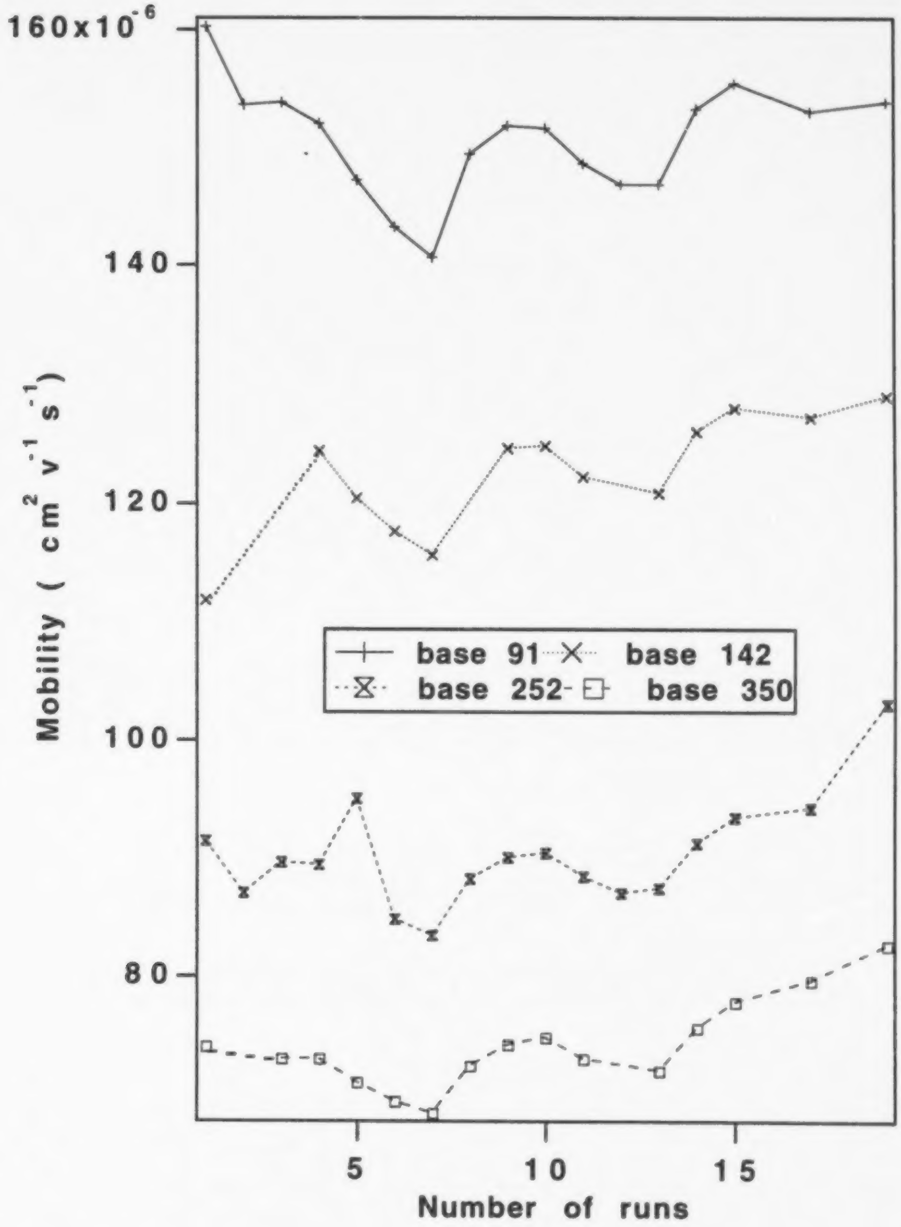

Figure 4.13 Mobility versus current for four subsequent runs done on a one-day old capillary. The polarity was not reversed in between runs.

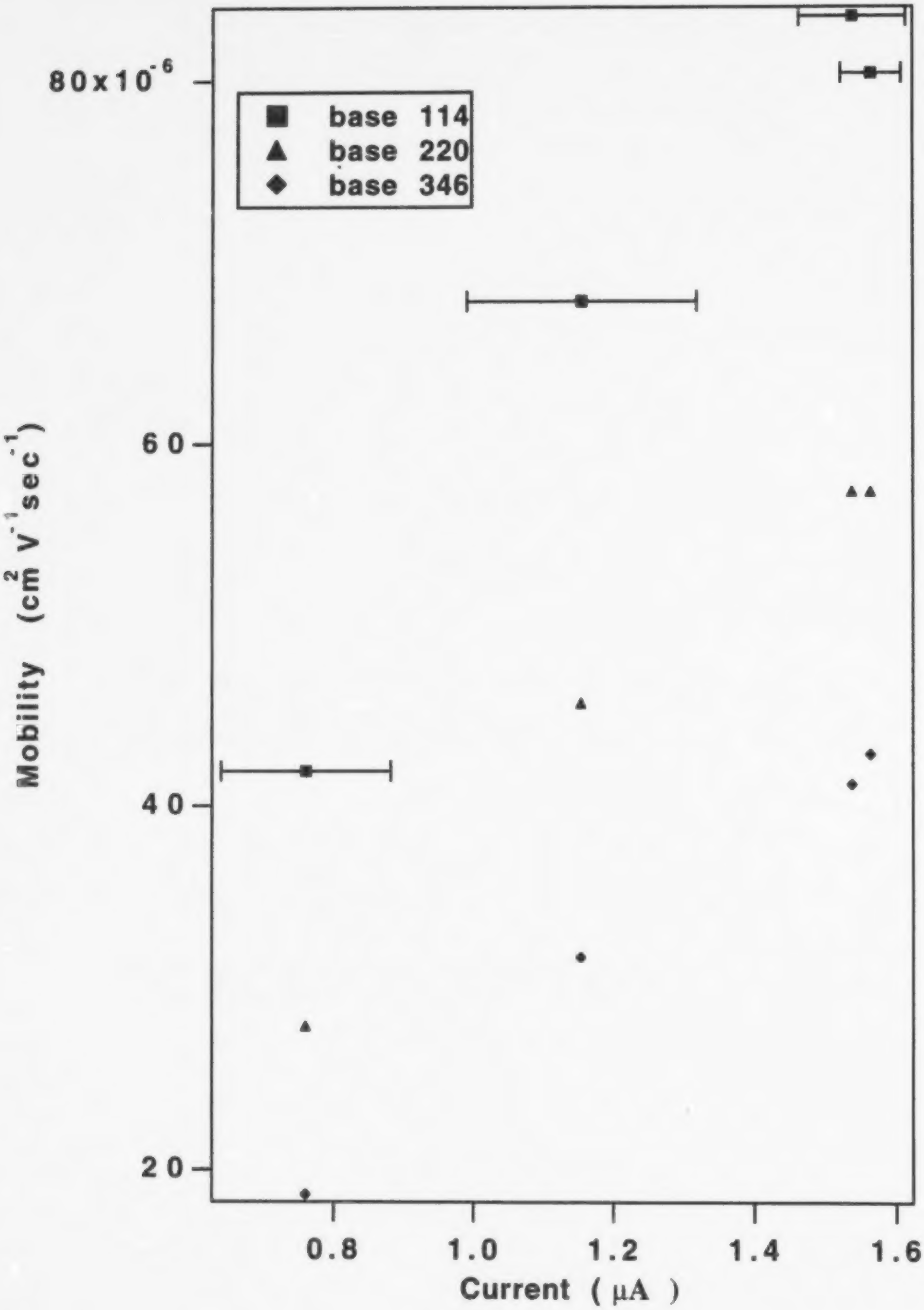

Figure 4.14 Resolution versus number of runs for different peaks. Other conditions as in fig. 4.10.

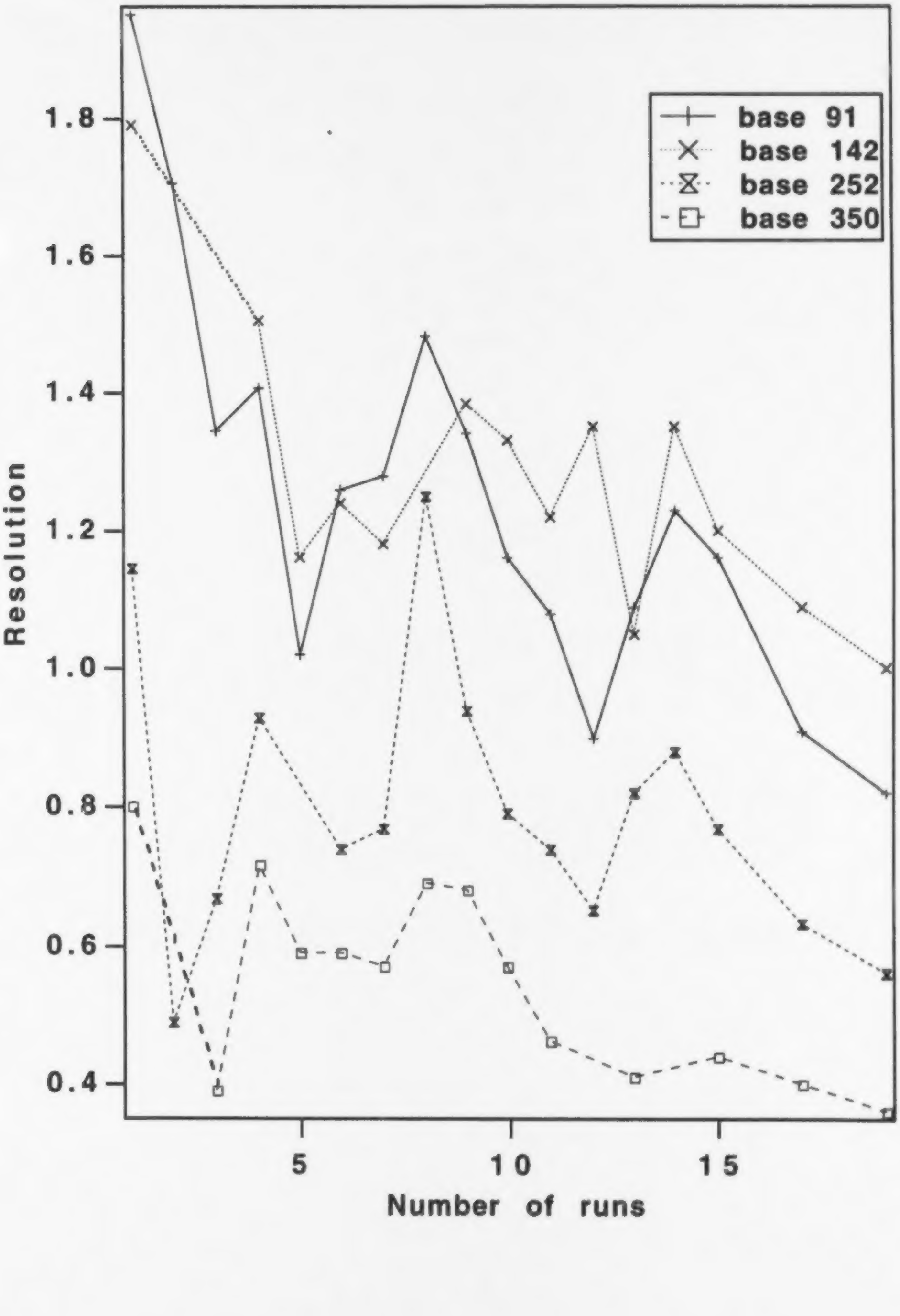

plug of NaCl before injecting some of the samples, because we observed the appearance of shoulder peaks, or double peaks, for longer fragments. This problem, due to sample preparation, could be easily eliminated by desalting the sample before injection. We did not attempt in this study to optimize the capillary length, the voltage, the buffer, or the sample preparation to obtain better results.

4.4.2 Conclusion

We have shown that it is possible to perform multiple runs on the same capillary without refilling it. Up to 19 subsequent runs were obtained on the same capillary. Based on the final current, it can be predicted that the number of runs is not limited to 19. The resolution is satisfactory for fragments less than 200 bases. The authors preferred to limit themselves to 19 runs, and instead, concentrate on reproducing their results with many different capillaries prepared with completely different solutions.

4.5 Bibliography

(1) Chen, D.; Harke, H. R.; Dovichi, N. J. *Nucleic Acids Research* **1992**, *20*, 4873-4880.

(2) Pentoney, S. L.; Konrad, K. D.; Kaye, W. *Electrophoresis* **1992**, *13*, 467-474.

(3) Swerdlow, H.; Zhang, J. Z.; Chen, D. Y.; Harke, H. R.; Grey, R.; Wu, S.; Dovichi, N. J.; Fuller, C. *Analytical Chemistry* **1991**, *63*, 2835-2841.

(4) Swerdlow, H.; Gesteland, R. *Nucleic Acids Research* **1990**, *18*, 1415-1419.

(5) Chen, D. Y.; Swerdlow, H. P.; Harke, H. R.; Zhang, J. Z.; Dovichi, N. J. *Journal of Chromatography* **1991**, 237.

(6) Huang, X. C.; Quesada, M. A.; Mathies, R. A. *Analytical Chemistry* **1992**, *64*, 967-972.

(7) Kambara, H.; Takahashi, S. *Nature* **1993**, *361*, 565-566.

(8) Ruiz-Martinez, M. C.; Berka, J.; Belenkii, A.; Foret, F.; Miller, A. W.; Karger, B. L. *Analytical Chemistry* **1993**, *65*, 2851-2858.

(9) Drossman, H.; Luckey, J. A.; Kostichka, A. J.; D'Cunha, J.; Smith, L. M. *Analytical Chemistry* **1990**, *62*, 900-903.

(10) Cohen, A. S.; Najarian, D. R.; Karger, B. L. *Journal of Chromatography* **1990**, *516*, 49-60.

(11) Luckey, J. A.; Drossman, H.; Kostichka, A. J.; Mead, D. A.; D'Cunha, J.; Norris, T. B.; Smith, L. M. *Nucleic Acids Research* **1990**, *18*, 4417-4421.

(12) Sanger, F.; Nicklen, S.; Coulson, A. R. *Proceedings of the National Academy of Sciences USA* **1977**, *74*, 5463-5467.

(13) Rocheleau, M. J.; Dovichi, N. J. *Journal of Microcolumn Separations* **1992**, *4*, 449-453.

(14) Harke, H. R.; Bay, S.; Zhang, J. Z.; Rocheleau, M. J.; Dovichi, N. J. *Journal of Chromatography* **1992**, *608*, 143-150.

(15) Figeys, D.; Dovichi, N. J. *Journal of Chromatography* **1993**, *645*, 311-317.

(16) Lu, H.; Arriaga, E.; Chen, D. Y.; Figeys, D.; Dovichi, N. J. *Journal of Chromatography* **1994**, *680*, 503-510.

(17) Swerdlow, H.; Dew-Jager, K. E.; Brady, K.; Grey, R.; Dovichi, N. J.; Gesteland, R. *Electrophoresis* **1992**, *13*, 475-483.

(18) Figeys, D.; Renborg, A.; Dovichi, N. J. *Electrophoresis* **1994**, *15*, 1512-1517.

(19) Sudor, J.; Foret, F.; Bocek, P. *Electrophoresis* **1991**, *12*, 1056-1058.

(20) Chiari, M.; Nesi, M.; Fazio, M.; Righetti, P. G. *Electrophoresis* **1992**, *13*, 690-697.

(21) Baba, Y.; Matsuura, T.; Wakamoto, K.; Morita, Y.; Nishitsu, Y.; Tsuhako, M. *Analytical Chemistry* **1992**, *64*, 1221-1225.

(22) Baba, Y.; Matsuura, T.; Wakamoto, K.; Tsuhako, M. *Chemistry Letters* **1991**, 371-374.

(23) Guttman, A.; Wanders, B.; Cooke, N. *Analytical Chemistry* **1992**, *64*, 2348-2351.

(24) Huang, X. C.; Quesada, M. A.; Mathies, R. A. *Analytical Chemistry* **1992**, *64*, 2149-2154.

(25) Spencer, M. *Electrophoresis* **1983**, *4*, 36-41.

(26) Spencer, M. *Electrophoresis* **1983**, *4*, 41-45.

(27) Spencer, M. *Electrophoresis* **1983**, *4*, 46-52.

(28) Slater, G. W.; Mayer, P.; Drouin, G. *Analusis Magazine* **1993**, *21*, M25-M28.

(29) Slater, G. W.; Mayer, P.; Drouin, G. *Electrophoresis* **1993**, *14*, 962-966.

(30) Seida, Y.; Nakano, Y. *Journal of Chemical Engineering of Japan* **1991**, *24*, 755-760.

CHAPTER 5 [1, 2]

LABELING AND SEPARATION BY CAPILLARY ELECTROPHORESIS OF DOUBLE-STRANDED DNA.

---

[1] A part of this chapter has been published.
Figeys, D., Arriaga, E., Renborg, A. and Dovichi, N.J. 1994. Journal of Chromatography A 669:205-216.

[2] A part of this chapter has been published.
Figeys, D., Renborg, A. and Dovichi, N.J. 1994. Analytical Chemistry 66:4382-4383.

5.1 Introduction

DNA is one of the most important substances in the living world. It contains all the necessary information to create and maintain life. Most of the information within the DNA is usually hereditary transferred without any change, but some of it changes leading to, virtually, an infinity of possible results. This variability of DNA is involved in the process of evolution.

Geneticists are interested in using this variability of the DNA to change or correct DNA. For example, they are able to create genetically altered crops or work on genetic treatments for diseases, like cancer. In these processes, they would need to cut or insert a piece of DNA at an exact position into the target DNA; this involves techniques such as restriction mapping and genomic mapping. In these mapping techniques, minute amounts of DNA restriction fragments have to be separated.

Traditionally, the separation of double-stranded DNA fragments was done by slab gel electrophoresis [1-3]. The demand for new techniques for efficient and fast separation of small amounts of DNA fragments has greatly increased in the last few years. Capillary electrophoresis, using polymers as sieving media, is one of the emerging techniques[4-23]. The advantage of capillary electrophoresis using sieving media over other techniques is its separation of a wide range of DNA fragments using different sieving media.

Agarose is used for the separation of long fragments and short fragments. Separation up to 12,000 base pairs of 1Kb ladders of DNA fragments was achieved by using 1.7% agarose[7]; 72-1353 bp fragments (ϕx174 RF/HaeIII) were separated using 0.3-2.8% agarose[24]. A low melting-point agarose solution was used to separate DNA fragments by capillary zone electrophoresis[8]. Agarose cannot be used in our capillary electrophoresis system because agarose tends to extrude from the capillary and plug the sheath flow cuvette.

Polyacrylamide gels are used for the separation of small fragments (<2000bp). Heiger *et al.* [11] used polyacrylamide (3%T 0.5%C) for the separation of ϕx174 RF/HaeIII fragments and 1000 bp ladder DNA fragments. Guttman[12] also used polyacrylamide to separate ϕx174 RF/HaeIII, and pBR322 DNA Hae III, but used gradient and step fields to obtain better resolutions. Capillaries filled with cross-linked polyacrylamide gel are very susceptible to the formation of bubbles, they cannot be refilled, and they usually have a short life.

Open-tube capillary electrophoresis has been used to separate a mixture of λDNA/Hind III digest and ϕx174 RF/Hae III digest (72 to 23130 bp) using a buffer made of 0.1M TRIS-borate, 2.5 mM EDTA, 0.1% SDS, and 7 M urea[25]. Although borate, urea, and SDS are presumed to bind to DNA and change its conformation, the mechanism of the separation is not well understood[17]. Also, the success of the experiment highly depends on careful handling and pretreatment of the sample.

Chin and Colburn[26] have written a report on the separation of restriction fragments by counter-migration capillary electrophoresis. In this technique, an uncoated capillary is filled with a TRIS-borate-based system that contains hydrophilic derivatives of cellulose. This technique takes advantage of high electroendosmotic flow to propel the bulk solution towards the detector.

Coated capillaries and entangled polymers seem to be very promising. The capillary filled with these polymers can usually be refilled, and used quite extensively. Novotny used hydroxyethylcellulose 0.2 to 1% for the separation of pBR322 DNA Hae III (22 fragments from 8 to 587 bp)[27]. Mathies and Clark [28] succeeded in the separation of ϕx174 RF/Hae III digest using capillary array electrophoresis on hydroxyethylcellulose. Grossman and Soane[15] did a rheological study of the separation of DNA restriction fragments in hydroxyethyl cellulose using capillary electrophoresis. Strege and Lagu[17] used a polyacrylamide-coated capillary in conjunction with 50 mM TRIS-borate, 2.5mM EDTA and 0.5% methylcellulose for the separation of 1Kb ladder (75 to 12 216bp) and λDNA/Hind III digest (125 to 23 130bp). Hydroxypropylmethylcellulose (HPMC) has been used by Schwartz *et al.*[5] at a concentration of 0.5% (4000cp) to separate ϕx174 RF/Hae III digest. He indicated that this polymer is well suited for the separation of small DNA fragments (1.8 million plates/m for the 118bp fragment). Schomburg *et al.* [29] separated different samples of DNA restriction fragments in linear polyacrylamide, hydroxyethylcellulose, and polyvinylalcohol. Morris and Kim[23] used pulsed-field capillary electrophoresis in dilute methylcellulose to separate multikilobase length nucleic acids. Sudor and Novotny[30] used pulsed-field capillary electrophoresis in a linear polyacrylamide solution for the separation of 48.5 kilobases to 1 megabase DNA fragments.

5.1.1 Intercalating Dyes

Most capillary electrophoresis analysis of double-stranded DNA has relied on ultraviolet absorbance for detection. Because of the large molar absorptivity of large DNA fragments, ultraviolet absorbance has produced detection limits of 10^{-18} mol of injected DNA.

Fluorescence detection is required for the study of minute amounts of analytes. Native fluorescence of DNA generates useful fluorescence signals upon excitation in the ultraviolet portion of the spectrum [18,31]. Usually, dyes have better quantum yields than native DNA, and they fluoresce in the visible spectrum. Non-intercalating dyes such as 33258 and 33342 Hoescht dyes can be added to the running buffer to achieve fluorescence emission; however, the sensitivity attained is roughly equivalent to UV detection [5]. Other dyes insert themselves between adjacent base pairs of double-stranded DNA. These dyes have planar aromatic or heteroaromatic rings, and they are know as intercalating dyes. Guttman and Cooke[32] studied the effects of the presence of an intercalating dye (ethidium bromide) on the separation of a few DNA samples. They indicated that the presence of ethidium bromide increases the resolution of DNA fragments, increases the UV absorbance of the DNA, and changes the velocity of the DNA fragments. Some intercalating dyes do not fluoresce unless they are inside a DNA strand, resulting in better sensitivities[33-35]. Ethidium homodimer (EthD), shows a better sensitivity than non-intercalating dyes, it allows picogram fluorescence detection of DNA[1].

A new line of ultra-sensitive intercalating dyes has been recently developed by Glazer *et al.* at Berkeley[33,35-38]. These dyes are dimers of intercalating dyes that have been modified to produce high affinities for DNA. The benzothiazolium-4-quinolinium dimer (TOTO-1) and the benzoxazolium-4-quinolinium dimer (YOYO-1) are examples of these types of dyes. The structure of the dyes used in our experiment are quite similar (Figure 5.1). By changing part of the structure, like replacing quinolinium by pyridinium, or benzothiazolium by benzoxazolium, it is possible to obtain a variety of dyes that absorb and fluoresce at different wavelengths, with a different quantum yield and a different affinity for the DNA (Table 5.1). The values in Table 5.1[36] are for the dyes intercalated in DNA. These dyes were selected because each one is excited with a specific laser. YOYO-1 is excited by the blue line (488 nm) of an Ar^+ laser, YOYO-3 is excited with the orange line (612 nm) of the He-Ne laser, and POPO-3 is excited with the green line (543 nm) of a He-Ne laser. These novel intercalating dyes have a much higher fluorescence enhancement (fluorescence signal for bound dye versus free dye) than Ethidium homodimer-1(EthD-1): EthD-1 has an enhancement of 40, TOTO-1 has an enhancement of 1,100, and YOYO-1 has an enhancement of 3,200 [33].

Rye *et al.* [34] used the TOTO and YOYO intercalating dyes to perform fluorometric assay on double-stranded DNA with a laser-excited confocal fluorescence scanner; as little as 20 pg of double-stranded DNA was detected.

There are a few preliminary reports on the use of these dyes in capillary gel electrophoresis. Schwartz *et al.* [5] used ethidium bromide to improve the resolution of restriction fragments; ultraviolet absorbance was used for detection. Schwartz and Ulfelder [4] did a comparative study of the separation of PCR fragments by capillary electrophoresis. They used ultraviolet detection and laser-induced fluorescence detection

Figure 5.1 Structures of the intercalating dyes POPO-3, YOYO-1, and YOYO-3.

POPO-3

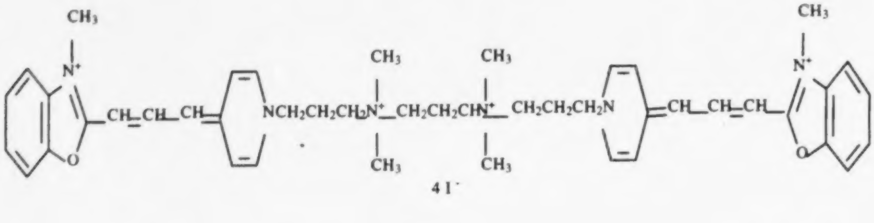
CH3
N+
O
CH=CH–CH=
NCH2CH2CH2N+–CH2CH2CH2N+–CH2CH2CH2N
=CH–CH=CH–
4 I-

YOYO-1

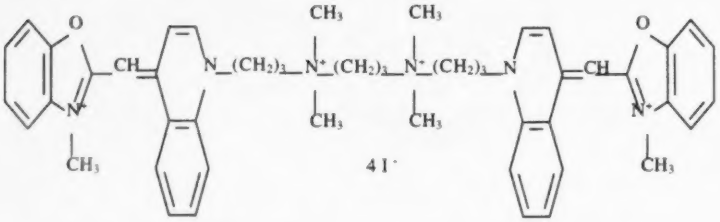
O
N+
CH3
CH=
N–(CH2)3–N+–(CH2)3–N+–(CH2)3–N
=CH
4 I-

YOYO-3

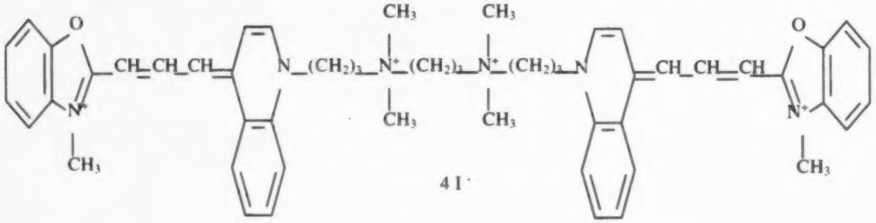
O
N+
CH3
CH=CH–CH=
N–(CH2)3–N+–(CH2)3–N+–(CH2)3–N
=CH–CH=CH
4 I-

Table 5.1 Characteristics of the dyes.

Dye	EX_{max} $/EM_{max}$ (nm)	$\varepsilon^1 x10^{-3}$ (QY^2)	$K_p{}^3$
YOYO-1	**491/509**	**84(0.52)**	**$6.0x10^{-8}$**
YOYO-3	**612/631**	**167(0.15)**	**$1.5x10^{-8}$**
POPO-3	**534/570**	**146(0.46)**	**nd**[4]
EthD-1	**528/617**	**7.4(0.08)**	**$5.0x10^{-8}$**

[1] cm^{-1} M^{-1} [2] QY=quantum yield [3] K_p=partition coefficient of the dye between DNA and solution [4] nd=not determined

with thiazole orange as the intercalating dye. Guttman and Cooke reported the use of ethidium bromide as a complexing ligand to improve electrophoretic resolutions. Ultraviolet absorbance was used in this report[32]. Morris *et al.* reported the use of ethidium bromide with helium-cadmium laser excited fluorescence and velocity modulated capillary electrophoresis[20]. More recently, Sepaniak *et al.* reported fluorescence detection for ethidium bromide and POPO-3 labeled DNA[28]. Detection limits (3σ) were 8.9 fg ($9\text{x}10^{-20}$ mol) for a 310 base-pair fragment. Assuming one dye molecule per four base pairs, the detection limit for the dye molecule is $3\text{x}10^{-19}$ mol intercalated into DNA. Keller *et al.* [39] and Shera *et al.* [40] at Los Alamos National Laboratory have reported size determinations of individual double-stranded DNA molecules that have been labeled with intercalating dyes. In these experiments, a large number of intercalating dye molecules are used to label the DNA fragments. When a highly diluted solution was analyzed in a modified flow cytometry instrument, the amplitude of the fluorescent burst was used to identify the size of the DNA fragment. Morris and Kim[21] used the bis-intercalating dyes ethidium homodimer-1 and ethidium homodimer-2 for the separation of ϕx174 RF/HaeIII digest in HPMC.

In this study, we show fast separations of DNA restriction fragments intercalated with ultra sensitive dyes (POPO-3, YOYO-1, and YOYO-3) using HPMC and linear polyacrylamide as sieving mediums in capillary electrophoresis. We use micellar electrokinetic capillary chromatography (MECC) to demonstrate the possibility of detecting a single 6 kb long DNA fragment. High sensitivity laser-induced fluorescence is used to detect fluorescently labeled analytes.

5.1.2 ROX-Dideoxycytosine Triphosphate

While intercalating dyes are very convenient to use, they suffer from a few limitations. First, the positive charge on the intercalating dyes changes the mobility and the stiffness of the DNA fragments. Second, only one sample can be processed at one time on the same capillary due to the rapid exchange of different dyes between DNA fragments. This limitation is particularly acute in capillary electrophoresis, where it is very useful to include a size marker along with the unknown DNA for analysis in a single capillary. The throughput of each capillary can also increase if several samples labeled with different fluorescence labels are analyzed simultaneously. We have attempted to use different intercalating dyes to label double-stranded DNA originating from two different restriction endonuclease digests; inevitably, an exchange of dyes was observed, resulting in the inability to distinguish the fluorescence from the two digests. Thus, it appears necessary to covalently label DNA with fluorescent dyes. The covalently bound dye is unable to be exchanged between DNA molecules, allowing analysis of many different analytes simultaneously in a single capillary. This approach also minimizes the effect of the label on the mobility of the DNA.

We report the use of terminal deoxynucleotidyl transferase to label covalently blunt and sticky ended DNA fragments with a fluorescently labeled dideoxynucleotide. Terminal deoxynucleotidyl transferase is widely used for 3'-end labeling of DNA or RNA with radioisotopically labeled nucleotides[41,42]. A fluorescently labeled deoxynucleotide has been used to label RNA[43] with terminal deoxynucleotidyl transference. Trainor and Jansen[44] used succinylfluorescein-labeled dideoxynucleoside triphosphate to label 17 bp oligonucleotide. Igloi and Schiefermayr[45] used terminal deoxynucleotidyl transferase to incorporate a fluorescently labeled dUTP to a single-stranded primer; however, to the best of our knowledge, terminal deoxynucleotidyl transferase has not been used to fluorescently label restriction fragment digests.

5.2 Intercalating Dye Experiments

5.2.1 Experimental

The capillary electrophoresis system and the detector used in this experiment were described in chapter 1. The experiments were done using 50 μm id x 144 μm od capillaries (Polymicro, Phoenix, AR). The capillaries were silanized as described in chapter 1. For MECC experiments, the outside polyimide coating of the end of the capillary inserted in the sheath flow cuvette was removed by a gentle flame. When HPMC was used as a sieving medium, the inner wall of the capillary was coated with 2%T acrylamide solution. After the polymerization of acrylamide, 0.4% HPMC was introduced inside the capillary using a syringe with an appropriate glass fitting. The 0.4% HPMC in 1xTBE was prepared by diluting a 4000 cp, 2% HPMC stock solution (Sigma, St. Louis, MO). For use with linear polyacrylamide, capillaries were also silanized as described in chapter 1. The detector used is similar to others reported from this laboratory[46], and it has been described in chapter 1.

Five different samples were used in this study. The first one is ϕx174 RF/HaeIII digest, which is commercially available. This sample includes the following fragment sizes: 72, 118, 194, 234, 271, 281, 310, 603, 872, 1078 and 1353 bp. Fragments 271 and 281 can show anomalous mobilities (281 coming out before 271 according to manufacturer). The second sample is a commercially available 100 bp DNA ladder that includes 16 fragments from 100 to 1500 bp every 100 bp, and one fragment at 2072 bp. Fragments 600 bp and 1500 bp are more intense than the others, except for fragment 2072 bp. Part of fragment 600 bp can show an anomalous mobility (two peaks, according to manufacturer). The third sample is a 123 bp DNA ladder ranging from 123 bp up to 4182 bp every 123 bp. Fragment 246 and higher can show a side peak. The fourth sample is a λ DNA/Hind III digest. It includes the following fragments: 125, 564, 2027, 2322, 4361, 6557, 9416 and 23130 bp. The last sample is a M13mp18 double-stranded DNA, digested by Taq I restriction enzyme. This sample was prepared by ourselves and includes 12 fragments: 30, 239, 381, 441, 552, 579, 618, 703, 791, 927, 971, and 1018 bp.

Unless otherwise indicated, stock solutions of POPO-3, YOYO-1 or YOYO-3 were diluted to 10^{-6} M with 0.1xTBE (pH 8.4) and then diluted ten-fold in the same buffer (10^{-7} M). To this solution, sufficient double-stranded DNA was added to obtain a 9.3 to 15 base pair-to-dye molecule ratio (bp:dye). The preparation was kept in the dark for about half an hour prior to further dilution or injection.

For polymer-filled capillary electrophoresis, sample injection was typically five seconds at -100 V/cm, unless otherwise indicated. In general, electrophoresis was done at -200 V/cm with 1XTBE buffer . For MECC, samples were diluted in a pH 9.4, 10 mM borate + 10 mM SDS buffer and electrophoresis was performed at +400 V/cm.

5.2.2 Results and Discussion

In this work we studied the separation of double-stranded DNA on HPMC and polyacrylamide. The peak resolution, the peak width, and the total time for the separation are used to characterize each polymer. At the time of this work, there were no previous reports on CE separation of double-stranded DNA with intercalated POPO-3, YOYO-1 and YOYO-3. We have investigated the effect of the bp:dye ratio, ionic strength, and HPMC and polyacrylamide concentrations in matrix composition. The limit of detection, obtained by MECC, for the three dyes intercalated inside double-stranded DNA is also reported.

5.2.2.1 Base Pair-to-Dye Molecule Ratio

The proportion of DNA base pairs to intercalating dye affects the intensity and the peak width of each DNA fragment. When the ratio of bp:dye is changed from 20% to 3%, we observe that the number of theoretical plates are highest when one POPO-3 molecule is added for twenty base pairs of DNA for fragments 194 and 600 base pairs in length, Figure 5.2.

The peak height increased linearly ($r>0.95$) with fragment length for all the fragments studied. The number of intercalated dye molecules is proportional to the

Figure 5.2 Number of theoretical plates versus base pair:POPO-3 ratio for ϕx174 RF/HaeIII. Data were obtained with HPMC in 32 μm capillary at -200V/cm.

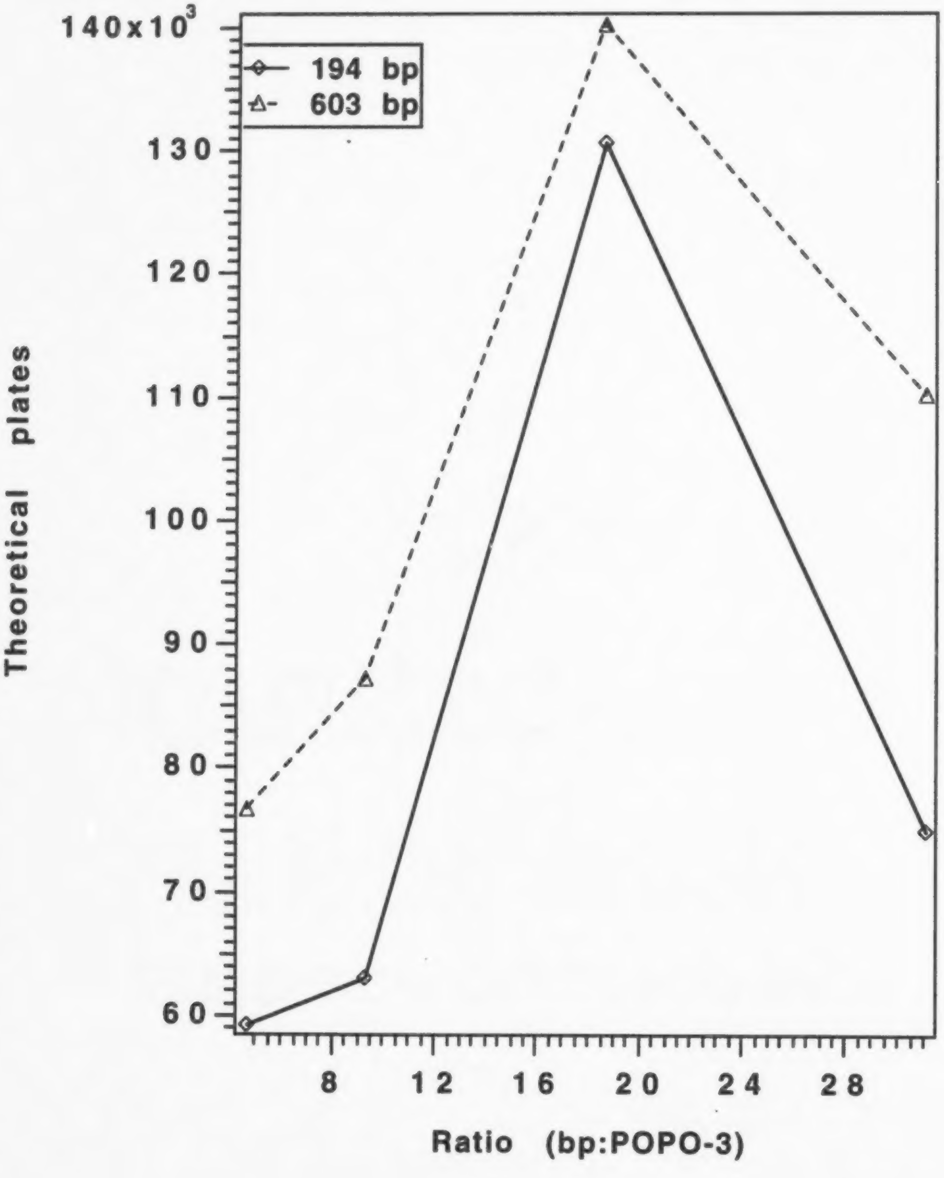

fragment length. The peak height (normalized to 1 bp) was not affected by bp:dye ratio 5, 20, and 33. The signal was, however, twice as high for a bp:dye ratio of 10, Figure 5.3.

5.2.2.2 Ionic Strength

The ionic strength of the running buffer (1xTBE) affected the peak width. The ionic strength was changed by adding up to 200 mM NaCl in the running and the sheath flow buffer. ϕx174 RF/HaeIII digest was separated on HPMC 0.4% with different concentrations of NaCl. The number of theoretical plates was extracted from these results, Figure 5.4.

These data were fitted with a function of the form,

$$\text{plates} = \frac{a}{\frac{b}{[\text{NaCl}]} + 1} \qquad (5.1)$$

The limiting number of theoretical plates ranged from 64,000 to 91,000, with a mean of 81,000 ± 12,000 plates. This improvement in resolution with the increasing sodium chloride concentration has been observed on slab gels[47]. It is proposed that the intercalating dye is more tightly held by the double-stranded DNA at a higher ionic strength; the partition ratio of the relatively non-polar dye increases at a higher ionic strength. An increase in the partition ratio means an increase in the number of dyes intercalated per molecule of DNA. Without NaCl, the amount of dye molecules for a particular DNA fragment is very variable. Also, the dye molecules are charged and their amount inside DNA fragments influence the mobility of these fragments. Thus, if the DNA molecules of a particular size do not have the same amount of dye intercalated, the average mobility will have a broad distribution. As the concentration of NaCl increases, the variance on the amount of dye intercalated decreases, and thus, the variance on the average mobility of a particular fragment size decreases. The retention time of all the fragments increases with the NaCl concentration, and the number of theoretical plates

Figure 5.3 Normalized peak height versus base pair:POPO-3 ratio. Conditions as Fig. 5.2.

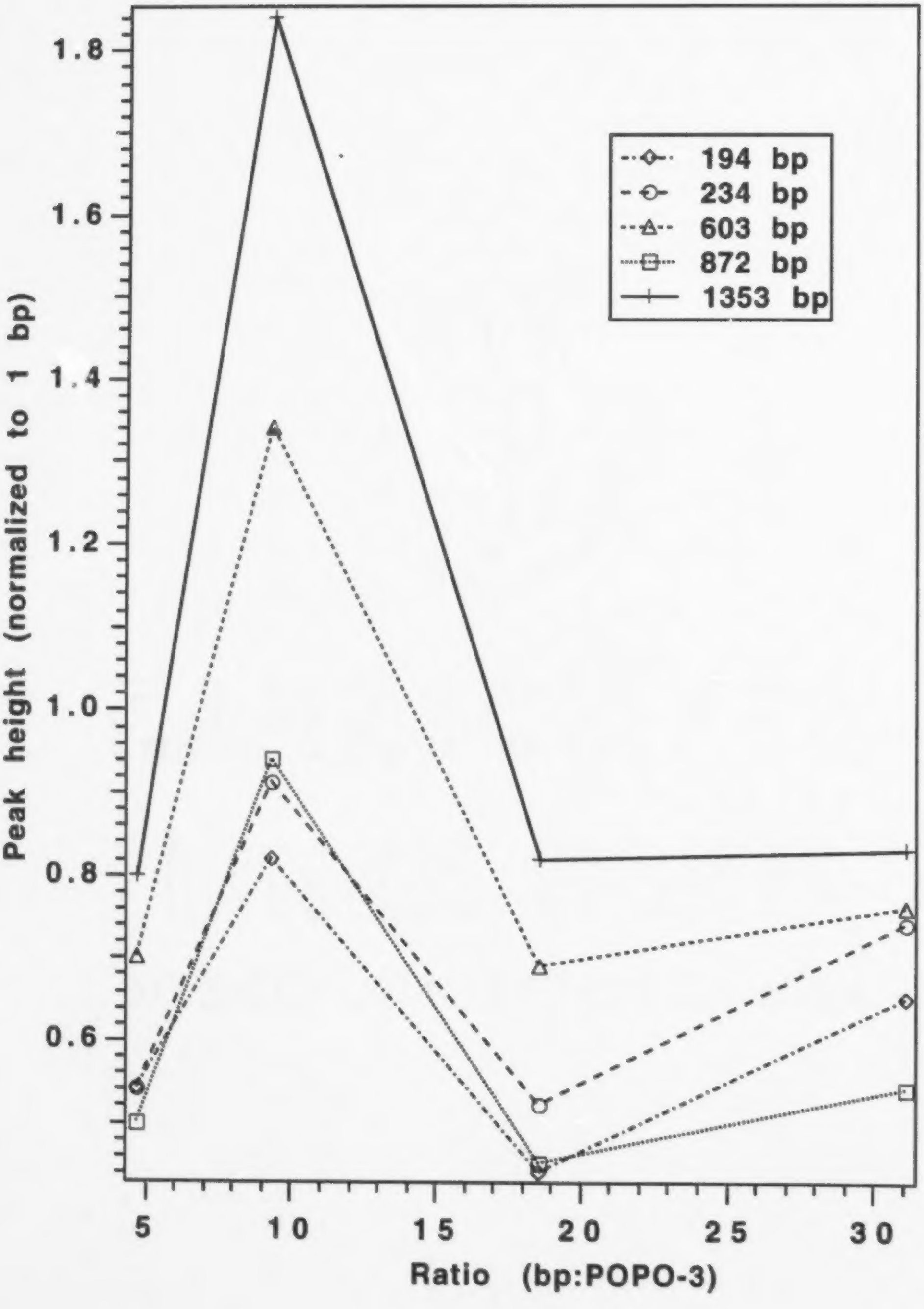

Figure 5.4 Theoretical plates versus NaCl concentration. Conditions as in Fig. 5.2.

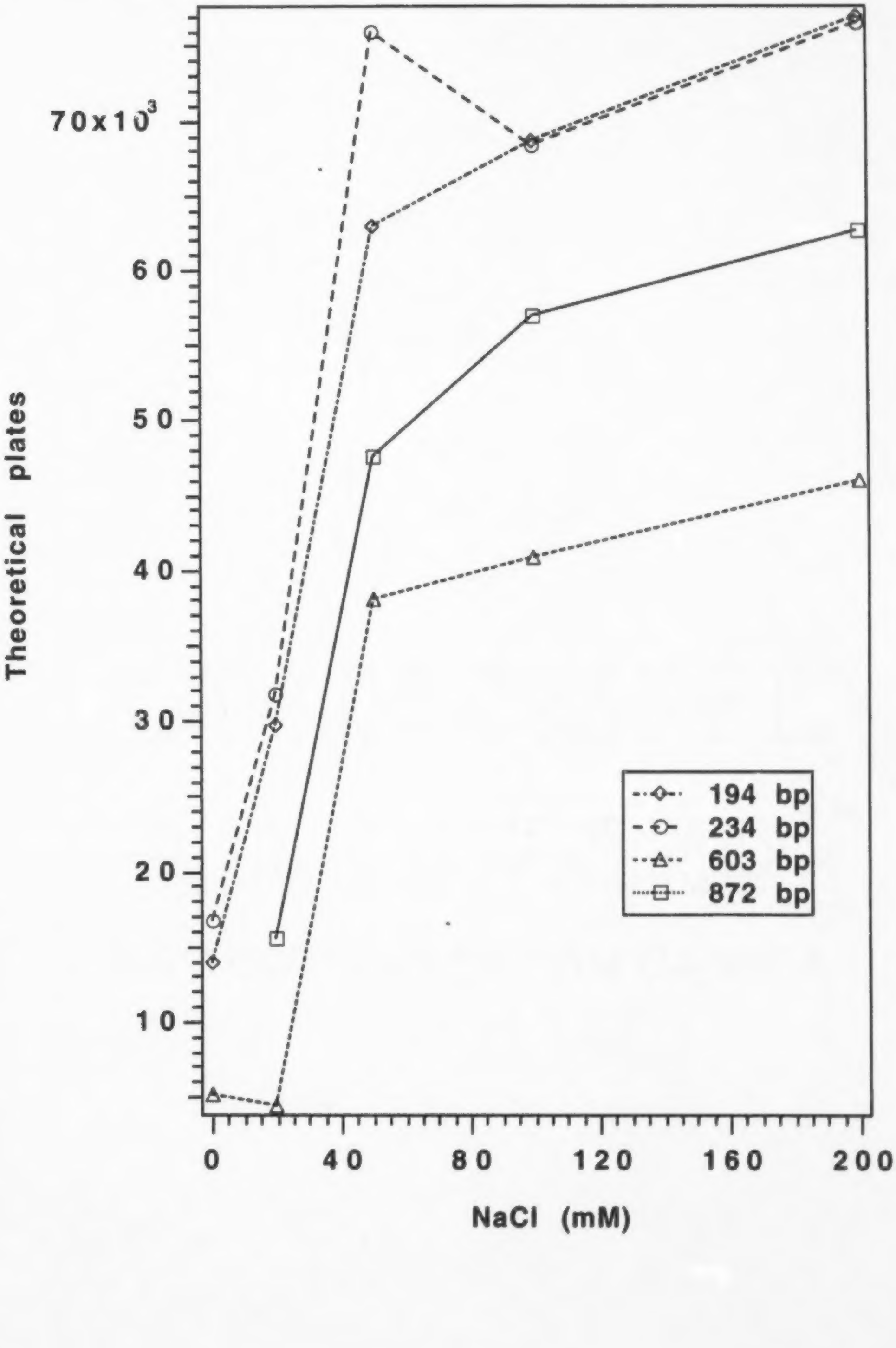

also increases with the NaCl concentration up to a plateau area between 40 to 200 mM NaCl. The increment in the migration time is greater for longer fragments. Similar results have been obtained by Oefner *et al.*[47]. They noticed an increase in the resolution, and a decrease in the mobility with the increase in the NaCl concentration.

5.2.2.3 Separation Matrix Composition

Separation of ϕx174 RF/HaeIII digest was obtained in 0.2%, 0.4%, and 0.8% HPMC, and in 4%T , 6%T, and 8%T linear polyacrylamide. The electropherograms obtained in HPMC and in polyacrylamide are shown in Figure 5.5 and Figure 5.6 respectively. The migration time increases with the concentration of the polymers.

The mobility of the fragments were calculated using equation 2.1 and are reported in Figure 5.7 versus the inverse of the fragment lengths in base pairs. The highest mobility is produced in the lowest concentration of HPMC; the relatively low viscosity of this medium produces little retardation of the double-stranded DNA. The lowest mobility is obtained in 8%T linear polyacrylamide; the high viscosity of this medium produces a significant retardation of the fragments. Mobility is plotted versus the inverse fragment length. As explained in Chapter 1, the small fragments migrate according to the Ogston model, and larger fragments migrate according to the biased reptation model. The range of fragment sizes which are subjected to biased reptation should have a linear relationship between mobility and the inverse of the fragment length (equation 1.22). The plot reveals that the onset of biased reptation occurs for fragments roughly 500 base pairs in length.

A non-linear least-squares routine was used to fit a four-parameter Gaussian function (equation 1.9) to the peaks of the electropherograms. The number of theoretical plates is estimated from the peak width and the retention time using equation 1.10. The number of theoretical plates decreased slightly with the fragment lengths for all the polymers studied, Figure 5.8.

Figure 5.5 Separation of ϕx174 RF/HaeIII digest intercalated with YOYO-3 on different HPMC at -200V/cm with 1xTBE, 0.1M NaCl.

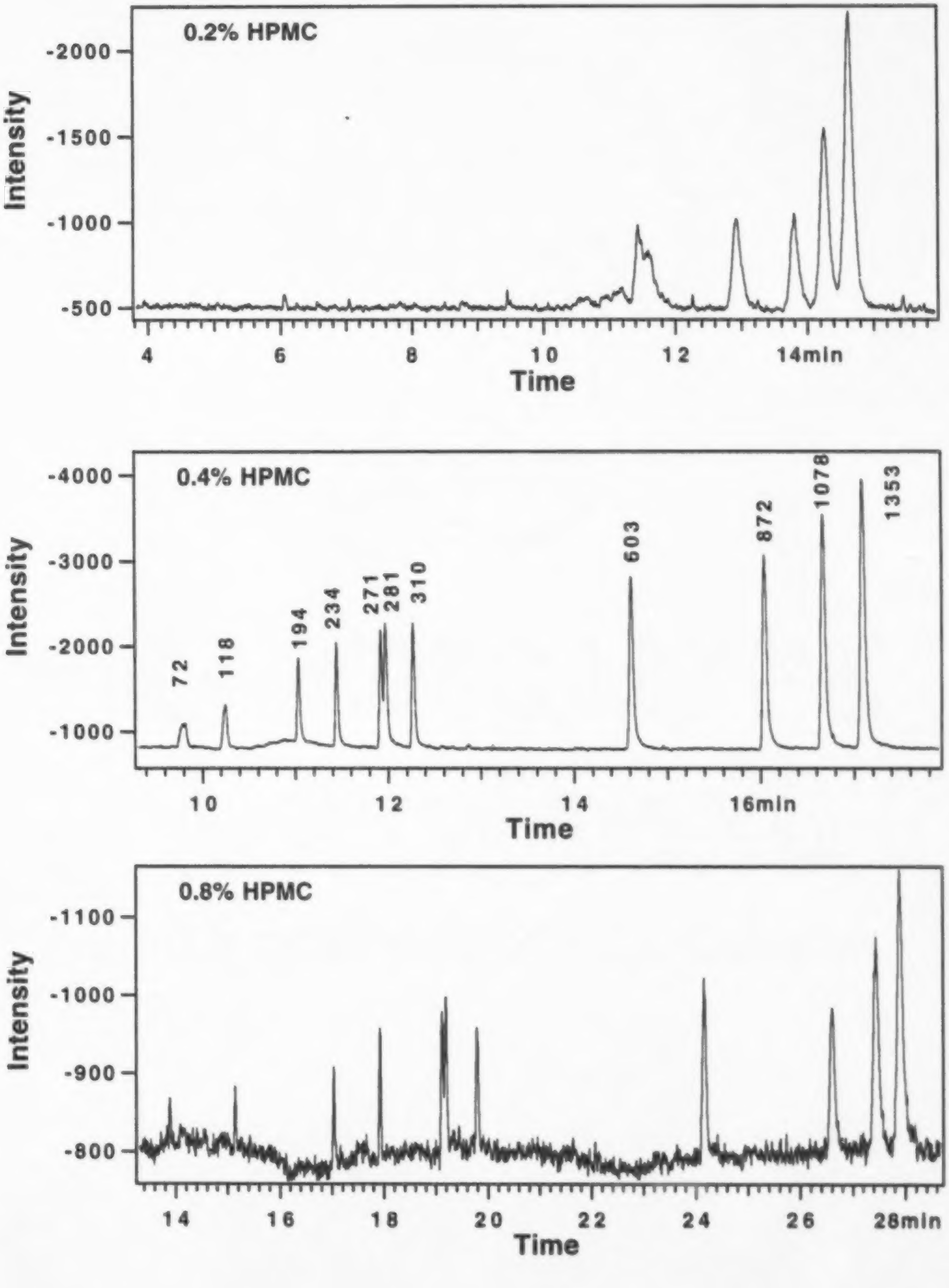

Figure 5.6 Separation of ϕx174 RF/HaeIII digest intercalated with YOYO-3 on different linear polyacrylamide at -200V/cm with 1xTBE, 0.1M NaCl.

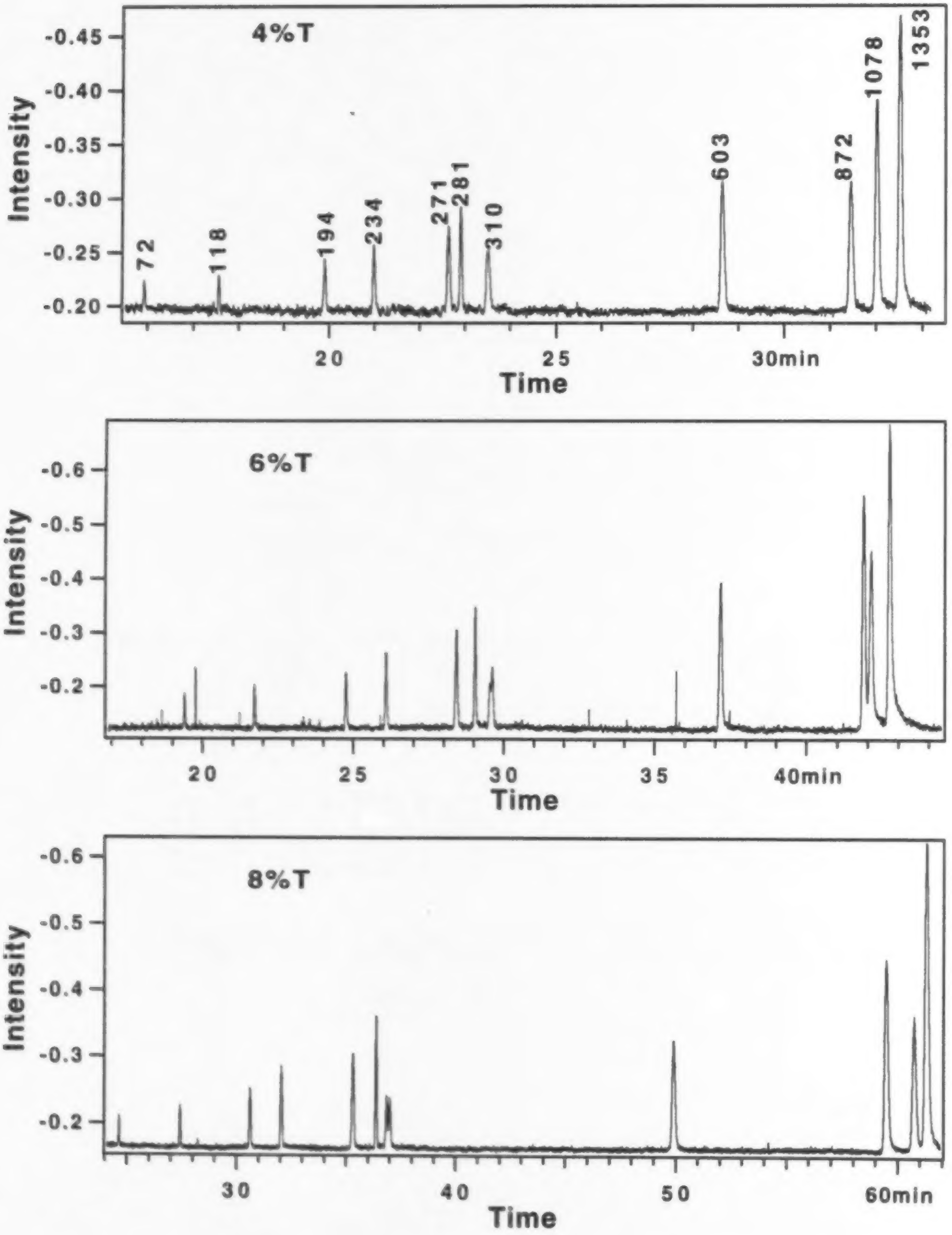

Figure 5.7 Mobility versus reciprocal fragment length for different polymers. The mobility was normalized to 30 cm capillary. Other conditions as in Fig. 5.5.

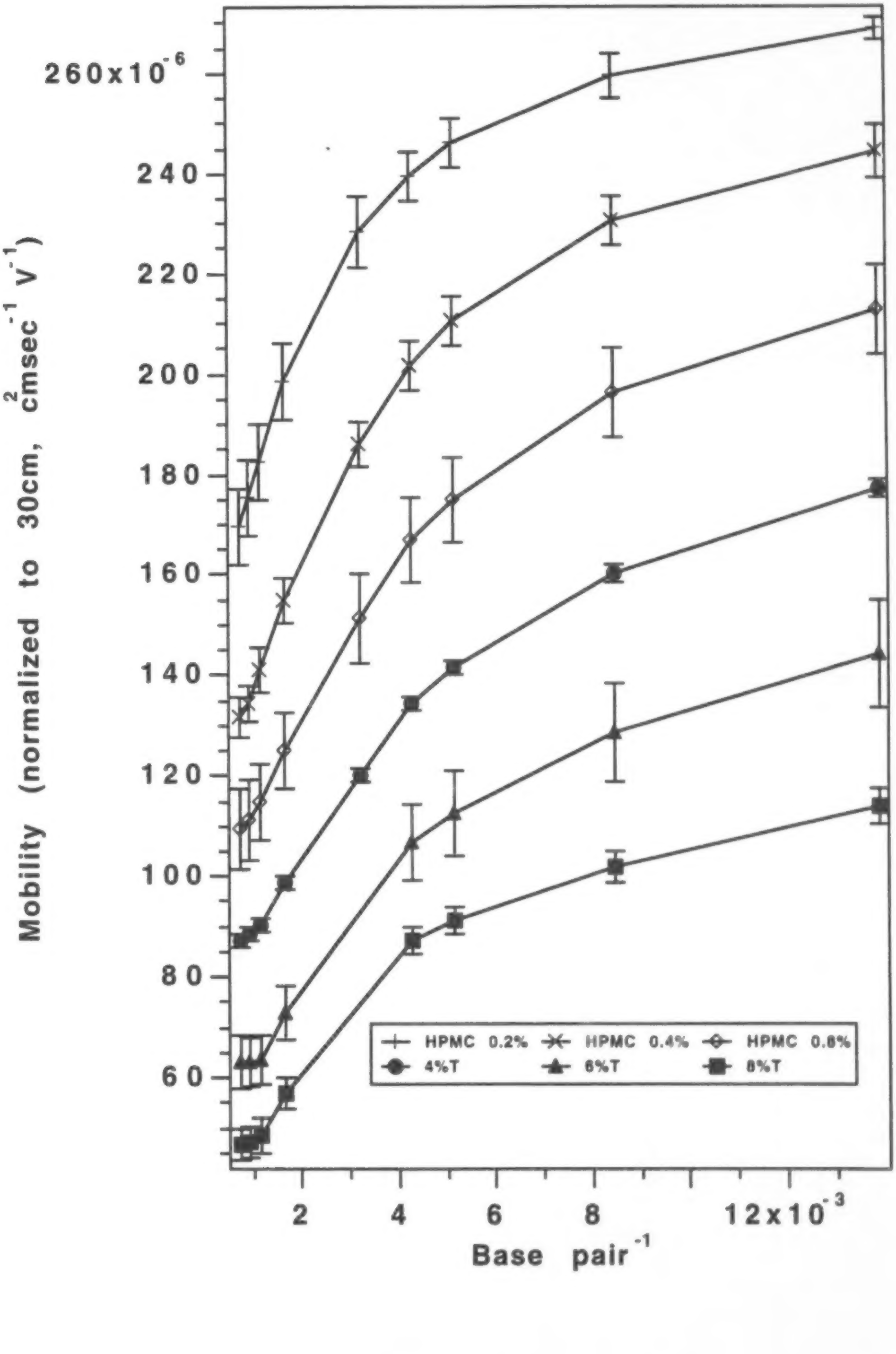

Figure 5.8 Theoretical plates versus fragment lengths for different polymers. Only the standard deviation for 8%T LPA and 0.8% HPMC are reported for clarity. Other conditions as in Fig. 5.5.

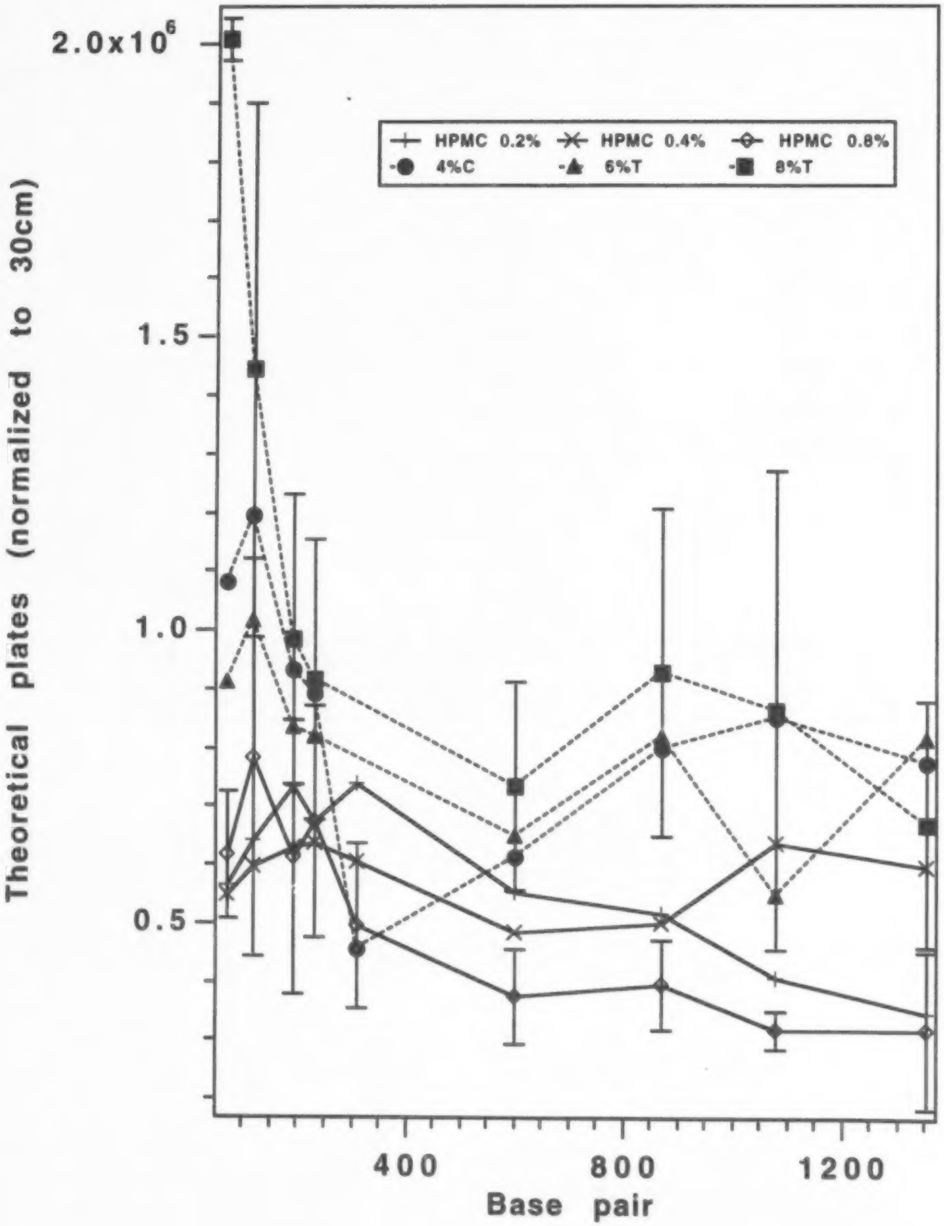

For linear polyacrylamide, the number of theoretical plates reached an asymptotic value of about 0.8 x 10^5 plates for the longest fragments; whereas for HPMC, the limiting plate count was about half that value. This trend towards lower number of theoretical plates for the longer fragments mirrors the onset of biased reptation; long fragments that undergo biased reptation appear to produce similar number of theoretical plates. Presumably, the change in conformation accompanying biased reptation produces a change in the diffusion coefficient of the fragments that matches the change in mobility.

Resolution for fragments differing by 10 base pairs (R_{10}) was estimated as,

$$R_{10} = 10 \text{ X } \frac{\Delta T}{2.83 \text{ x } \overline{A_2} \text{ X } \Delta BP} \tag{5.2}$$

Where ΔT is the difference in retention time of two fragments, $\overline{A_2}$ is the average peak width for the two peaks, and Δ BP is the difference in fragment length in base pairs. Note that the resolution is for a 10 base pair difference in fragment length; when the resolution drops below 1, fragments differing by 10 base pairs in length will produce overlapping peaks. Figure 5.9 shows that the resolution decreases nearly exponentially with fragment length. While resolution for fragments shorter than 300 base pairs is superior in linear polyacrylamide than in HPMC, longer fragments produce similar resolutions.

In general, HPMC seems to be superior to linear polyacrylamide for the analysis of fragments longer than 300 base pairs. The high mobility of fragments in HPMC leads to rapid separations with no loss of resolution compared to the use of linear polyacrylamide. In Figures 5.10 to 5.13, we present several examples of the separation of double-stranded DNA in HPMC. In Figure 5.10, a 100 base pair ladder is separated in 22 minutes at an electric field of -200 V/cm. Note that two peaks are generated for the 600 base pair fragment. This behavior is also observed in slab gels and is evident in the electropherogram supplied by the manufacturer.

Figure 5.9 Resolution versus fragment length for different polymers. The resolution was normalized to 10bp. Other conditions as in Fig. 5.5.

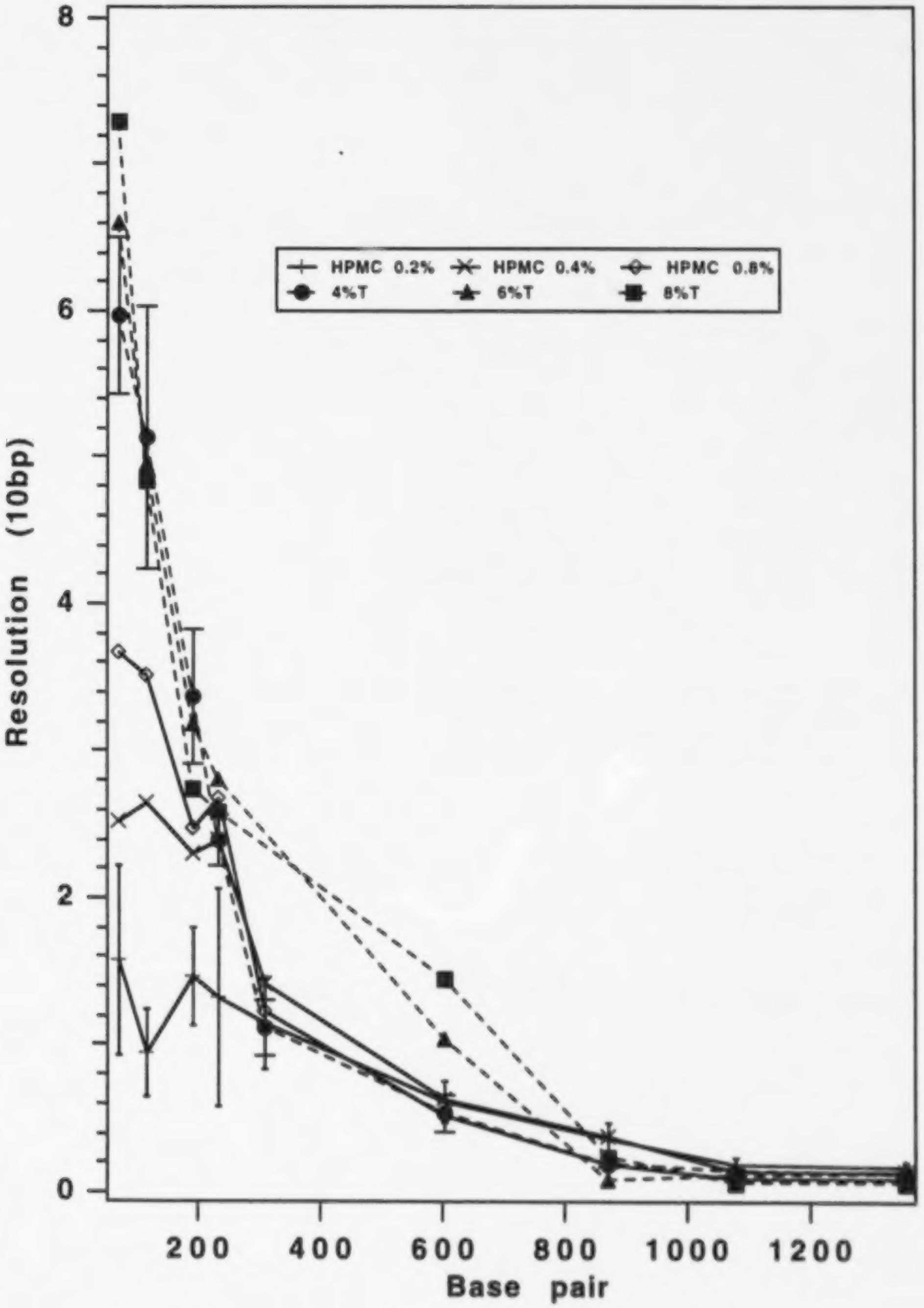

Figure 5.10 Separation of 100-bp ladder intercalated with YOYO-3 on HPMC 0.4% at -200V/cm with 1xTBE, 0.1M NaCl.

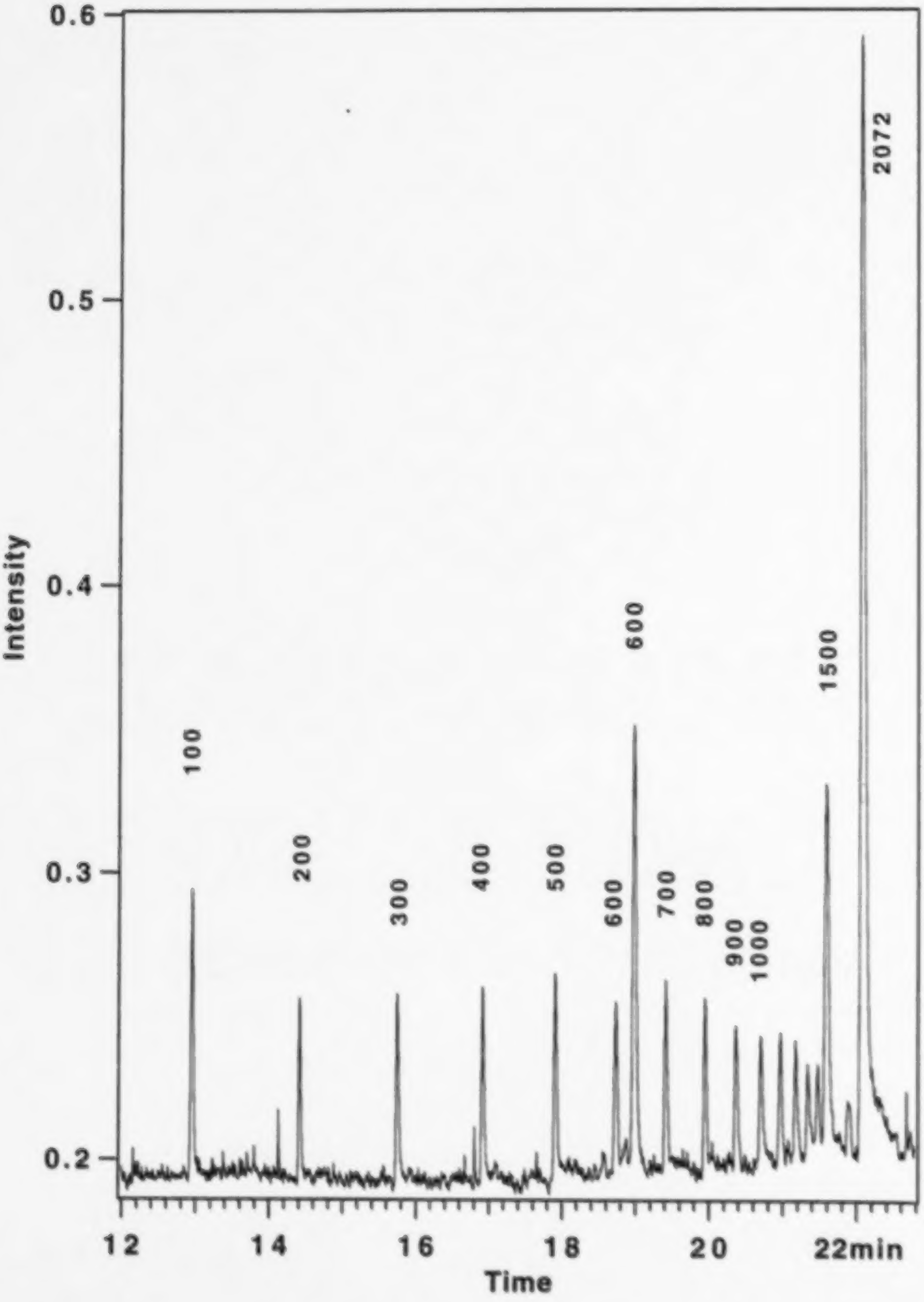

Figure 5.11A Separation of a 123-bp ladder. Other conditions as in Fig 5.10.

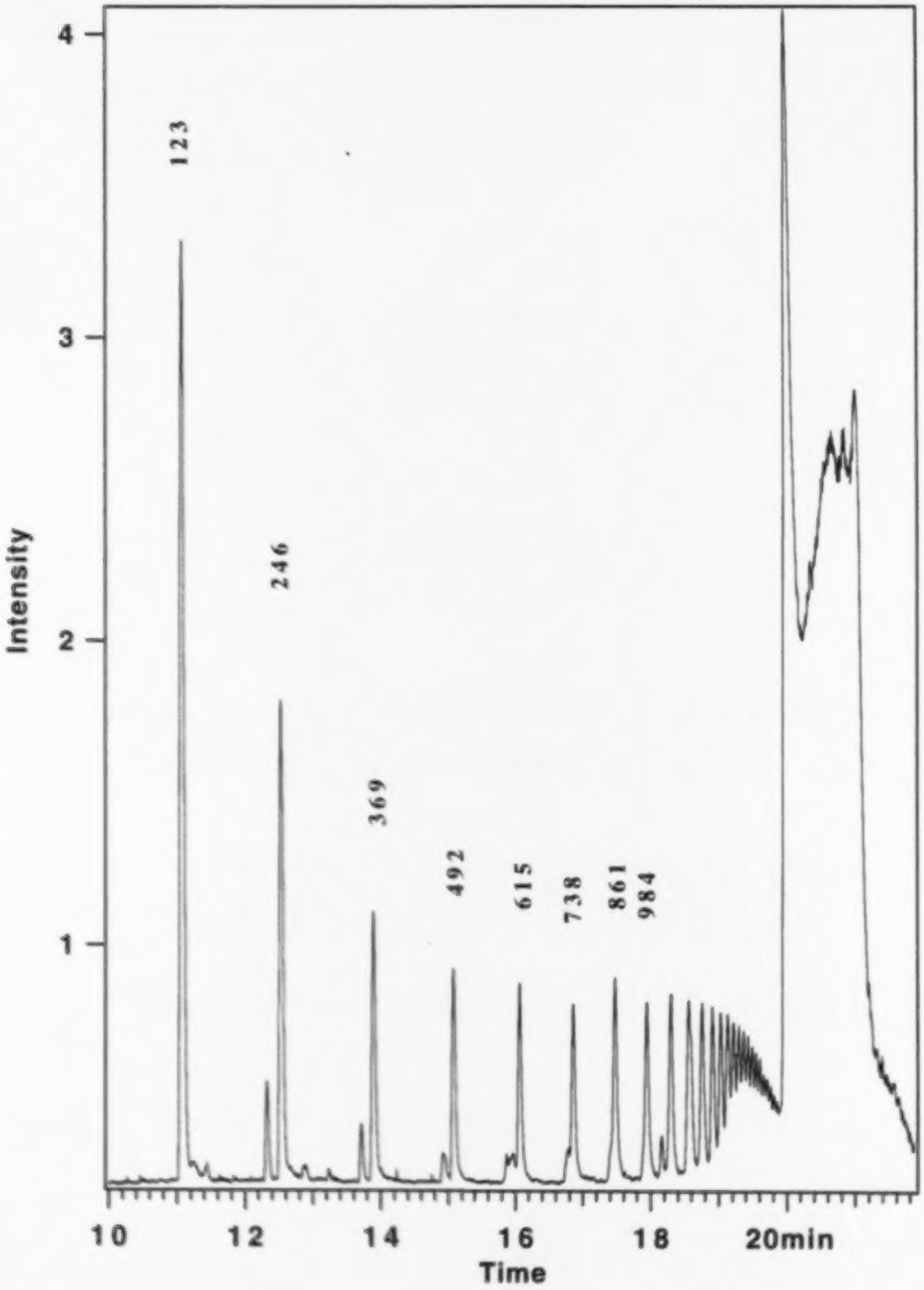

Figure 5.11B Expanded area of Figure 5.11A from 18 to 20 minutes.

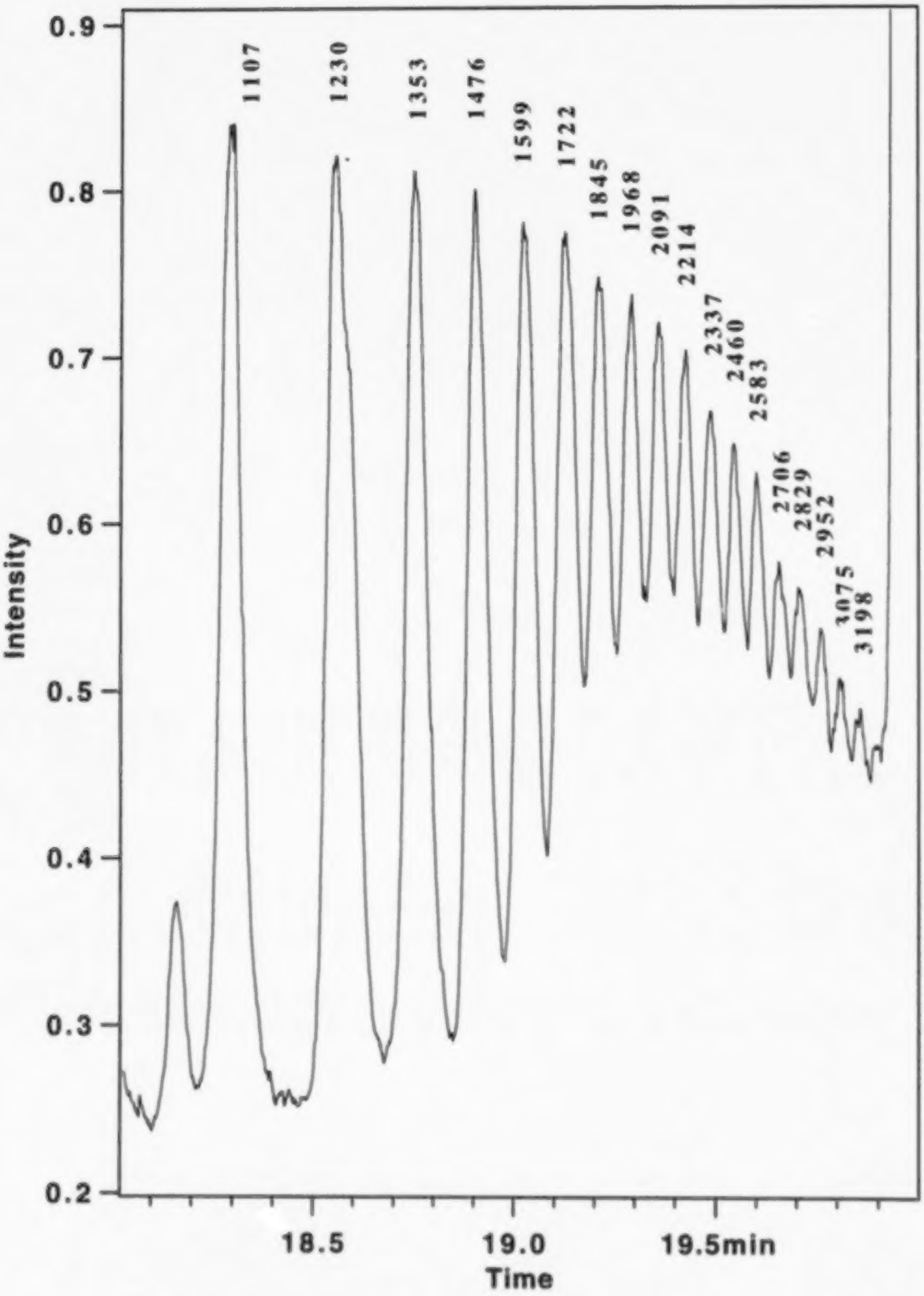

Figure 5.12 Separation of λ DNA/ Hind III. Other conditions as in Fig 5.10.

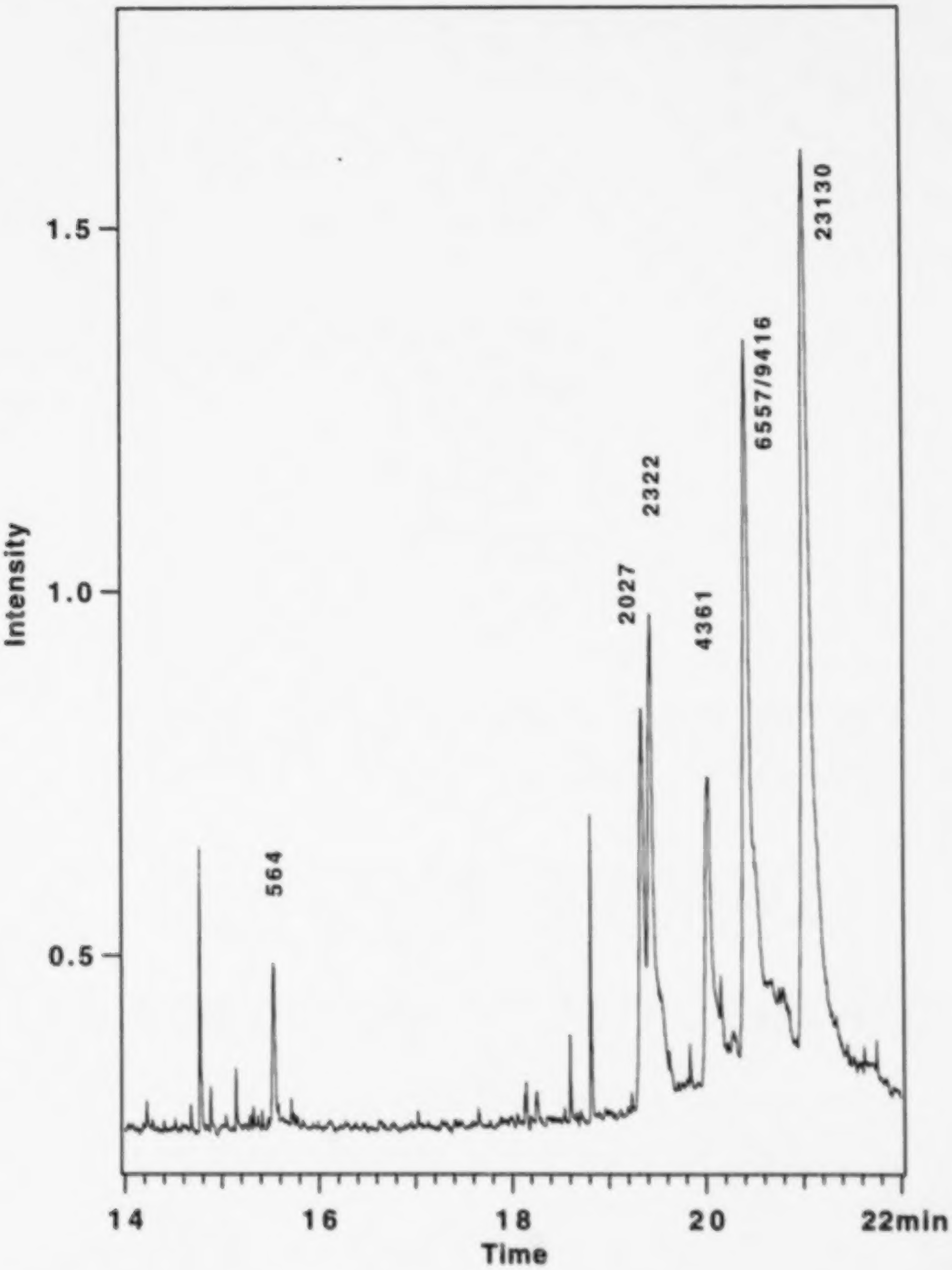

Figure 5.13 Separation of Taq I digest of M13mp18.
Other conditions as in Fig 5.10.

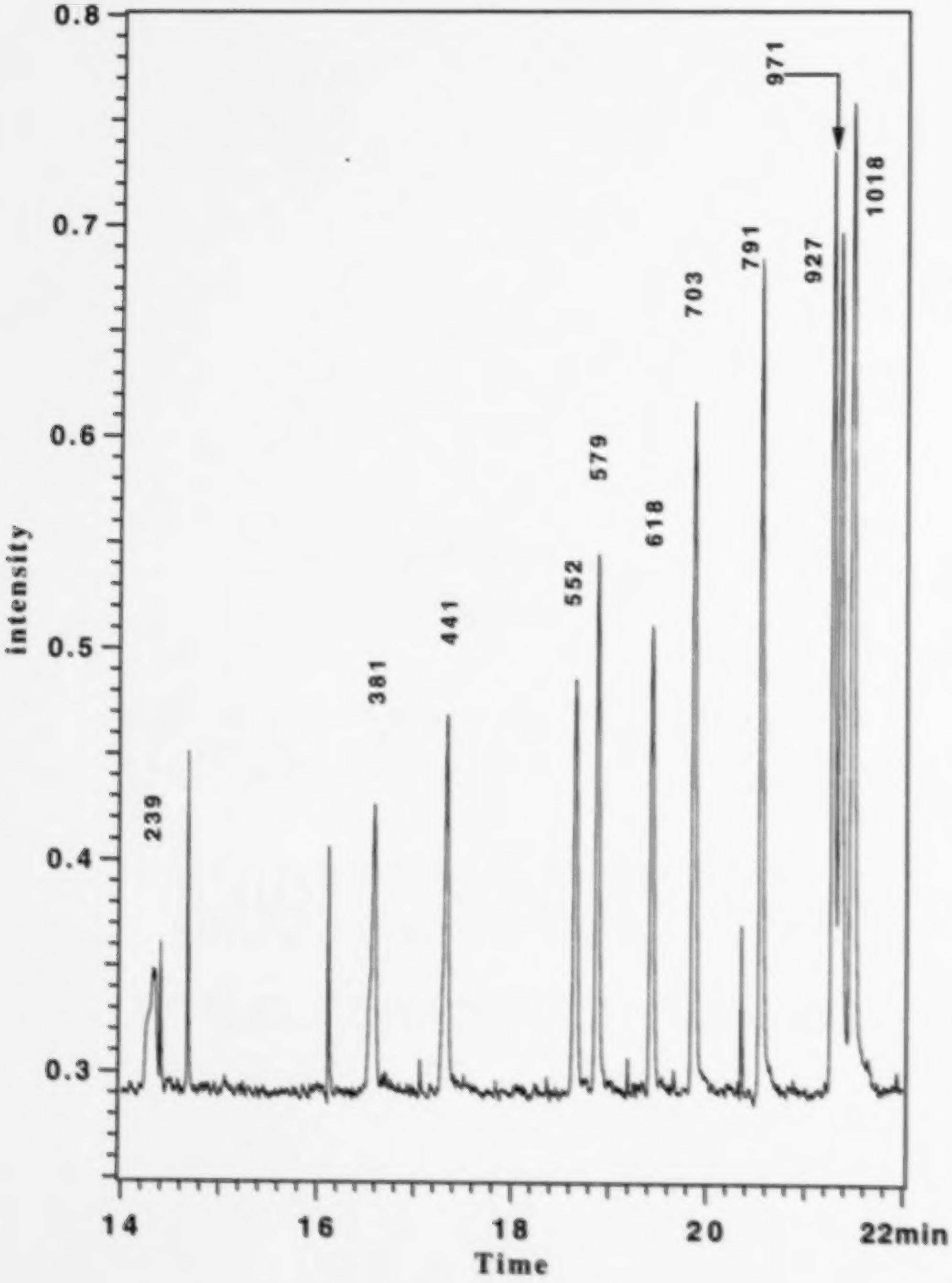

Figure 5.11 shows a 123 base pair ladder separated at -200V/cm in HPMC. The resolution extends to fragment 3198 base pairs in length. The longer fragments generate a single peak associated to the biased reptation phenomena. Figure 5.12 presents a λ phage that has been digested with Hind III restriction endonuclease. Finally, Figure 5.13 shows the separation of a home-made sample prepared by digesting M13mp18 with TaqI restriction endonuclease. This shows that a clean electropherogram can be obtained with a non-purified sample and the intercalating dyes. The resolution obtained in our experiment is much higher than the one obtained by other groups [21,48].

5.2.2.4 Detection Limits

These dyes undergo a significant increase in fluorescence intensity when intercalated in double-stranded DNA. Because of the large partition coefficient of these dyes (YOYO-3 1.5×10^8, and YOYO-1 6.0×10^8), we assume that all the dye molecules are intercalated inside the double helix[36]. Rather than using one double-stranded DNA fragment, we chose to use micellar electrophoresis to determine the limits of detection, because only the total DNA concentration is known. Under MECC conditions, the Hae III digest of ϕx174 RF yields a single electrophoresis peak with POPO-3, YOYO-1 and YOYO-3. This allows us to use the total concentration of DNA in our calculation, and to obtain limits of detection in number of mol. Table 5.2 gives the observed limits of detection for the dyes. Limits of detection were also measured by CZE(without SDS) and were similar to the results in Table 5.2. This indicates that the presence of SDS does not enhance the signal.

These limits of detection are for intercalated dyes; a large number of these dyes can be intercalated into large DNA fragments. For example, if the bp:dye ratio is 10, then a single 5,000 base pair DNA fragment will contain a 500 dye molecules. This number of dye molecules is in the range of the limit of detection on this system. Thus, the limit of detection for large DNA molecules approaches the single molecule limit in this

Table 5.2 Limits of detection of intercalated dyes. Data were obtained in MECC at an electric field of +400 V/cm with a 10 mM borate and 10 mM SDS buffer at pH=9.4.

Dye	Limit of detection (3 σ)
POPO-3	$1.1 \pm 0.1 \times 10^{-21}$ mol
YOYO-3	$1.9 \pm 0.4 \times 10^{-21}$ mol
YOYO-1	$5 \pm 2 \times 10^{-21}$ mol

capillary electrophoresis instrument. The limits of detection reported in this experiment need to be considered as conservative due to the assumptions involved in our calculation. These results are similar to the ones reported by Keller *et al.* for the analysis of neat solutions of highly dilute samples of DNA fragments labeled with intercalating dyes[39].

5.3 ROX-Dideoxycytosine Triphosphate

5.3.1 Experiment

The capillary electrophoresis system and the detector used in this experiment were described in Chapter 1 (Figures 1.19 and 1.20). A yellow He-Ne laser (8 mW at 594 nm) was used for the excitation of fluorescence. The experiments were done using 32 µm id x 144 µm od x 28.6 cm capillaries (Polymicro, Phoenix, AR). The capillaries were silanized as described in chapter 1. The HPMC and polyacrylamide were prepared as described in Chapter 5.2.1. The separations performed on 0.4% HPMC were done at an electric field of -100 V/cm, and the separations performed on polyacrylamide were done at -200V/cm.

One µL of DNA [ϕx174 RF/HaeIII (Gibco BRL) 0.6 µg/µL or M13mp18 RF1 (Sigma) / TaqI (Gibco BRL) 0.045 µg/µL], 4 µL of a 5X reaction buffer (Boehringer Mannheim), 1 µL of ROX-ddCTP (90 pmol, ABI), 2 µL of $COCl_2$ (2.5 mM, Boehringer Mannheim), 10 µL of water, and 1 µL of terminal deoxynucleotidyl transferase (10U, Boehringer Mannheim) from calf thymus were mixed together. The mixture was incubated at 37°C for 1 hour. EDTA was added to terminate the reaction. The sample was ethanol precipitated and dissolved in 10µL of 1xTBE.

5.3.2 Results and Discussion

We used ROX-dideoxycytosine triphosphate (Applied Biosystems Division of Perkin-Elmer) to label blunt and sticky ended restriction fragments. We successfully labeled ϕx174 RF/HaeIII and M13mp18RF/TaqI restriction fragments. Figure 5.14

Figure 5.14 Separation of ϕx174 RF/Hae III on a 28.6 cm capillary filled with HPMC 0.4% and 1xTBE 0.1MNaCl at -100V/cm.

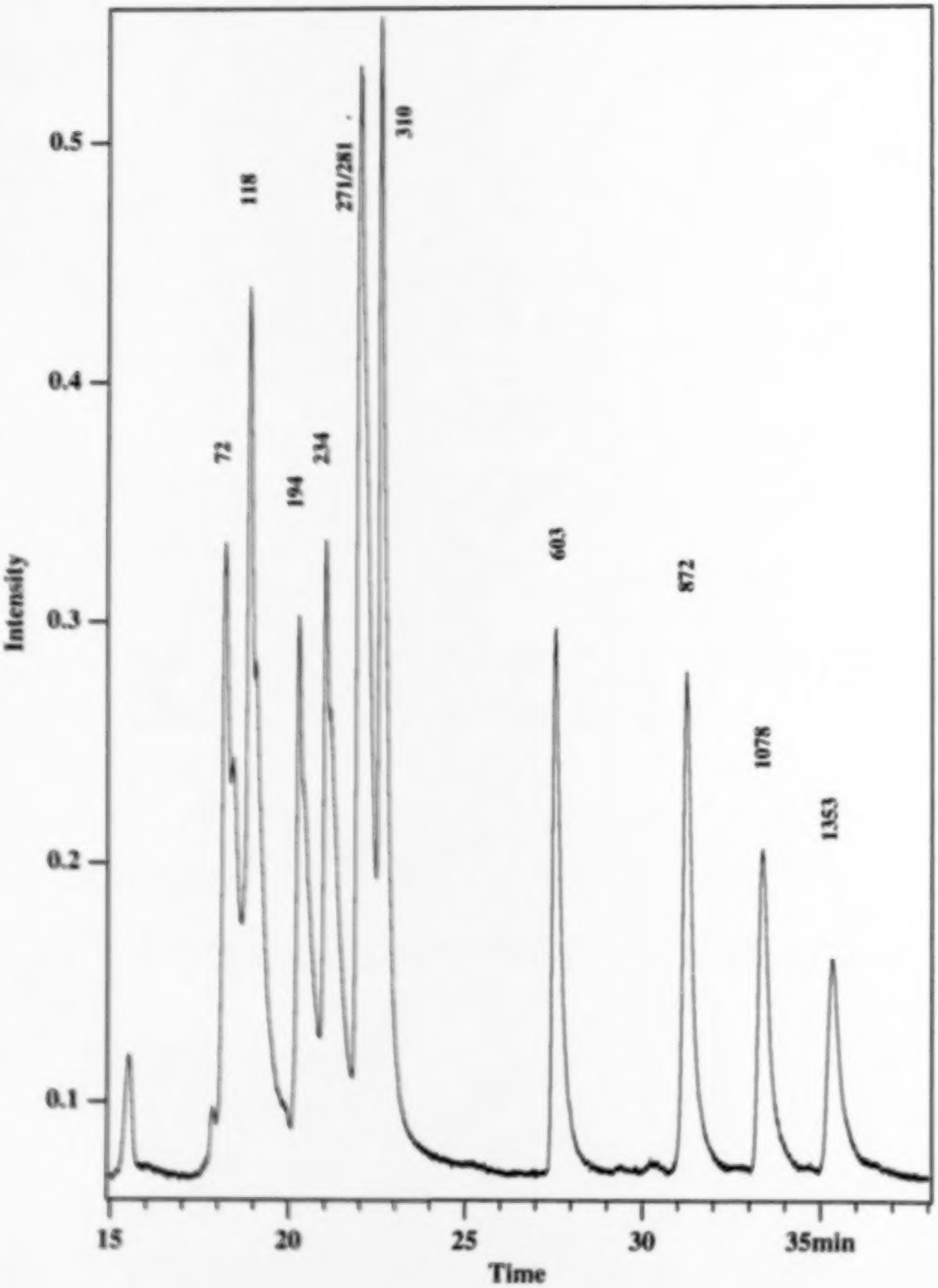

shows the separation of ϕx174 RF/HaeIII fragments on hydroxypropylmethylcellulose 0.4%.

While HPMC is convenient for the analysis of double-stranded DNA, linear polyacrylamide solutions provide higher resolution separations. Figure 5.15 presents the separation of ϕx174 RF/HaeIII fragments on polyacrylamide. Each fragment generates a major peak and a smaller satellite peak; presumably, the first peak is due to fragments that have incorporated a single label at one 3' end, and the second peak is associated with fragments that have been labeled at both 3' ends. For the largest peaks, the resolution presumably is insufficient to resolve the satellite peaks. A decrease in the relative amount of dideoxynucleotide should reduce the formation of the satellite peaks.

The use of fluorescent dideoxynucleotides is attractive for labeling double-stranded DNA. In particular, the labeling procedure will be of value in the analysis of restriction endonuclease digested DNA. Alternative technology based on the use of intercalating dyes, does not easily allow the analysis of mixed samples. Many different dideoxynucleotides labeled with unique fluorescent label are available.

5.4 Conclusion

We are able to separate different DNA restriction digests in the presence of the intercalating dyes YOYO-3, YOYO-1, and POPO-3. The dye is added in a ratio between 9 to 15 bp:dye. Adding NaCl to the running and the sheath flow buffer increases the resolution and the number of theoretical plates. Separation of ϕx174 RF/HaeIII was done on HPMC and linear polyacrylamide. The best results were obtained on 0.4% HPMC and 8%T linear polyacrylamide. Resolution for fragments less than 300 bp are better on linear polyacrylamide than on HPMC. HPMC allows larger fragments to be separated in a shorter time. The limits of detection were calculated for each of the intercalating dyes and were in agreement with the results obtained on more complicated systems. Overall,

Figure 5.15 Separation of ϕx174 RF/Hae III on a 30 cm capillary filled with 5% T LPA and 1xTBE 0.1M NaCl at -300V/cm.

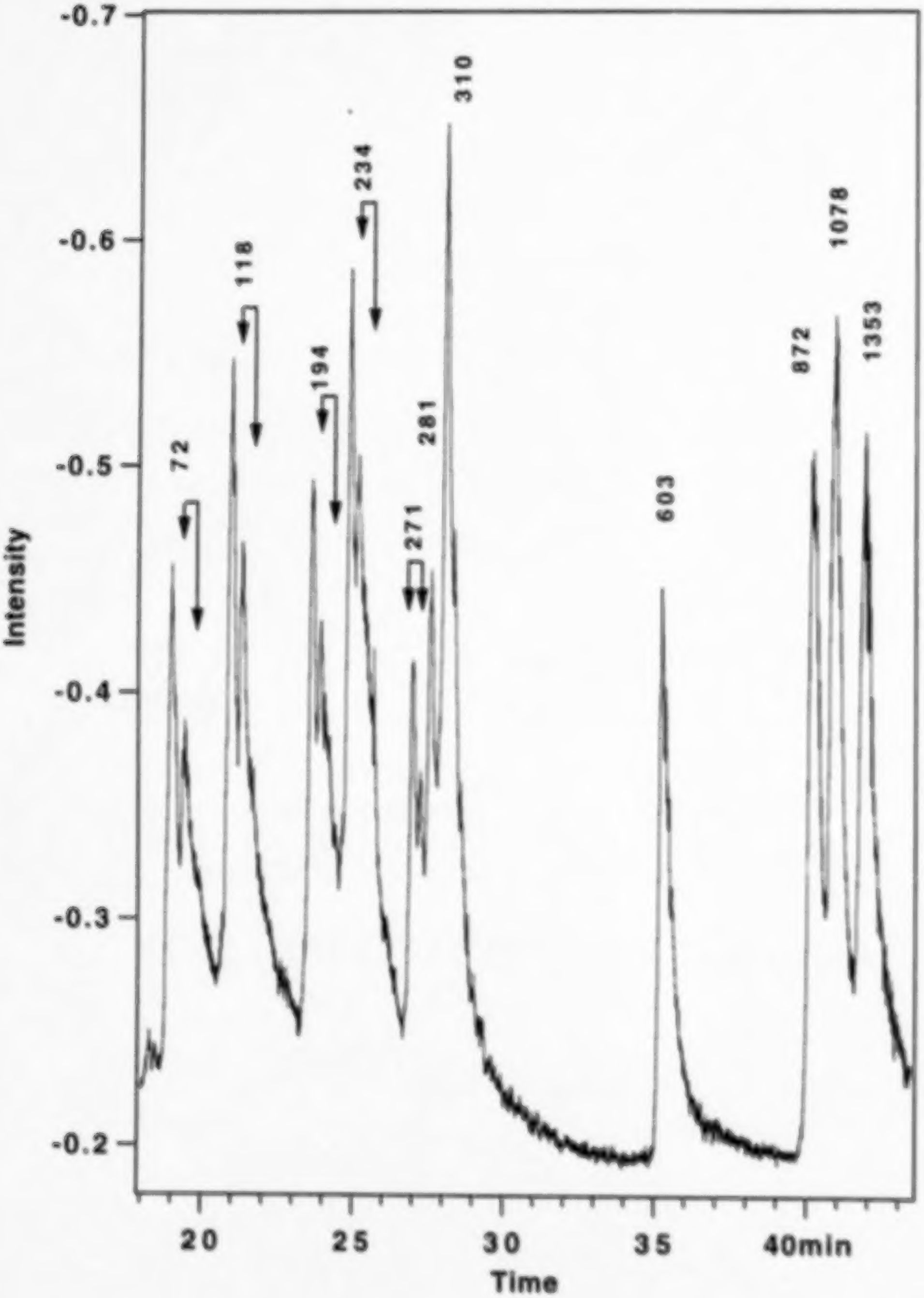

the resolution and the number of theoretical plates are lower when the intercalating dye YOYO-3, YOYO-1, and POPO-3 are used instead of no dye or ethidium bromide.

We used terminal deoxynucleotidyl transferase and ROX-dideoxycytosine triphosphate to label blunt and sticky ended DNA. Separation on HPMC and linear polyacrylamide were presented. Although double peaks were obtained due to incomplete labeling of fragments, it is expected that single peaks could be obtained. Thus, this technique should be useful for the labeling of restriction endonuclease fragments.

5.5 Bibliography

(1) Glazer, A. N.; Peck, K.; Mathies, R. A. *Proceedings of the National Academy of Sciences USA* **1990**, *87*, 3851-3855.

(2) Paulus, A.; Husken, D. *Electrophoresis* **1993**, *14*, 27-35.

(3) Lamerdin, J. E.; Carrano, A. V. *BioTechniques* **1993**, *15*, 294-302.

(4) Schwartz, H. E.; Ulfelder, K. J. *Analytical Chemistry* **1992**, *64*, 1737-1740.

(5) Schwartz, H. E.; Ulfelder, K.; Sunzeri, F. J.; Busch, M. P.; Brownlee, R. G. *Journal of Chromatography* **1991**, *559*, 267-283.

(6) Sudor, J.; Foret, F.; Bocek, P. *Electrophoresis* **1991**, *12*, 1056-1058.

(7) Bocek, P.; Chrambach, A. *Electrophoresis* **1992**, *13*, 31-34.

(8) Kleparnik, K.; Fanali, S.; Bocek, P. *Journal of Chromatography* **1993**, *638*, 283-292.

(9) Bocek, P.; Chrambach, A. *Electrophoresis* **1991**, *12*, 1056-1058.

(10) Guttman, A.; Cohen, A. S.; Heiger, D. N.; Karger, B. L. *Analytical Chemistry* **1990**, *62*, 137-141.

(11) Heiger, D. N.; Cohen, A. S.; Karger, B. L. *Journal of Chromatography* **1990**, *516*, 33-48.

(12) Guttman, A.; Wanders, B.; Cooke, N. *Analytical Chemistry* **1992**, *64*, 2348-2351.

(13) Garner, M. M.; Chrambach, A. *Electrophoresis* **1992**, *13*, 176-178.

(14) Chiari, M.; Nesi, M.; Fazio, M.; Righetti, P. G. *Electrophoresis* **1992**, *13*, 690-697.

(15) Grossman, P. D.; Soane, D. S. *Journal of Chromatography* **1991**, *559*, 257-266.

(16) Grossman, P. D.; Soane, D. S. *Biopolymers* **1991**, *31*, 1221-1228.

(17) Strege, M.; Lagu, A. *Analytical Chemistry* **1991**, *63*, 1233-1236.

(18) Milofsky, R. E.; Yeung, E. S. *Analytical Chemistry* **1993**, *65*, 153-157.

(19) Dolnik, V.; Novotny, M. *Journal of Microcolumn Separations* **1992**, *4*, 515-519.

(20) Demana, T.; Lana, M.; Morris, M. *Analytical Chemistry* **1991**, *63*, 2795-2797.

(21) Kim, Y.; Morris, M. D. *Analytical Chemistry* **1994**, *66*, 1168-1174.

(22) Navin, M. J.; Rapp, T. L.; Morris, M. D. *Analytical Chemistry* **1994**, *66*, 1179-1182.

(23) Kim, Y.; Morris, M. D. *Analytical Chemistry* **1994**, *66*, 3081-3085.

(24) Bocek, P.; Chrambach, A. *Electrophoresis* **1991**, *12*, 1059-1061.

(25) Cohen, A. S.; Najarian, D.; Smith, J. A.; Karger, B. L. *Journal of Chromatography* **1988**, *458*, 323-333.

(26) Chin, M.; Colburn, J. C. *American Biotechnology Laboratory* **1989**, 16.

(27) Novotny, M.; Dolnfk, V. *Journal of Microcolumn Separations* **1992**, *4*, 515-519.

(28) Clark, S. M.; Mathies, R. A. *Analytical Biochemistry* **1993**, *215*, 163-170.

(29) KleemiB, M. H.; Gilges, M.; Schomburg, G. *Electrophoresis* **1993**, *14*, 515-522.

(30) Sudor, J.; Novotny, M. V. *Analytical Chemistry* **1994**, *66*, 2446-2450.

(31) Hogan, B. L.; Yeung, E. S. *Analytical Chemistry* **1992**, *64*, 2841-2845.

(32) Guttman, A.; Cooke, N. *Analytical Chemistry* **1991**, *63*, 2038-2042.

(33) Glazer, A. N.; Rye, H. S. *Nature* **1992**, *359*, 859-861.

(34) Rye, H. S.; Dabora, J. M.; Quesada, M. A.; Mathies, R. A.; Glazer, A. N. *Analytical Biochemistry* **1993**, *208*, 144-150.

(35) Rye, H. S.; Yue, S.; Wemmer, D. E.; Quesada, M. A.; Haugland, R. P.; Mathies, R. A.; Glazer, A. N. *Nucleic Acids Research* **1992**, *20*, 2803-2812.

(36) Haugland, R. P. *MOLECULAR PROBES Handbook of Fluorescent Probes and Research Chemicals*; 1992.

(37) Benson, S. C.; Mathies, R. A.; Glazer, A. N. *Nucleic Acids Research* **1993**, *21*, 5720-5726.

(38) Benson, S. C.; Singh, P.; Glazer, A. N. *Nucleic Acids Research* **1993**, *21*, 5727-5735.

(39) Goodwin, P. M.; Johnson, M. E.; Martin, J. C.; Ambrose, W. P.; Marrone, M.; Jett, J. H.; Keller, R. A. *Nucleic Acids Research* **1993**, *21*, 803.

(40) Castro, A.; Fairfield, F. R.; Shera, E. B. *Analytical Chemistry* **1993**, *65*, 849-852.

(41) Tu, C.-P. d.; Cohen, S. N. *Genetic* **1980**, *10*, 177-183.

(42) Roychoudhury, R.; Jay, E.; Wu, R. *Nucleic Acids Research* **1976**, *3*, 863-877.

(43) Dirks, R. W.; VanGijlswijk, R. P. M.; Vooijs, M. A.; Smit, A. B.; Bogerd, J.; VanMinnen, J.; Raap, A. K.; VanDerPloeg, M. *Experimental Cell Research* **1991**, *194*, 310-315.

(44) Trainor, G. L.; Jensen, M. A. *Nucleic Acids Research* **1988**, *16*, 11846.

(45) Igloi, G. L.; Schiefermayr, E. *BioTechniques* **1993**, *15*, 486-495.

(46) Wu, s.; Dovichi, N. J. *Journal of Chromatography* **1989**, *480*, 141-145.

(47) Nathakarnkitkool, S.; Oefner, P. J.; Bartsch, G.; Chin, M. A.; Bonn, G. K. *Electrophoresis* **1992**, *13*, 18-31.

(48) Clark, B. K.; Sepaniak, M. J. *Journal of Microcolumn Separations* **1993**, *5*, 275-282.

CHAPTER 6

CONCLUSION

The human genome is made up of over 3,000,000 kb and includes between 50,000 to 150,000 genes[1,2]. In the last two decades, scientists have lobbied for the need to study and sequence the human genome, to gain massive information and understanding in a short period of time. Hopefully, once this information is processed, new drugs and therapies for genetic diseases will be produced. A few years ago, the Human Genome Project was created. It is a cooperative project between many countries and is the most ambitious project ever attempted in the biological field.

In the first few years of the project, new techniques are being developed for fast determination of DNA sequences and for restriction fragments analysis. Two schemes have been put forward for fast DNA sequence analysis: the first one suggests pushing the limit of existing techniques, and the second one suggests the development of new techniques. Capillary gel electrophoresis falls in the first category.

Capillary gel electrophoresis with laser induced fluorescence detection provides faster DNA sequencing than the classical slab gel electrophoresis with radioactive labeling. There are two reasons for this. The first reason is that higher electric fields can be used, due to efficient heat dissipation through the capillary wall. Thus, the higher electric field, used with capillary electrophoresis, allows faster separations with higher resolutions than slab gel electrophoresis. The second reason is the replacement of radioactive labeling by fluorescence detection. In classical slab gel electrophoresis, DNA is separated into bands of various sizes on a slab of polyacrylamide, and then, a film is exposed to the emission from the radioactive elements inserted in the DNA sequence. The exposure of the film can take hours, depending on the amount of DNA present in the bands. In the case of fluorescence detection, enough signal is generated in a very short period of time. Thus, fluorescence detection is not a time limiting process.

Capillary gel electrophoresis for DNA sequencing is still in its early stages, and is not commercially available. There are three main problems with capillary gel electrophoresis. First, the samples are run in series compared to slab gel electrophoresis in which the samples are run in parallel. Even though capillary electrophoresis is faster than slab gel electrophoresis, the throughputs are similar. A few groups are working on increasing the throughput of capillary electrophoresis by running capillaries in parallel[3-7]. The second problem is related to the gel performance and reproducibility in high electric fields. This problem is the main subject of this thesis. Finally, the third problem is a lack of confidence in capillary gel electrophoresis by the potential users and sometimes from the developers of the technique. This lack of confidence comes from the poor understanding and mishandling of the gel during the first years of capillary gel electrophoresis. In the last few years, a few groups[8-13] have studied gel stability. The result of these studies was good stability and reproducibility of the gel as well as understanding of the phenomena occurring in the gel.

In chapter 2, the effect of the concentration of cross-linker on the separation of a DNA sequencing standard was studied. We observed that higher resolution is obtained for cross-linked polyacrylamides compared to linear polyacrylamide; however, linear polyacrylamide is less affected by the formation of bubbles, and can be easily refilled into capillaries. Refilling the capillaries with linear polyacrylamide will become necessary for the multiple capillary system, because there would be too much work if the capillaries had to be replaced after each run. The sequencing obtained in linear polyacrylamide is faster than in cross-linked polyacrylamides. Also, because the biased reptation effect is less severe in linear polyacrylamide than in cross-linked polyacrylamides, longer sequences should be obtained. Therefore, linear polyacrylamide is more suitable for DNA sequencing by capillary gel electrophoresis than cross-linked polyacrylamides.

Chapter 3 presents a study of the stability of linear polyacrylamide. Two parameters were studied. The first is the effect of changes in transference numbers at the capillary:reservoir interfaces. It is demonstrated that, when 1xTBE buffer is used, an ionic depletion area forms at the cathodic end of the capillary, and no change in ionic concentration is observed at the anodic end. This depletion of ions at the cathodic end of the capillary was demonstrated to be less severe in aged linear polyacrylamides than in fresh ones. In fact, the effect of the depletion of ions appears to decrease exponentially with the age of the polyacrylamide and has a time constant of 5 days. We demonstrated that, when KCl is added to 1xTB, an area of increased ionic concentration forms at the anodic end of the capillary, and no change in ionic concentration is observed at the cathodic end. By using polyacrylamide filled reservoirs, we noticed no changes in ionic concentration at either end; however, polyacrylamide filled reservoirs cannot be used with post-column detectors. The second parameter studied is the effect of the concentration of the template on the stability of the current. Important decreases in current are observed when template is injected into linear polyacrylamide, but this effect is reversible if the polymer is allowed to relax. The results suggest that the effect of the template on the current is less important when more diluted template solutions are used. This is the first time that quantitative information is extracted from the measurement of the current in a capillary. Also, it is the first time that the effect of changes in transference number at the reservoir:capillary interfaces is demonstrated. From now on, separation studies by CGE will have to take into account this effect.

In chapter 4, we studied the effects of the observations from chapter 3 on the separation of a sequencing standard. First, the effect of aging of linear polyacrylamide was studied. We noticed that more stable migration times were obtained within four subsequent sequencing runs if 5- to 34-day old linear polyacrylamides were used. In fresh polyacrylamide, the migration times double within a few runs. In 115-day old polyacrylamide, the migration times decrease from run to run. These results are probably caused by changes in polyacrylamide properties with time. We postulated that hydrolysis, with time, of the amino group of some acrylamide units to a carboxylic group could be the cause of the changes. Thus, the migration times change from increasing, to being stable, and to decreasing from run to run with aging linear polyacrylamide.

In the second part of Chapter 4, the polarity of the electric field was reversed between sequencing runs, in order to replenish the depleted area at the injection end with ions. By using this technique, up to 19 subsequent sequencing runs were performed. This is the first report of multiple separations of sequencing sample by CGE. The migration time was shown to be related to the current, as the current decreases, the migration time increases. Reversing the polarity between runs allows the stabilization or quasi-stabilization of the current. Thus, the migration times of the DNA fragments are stable from sequencing runs to sequencing runs. Reversing the polarity between runs is only useful if the depletion of ions does not proceed too quickly, which means using older polyacrylamides. Therefore, by reversing the polarity between sequencing runs and using aged polyacrylamides, the migration times of the DNA fragments are stabilized; however, the resolution still decreases from run to run.

The labeling and the separation of double-stranded DNA by capillary gel electrophoresis is presented in Chapter 5. The intercalating dyes POPO-3, YOYO-3, and YOYO-1 were used to label double stranded DNA. Different restriction fragments were separated on polyacrylamide and HPMC. The results indicate that polyacrylamide gives better resolutions than HPMC, for fragments smaller than 300bp. For fragments bigger than 300bp, HPMC is preferable. Although these dyes are very efficient chromophores, they cause important band broadening because of their slow partition kinetics between the DNA and the solvent. In a different approach, the enzyme terminal deoxynucleotidyl transferase was used with ROX-dideoxycytosine triphosphate to covalently label double-stranded DNA. The product of the labeling was separated in HPMC and in polyacrylamide. Two peaks were produced per fragment due to incomplete labeling. Changing the concentration of the reagents should help to generate one peak per fragment.

The objectives of this thesis were first to better understand the phenomena happening in the separation matrix during electrophoresis, and second, to use the knowledge gained to achieve separation of single- and double-stranded DNA. In the last few years, there have been many studies done on the polymerization properties of polyacrylamide used for electrophoresis[14-24]. A few groups have studied different parameters affecting the separation of DNA by capillary gel electrophoresis[25-30]. These studies mainly focus on optimizing a few parameters according to the resolutions and the experimental times. Only a handful of studies address the problem of the behavior of polyacrylamide during electrophoresis in more detail[8-13]. The results of this thesis indicate which parameters most affect the behavior of polyacrylamide used for capillary gel electrophoresis.

More work should be done on the changes in transference numbers between a capillary and its reservoirs. As briefly demonstrated in chapter 3, changing the buffer composition can modify the phenomenon occurring at both ends of the capillary. The pH in the capillary should be probed, because any changes in ionic concentration due to changes in transference numbers are also accompanied by changes in pH. These changes in pH were not specifically addressed in this thesis. Also the presence of charges on aging polyacrylamide should be verified.

6.1 **Bibliography**

(1) Brown, T. A. *Gene Clonning, an Introduction;* 2 ed.; Chapman & Hall: London, 1990, pp 286.

(2) Brown, T. A. *Genetics a Molecular Approach*; Chapman & Hall: London, 1993; Vol. 2, pp 467.

(3) Ueno, K.; Yeung, E. S. *Analytical Chemistry* **1994**, *66*, 1424-1431.

(4) Takahashi, S.; Murakami, K.; Anazawa, T.; Kambara, H. *Analytical Chemistry* **1994**, *66*, 1021-1026.

(5) Kambara, H.; Takahashi, S. *Nature* **1993**, *361*, 565-566.

(6) Huang, X. C.; Quesada, M. A.; Mathies, R. A. *Analytical Chemistry* **1992**, *64*, 967-972.

(7) Huang, X. C.; Quesada, M. A.; Mathies, R. A. *Analytical Chemistry* **1992**, *64*, 2149-2154.

(8) Spencer, M. *Electrophoresis* **1983**, *4*, 36-41.

(9) Spencer, M. *Electrophoresis* **1983**, *4*, 41-45.

(10) Spencer, M. *Electrophoresis* **1983**, *4*, 46-52.

(11) Swerdlow, H.; Dew-Jager, K. E.; Brady, K.; Grey, R.; Dovichi, N. J.; Gesteland, R. *Electrophoresis* **1992**, *13*, 475-483.

(12) Swerdlow, H.; Dew-Jager, K.; Gesteland, R. F. *BioTechniques* **1994**, *16*, 684-693.

(13) Figeys, D.; Renborg, A.; Dovichi, N. J. *Electrophoresis* **1994**, *15*, 1512-1517.

(14) Righetti, P. G.; Gelfi, C.; Bosisio, A. B. *Electrophoresis* **1981**, *2*, 291-295.

(15) Righetti, P. G.; Gelfi, C. *Electrophoresis* **1981**, *2*, 220-228.

(16) Gelfi, C.; Righetti, P. G. *Electrophoresis* **1981**, *2*, 213-219.

(17) Righetti, P. G.; Gelfi, C.; Bosisio, A. B. *Electrophoresis '82* **1983**, 147-156.

(18) Righetti, P. G.; Snyder, R. S. *Applied and Theoretical Electrophoresis* **1988**, *1*, 53-58.

(19) Gelfi, C.; deBesi, P.; Alloni, A.; Righetti, P. G. *Journal of Chromatography* **1992**, *608*, 333-341.

(20) Righetti, P. G.; Caglio, S.; Saracchi, M.; Quaroni, S. *Electrophoresis* **1992**, *13*, 587-595.

(21) Righetti, P. G.; Caglio, S. *Electrophoresis* **1993**, *14*, 573-582.

(22) Caglio, S.; Righetti, P. G. *Electrophoresis* **1993**, *14*, 997-1003.

(23) Righetti, P. G.; Chiari, M.; Nesi, M.; Caglio, S. *Journal of Chromatography* **1993**, *638*, 165-178.

(24) Righetti, P. G.; Bossi, A.; Giglio, M.; Vailati, A.; Lyubimova, T.; Briskman, V. A. *Electrophoresis* **1994**, *15*, 1005-1013.

(25) Lu, H.; Arriaga, E.; Chen, D. Y.; Figeys, D.; Dovichi, N. J. *Journal of Chromatography* **1994**, *680*, 503-510.

(26) Best, N.; Arriaga, E.; Chen, D. Y.; Dovichi, N. J. *Analytical Chemistry* **1994**, *66*, 4063-4067.

(27) Harke, H. R.; Bay, S.; Zhang, J. Z.; Rocheleau, M. J.; Dovichi, N. J. *Journal of Chromatography* **1992**, *608*, 143-150.

(28) Rocheleau, M. J.; Grey, R. J.; Chen, D. Y.; Harke, H. R.; Dovichi, N. J. *Electrophoresis* **1992**, *13*, 484-486.

(29) Figeys, D.; Dovichi, N. J. *Journal of Chromatography* **1993**, *645*, 311-317.

(30) Luckey, J. A.; Smith, L. M. *Analytical Chemistry* **1993**, *65*, 2841-2850.

APPENDIX A

CALCULATION OF THE FRICTION COEFFICIENT AND THE GEL PORE SIZE.

The linear part of the mobility plot versus N_{bead}^{-1} should follow the bias reptation model:

$$\mu = \frac{Q}{3 \quad \varepsilon_c} \left[\frac{1}{N_{bead}} + \left\langle\frac{q \quad E \quad \alpha_s}{3 \quad K_b \quad T_p}\right\rangle^2\right] \tag{A.1}$$

where N_{bead} is the number of pores filled by the fragment. Equation A.1 can be written as:

$$\mu = \frac{Q}{3 \quad \varepsilon_c} \quad \frac{1}{N_{bead}} + \frac{Q}{3 \quad \varepsilon_c} \quad \left\langle\frac{q \quad E \quad \alpha_s}{3 \quad K_b \quad T_p}\right\rangle^2 \tag{A.2}$$

We have fitted the mobility to the inverse of the base number(N) for the linear part, the coefficients obtained were reported in Table 2.2.

$$\mu = \frac{S}{N} + I \tag{A.3}$$

In equation A.3, N can be estimated in the case of DNA by:

$$N \approx \frac{N_{bead} \quad \alpha_s}{D_{b\text{-}b}} \tag{A.4}$$

where $D_{b\text{-}b}$ is the distance between two bases. Then,

$$\mu = \frac{S \quad D_{b\text{-}b}}{N_{bead} \quad \alpha_s} + I \tag{A.5}$$

Thus the slope (S) in Table 2.2 multiply by ($D_{b\text{-}b} * \alpha^{-1}$) is equal to $\frac{Q}{3 \quad \varepsilon_c}$. Once the change of the variable is done, we obtain:

$$\mu = \frac{S\ D_{b\text{-}b}}{\alpha_s} \left[\frac{1}{N_{bead}} + \left(\frac{q}{3}\ \frac{E}{K_b}\ \frac{\alpha_s}{T}\right)^2\right] \tag{A.6}$$

A.1 Slope

The slope (S) is related to the whole charge of the fragment (Q) and to the friction coefficient (ε_c) of the solution by the following relationship:

$$S = \frac{Q\ \alpha_s}{3\ \varepsilon_c\ D_{b\text{-}b}} \tag{A.7}$$

for a particular fragment, Q and ($D_{b\text{-}b} * \alpha^{-1}$) are constant, equation A.7 can be rewritten as:

$$\varepsilon_c = \frac{K}{S} \tag{A.8}$$

Thus, the friction coefficient is inversely related to S. The values of S^{-1} are reported in Table 2.2.

A.2 Intercept

The intercept (I) of the fit is related to the pore's size (α_s) through the second term of Equation A.6. If we make an approximation for the value of q (equation A.9), it is possible to calculate the radius from the intercept and the slope (equation A.10).

$$q = \frac{e\ \alpha_s}{D_{b\text{-}b}} \tag{A.9}$$

$$\alpha_s = \left[\frac{9 \quad I \ K_b^2 \quad D_{b\text{-}b} \quad T^2}{S \quad E^2 \quad e^2}\right]^{\frac{1}{3}} \qquad \text{(A.10)}$$

The values of the pore's size are reported in Table 2.2.

APPENDIX B

MORE MULTIPLE RUNS OF DNA SEQUENCING SAMPLES

Figure B.1 14 runs of sequencing samples on the same capillary at -300V/cm. Runs 2, 6, 9, and 14 are presented. The M13mp18 ddATP samples were used for runs 1 to 7, and M13mp18 ddGTP samples were used for runs 8 to 14. Bases 109-111 and bases 164-166 for ddATP, and bases 171-174 for ddGTP are identified on the electropherograms.

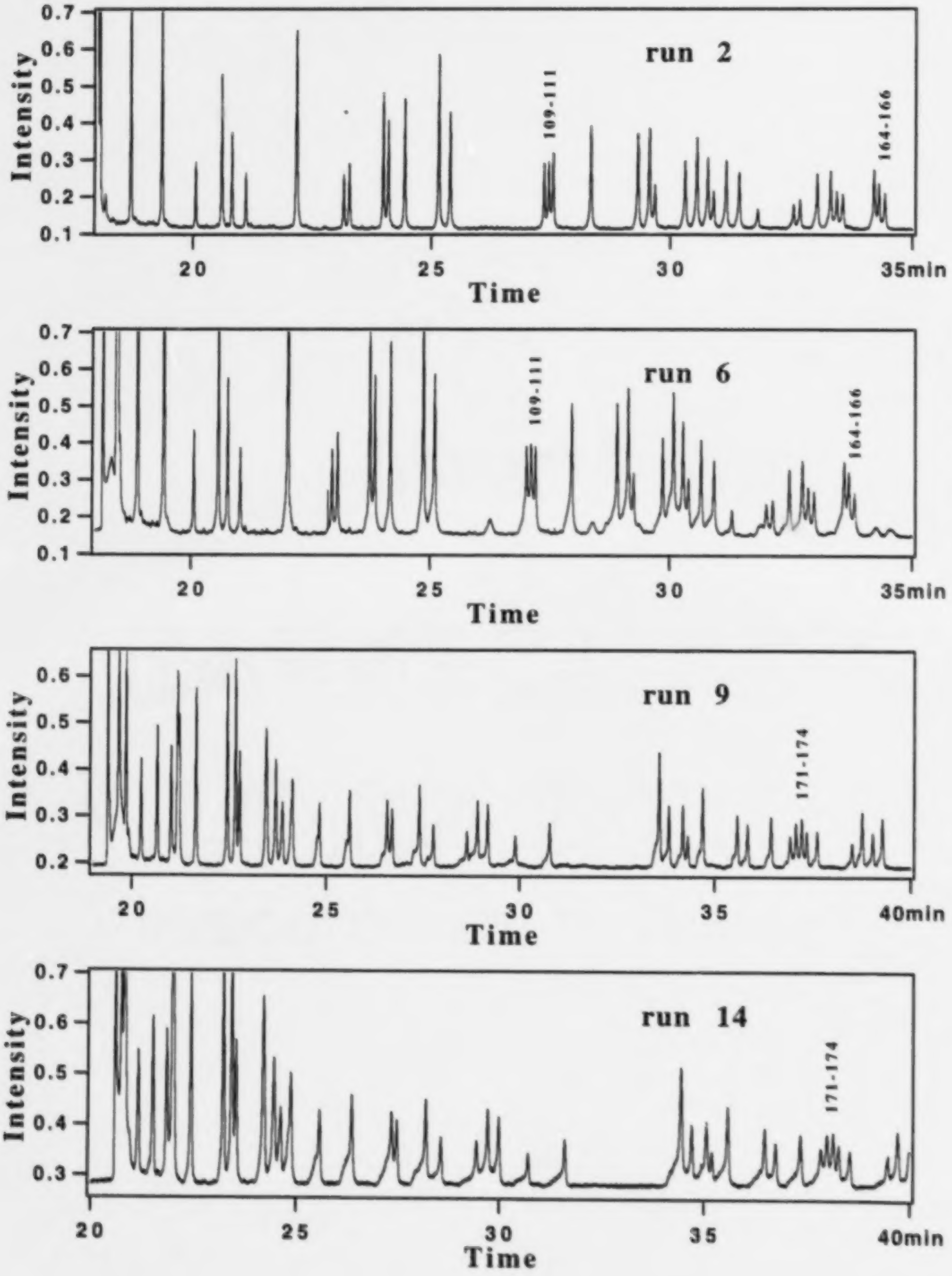

Figure B.2 15 runs of M13mp18 ddGTP sequencing samples on the same capillary at -300V/cm. Runs 2, 6, 10, and 14 are presented. Bases 171-174 are identified on the electropherograms.

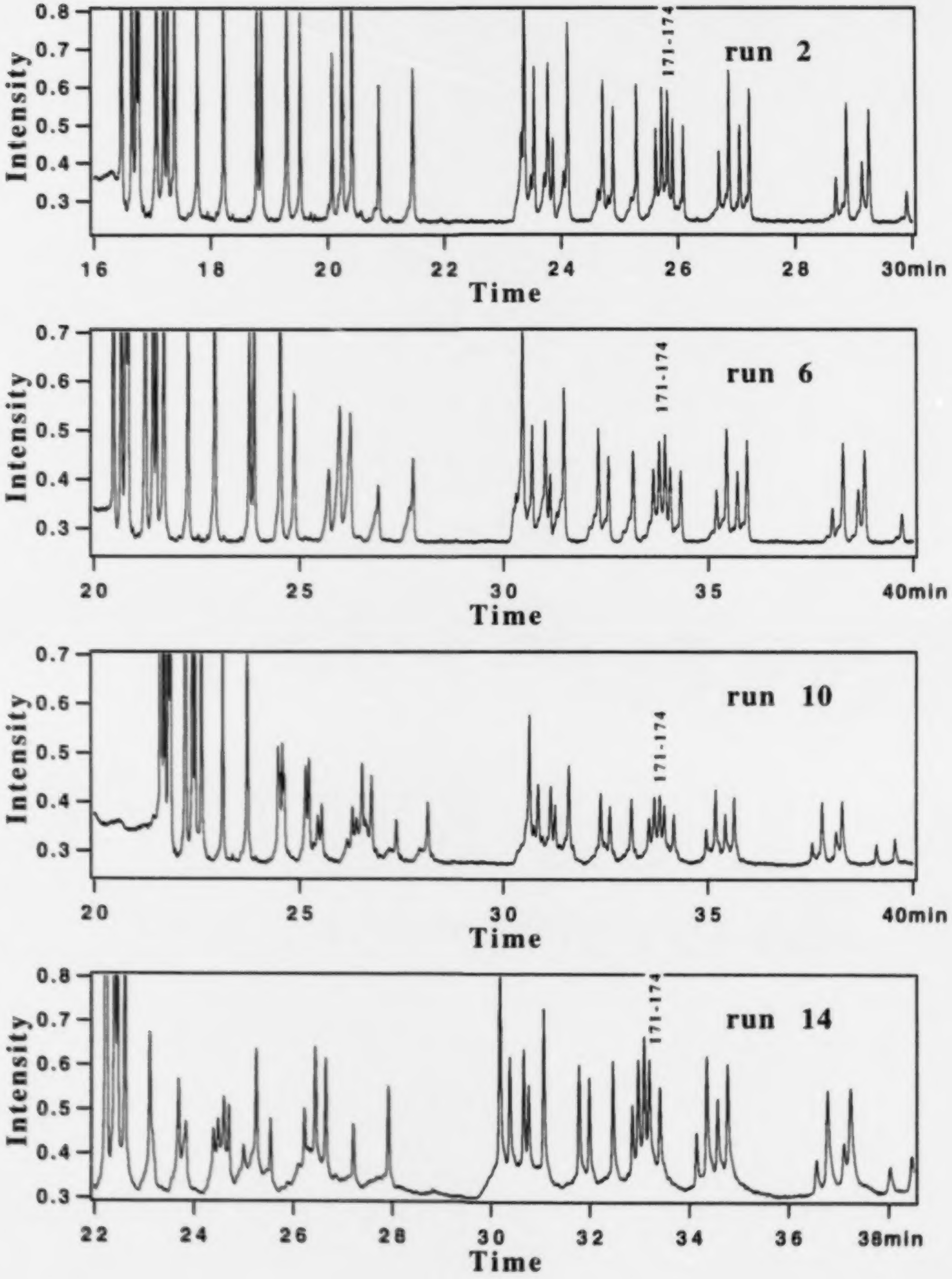

Figure B.3 7 runs of M13mp18 ddATP sequencing samples on the same capillary at -300V/cm. Runs 1, 2, 4, and 6 are presented. Bases 109-111 and bases 164-166 are identified on the electropherograms.